Leptin signaling in pancreatic β-cells: a mechanism to regulate K_{ATP} channel trafficking and β-cell electrical activity

By

Veronica Cochrane

A DISSERTATION

Presented to the Department of Chemical Physiology & Biochemistry

Oregon Health & Science University

School of Medicine

In partial fulfillment of the requirements for the degree of

Doctor of Philosophy

January 2021

Department of Chemical Physiology & Biochemistry
School of Medicine
Oregon Health & Science University

CERTIFICATE OF APPROVAL

This is to certify that the Ph.D. dissertation of

Veronica Cochrane

has been approved

Advisor: Show-Ling Shyng, Ph.D.
Professor of Chemical Physiology & Biochemistry
Oregon Health & Science University

Chair: Philip Stork, M.D.
Senior Scientist
Vollum Institute

Member: Beth Habecker, Ph.D.
Professor of Chemical Physiology & Biochemistry
Oregon Health & Science University

Member: Carsten Schultz, Ph.D.
Professor of Chemical Physiology & Biochemistry
Oregon Health & Science University

Member: Jonathan Purnell, M.D.
Professor of Medicine
Oregon Health & Science University

Member: Paul Kievit, Ph.D.
Assistant Professor
Oregon National Primate Research Center

Table of Contents

List of Figures and Tables

Chapter 1

Chapter 2

Chapter 3

Chapter 4

Chapter 5

Appendices

List of Abbreviations

2-APB	2-aminoethyldiphenyl borate
8Br	8-Bromo-cAMP
AC	adenylyl cyclase
ACC	Acetyl CoA carboxylase
ADP	adenosine diphosphate
AICAR	5-Aminoimidazole-4-carboxamide ribonucleotide
AKAP	A-kinase anchoring protein
AKAR4	A-kinase activity reporter 4
AM	acetoxylmethyl ester
AMP	Adenosine monophosphate
AMPA	α-amino-3-hydroxy-5-methyl-4-isoxazolepropionic acid
AMPK	5'AMP-activated protein kinase
ATP	Adenosine triphosphate
AUC	area under the curve
AZD	AZD0530
BAPTA	1,2-bis(o-aminophenoxy)ethane-N,N,N′,N′-tetraacetic acid
BSA	bocine serum albumin
BTX	α-bungarotoxin
Ca2+	calcium
CaMKKβ	Ca^{2+}/calmodulin kinase kinase β
cAMP	Cyclic adenosine monophosphate
CC	Compound C (Dorsomorphin)
CDK5	Cyclin Dependent Kinase 5
CFP	cyan fluorescent protein
CNBD	cyclic nucleotide binding domain
CUTie	cAMP Universal Tag for imaging experiments

D-APV	D-2-amino-5-phosphonovalerate
Das	dasatinib
Diaz	Diazoxide
DMSO	Dimethyl sulfoxide
DPBS	Dulbecco's phosphate-buffered saline
DTT	dithiothreitol
DXM	dextromethorphan
EAAT	excitatory amino acid transporter
EGTA	ethylene glycol-bis(β-aminoethyl ether)-N,N,N′,N′-tetraacetic acid
EPAC	exchange factor directly activated by cAMP
ER	endoplasmic reticulum
FBS	Fetal bovine serum
FRET	fluorescence resonance energy transfer
Fsk	forskolin
GD	glucose deprivation
GEF	guanine nucleotide exchange factors
GFP	green fluorescent protein
GIRK	G-protein coupled Kir channels
GLP-1	glucagon-like peptide 1
GLT1	glial glutamate transporter 1
Go 6983	3-[1-[3-(Dimethylamino)propyl]-5-methoxy-1*H*-indol-3-yl]-4-(1*H*-indol-3-yl)-1*H*-pyrrole-2,5-dione
GSIS	glucose-stimulated insulin secretion
GSK3β	glycogen synthase kinase 3 β
HEPES	4-(2-hydroxyethyl)-1-piperazineethanesulfonic acid
IBMX	isobutyl-methylxanthine
IIDP	Integrates Islets Distribution Program
INS-1 832/13	INS-1 clone 832/13
IP_3R	1,4,5-triphosphate receptors

JAK	Janus kinase
K^+	potassium
K_{ATP}	ATP-sensitive potassium channel
KD	knockdown
LKB1	liver kinase B1
LY294002	2-Morpholin-4-yl-8-phenylchromen-4-one
MK-801	Dizocilpine
ML-204	4-Methyl-2-(1-piperidinyl)quinoline
mRNA	messenger ribonucleic acid
NEDH	New England Diaconess Hospital
NES	nuclear export signal
NMDA	N-Methyl-D-Aspartate
NMDAR	N-Methyl-D-Aspartate Receptor
ObR	leptin receptor
PBS	phosphate-buffered saline
PBST	phosphate-buffered saline plus 0.1% Tween-20
PDE	phosphodiesterase
PI3K	phosphoinositide 3-kinase
PIP3	phosphatidylinositol (3,4,5)-trisphosphate
PKA	protein kinase A
PKC	protein kinase C
PKI	protein kinase A-specific inhibitor peptide
PP	pancreatic polypeptide
PP2B	protein phosphatase 2B
PTEN	phosphatase and tensin homolog
PTP1B	protein tyrosine phosphatase 1B
Ro 25-6981	(α*R*,β*S*)-α-(4-Hydroxyphenyl)-β-methyl-4-(phenylmethyl)-1-piperidinepropanol maleate
Ros	roscovitine

RT-PCR	reverse transcriptase-polymerase chain reaction
SEM	standard error of the mean
SFK	Src family kinase
shRNA	short hairpin ribonucleic acid
SH	Src homology
siRNA	small interfering ribonucleic acid
SOCS3	suppressor of cytokine signaling
st	stearate
STAT	signaling transducers and activators of transcription
STO-609	7-Oxo-7*H*-benzimidazo[2,1-*a*]benz[de]isoquinoline-3-carboxylic acid acetate
Sulfo-NHS-biotin	sulfosuccinimidobiotin
SUR1	sulfonylurea receptor 1
T2D	Type 2 Diabetes
TBST	Tris-buffered saline plus 0.1% Tween-20
TCN-201	3-Chloro-4-fluoro-*N*-[4-[[2-(phenylcarbonyl)hydrazino]carbonyl]benzyl]benzenesulfonamide
TEA	tetraethylammonium
Tolb	tolbutamide
TRPC4	Transient receptor potential channel
VGLUT	vesicular glutamate transporters
WT	wild type
YEEI	phosphopeptide EPQpYEEIPIYL
YFP	yellow fluorescent protein

Acknowledgements

Thanks to my mentor Show-Ling Shyng, who not only turned me into a scientist but also improved me as a person; my committee members Phil Stork, Beth Habecker, Carsten Schultz, and Jonathan Purnell, for their valuable insights and encouragement; my collaborators Chuck Allen, Nate Klett, Paul Kievit, and Mark Dell'Acqua; the Shyng lab, both past and current members; and my friends and family, for their love and support throughout my time as a graduate student.

Abstract

Insulin is a hormone secreted by pancreatic β-cells in response to glucose stimulation. Proper insulin secretion keeps blood glucose in a physiological range by promoting the uptake of glucose by insulin-sensitive target tissues. In addition to glucose, various other metabolic and hormonal stimuli act on β-cells to modulate insulin secretion and maintain metabolic homeostasis. One such hormone is the adipocyte-derived peptide hormone leptin. Leptin acts directly on β-cells to suppress insulin secretion and prevent excessive serum insulin levels. Disrupted leptin signaling is associated with various metabolic disorders including obesity and type 2 diabetes (T2D). Leptin was found to suppress insulin secretion from pancreatic β-cells by increasing conductance of ATP-sensitive potassium (K_{ATP}) channels resulting in β-cell hyperpolarization. However, the mechanism by which leptin increased K_{ATP} channel activity remained elusive.

Recent studies by our group and others have determined that leptin increases K_{ATP} currents by promoting trafficking of K_{ATP} channels to the β-cell surface. Mechanistic studies determined that leptin activates Ca^{2+}/calmodulin kinase kinase β (CaMKKβ), which then phosphorylates and activates 5'AMP-activated protein kinase (AMPK). Downstream of AMPK actin remodeling occurs in a protein kinase A (PKA)-dependent manner allowing for vesicles containing K_{ATP} channels to traffic to the cell surface. These studies provided valuable insight into the signaling mechanism underlying K_{ATP} channel trafficking, but several questions were left unanswered including: 1) what is the Ca^{2+} source to activate CaMKKβ and 2) what is the relationship between leptin and PKA?

In this thesis, leptin is shown to induce a Ca^{2+} influx via Src kinase potentiation of N-Methyl-D-Aspartate (NMDA) receptors that initiates the CaMKKβ-AMPK signaling pathways. Then it is determined that leptin signaling via the NMDAR-CaMKKβ-AMPK axis increases the

activity of PKA anchored to the scaffolding A-kinase anchoring protein (AKAP) AKAP79/150. The role of AKAP79/150 in mediating leptin signaling indicates that leptin signaling is spatially localized within β-cells to promote K_{ATP} channel trafficking, which is significant as both Ca^{2+} and PKA may also serve as positive regulators of insulin secretion. Finally, the work presented here provides evidence that leptin signaling in β-cells is disrupted in the pathology of T2D, but that this may be overcome by targeting leptin signaling molecules. In summary, the work in this thesis significantly advances our mechanistic understanding of leptin-induced K_{ATP} channel trafficking, and it identifies leptin signaling molecules as potential therapeutic targets for preventing or treating T2D.

Chapter 1: Introduction

Diabetes mellitus affects >400 million people worldwide and the prevalence of diabetes continues to grow. Diabetes is characterized by pathologically high blood glucose levels, also known as hyperglycemia. Over time, diabetes can lead to other health problems including heart disease, nerve damage, and kidney disease. Diabetes and its associated complications increase the risk of premature death and burden health care systems. The vast majority (~90%) of diabetes patients are diagnosed with Type 2 Diabetes (T2D). Typically, T2D afflicts older adults who are obese and have sedentary lifestyles. In healthy individuals, pancreatic β-cells secrete the hormone insulin in response to a rise of blood glucose levels, insulin then signals to its target tissues such as skeletal muscle and fat to promote the uptake of glucose for usage and storage to restore blood glucose levels. However, in T2D patients, the body does not respond to insulin (i.e. insulin resistance) and β-cells are unable to secrete sufficient insulin to overcome this, resulting in excessive glucose remaining in the blood. The high correlation between T2D and obesity is indicative of disrupted mechanisms that integrate energy homeostasis and glucose homeostasis. One such mechanism is a dual hormonal feedback loop between the hormones insulin and leptin termed the 'adipoinsular axis'(1). In this model, insulin promotes the production and secretion of the adipocyte hormone leptin in addition to stimulating glucose uptake, adipogenesis, and increasing fat mass; leptin in turn inhibits insulin secretion from β-cells as well as suppressing food intake and increasing energy expenditure. Disruption of this feedback loop as a result of insulin or leptin resistance is predicted to upset the balance of fat and glucose regulation, as observed in obese T2D patients. Understanding the signaling pathway underlying the adipoinsular axis is therefore of high significance. The following sections will cover a brief history of leptin with an emphasis on leptin as a regulator of glucose homeostasis and our understanding at the start of this thesis of how leptin suppresses insulin secretion from pancreatic β-cells.

Sections 1.1. – 1.6.4.2. are adapted from a review article originally published by

Cochrane V. & Shyng S-L.

International Journal of Molecular Sciences 2019; 20(11): 2660.

DOI: 10.3390/ijms20112660

1.1. Leptin

The discovery of leptin and its receptor began when Doug Coleman performed parabiosis experiments using wild type mice and the genetically obese *ob* and *db* mouse strains. Coleman discovered that when *ob* mice were paired with wild type or *db* mice they ate less and lost weight (Fig. 1.1.)(2,3). However, wild type and *ob* mice paired with *db* mice would eventually starve to death(2,3). From these studies, Coleman concluded that *ob* mice lacked a satiety hormone and *db* mice lacked the receptor for this hormone. Moreover, the finding that wild type and *ob* mice starved to death when surgically joined with *db* mice indicated that *db* mice overexpress the satiety hormone and it was implicated that overexpression of this hormone was linked to obesity.

Coleman's predictions were proven correct when the *ob* and *db* genes were identified through cloning experiments. After identifying the *ob* gene(4) it was determined to encode a 167 amino acid peptide hormone belonging to the cytokine family. This peptide hormone was named "leptin" after the Greek root "leptos" for "thin". Although *ob* mice have upregulated expression levels of leptin mRNA(4), a missense mutation in the *ob* gene results in a truncated inactive form of leptin(5). Shortly after the discovery of the *ob* gene, the *db* gene was identified and found to encode the leptin receptor (ObR)(6). The *db* gene has six different splice variants that are each translated into a leptin receptor isoform (ObRa - ObRf)(7,8). The ObRb isoform is primarily expressed in the hypothalamus(7,9,10) and it is attributed with affecting the majority of leptin's actions due to its long intracellular signaling domain. ObRb signaling canonically occurs through Janus kinase (JAK)/signaling transducers and activators of transcription (STAT)

signaling pathways to elicit transcriptional changes of its target genes(11–14). However, in *db* mice, an insertion mutation causes the ObRb isoform to have a truncated intracellular signaling domain(7,8,10). In agreement with Coleman's predictions, leptin was found to signal through its ObRb receptor in the hypothalamus to suppress appetite(10,12,15,16), which is disrupted in *ob* and *db* mice. The notion that leptin was the long sought-after satiety hormone responsible for coordinating body weight with food intake and energy expenditure to regulate energy homeostasis was further supported by the findings that leptin is predominantly produced and secreted by white adipocytes, and plasma leptin levels are highly correlated with body fat mass. While the role of leptin in energy homeostasis has garnered much attention, leptin has also been implicated in numerous other biological processes including glucose homeostasis.

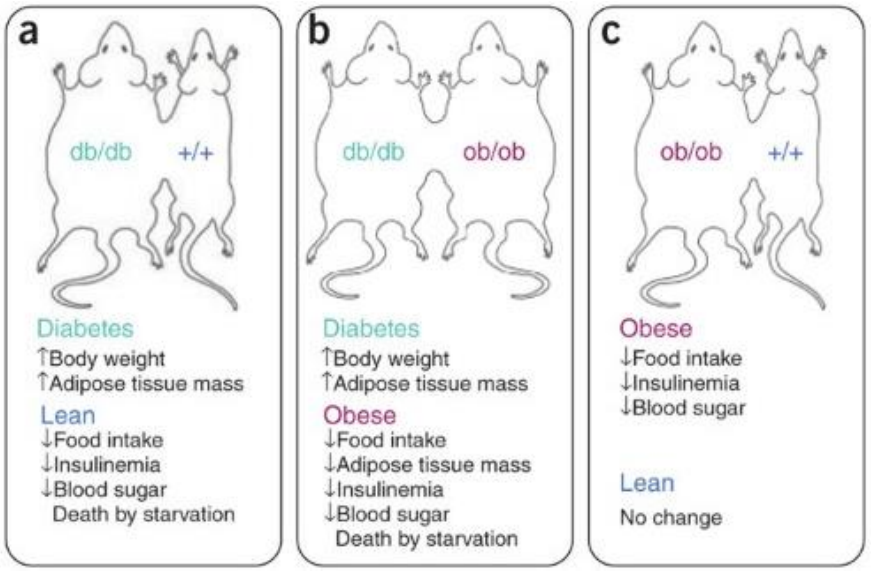

Figure 1. 1. *ob* and *db* mice.
Summary of parabiosis experiments between wild type, *ob*, and *db* mice. DOI: https://doi.org/10.1038/nm1010-1097

1.2. Leptin as a regulator of glucose homeostasis

Evidence that leptin was critical for regulating glucose homeostasis also came from the *ob* and *db* mouse strains. In addition to developing obesity, indicative of an energy imbalance, *ob* and *db* mice exhibit hyperinsulinemia, insulin resistance, and high blood glucose levels reminiscent of T2D in humans(2,3). Both *ob* and *db* mice develop hyperinsulinemia prior to

developing insulin resistance, obesity and hyperglycemia(3,17–20) indicating that the effects of leptin on glucose homeostasis are independent of leptin's effects on energy homeostasis. Consistent with these findings, disrupting endogenous leptin signaling in wild type mice with a leptin antagonist also causes hyperinsulinemia prior to any effects on body weight(21). Moreover, administering leptin to *ob/ob* mice normalizes serum insulin and glucose concentrations before any changes in the animals' weight are observed(15,22). It should be noted that while the *ob* and *db* mouse strains do display some of the characteristics of T2D observed in humans, there are several significant differences in the pathology with the most notable one being that T2D in humans is predominantly the result of multiple genetic variants and environmental factors. Nevertheless, the above findings demonstrate that leptin serves a direct role in maintaining glucose homeostasis in addition to regulating energy balance, which has indirect consequences for glucose metabolism.

1.3. The Pancreas

The pancreas is an abdominal organ central to glucose homeostasis. It is located in the upper abdomen behind the stomach, and it is shaped like a tadpole with the head of the pancreas connecting to the duodenum near the center of the abdomen and the tail extending to the left. The pancreas comprises an exocrine gland and an endocrine gland (Fig. 1.2.), which are important for digestion and glucose metabolism, respectively. The exocrine gland makes up the bulk of the pancreatic volume and is composed of acinar and ductal cells(23–25). These cells produce digestive enzymes that flow through the pancreatic duct and into the duodenum to breakdown food for absorption by the body. The endocrine gland makes up only 1-4% of the pancreas and consists of cell clusters that appear as 'islands' throughout the exocrine pancreas(23–27). These cell clusters were discovered by Paul Langerhans in 1869 and have

been aptly named “islets of Langerhans”. Islet cells produce several hormones important for glucose metabolism; most notably insulin is synthesized and secreted by islets.

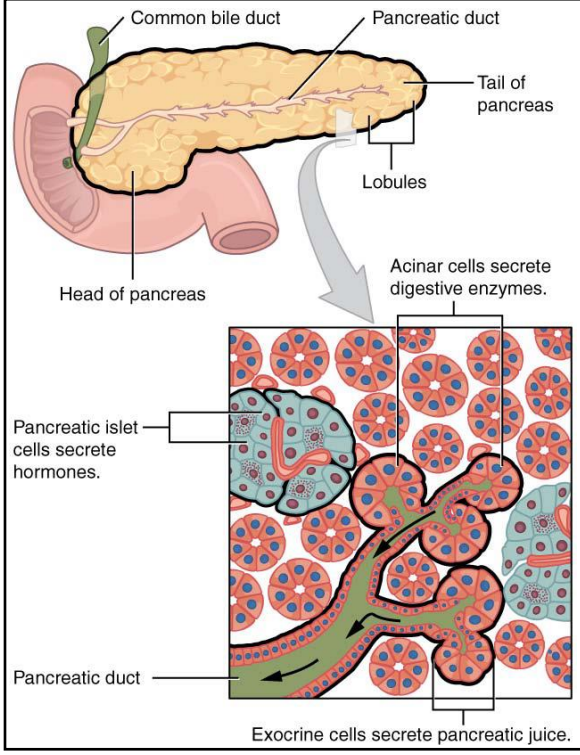

Figure 1. 2. Anatomy of the pancreas.
The pancreas is an organ situated in the upper abdomen comprised of exocrine and endocrine glands that regulate digestion and glucose metabolism, respectively. The exocrine gland consists of acinar and duct cells that make up the bulk of the pancreatic volume and secrete ‘pancreatic juices’ through the duct into the duodenum to promote digestion. The endocrine gland clusters of cells termed ‘islets’. Islets produce hormones including insulin that are critical for glucose metabolism.

Image: ‘Exocrine and Endocrine Pancreas’ by Phil Schatz. https://philschatz.com/anatomy-book/contents/m46496.html

License: CC BY 2.0

1.3.1 Pancreatic islets

Pancreatic islets are made up of five major cell types and each produces a distinct hormone: α-cells (glucagon), β-cells (insulin), δ-cells (somatostatin), PP cells (pancreatic polypeptide), ε-cells (ghrelin)(25,28). The most prevalent cell types in islets are β-cells and α-cells. In mice, islets are made up of 60-80% β-cells and 10-20% α-cells, whereas in humans, β-cells and α-cells make up 50-70% and 20-40% of cells in islets, respectively(25). Islets, in mice and most animals, form a mantle-core pattern with an almost exclusively β-cell core and non-β-cell mantle (Fig. 1.3.). In contrast, human islets appear to be largely unorganized(29,30), although more recently it has been reported that human islets form trilaminar plates in which β-cells are sandwiched between α-cell layers(31). The organization of cells within islets has implications for islet function(32,33), and this should be considered when making comparisons

across organisms. Interestingly, one study found that mouse islets assume an architecture similar to human islets when there is a greater physiological demand for insulin(33,34). Another key feature of islets is that they are highly vascularized. This allows for the hormones produced by islet cells to be readily introduced into the bloodstream. Both glucagon and insulin play critical roles in maintaining glucose homeostasis. While insulin decreases blood glucose levels, glucagon increases them. Although there are several hormones that, like glucagon, increase blood glucose levels, insulin is the only hormone that promotes glucose uptake and it is indispensable for glucose homeostasis.

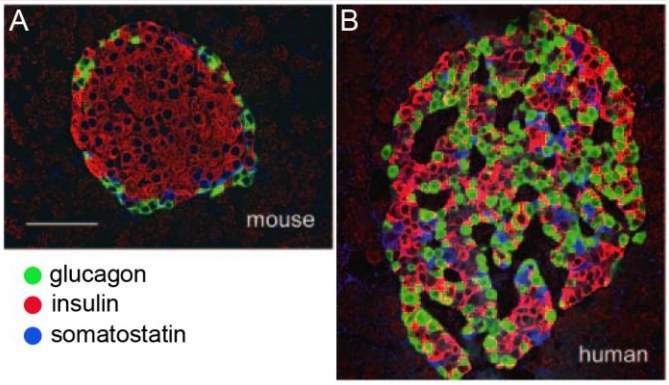

Figure 1. 3. Architectural differences between mouse and human islets. Mouse (A) and human (B) Islets were immunnostained for glucagon (green), insulin (red), and somatostatin (blue). The black space within the human islets is occupied by blood vessels. (Scale bar, 50μm).

1.3.2 Insulin secretion from β-cells

Pancreatic β-cells are the sole source of insulin for the body, and proper insulin secretion from β-cells is critical for maintaining glucose homeostasis. Blood glucose is a main energy source for the body and the primary stimulus that governs insulin secretion. As glucose is a principal component of food, blood glucose levels rise following a meal and decline during fasting periods. A key link between serum glucose levels and insulin secretion is the ATP-sensitive potassium (K_{ATP}) channel, which sets the β-cell resting membrane potential. K_{ATP} channels are regulated by the intracellular ATP/ADP ratio, enabling them to effectively serve as metabolic sensors that couple serum glucose to insulin secretion (Fig. 1.4.)(35–37). At high

blood glucose levels, glucose enters β-cells and is metabolized leading to an increase in the intracellular ATP/ADP ratio; this favors K_{ATP} channel closure, resulting in cell depolarization, activation of voltage-gated Ca^{2+} channels, and insulin exocytosis. Conversely, at low blood glucose concentrations the low intracellular ATP/ADP ratio favors K_{ATP} channel opening, which hyperpolarizes the cell and inhibits insulin secretion. In addition to glucose, there are numerous other physiological stimuli that function to either augment or inhibit glucose-stimulated insulin secretion (GSIS). The consequent changes in serum insulin levels maintain blood glucose levels within a narrow range, 4.0 mM – 7.8 mM (72 mg/dL – 140 mg/dL) in humans, regardless of feeding status.

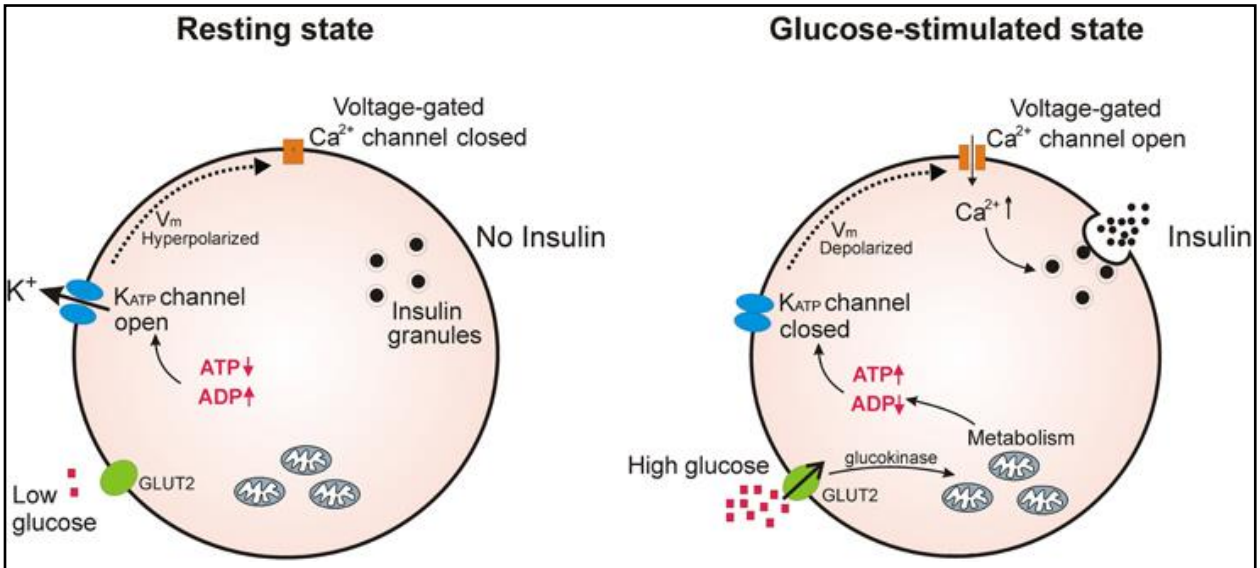

Figure 1. 4. Insulin secretion from pancreatic β-cells.
At low blood glucose concentrations, K_{ATP} channels are activated by the relatively low ATP/ADP ratio. This leads to β-cell hyperpolarization and inhibition of insulin secretion. Upon a rise in blood glucose levels, glucose enters the cell and is metabolized resulting in an elevated ATP/ADP ratio. Under these conditions K_{ATP} channels close and the cell membrane depolarizes and activates voltage-gated Ca^{2+} channels; the ensuing Ca^{2+} influx promotes insulin exocytosis.

Image is from Martin G. et al., Front. Physiol., 2013; 4:386. DOI: 10.3389/fphys.2013.00386.

1.4. β-cell K_{ATP} channels as a target of leptin

In light of the finding that leptin rapidly normalizes serum insulin levels in hyperinsulinemic *ob/ob* mice (see section 1.2.), pancreatic β-cells were proposed to be a peripheral target of leptin. Several groups have since shown that leptin receptors are expressed in islets and β-

cells(38–43), bolstering the notion that leptin targets β-cells. Many of these studies also found that leptin reduces insulin secretion when directly applied to isolated islets(40–44), but a few reported that leptin had no effect or a stimulatory effect(45–47). These contradicting findings sparked a controversy over whether leptin acts directly on β-cells to regulate insulin secretion. In an attempt to address this, multiple groups used genetic approaches to create mice that lack leptin signaling in β-cells(48–51). Unfortunately, these studies have also produced inconsistent results. For example, Covey et al. found that disrupting leptin signaling at the β-cell level led to hyperinsulinism followed by insulin resistance and diabetes(48,49), whereas Soedling et al. reported only a limited impact on glucose homeostasis(51). The reason for this discrepancy has not been resolved but it may in part be due to these studies using different genetic approaches and mouse strains. Despite the conflicting data from islets and mice, leptin has repeatedly been shown to have an effect on isolated β-cells.

Consistently leptin stimulation causes β-cell hyperpolarization at high glucose concentrations, when the majority of K_{ATP} channels are mostly closed and β-cells are depolarized(39,52–59). This discovery made researchers question whether leptin influences K_{ATP} channel activity, as K_{ATP} channels were known to regulate the resting potential of β-cells(60). Indeed, leptin was found to cause membrane hyperpolarization by increasing β-cell membrane K^+ conductance, which could be reversed upon application of a K_{ATP} channel specific sulfonylurea inhibitor, tolbutamide(39,52) (Fig. 1.5.). Based on these findings it was proposed that leptin reduces insulin secretion by enhancing K_{ATP} channel activity.

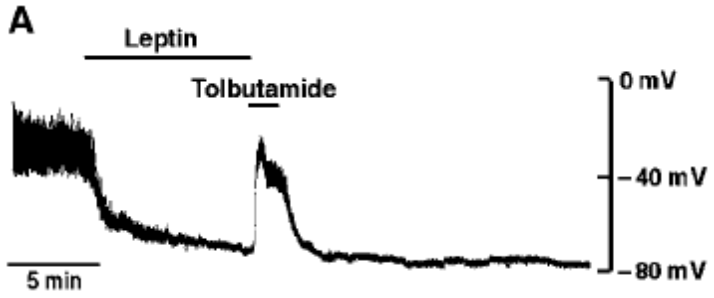

Figure 1. 5. Leptin causes β-cell hyperpolarization.

(A) Representative whole-cell current clamp recording from a mouse β-cell. Leptin-induced hyperpolarization is reversed upon application of the K_{ATP} channel inhibitor Tolbutamide.

Image is from Ning K. et al., EMBO J., 2006. DOI: 10.1038/sj.emboj.7601118.

Follow-up studies attempted to elucidate how leptin signaling enhanced K_{ATP} channel activity. This work was conducted under the assumption that leptin increased activity of K_{ATP} channels already present in the membrane. Initially the studies tested the ability of leptin to increase phosphatidylinositol (3,4,5)-trisphosphate (PIP_3) levels by activating phosphoinositide 3-kinase (PI3K), as PIP_3 has been shown to increase K_{ATP} channel activity(61). Although application of exogenous PIP_3 did increase K_{ATP} channel activity(55), it was revealed that the increase of endogenous PIP_3 levels in response to leptin stimulation was insufficient(54,59). Moreover, they found that PIP_3 levels increased as the result of phosphatase and tensin homolog (PTEN) inhibition rather than PI3K activation. PTEN is a dual lipid and protein phosphatase that has been extensively studied for its role in tumorigenesis with the majority of its actions being attributed to its phosphatase activity towards lipids especially PIP_3(62). In addition to increasing PIP_3 levels PTEN inactivation by leptin was shown to cause actin remodeling. This was a particularly interesting finding since a prior study in cardiomyocytes had shown that actin destabilizing agents could increase K_{ATP} channel activity(63). It was further determined that the effect leptin has on β-cell K_{ATP} channels is dependent on actin depolymerization and could be recapitulated by actin destabilizing agents(54,56,59). While this work identified potential signaling steps required for leptin to exert its effects on K_{ATP} channels, it was largely unsuccessful in proving the hypothesis that leptin modulates K_{ATP} channel gating.

1.5. Leptin increases K_{ATP} channel surface density

In recent years, increased K_{ATP} channel surface density has emerged as the predominant mechanism by which leptin increases K_{ATP} channel conductance. This finding was first reported by Park et al. and months later by our group(57,58). Our lab found that following leptin treatment K_{ATP} channels do not display altered sensitivity to ATP or ADP indicating that the effects of leptin are not due to changes in K_{ATP} channel gating(58). Using surface biotinylation assays to monitor K_{ATP} channel surface density in the rat insulinoma cell line INS-1 clone 832/13 (INS-1 832/13)(64) there was a detectable increase observed as early as 5 minutes following leptin treatment with the response peaking at 30 minutes and signs of reversal within 60 minutes (Fig. 1.6.)(57,58). The transient nature of the response is likely to be physiologically significant and may serve to prevent prolonged inhibition of insulin secretion. The increase in K_{ATP} channel surface density was primarily due to insertion of K_{ATP} channels into the β-cell membrane and to a lesser extent reduced K_{ATP} endocytosis. Based on the time frame in which K_{ATP} channel surface density increases, it is likely that the channels reside in a readily available vesicle reserve rather than increased K_{ATP} channel biogenesis. Consistent with this there was no apparent change in total K_{ATP} channel protein content over the course of leptin treatment. Of note, the increase of surface K_{ATP} channels within 5 minutes coincides with leptin-induced K_{ATP} channel conductance and hyperpolarization(39,52,65). By analyzing K_{ATP} channel currents it is estimated that ~800 channels are inserted into the β-cell membrane in response to leptin and that the total number of K_{ATP} channels in the membrane increases from ~400 to ~1200, which is in agreement with the 3- to 4-fold increase observed using surface biotinylation(57,58). Importantly, blocking the ability of leptin to increase K_{ATP} channel surface density by blocking downstream signaling events (see section 1.6. below) also prevented cell hyperpolarization, confirming K_{ATP} channel surface density regulation as a mechanism for modulating β-cell excitability.

Although the majority of the mechanistic studies have been conducted using INS-1 832/13 cells there is substantial evidence that this mechanism is conserved in rodent and human β-cells. Park et al. confirmed the effects of leptin on K_{ATP} channels in isolated mouse β-cells via immunostaining and whole-cell currents(57). Our group has demonstrated that isolated human β-cells also hyperpolarize in response to leptin and as will be discussed in the following sections, inhibiting leptin signaling molecules necessary for K_{ATP} channel trafficking blocks human β-cell hyperpolarization(65). Collectively, the above findings provided the foundation for establishing K_{ATP} channel trafficking as a physiologically relevant mechanism by which leptin inhibits insulin secretion.

Notably, our lab has shown that leptin also increases surface density of the voltage-gated delayed rectifier channel Kv2.1 but not several other ion channels including G-protein coupled Kir channels (GIRK), sodium and calcium currents(65). Remarkably, trafficking of Kv2.1 and K_{ATP} channels in response to leptin occurs through a common mechanism. As Kv2.1 channels are the dominant delayed inward rectifier and have a prominent role in the repolarization of action potentials in β-cells, at least in mice(66), the concerted regulation of K_{ATP} and Kv2.1 channels by leptin would synergistically reduce β-cell excitability at elevated glucose concentrations to suppress insulin secretion. However, K_{ATP} channels will be the primary focus of this thesis.

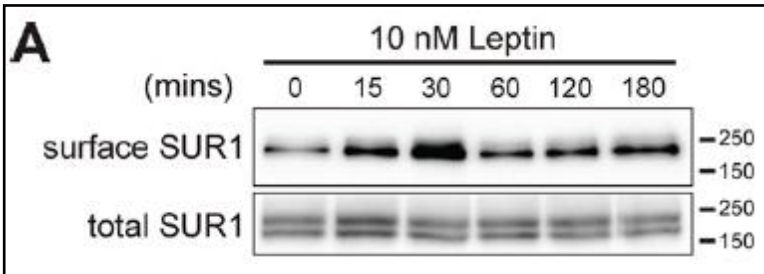

Figure 1. 6. Leptin increases K_{ATP} channel surface density.
(A) INS-1 832/13 cells treated with leptin over a time course. Surface biotinylation experiments followed by western blot analysis of surface and total cell lysate for the SUR1 subunit of K_{ATP} channels.

Image is from Chen P-C. et al., J. Biol. Chem., 2013. DOI: 10.1074/jbc.M113.516880

1.6. K_{ATP} channel trafficking signaling molecules

Since the initial reports that leptin regulates K_{ATP} channel trafficking, there has been significant progress towards delineating the signaling cascade underlying this regulation. A model based on published studies is shown in Figure 1.7. In this model, activation of leptin receptors by leptin leads to an influx of Ca^{2+} that stimulates Ca^{2+}/calmodulin-dependent kinase kinase β (CaMKKβ) to phosphorylate and activate 5'AMP-activated protein kinase (AMPK). Downstream of AMPK actin remodeling occurs to allow trafficking of vesicles containing K_{ATP} channels to the β-cell surface. The following sections will evaluate the role of the signaling molecules that have been implicated in leptin mediated K_{ATP} channel trafficking.

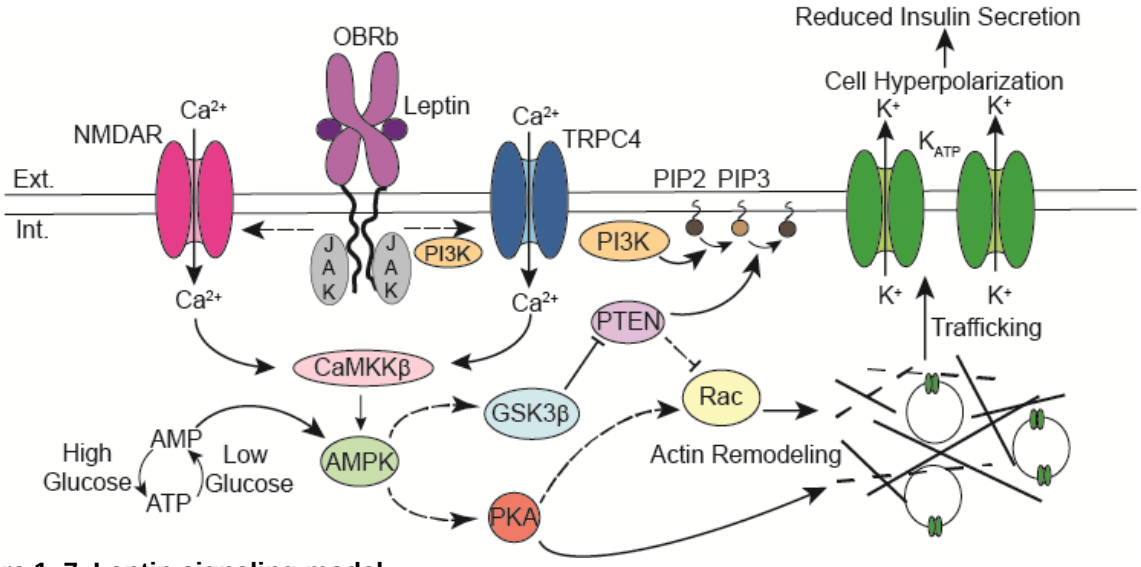

Figure 1. 7. Leptin signaling model.
Leptin binding to its receptor (OBRb) leads to a calcium influx through Ca^{2+}-permeant ion channels. The rise in intracellular Ca^{2+} activates CaMKKβ, which then phosphorylates and activates AMPK. Downstream of AMPK actin remodeling is triggered. Depolymerization of the cortical actin cytoskeleton allows vesicles containing K_{ATP} channels to traffic to the membrane. The increased abundance of K_{ATP} channels reduces β-cell excitability thereby suppressing insulin secretion. Abbreviations: Extracellular (Ext.), Intracellular (Int.), N-methyl-D-Aspartate Receptor (NMDAR), Janus Kinase (JAK), Ca^{2+}/calmodulin kinase kinase β (CaMKKβ), AMP-dependent protein kinase (AMPK), Leptin receptor (OBRb), phosphoinositide 3-kinase (PI3K), phosphatidylinositol (4,5)-bisphosphate (PIP2), phosphatidylinositol (3,4,5)-trisphosphate (PIP3), phosphatase and tensin homolog (PTEN), Glycogen synthase kinase 3 β (GSK3β), cAMP-dependent protein kinase A (PKA), Transient receptor potential channel 4 (TRPC4), Potassium (K^+).
Image is from Cochrane V. & Shyng S-L. Int. J. Mol. Sci. 2019; 20(11):2660. CC BY 4.0.
DOI: 10.3390/ijms20112660

1.6.1. AMPK

AMPK is known for its role as a master regulator of cellular energy and glucose homeostasis(67). This is due to AMPK being activated by AMP/ADP and inhibited by ATP. AMP/ADP binding to the AMPK γ-subunit induces a conformational change that promotes phosphorylation of Thr172 in the activation loop of the AMPK α-subunit by upstream kinases, while also preventing dephosphorylation of Thr172 by phosphatases. Additionally, AMP, but not ADP, allosterically activates AMPK. Activation of AMPK in response to a rise in the AMP/ADP:ATP ratio promotes catabolic processes to increase ATP concentrations and inhibits anabolic processes. A role of AMPK in K_{ATP} channel trafficking was first documented by Lim et al. who showed that under low glucose culturing conditions (0-3 mM), K_{ATP} channels translocate to the β-cell membrane in an AMPK-dependent manner to reduce insulin secretion(68). This study uncovered a physiological mechanism by which β-cells adapt to glucose starvation. Interestingly, a subsequent study showed that β-cells lacking AMPKα2 or expressing a kinase-dead AMPKα2 failed to hyperpolarize under low glucose conditions(69). Although K_{ATP} channel trafficking was not examined, dysregulation of K_{ATP} trafficking likely contributed to the observed β-cell dysfunction.

In addition to responding to changes in intracellular energy levels AMPK activity is modulated by various hormones including leptin. The effect of leptin on AMPK activity is cell-type specific. For example, in skeletal muscle leptin stimulates AMPK(70), whereas it inhibits AMPK in parts of the hypothalamus(71). In the case of INS-1 832/13 and mouse β-cells, leptin treatment was found to cause a marked increase in phosphorylation of the AMPK catalytic α subunit at Threonine 172 (pAMPKα) and its substrate Acetyl CoA carboxylase (pACC) indicative of increased AMPK activity(57,58). The increase in pAMPKα was transient and peaked at 30 minutes similar to the changes observed in surface K_{ATP} channel density. To test whether AMPK is involved in leptin-induced K_{ATP} channel trafficking both pharmacological and genetic

approaches were employed. While inhibition of AMPK occluded the effects of leptin, AMPK activation mimicked the effects of leptin on K_{ATP} channel translocation(57,58). These findings provide strong evidence that leptin activates AMPK to recruit K_{ATP} channels to the β-cell surface.

1.6.2. CaMKKβ

AMPK activity is also regulated by liver kinase B1 (LKB1) and CaMKKβ(67). LKB1 is the primary kinase that phosphorylates Thr172 on the α-subunit when AMPK is bound to AMP/ADP. In doing so, LKB1 can enhance AMPK activity up to 100-fold. Alternatively, AMPK may be activated independent of AMP/ADP via a rise of cytoplasmic Ca^{2+} that binds and activates the Ca^{2+}/CaM kinase CaMKKβ, which then phosphorylates AMPKα residue Thr172. While at low glucose concentrations AMPK may be activated in an AMP/ADP-dependent fashion(68), this is unlikely to be how leptin activates AMPK to promote K_{ATP} channel trafficking at higher glucose conditions.

Both LKB1 and CaMKKβ were investigated as potential AMPK activators in leptin signaling. Inhibition of CaMKKβ by pharmacological inhibitors or genetic knockdown completely ablated leptin activation of AMPK. In contrast, genetic knockdown of LKB1 had no effect(57,65). Furthermore, increased K_{ATP} channel surface density in response to leptin was also dependent on CaMKKβ activity. From these studies it was concluded that leptin signals via CaMKKβ to activate AMPK. Interestingly, CaMKKβ had previously been identified as a regulator of insulin secretion due to islets from CaMKKβ knockout mice showing increased insulin secretion(72). It is plausible that disrupted K_{ATP} channel trafficking may be a contributing factor to the observed phenotype in CaMKKβ knockout islets.

1.6.3. Ca^{2+}

Taking into consideration that CaMKKβ activation is dependent on Ca^{2+} it follows that leptin must somehow elevate intracellular calcium levels. Consistently, Ca^{2+}-chelating agents

such as BAPTA-AM and EGTA completely blocked leptin activation of AMPK and leptin-induced increase of K_{ATP} surface expression(57,65). In the next sections, potential Ca^{2+} sources for leptin signaling will be discussed.

1.6.3.1. TRPC4 channels

To identify where Ca^{2+} is coming from Park et al. used pharmacological inhibitors and ruled out voltage-gated Ca^{2+} channels or the ER Ca^{2+} store as the source(57). They focused on transient receptor potential channels (TRPC) instead based on attenuation of the leptin effect by the drug 2-aminoethyldiphenyl borate (2-APB). Here, it is worth noting that although 2-APB does block TRPC channels, it also blocks a number of other channels including inositol 1,4,5-triphosphate receptors (IP_3Rs) and store-operated Ca^{2+} channels(73,74). Nevertheless, they went on to show that knocking down TRPC4, but not TRPC5, by siRNA or inhibition of TRPC4 by ML-204 abrogated the effect of leptin. Moreover, they concluded that leptin activates TRPC4 channels by activating PI3-kinase because LY294002, a PI3K inhibitor, abolished leptin-induced increase of TRPC4 conductance. Of note, an earlier study also implicated a role of PI3K in leptin regulation of K_{ATP} channel activity, again using PI3K inhibitors(55). However, it is important to keep in mind that it is now known that LY294002 also directly inhibits some potassium channels(75), thus results should be interpreted with caution.

Although TRPC4 channels were identified as the Ca^{2+} source for leptin by Park et al.(57), our lab was unable to block the leptin effect using the TRPC4 inhibitor ML-204 (see chapter 3) The reason for this discrepancy remains unclear but may depend on experimental conditions. Below, N-Methyl-D-Aspartate (NMDA) receptors are discussed as a potential alternative Ca^{2+} source for leptin signaling.

1.6.3.2 NMDA Receptors

NMDA receptors (NMDARs) are ionotropic glutamate receptors that are permeant to monovalent cations and Ca^{2+} (76). They are activated by co-agonists glutamate and glycine and

require membrane depolarization to remove external Mg^{2+} block for conduction. Upon activation, NMDARs allow an influx of Ca^{2+} into cells and trigger various Ca^{2+}-dependent signaling cascades. NMDARs are highly expressed throughout the central nervous system where they play important roles in synaptic plasticity. Interestingly, a prior study had linked leptin to enhanced NMDAR activity for long-term potentiation in hippocampal neurons(77). Although NMDARs have been primarily studied in the brain there is increasing evidence that they have important function in pancreatic β-cells(78–81). A recent study showed that NMDAR antagonism increased GSIS both in vivo and in vitro; moreover, this effect was dependent on the expression of functional K_{ATP} channels in islets(82). In chapter 3, a role for NMDARs in recruitment of K_{ATP} channels in β-cells is investigated.

In addition to being activated by their co-agonists glutamate and glycine, NMDAR activity can be modulated via phosphorylation. NMDARs are heterotetramers composed of two obligatory glycine binding GluN1 subunits and two glutamate binding GluN2 subunits (GluN2A-D). The GluN2A and GluN2B subunits have long cytoplasmic tails that can be phosphorylated by serine/threonine or tyrosine kinases to alter NMDAR trafficking and gating(83). For example, Src and Fyn kinases are tyrosine kinases belonging to the Src family kinases (SFKs) that have been shown to enhance NMDAR activity by phosphorylating tyrosine residues on GluN2A(84) and GluN2B(85), respectively. Interestingly, Src kinase has also been implicated as an effector of leptin(77,86,87). In chapter 4, Src kinase is investigated as a link between leptin and NMDARs in K_{ATP} channel trafficking.

1.6.4 Actin remodeling molecules

Although early studies presumed that leptin-induced actin depolymerization activated K_{ATP} channels already present in the β-cell membrane(59), more recent studies have concluded that actin remodeling allows trafficking of vesicles containing K_{ATP} channels to the cell surface(58). Cortical actin is predicted to serve as a barrier for vesicle exocytosis and as such

actin remodeling typically occurs prior to exocytotic events(88–91). It has been shown that actin remodeling downstream of AMPK in the leptin signaling cascade is a necessary step for K_{ATP} channel trafficking to the membrane(58). AMPK has previously been shown to be involved in actin depolymerization in other cell types but how it does so in β-cells is still unresolved. The following sections will discuss potential signaling molecules that may act downstream of AMPK.

1.6.4.1. PTEN

Soon after leptin was found to recruit K_{ATP} channels to the β-cell surface the role of PTEN, which was previously implicated in mediating the effect of leptin on K_{ATP} conductance(54,59), was re-examined. In agreement with early studies, inhibition of both PTEN's lipid and protein phosphatase activities are required for actin remodeling and leptin-induced K_{ATP} channel trafficking(92,93). Leptin inhibition of PTEN was determined to be dependent on AMPK and glycogen synthase kinase 3 β (GSK3β)(92). Blocking AMPK activity prevents both activation of GSK3β and inhibition of PTEN in response to leptin, whereas GSK3β inhibitors prevent PTEN inhibition without affecting AMPK activation. These studies indicate that GSK3β lies downstream of AMPK; however, the relationship between the two is unclear since GSK3β activation requires phosphorylation of Tyr216 but AMPK is a Ser/Thr kinase(92).

In an effort to elucidate how PTEN inactivation following leptin stimulation leads to actin remodeling, Rac was examined(93). Rac is a Rho family small GTPase molecular switch that is known to regulate actin dynamics for vesicle transport(94). These studies showed that leptin stimulation increased Rac activity and that Rac activity was necessary for the recruitment K_{ATP} channels to the β-cell surface(93). As PIP_3 has been reported to enhance Rac activity by recruiting guanine nucleotide exchange factors (GEFs)(95–97), PIP_3 elevation following PTEN inactivation could be an underlying mechanism of actin depolymerization. Following Rac activation there was evidence for increased activation of Myosin II(93), which has also been implicated in actin disassembly and vesicular trafficking(98). Thus, these studies proposed that

leptin signaling inhibits PTEN to activate Rac and Myosin II, leading to actin depolymerization and trafficking of K_{ATP} channels(93).

Although the above studies provide a framework for understanding how PTEN participates in the leptin signaling pathway to regulate K_{ATP} channel trafficking, many details are still missing. In addition, studies involving actin and actin regulatory proteins are not always straightforward. Many of these proteins are also modulated by AMPK or PKA (see section 1.6.4.2.) directly or indirectly and global cellular manipulation of these molecules can have unintended consequences that confound data interpretation. Moving forward it will be important to design more sophisticated methods and molecular tools to evaluate actin remodeling events specific to K_{ATP} channel trafficking regulation by leptin.

1.6.4.2. PKA

PKA is a Ser/Thr kinase that is activated by cAMP binding its regulatory subunits causing the active catalytic subunits to be released. PKA is known to modulate the activity of many molecules involved in actin dynamics, including Rac mentioned above, and has been shown to regulate the trafficking of a number of ion channels(99–101). Studies by our lab found that PKA is involved in actin remodeling downstream of AMPK(58). Activation of PKA directly by cAMP elevating agents mimics the effects of leptin and an AMPK activator, while pharmacological inhibition of PKA blunts leptin- and AMPK-induced actin depolymerization and K_{ATP} channel trafficking. These findings raise the possibility that AMPK may activate PKA to cause actin depolymerization necessary for channel trafficking. Interestingly, crosstalk between AMPK and PKA has been reported in smooth muscle cells and cardiomyocytes where activation of AMPK coincides with increased PKA activity(102,103). However, in the absence of a mechanism by which AMPK activates PKA, a permissive role of PKA in allowing leptin-induced actin remodeling rather than being part of the signaling cascade cannot be ruled out. In chapter 5, the role of PKA for leptin-mediated K_{ATP} channel translocation is investigated.

1.7. β-cell signaling microdomains

Many of the molecules discussed in the previous sections also have roles as positive regulators of GSIS, which begs the question of how β-cells appropriately process signals. The importance of β-cell subcellular organization in regulating insulin secretion is becoming increasingly apparent. For example, one study found that glucose sensing and insulin secretory machinery co-localize creating a signaling microdomain that efficiently couples glucose uptake to insulin secretion(104). Identifying additional signaling microdomains may elucidate how β-cells coordinate numerous complex signaling pathways that mediate insulin secretion—many of which share common signaling molecules. Below, evidence is provided of signaling microdomains in β-cells with a specific focus on molecules involved in both K_{ATP} channel trafficking and GSIS.

1.7.1. Ca^{2+}

Ca^{2+} microdomains are essential to insulin secretion. A subplasma membrane Ca^{2+} microdomain forms at sites where voltage-gated L-type Ca^{2+} channels co-localize with insulin granules and exocytic machinery. Ca^{2+} influx via L-type channels combined with cytosolic Ca^{2+} buffers creates a localized region of high Ca^{2+} concentrations (μM) that is sufficient to activate exocytic factors and increase insulin exocytosis(105). Another Ca^{2+} microdomain forms at endoplasmic reticulum (ER)-mitochondria contact sites where ER IP_3Rs release Ca^{2+} that is taken up by the tethered mitochondria to regulate cell bioenergetics(106,107). Ca^{2+} exchange between the ER and mitochondria is stimulated by high glucose concentrations and promotes mitochondrial ATP synthesis and insulin secretion(108). Both of these examples highlight the role of localized Ca^{2+} signaling in GSIS. However, Ca^{2+} is critical for many additional β-cell processes suggesting that there are Ca^{2+} microdomains in β-cells that have yet to be identified.

1.7.2. PKA

The cAMP effector PKA is involved in several processes pertaining to insulin secretion. This is not surprising since cAMP is intimately linked to GSIS and many cAMP elevating agents, including glucagon and glucagon-like peptide 1 (GLP-1), potentiate insulin secretion. A rise of cAMP levels in response to GLP-1 increases L-type Ca^{2+} channel activity via PKA, resulting in enhanced Ca^{2+} influx and augmented GSIS(109). The increase in L-type Ca^{2+} channel activity is likely due to PKA phosphorylation of the channel, as has been shown in neurons(110). Moreover, glucagon and GLP-1 activation of cAMP-PKA signaling potentiates IP_3R activity allowing an efflux of Ca^{2+} from the ER into the cytosol that promotes insulin granule trafficking and exocytosis(109,111). Originally, all of cAMP's actions were attributed to PKA because it was the only known cAMP effector at the time. However, once the exchange factor directly activated by cAMP (EPAC)(112) family of cAMP effectors was discovered it became evident that cAMP signals via PKA for some processes and EPAC for others. For example, cAMP-EPAC signaling enhances the secretion of insulin granules from a readily releasable pool, whereas PKA replenishes this pool(109,113,114). It has been proposed that cAMP signaling is regulated through the formation of cAMP microdomains (113) and there is strong evidence of this in the case of cAMP-PKA signaling (see below).

1.7.3. AKAP

A-kinase anchoring proteins (AKAPs) are a family of scaffolding proteins that are distinguished by their ability to anchor PKA(115). AKAPs are targeted to subcellular locations and anchor cAMP producing proteins, cAMP degrading proteins, and PKA effectors in addition to PKA. Thus, AKAPs form signaling complexes that allow cAMP-PKA signaling to be highly spatiotemporally regulated. In some contexts, disrupting the interaction between PKA and AKAPs hinders insulin secretion from β-cells(116,117). Several attempts aimed at identifying the AKAP-PKA complexes involved in regulating insulin secretion have since been made. AKAP18α

is a membrane-targeted AKAP that has been shown to enhance GLP-1 potentiation of insulin secretion when it is overexpressed(118). Consistent with this, another study found AKAP18α expression is upregulated by high glucose concentrations and that silencing AKAP18α using siRNA decreases GSIS(119). Interestingly, the same study showed that the opposite was true for AKAP18γ; glucose decreases AKAP18γ expression and siRNA knockdown of AKAP18γ increases GSIS(119). From these findings it has been proposed that AKAP18α and AKAP18γ have opposing actions on insulin secretion(119). AKAP79/150 (human/rodent proteins; *AKAP5* gene) has also been investigated as a potential regulator of insulin secretion. Using genetic techniques, a mouse strain was created that lacked expression of AKAP150 (AKAP150 KO) in β-cells(120). Islets from these mice have significantly diminished GSIS compared to controls. Further investigation showed that AKAP150 KO islets have reduced Ca^{2+} currents and glucose-induced Ca^{2+} influx, which may underlie the low level of insulin secreted by these islets. Taken together, these studies have identified several AKAPs that may be involved in insulin secretion, but the precise mechanisms by which they do so are poorly understood.

Chapter 5 of this thesis will focus on determining whether leptin signaling is spatially localized within β-cells with the goal of reconciling the dual functions of several molecules in promoting insulin secretion and K_{ATP} channel translocation.

1.8. Thesis overview

The purpose of this thesis is to further elucidate the signaling mechanism underlying leptin-mediated K_{ATP} channel trafficking in β-cells and how it may be disrupted during the pathology of T2D. At the start of this thesis leptin had been shown to activate AMPK via CaMKKβ, which is followed by PKA-dependent actin remodeling and subsequent K_{ATP} channel trafficking. However, the Ca^{2+} source for leptin activation of CaMKKβ and the relationship between leptin and PKA remained elusive (Fig. 1.8.). The following studies use a combination of biochemical, electrophysiological, immunocytochemistry, and live cell imaging techniques to investigate NMDA receptors as a Ca^{2+} source for leptin signaling, the ability of leptin to activate Src kinase to potentiate NMDAR activity, the role of PKA for leptin signaling, and mediation of leptin signaling by a PKA-AKAP signaling complex.

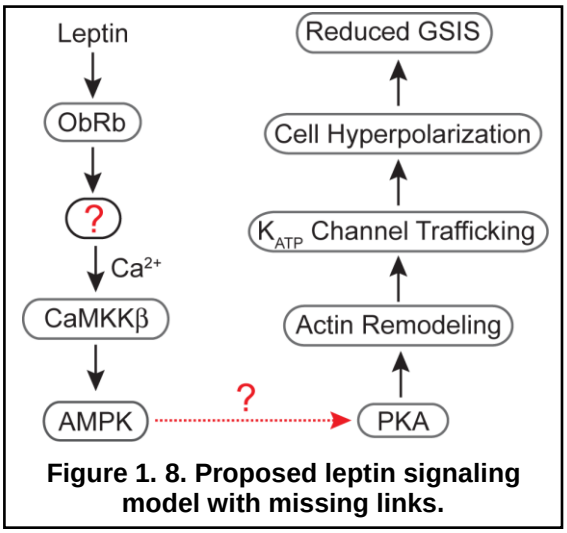

Figure 1. 8. Proposed leptin signaling model with missing links.

In Chapter 3, NMDARs are examined as a potential Ca^{2+} source for leptin signaling. Biochemical and electrophysiology experiments in INS-1 832/13 cells demonstrate that leptin activation of AMPK and downstream K_{ATP} channel trafficking requires NMDARs. Consistent with NMDARs being a Ca^{2+} source, Ca^{2+} imaging experiments show that direct activation of NMDARs increases intracellular Ca^{2+} levels and that NMDAR inhibitors block leptin-induced Ca^{2+} influx. Moreover, through monitoring NMDAR currents it is revealed that leptin stimulation enhances NMDAR activity. Finally, by repeating key experiments in dissociated human islets, the role of NMDARs for leptin signaling is found to be conserved. Collectively, these experiments show that leptin potentiates NMDAR activity in β-cells to allow a Ca^{2+} influx that initiates downstream signaling events for K_{ATP} channel trafficking.

In chapter 4, follow-up studies investigate how leptin potentiates NMDAR activity. A combination of electrophysiological and biochemical experiments in INS-1 832/13 cells determine that NMDARs involved in leptin signaling are composed of GluN2A subunits in addition to the obligatory GluN1 subunit. Leptin-induced K_{ATP} channel trafficking and potentiation of NMDAR currents was blocked by overexpression of a kinase-dead Src mutant or pharmacological inhibition of Src kinase, which had previously been found to enhance NMDAR activity by phosphorylating GluN2A tyrosine residues. Furthermore, mutating GluN2A tyrosine residues known to be phosphorylated by Src kinase to phenyalanine also prohibited the effects of leptin. Another significant finding from this work is that directly activating NMDARs could restore leptin signaling in leptin-resistant β-cells from *db/db* mice and obese T2D human donors. Overall, these studies uncover a role for Src kinase in mediating leptin potentiation of NMDARs in β-cells and that targeting NMDARs may overcome leptin resistance.

In chapter 5, whether PKA plays an active or permissive role for leptin signaling is investigated. Here, a fluorescence resonance energy transfer (FRET)-based PKA activity reporter is utilized to demonstrate that leptin does indeed increase PKA activity and that this occurs via our previously identified NMDAR-CaMKKβ-AMPK signaling cascade. Additional experiments show that a PKA-AKAP interaction is necessary for leptin to increase K_{ATP} channel trafficking and that this is conserved in human β-cells. Through a series of genetic knockdown and rescue experiments AKAP79/150 is determined to anchor PKA for leptin signaling. Importantly, overexpression of an AKAP79/150 mutant that cannot bind protein phosphatase 2B (PP2B), which has been shown to increase basal AKAP79/150-anchored PKA activity(110), promotes K_{ATP} channel trafficking even in the absence of leptin. This work identifies a novel mechanism by which leptin increases AKAP79/150-anchored PKA activity for K_{ATP} channel translocation in β-cells.

These studies have significantly advanced our understanding of the leptin signaling mechanism underlying K_{ATP} channel trafficking in β-cells. Specifically, this work shows that leptin activates Src kinase to potentiate NMDARs and enhance a Ca^{2+} influx that activates CaMKKβ, which phosphorylates and activates AMPK; AMPK then increases AKAP79/150-anchored PKA activity resulting in actin remodeling and increased K_{ATP} channel trafficking. Of note, the findings presented in this thesis provide evidence that leptin signaling is disrupted at the β-cell level during the pathology of T2D and that this may be overcome by directly targeting leptin signaling molecules. In conclusion, this work has uncovered a novel mechanism by which leptin promotes K_{ATP} channel trafficking in pancreatic β-cells that may be targeted to restore the effects of leptin in leptin-resistant β-cells.

Chapter 2: Methods Background

This chapter covers background information on the methods used in the following research chapters. A detailed description of the experimental methods can be found in the 'materials and methods' sections provided in each chapter.

2.1. INS-1 832/13 cells

Fully functional pancreatic islets isolated from humans and mice are not always readily available and even when they are their responses to glucose and other stimuli begin to decline within hours of isolation(64). Therefore, cell lines that can be easily maintained in the lab and behave physiologically similar to β-cells are instrumental for defining the mechanisms that govern insulin secretion. To generate the β-cell-like INS-1 cell line a radiation-induced insulinoma tumor from NEDH rats was dispersed into tissue culture(121). Although low passage numbers of the INS-1 cell line robustly secrete insulin in response to glucose, the magnitude of the response is notably less than that from freshly isolated rat islets in older INS-1 passages. This may be explained by INS-1 cells being a polyclonal cell line that becomes enriched with glucose-nonresponsive cells over several passages. In order to create cell lines with sustained glucose responsiveness INS-1 cells were stably transfected with the human proinsulin gene(64). This generated several INS-1 clones that produced greater amounts of insulin, but only 16% of these clones showed robust insulin secretion in response to glucose. Among these strong responders was clone 832/13 (referred to herein as INS-1 832/13)(64). INS-1 832/13 cells have sustained responsiveness to glucose for more than 66 passages with a half maximal stimulation at 6 mM glucose. Further characterization of INS-1 832/13 showed that known potentiators of GSIS [isobutyl-methylxanthine (IBMX), oleate palmitate, GLP-1, and the sulfonylurea tolbutamide] augment insulin secretion at 15 mM glucose(64). Moreover, GSIS from INS-1 832/13 cells is completely blocked by the K_{ATP} channel opener diazoxide consistent with K_{ATP}

channels being critical for the glucose response(64). Lastly, at depolarizing K^+ (35 mM) concentrations, glucose stimulates additional insulin secretion indicating that INS-1 832/13 cells maintain K_{ATP}-independent insulin secretion pathways similar to isolated islets(64). Collectively, these findings indicate that the INS-1 832/13 cell line is an improved model for studying processes that regulate insulin secretion from β-cells.

2.2. Electrophysiology

Electrophysiology allows us to study the electrical properties of cells. Some of the first electrophysiology experiments involved inserting a fine capillary electrode into squid giant axons to record the potential differences across the membrane(122). This method was suitable for large cells, like the squid giant axon, but not for smaller cells such as β-cells. Later, when the patch-clamp technique was developed(123), it became possible to perform electrophysiology on smaller cells. For patch-clamp recordings, a glass micropipette with a relatively large diameter is filled with an ionic solution and a recording electrode; the micropipette is then attached to a cell membrane by applying light suction to form a gigaseal. Applying the patch-clamp technique to β-cells revealed that electrical activity underlies insulin secretion. For example, electrophysiology experiments led to the discovery that K_{ATP} channels are expressed on β-cells and that glucose stimulation causes K_{ATP} channels to close, depolarizing the β-cell and initiating electrical activity to promote insulin secretion(60). Patch-clamp can be performed in various configurations depending on the research question. In cell-attached patch-clamp, recordings are made from a patch of the cell membrane and the membrane of the cell is left intact, whereas in the whole-cell configuration, the cell membrane is disrupted resulting in the micropipette ionic solution being continuous with the cytoplasm and recordings being made from the entire cell (Figure 2.1.). The advantage of cell-attached recordings is that the composition of the cytoplasm is not altered by the ionic solution of the pipette. However, the whole-cell configuration can be beneficial for introducing cell-impermeable reagents into the cell, or if it is necessary to record

electrical potentials and currents from the entire cell. Additionally, cell-attached and whole-cell recordings can be made in voltage-clamp or current-clamp mode to record ionic currents across the membrane or the membrane potential, respectively. The following research chapters use a combination of these strategies to answer questions pertaining to β-cell electrical activity.

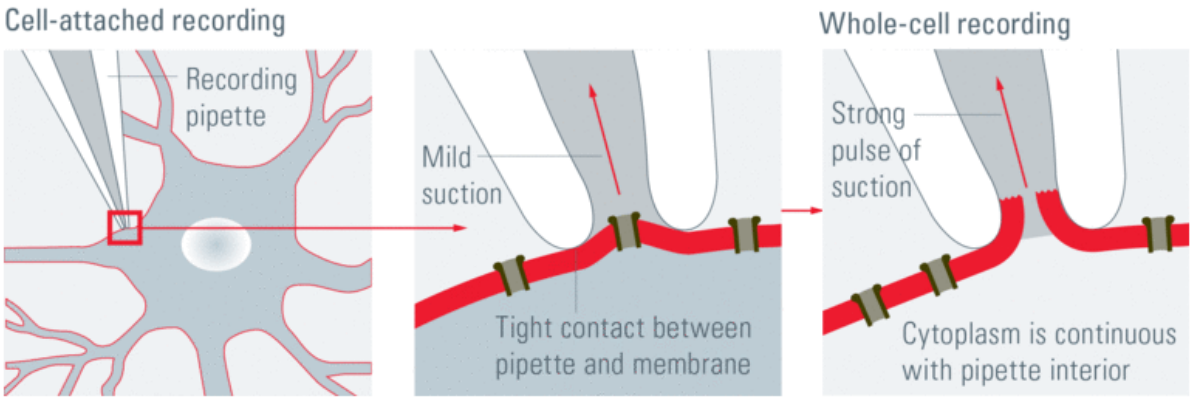

Figure 2. 1. Patch-clamp configurations.

For the cell-attached configuration, the micropipette is brought into close proximity to the cell and then suction is applied to attach the micropipette to the cell. Applying another brief suction will rupture the cell membrane to create the whole-cell configuration.

Image has been modified from Patch me if you can – What is the patch-Clamp Technique?, puzzledponderer.wordpress.com

2.3. Surface biotinylation

Surface biotinylation is an excellent method for isolating and quantifying proteins expressed at the cell membrane. Throughout this thesis, surface biotinylation followed by western blot analysis is used to monitor the surface expression of K_{ATP} channels. To do so, cells are incubated with EZ-Link™ Sulfo-NHS-biotin (sulfosuccinimidobiotin) (Thermo Scientific™) to label surface proteins. Sulfo-NHS-biotin is cell impermeable and reacts with primary amines ($-NH_2$) such as the side chain of lysines and the amino-termini of polypeptides. Following biotin labeling of surface proteins the cells are lysed and biotin-labeled proteins are isolated by immunoprecipitation with the high affinity biotin-binding NeutrAvidin protein covalently immobilized onto beaded agarose. The biotinylated proteins are then eluted using sample buffer that contains dithiothreitol (DTT) and analyzed by western blot. Immunoblotting for K_{ATP} channel

subunits is used to determine if there are changes in surface K_{ATP} channel expression. β-cell K_{ATP} channels are tetramers composed of four Kir6.2 subunits that form the potassium conducting pore and four surrounding regulatory sulfonylurea receptor SUR1 subunits. Each SUR1 subunit contains two lysine residues exposed to the extracellular culture medium that can be biotinylated by Sulfo-NHS-biotin. For this reason, surface biotinylation eluents are typically analyzed for K_{ATP} channels by immunoblotting for the SUR1 subunits, although it is possible to detect Kir6.2 as Kir6.2 remains associated with SUR1 in the buffer used to lyse the cells. It should be noted that the co-assembly of Kir6.2 subunits with SUR1 subunits is necessary for K_{ATP} channels to exit the ER; therefore, probing for only SUR1 should be sufficient for monitoring surface K_{ATP} channels.

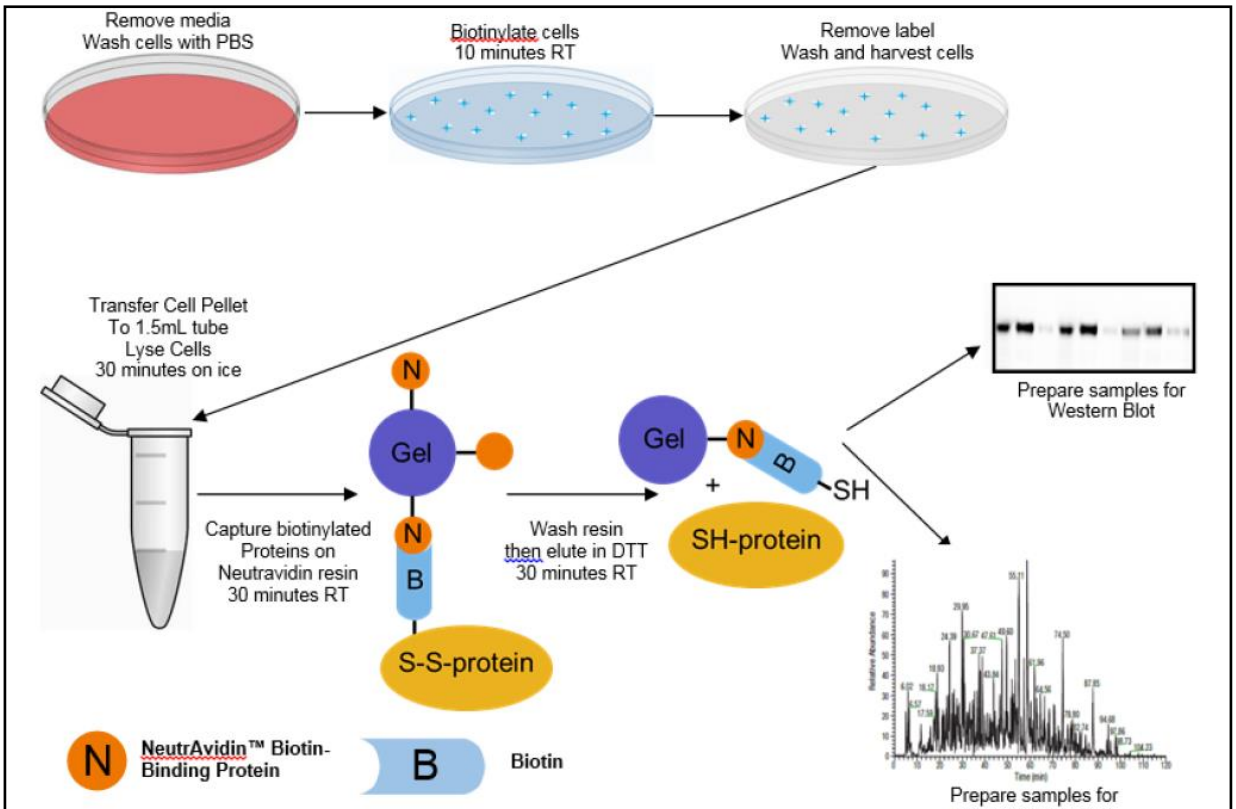

Figure 2. 2. Surface biotinylation work-flow.
Cell surface proteins are biotinylated with Sulfo-NHS-biotin and then washed to remove excess Sufo-NHS-biotin. Next, cells are lysed and biotinylated proteins are captured on NeutrAvidin agarose. The biotinylated proteins are eluted in a buffer containing DTT. Samples can then be analyzed by western blot or mass spectrometry.

Image is from the Pierce™ Cell Surface Biotinylation and Isolation Kit Manual.

2.4. K_{ATP} channel surface staining

Another strategy developed by the lab to monitor surface K_{ATP} channels is surface staining. In order to visualize K_{ATP} channels at the cell surface an α-bungarotoxin (BTX) binding peptide tag (WRYYESSLEPYPD) was placed at the N-terminus of SUR1 (referred to as BTX-SUR1). Infecting INS-1 832/13 cells with adenoviruses containing BTX-SUR1 and Kir6.2 results in the expression of exogenous K_{ATP} channels containing BTX-SUR1 subunits. The BTX tag on SUR1 is extracellular and can be labeled by incubating Infected INS-832/13 cells with culture medium containing α-bungarotoxin. The α-bungarotoxin used for labeling K_{ATP} channels can be conjugated with biotin for surface biotinylation experiments or with fluorescent dyes, such as Alexa Fluor 555, for confocal microscopy imaging. Surface biotinylation experiments using biotin-conjugated α-bungarotoxin demonstrate that the exogenous BTX-tagged K_{ATP} channels respond similar to endogenous K_{ATP} channels when INS-1 832/13 cells are stimulated with leptin.

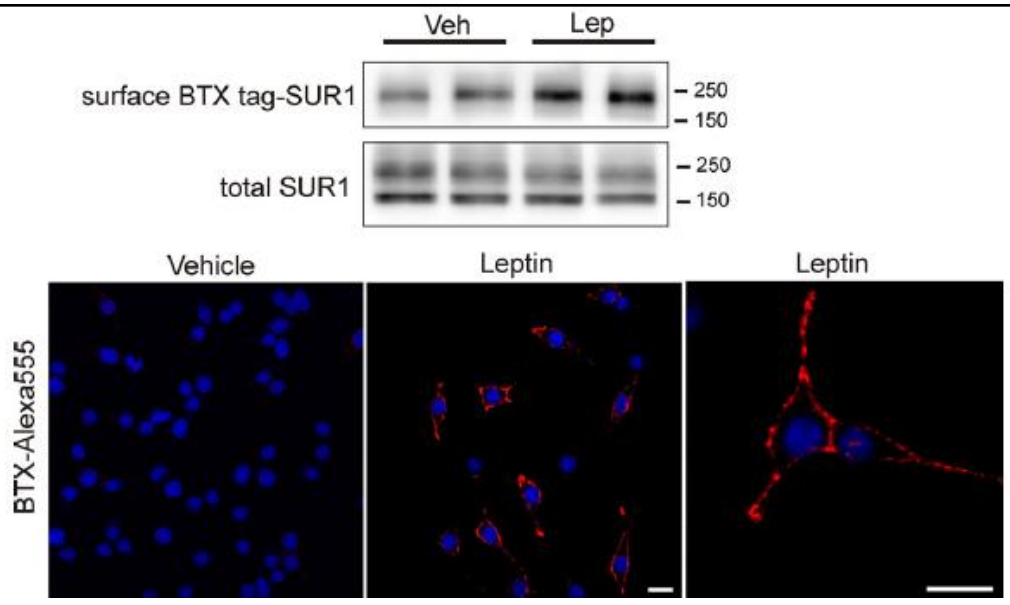

Figure 2. 3. BTX-tagged K_{ATP} channels.

INS-1 832/13 cells were transduced with adenoviruses containing BTX-tagged SUR1 and Kir6.2. Cells were then treated with vehicle (Veh) or leptin (Lep, 10nM) for 30 minutes and labeled with biotin-conjugated BTX and analyzed by western blot (top), or with Alexa 555-conjugated BTX (red) and imaged by confocal microscopy (bottom). Nuclei were stained with DAPI (blue). *Scale bar 10μm*.

Image is from Chen P-C. et al., J. Biol. Chem., 2013. DOI: 10.1074/jbc.M113.516880

2.5. Live cell imaging

Advancing our understanding of cell signal transduction pathways requires tools that are capable of recording dynamic processes in cells. For example, in cell-attached patch-clamp recordings hyperpolarization is commonly observed following ~6 minutes of leptin stimulation indicating that leptin signaling events for K_{ATP} channel trafficking occur on a timescale of seconds to minutes. While electrophysiology techniques are very sensitive to cellular changes and produce results in real-time, they are limited to detecting electrical events. On the other hand, biochemical approaches can be very time-consuming and labor intensive, and they are not always sensitive enough to detect rapid signaling events. To overcome the limitations of these approaches, live cell imaging has been implemented to study leptin signaling. By introducing fluorescent sensors into cells that can detect changes in leptin signaling molecules it is possible to dissect leptin signaling in intact living cells in real-time using fluorescent microscopy. The next sections will describe the fluorescent sensors used in this thesis.

2.5.1. Fluo4-AM

The finding that leptin activates AMPK in a CaMKKβ-dependent manner suggests that leptin induces a Ca^{2+} influx to activate CaMKKβ. To monitor Ca^{2+} levels in response to leptin, the Ca^{2+} sensor Fluo-4 is utilized (see Chapter 3). Fluo-4 is a single-wavelength green-fluorescent Ca^{2+} indicator(124). Modification of Fluo-4 with a cell-permeable acetoxylmethyl ester (Fluo-4AM) allows the sensor to be easily loaded into cells. Once inside the cell the AM ester is cleaved to give free, fluorescent Fluo-4. Upon binding Ca^{2+} ions Fluo-4 exhibits increased fluorescence; thus, increased Fluo-4 fluorescence indicates increased intracellular Ca^{2+} levels. Fluo-4 was selected for experiments in chapter 3 because of its relatively high affinity for Ca^{2+} (K_d= 345 nM) and ability to detect Ca^{2+} at concentrations in the 100 nM to 1 μM range. A Ca^{2+} sensor with a high affinity was preferable because it is assumed that leptin

induces a very limited Ca^{2+} influx that is sufficient to initiate signaling for K_{ATP} channel trafficking without promoting insulin exocytosis.

Note: Fluo-4 is an anion that may be extruded from the cell or transported into lysosomes via organic anion transporters endogenously expressed by cells. To prevent this and keep Fluo-4 dispersed throughout the cell cytoplasm, cells may be incubated with the anion transporter inhibitor probenecid.

2.5.2. AKAR4 sensors

A primary focus of this thesis was to determine if PKA plays an active or permissive role in leptin signaling. To investigate the role of PKA, a FRET-based PKA activity sensor was implemented. This sensor is termed A-kinase activity reporter 4 (AKAR4) and it is a genetically-encoded single-chain FRET sensor (Figure 2.4.) that can be introduced to cells through plasmid transfection(125). AKAR4 is a recombinant protein that is composed of a donor cyan fluorescent protein (CFP) and an acceptor yellow fluorescent protein (YFP) that are separated by a phosphoamino acid binding domain and a PKA-specific substrate. PKA phosphorylation of its substrate on AKAR4 leads to intramolecular binding of the substrate and the phosphoamino acid binding domain. This intramolecular binding drives a conformational change of the sensor that yields increased FRET between CFP and YFP, indicative of increased PKA activity. AKAR4 has been modified with a farnesylation motif (CAAX) to target it to the cell membrane(125) and a nuclear export signal (NES) to target it to the cell cytoplasm(126). These targeted sensors have been successful in visualizing PKA activity specifically localized to the cell membrane or in the cytosol(125,126). In chapter 5, both of these sensors are employed to investigate the relationship between leptin and PKA.

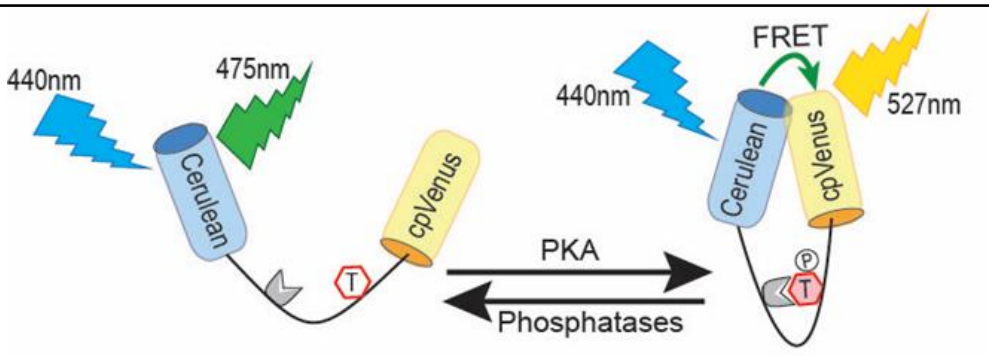

Figure 2. 4. AKAR4 Schematic.

AKAR4 schematic showing the sensor components and conformational change induced by PKA phosphorylation. In the relaxed conformation unphosphorylated conformation excitation of the CFP (cerulean) donor produces CFP emission (left). When phosphorylated by PKA, the sensor undergoes a conformational change so that now when CFP is excited energy is resonately transferred to the acceptor YFP (cpVenus) molecule to yield increased YFP emission.

2.5.3. CUTie sensors

Following the finding that leptin signaling increases PKA activity (Chapter 5), I sought out to determine if leptin does so by increasing the intracellular concentration of the PKA activator cAMP. In light of my finding that the scaffolding protein AKAP79/150 anchors PKA for leptin signaling, I selected cAMP sensors that have been targeted to AKAPs. In addition to PKA, AKAPs anchor adenylyl cyclases (ACs) and phoshpodiesterases (PDEs) that produce and degrade cAMP, respectively. Highly regulated levels of cAMP near AKAPs have been proposed to tightly control PKA activity. The development of a universal cAMP sensor that can be targeted to proteins of interest allows cAMP levels to be monitored at AKAPs. This sensor is called cAMP Universal Tag for imaging experiments (CUTie)(127). Similar to AKAR4, CUTie is a FRET-based recombinant protein construct that can be introduced to cells via transfection. CUTie consists of a cyclic nucleotide binding domain (CNBD) from the PKA regulatory subunit RIIβ that serves as the cAMP-sensing moiety (Figure 2.5.). A YFP acceptor molecule has been inserted into the 4-5 loop of the CNBD region and the CFP donor molecule was placed at the C-terminal end of CNBD. When cAMP binds the CNBD region, the sensor undergoes a conformational change that brings the YFP acceptor into proximity with the CFP donor yielding increased

FRET. CUTie has been targeted to a few AKAPs including the membrane-targeted AKAP79 and the cytosolic AKAP18. In chapter 5, AKAP79 and AKAP18δ are used to determine whether leptin increases cAMP levels as a possible means to activate PKA.

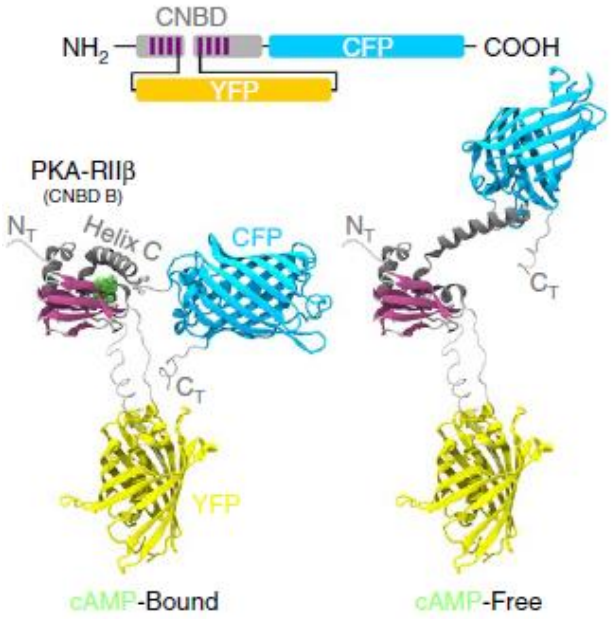

Figure 2. 5. CUTie schematic.

A schematic representative of CUTie (top). Below shows the predicted ribbon molecular structures of CUTie in the cAMP-bound and cAMP-free conformations. cAMP is shown in green.

Source: Surdo, N. et al.,Nat Commun, 2017; 8:15031. DOI: 10.1038/ncomms15031

License: CC BY 4.0

2.6. AKAP79 rescue of AKAP150 knockdown

AKAPs are identified by their ability to bind the regulatory subunits of PKA and are often named after their molecular mass. The *AKAP5* gene encodes AKAP79 in humans and AKAP150 in rodents(128). The size difference between AKAP79 and AKAP150 is due to AKAP150 containing multiple octapeptide repeats with unknown function(129). Regardless, AKAP79 and AKAP150 share many common features. Both AKAP79 and AKAP150 contain membrane binding domains(130) as well as binding sites for PKA, protein kinase C (PKC), and

PP2B(131). Importantly, several reciprocal knockdown and rescue experiments have shown that AKAP79 and AKAP150 are functionally equivalent(132–134). In chapter 5, knockdown of AKAP150 expression in INS-1 832/13 cells is used to determine whether AKAP150 is involved in K_{ATP} channel trafficking. INS-1 832/13 cells were transfected with AKAP150 shRNAi plasmids. 3-4 days post-transfection the cells were subjected to surface biotinylation experiments and western blot analysis of surface K_{ATP} channel expression and total cell lysate expression of AKAP150. For rescue experiments, INS-1 832/13 were co-transfected with the AKAP150 shRNAi plasmid and a plasmid containing wild type (WT) AKAP79 tagged with green fluorescent protein (AKAP79-GFP). Surface biotinylation experiments and western blot analysis was then performed the same as in AKAP150 knockdown experiments except that total cell lysate was also probed for GFP to confirm expression of AKAP79-GFP. Prior to this work, our collaborator Mark Dell'Acqua had generated AKAP79-GFP mutants that cannot bind PKA or PP2B. These mutants were also evaluated for their ability to rescue K_{ATP} channel trafficking in AKAP150 knockdown cells.

The AKAP150 shRNAi plasmid was a gift from John Scott (UW, Washington)(132). AKAP79-GFP and AKAP79-GFP mutants were provided by our collaborator Mark Dell'Acqua(110,130,134,135).

Note: AKAPs contain a common region that forms an amphipathic helix and binds the regulatory subunits of PKA. The peptide Ht31 is derived from this PKA binding region(136,137), and it is frequently used to disrupt PKA-AKAP interactions. A cell permeable, stearated form of Ht31 (st-Ht31) is used in chapter 5 to investigate the significance of AKAP-anchored PKA for leptin signaling.

Chapter 3: NMDA receptors mediate leptin signaling and regulate potassium channel trafficking in pancreatic β-cells

Yi Wu[1*], Dale A. Fortin[1*], Veronica A. Cochrane[1], Pei-Chun Chen[2†] and Show-Ling Shyng[1†]

[1]Department of Biochemistry and Molecular Biology, Oregon Health & Science University, Portland, OR 97239, USA; [2]Department of Physiology, College of Medicine, National Cheng Kung University, Tainan 701, Taiwan.

This work was originally published in

The Journal of Biological Chemistry 2017; 292: 15512-15524

DOI: 10.1074/jbc.M117.802249

*These authors contributed equally to the work. †To whom correspondence may be addressed: Pei-Chun Chen, Department of Physiology, College of Medicine, National Cheng Kung University, No.1 University Road, Tainan 701, Taiwan, Tel. 011-886-6-235-3535 ext. 5423; Fax: 011-886-6-236-2780; Email: pcchen@mail.ncku.edu.tw; or Show-Ling Shyng, Department of Biochemistry and Molecular Biology, School of Medicine, Oregon Health & Science University, 3181 S.W. Sam Jackson Park Road, Portland, OR 97239, Tel. (503) 494-2694; Fax: (503) 494-3849; Email:shyngs@ohsu.edu

Author Contributions: YW designed and performed experiments, analyzed data, and edited the manuscript; **DF** designed and performed experiments, analyzed data, and wrote the manuscript; **VC** designed and performed calcium imaging experiments (Fig. 3.6.), analyzed data, and edited the manuscript; **PCC** conceived the project, designed and performed experiments, and analyzed data; **SLS** conceived the project, designed experiments, and wrote the manuscript. All authors have full access to all the data in the study and take responsibility for the integrity of the data and the accuracy of the data analysis.

Acknowledgements: We thank Dr. Christopher Newgard for the rat insulinoma INS-1 832/13 cells. We are grateful to Dr. Charles Allen for sharing calcium imaging equipment and Dr. Nathan Klett for assistance with calcium imaging experiments. This work was supported by National Institutes of Health grant R01DK057699 and 3R01DK057699-14S1 (to Show-Ling Shyng) and by Ministry of Science and Technology grant MOST105-2628-B-006-006-MY3 (to Pei-Chun Chen). Veronica Cochrane was supported by the NIH T32 training grant GM071338. The authors declare that they have no conflict of interest.

3.1. Abstract

NMDA receptors (NMDARs) are Ca^{2+}-permeant, ligand-gated ion channels activated by the excitatory neurotransmitter glutamate and have well-characterized roles in the nervous system. The expression and function of NMDARs in pancreatic β cells, by contrast, are poorly understood. Here, we report a novel function of NMDARs in β-cells. Using a combination of biochemistry, electrophysiology, and imaging techniques we now show that NMDARs have a key role in mediating the effect of leptin to modulate β-cell electrical activity by promoting AMP-activated protein kinase (AMPK)-dependent trafficking of K_{ATP} and Kv2.1 channels to the plasma membrane. Blocking NMDAR activity inhibited the ability of leptin to activate AMPK, induce K_{ATP} and Kv2.1 channel trafficking, and promote membrane hyperpolarization. Conversely, activation of NMDARs mimicked the effect of leptin, causing Ca^{2+} influx, AMPK activation, increased trafficking of K_{ATP} and Kv2.1 channels to the plasma membrane, and triggered membrane hyperpolarization. Moreover, leptin potentiated NMDAR currents and triggered NMDAR-dependent Ca^{2+} influx. Importantly, NMDAR-mediated signaling was observed in rat insulinoma INS-1 832/13 cells and in human β-cells indicating that this pathway is conserved across species. The ability of NMDARs to regulate potassium channel surface expression and thus, β-cell excitability provides mechanistic insight into the recently reported insulinotropic effects of NMDAR antagonists, and therefore highlights the therapeutic potential of these drugs in managing type 2 diabetes.

3.2. Introduction

Insulin secretion by β-cells is under the control of a complex network of ion channels and signaling events(66). ATP-sensitive potassium (K_{ATP}) channels composed of Kir6.2 and sulfonylurea receptor 1 (SUR1) subunits have a key role by coupling glucose metabolism to the β-cell membrane potential(138). Upon glucose stimulation, K_{ATP} channels close in response to an increased intracellular ATP to ADP ratio, resulting in membrane depolarization, which activates voltage-gated calcium channels; the ensuing calcium influx then triggers insulin release(138,139). Cessation of insulin secretion occurs when the β-cell membrane potential returns to a hyperpolarized resting state. An important contributor of β-cell membrane repolarization is the voltage-gated delayed rectifier potassium channel Kv2.1. Reduction of Kv2.1 function in β-cells has been shown to enhance action potential duration, calcium influx, and insulin secretion(140,141). Recent studies showed that the density of K_{ATP} and Kv2.1 channels in β-cells is dynamically regulated by metabolic or hormonal signals to modulate cell excitability(57,58,68,142). In particular, leptin, a satiety hormone secreted by adipocytes to maintain energy and glucose homeostasis was reported to promote trafficking of K_{ATP} channels(57,58) and Kv2.1 channels(65) to the β-cell surface. Evidence suggests that leptin activates the AMP-activated protein kinase (AMPK) via its upstream kinase Ca^{2+}-calmodulin-dependent protein kinase kinase β (CaMKKβ)(57,65); however, the mechanism by which leptin activates the CaMKKβ/AMPK pathway in β-cells is unclear.

NMDA receptors (NMDARs) are ionotropic glutamate receptors whose activation requires the co-agonists glutamate and glycine as well as membrane depolarization, which removes external Mg^{2+} block(143). NMDARs are Ca^{2+}-permeable, which endows them the ability to trigger Ca^{2+}-dependent signaling events. For example, in hippocampal neurons Ca^{2+} influx through NMDARs is coupled to activation of the Ca^{2+}-dependent protein kinase CaMKK to induce long-term potentiation(144). Expression of NMDARs in β-cells has been reported since the mid-

nineties(79–81). However, in contrast to their well characterized functional role in the nervous system(145), the role of NMDARs in β-cells has remained elusive or even controversial. A recent study reported that inhibition of NMDARs *in vitro* and *in vivo* elicits increases in glucose stimulated insulin secretion (GSIS)(82), but the underlying mechanism has yet to be elucidated.

In the present study, we demonstrate that NMDARs are expressed by β-cells and are required for leptin-induced calcium influx, AMPK activation, increased K_{ATP} and Kv2.1 channel surface expression, and reductions in β-cell membrane excitability. Moreover, we show that activation of NMDARs alone induces channel trafficking and reduces β-cell membrane excitability. These findings reveal an important role of NMDARs in regulating β-cell excitability and provide a novel mechanistic paradigm for insulin secretion regulation.

3.3. Results

3.3.1. NMDARs are expressed in pancreatic β-cells

We previously reported that leptin increases the surface density of K_{ATP} and Kv2.1 channels in rat insulinoma INS-1 832/13 cells and human β-cells. In INS-1 832/13 cells, this increase is dependent upon activation of the AMP-activated protein kinase (AMPK), which is in turn dependent on its upstream effector Ca^{2+}-calmodulin-dependent protein kinase kinase β (CaMKKβ)(57,58). Studies in hippocampal neurons have linked calcium influx through NMDARs to activation of the CaMKKβ-AMPK pathway(146,147). Furthermore, NMDAR stimulation has been shown to increase K_{ATP} currents in an AMPK-dependent manner in subthalamic neurons(148,149). These reports prompted us to investigate whether NMDARs could be involved in the leptin signaling pathway that regulates surface expression of K_{ATP} and Kv2.1 channels in β-cells.

Although expression of NMDARs and their functional roles have been studied in a number of rodent β-cell lines or primary islets by measuring mRNA, protein, or currents, the results vary

and in some cases are controversial(79,81,82,150–152). We first determined whether NMDARs are expressed by INS-1 832/13 cells, which were used in our previous studies. Immunoblotting was used to probe the NMDAR subunit GluN1 which is the mandatory subunit for all functional NMDARs(153) in INS-832/13 cell lysate. While GluN1 protein was expressed by INS-1 832/13 cells, its expression level was less than that observed in whole brain homogenate (Fig. 3.1.A). No expression was observed in COS cells which lack NMDARs. Immunostaining illustrated that only 43% of insulin-positive INS-1 832/13 and 46% human β-cells expressed detectable levels of GluN1 protein (Fig. 3.1.B). Notably, while most GluN1-positive INS-1 832/13 and human β-cells showed low level of staining, some INS-1 832/13 cells showed intense GluN1 signals (Fig. 3.1.C, D). In addition, we found that a small percentage of dissociated islet cells (23%), while positive for GluN1, were not identified as β-cells implicating that other cell types within human islets also express NMDARs.

We next conducted whole-cell patch-clamp recordings and used local pressure (puff) application of NMDA (1 mM) to assess NMDAR function. In 10 out of 21 cells tested puff application of NMDA induced inward currents (holding potential -70 mV; no external Mg^{2+}), with a mean of 9.0±1.4 pA that was inhibited to 1.8±0.2 pA by the non-competitive NMDAR antagonist, MK-801 (50 μM; $p<0.001$, n=10 by paired *t*-test, Fig. 3.1.E). Application of the competitive NMDAR antagonist D-APV (50 μM) also reduced NMDAR currents (from 28.4±7.2 pA to 9.7±5.2 pA; $p<0.001$, n=12 by paired *t*-test; not shown). Consistent with immunostaining results, not all cells recorded had detectable NMDAR currents and those that did displayed a range of amplitudes that reflected the heterogeneity in NMDAR expression (Fig. 3.1.D). Importantly, NMDA-evoked currents were also observed in dispersed human β-cells and were reduced by MK-801 (from 21.3±8.9 pA to 6.3±3.0 pA; $p<0.001$, n=5 by paired *t*-test; Fig. 3.1.F). Puff application of glutamate (1 mM), a physiological ligand of the NMDAR, also elicited outward currents when cells were held at a positive potential of 40 mV, which were reversibly blocked by MK-801

(27.8±7.0 pA for glutamate, 2.3±1.4 pA for MK-801, and 23.5±6.7 pA for MK-801 washout; $p<0.01$, n=5 by paired *t*-test; Fig. 3.1.G). Together, these results show that both INS-1 832/13 cells and human β-cells express functional NMDARs.

3.3.2. NMDARs are required for leptin-induced surface trafficking of K_{ATP} and Kv2.1 channels

To test the role of NMDARs in leptin-induced surface trafficking of K_{ATP} and Kv2.1 channels, we monitored surface expression of these channels using surface biotinylation following treatment of INS-832/13 cells with 0.1% DMSO, 10 nM leptin, or 50 µM NMDA for 30 min in the absence or presence of MK-801. To test for specificity among ionotropic glutamate receptors, the effect of α-amino-3-hydroxy-5-methyl-4-isoxazolepropionic acid (AMPA) (50 µM), an agonist of the ionotropic AMPA receptor which has been reported to be expressed in β-cells(154,155), was also examined in the absence or presence of MK-801. As expected(58), leptin induced a significant increase (~2-fold) in surface SUR1 as compared to controls (Fig. 3.2.A). Strikingly, while treatment with NMDA induced a similar increase in biotinylated SUR1 protein, treatment with AMPA did not suggesting this is not a general response to ionotropic glutamate receptor activation (Fig. 3.2.A). Both leptin- and NMDA-induced increases in biotinylated SUR1 and Kv2.1 were inhibited by NMDAR antagonists (Fig. 3.2.A,C). While a previous study attributed the leptin-induced trafficking of K_{ATP} channels to activation of TRPC4 channels(57), we failed to see an effect of TRPC4 inhibition (ML204, 10µM)(156) on leptin-induced increases in surface expression of either K_{ATP} or Kv2.1 channels (Fig. 3.2.B,D).

Previously, we and others showed that leptin increases AMPK phosphorylation at residue T172 of the catalytic subunit, a signature of AMPK activation(57,65). The increase in phosphorylation was shown to be Ca^{2+}- dependent and required the Ca^{2+} dependent kinase, CaMKKβ. Importantly, activation of AMPK was required for the trafficking of K_{ATP} and Kv2.1 channels(68). We found that like leptin, NMDA also increased AMPK-pT172 and that the increase

was blocked by MK-801 in both cases, implying they activate similar signaling pathways (Fig. 3.3.A,B). Taken together, these results reveal a necessary role of NMDARs in mediating the effect of leptin on AMPK activation and the subsequent surface expression of K_{ATP} and Kv2.1 channels.

3.3.3. NMDARs mediate leptin-induced hyperpolarization in INS-1 832/13 cells

Delivery of K_{ATP} channels to the plasma membrane of INS-832/13 cells upon leptin signaling results in membrane hyperpolarization(65). We reasoned that this hyperpolarization should also be NMDAR dependent. To monitor changes in membrane potential we used cell-attached patch-clamp recording, which provides an accurate measure of membrane potential, maintains cell integrity, and prevents dialysis of soluble factors that may be important for proper signaling(157). Membrane potential was recorded in response to vehicle or leptin in the absence or presence of tolbutamide, an inhibitor of K_{ATP} channels, the competitive NMDAR antagonist D-APV or the TRPC4 inhibitor ML204. In addition, dextromethorphan (DXM), a NMDAR antagonist recently shown to stimulate insulin secretion and improve glucose tolerance in type 2 diabetes patients(82), was also tested.

In the majority of cells tested (23/32 cells) bath application of leptin in the presence of 11 mM glucose induced a significant membrane hyperpolarization (ΔVm= -0.2±0.7 and -23.1±3.5 mV for Veh and leptin, respectively, p<0.001) (Fig. 3.4.). Leptin induced similar results when cells were recorded under whole-cell mode (ΔVm= -26.6±3.6 mV, n=16), confirming the integrity of our cell attached recordings. The onset of hyperpolarization occurred ~ 1-10 min after the start of leptin perfusion and was largely abolished by co-application with tolbutamide(158) (ΔVm= -4.7±2.0 mV), indicating that the source of hyperpolarization was from K_{ATP} channels. These results are in good agreement with those reported previously in a different β-cell line CR1-G1(52). By contrast, in the absence of leptin, tolbutamide alone did not significantly alter the depolarized baseline potential of INS-1 832/13 cells bathed in 11 mM glucose (baseline = 3.6±2.5 mV; tolbutamide = 7.9±3.3 mV, n=9), indicating that under this condition most existing K_{ATP} channels

are closed, as expected. We next examined whether blockade of NMDARs, could inhibit the ability of leptin to hyperpolarize the cell membrane. Application of either, D-APV or DXM significantly reduced the level of hyperpolarization by leptin (ΔVm= -6.2±2.9 and -5.9±2.1 mV respectively) (Fig. 3.4.C). By contrast, cells receiving bath application of leptin with the TRPC4 inhibitor ML204 showed a similar level of hyperpolarization as with leptin alone (ΔVm= -25.8±3.6 mV; Fig.4B, C) suggesting that TRPC4 channels do not contribute significantly to leptin-induced membrane hyperpolarization.

3.3.4. NMDAR activation is sufficient to induce membrane hyperpolarization in β-cells

Since NMDA is sufficient to enhance surface expression of K_{ATP} channels, we asked whether it also regulates β-cell membrane excitability. In the majority of cells tested (~80%), perfusion of NMDA (50 μM) alone triggered a significant hyperpolarization in membrane potential in both INS-1 832/13 (ΔVm= -20.7±4.4 mV, p<0.01), and human β-cells (ΔVm= -30±5.4 mV, p<0.001; Fig. 3.5.C). The onset of hyperpolarization to NMDA treatment averaged ~7min but ranged from 1-14 min in INS-1 832-13 cells and human β-cells after the start of perfusion. In some instances, NMDA induced a small membrane depolarization, indicative of NMDAR activation, prior to the onset of hyperpolarization (Fig. 3.5.A, lower trace). Importantly, the NMDA-mediated hyperpolarization in both INS-1 832/13 and human β-cells was blocked by tolbutamide, suggesting that like leptin, NMDA affects β-cell membrane potential via K_{ATP} channels (Fig. 3.5.C). These data indicate that activation of NMDARs is sufficient to induce trafficking of K_{ATP} channels and subsequent membrane hyperpolarization in INS-1 832/13 and human β-cells.

We have previously shown that leptin increases AMPK phosphorylation via CaMKKβ, a known upstream kinase of AMPK, to regulate surface trafficking of Kv2.1 and K_{ATP} channels(65). Since NMDA also increased AMPK phosphorylation (Fig. 3.3.), we tested whether the observed NMDAR-mediated hyperpolarization requires CaMKKβ. We found that while NMDA alone triggered a significant hyperpolarization in membrane potential (ΔVm= -27.3±7.1 mV; n=8,

p<0.05), INS-1 832/13 cells pretreated with STO-609, a well-known inhibitor of CaMKKβ, failed to hyperpolarize in the presence of NMDA (baseline = 6.8±5.3 mV; NMDA = 3.1±7.5 mV; n=6) (Fig. 3.5.D,E). This result indicates that both leptin and NMDARs promote channel trafficking and INS-1 832/13 membrane hyperpolarization by CaMKKβ-dependent phosphorylation of AMPK.

3.3.5. Leptin causes increased Ca^{2+} influx through NMDARs

Given that CaMKKβ requires Ca^{2+} for its catalytic activity, we hypothesized that Ca^{2+} influx through NMDARs might be critical for leptin signaling. To directly monitor changes in intracellular [Ca^{2+}], β-cells were loaded with the cell permeant fluorescent indicator dye, Fluo-4 AM. Local puff application of NMDA caused a robust transient increase in intracellular [Ca^{2+}] in 70% of cells tested (Fig. 3.6.A, B, C). On average NMDA increased intracellular [Ca^{2+}] by 2.00±0.26 fold. Importantly, the increase in intracellular [Ca^{2+}] by NMDA was abolished by co-application of either D-APV (1.02±0.06 fold), MK-801 (1.12±0.07 fold), or DXM (0.96±0.03 fold), but not by ML204 (2.61±0.64 fold) (Fig. 3.6.C). These results demonstrate that NMDARs permit Ca^{2+} influx in INS-1 832/13 cells.

Next, we tested whether leptin induces Ca^{2+} influx through NMDARs. Bath application of leptin triggered a more sustained increase in intracellular Ca^{2+} as compared to puff application of NMDA (Fig. 3.6.D); however, similar sustained increases in Ca^{2+} were observed when NMDA was bath applied (see inset Fig. 3.6.D). On average leptin induced a rise in intracellular Ca^{2+} that was 2.48±0.15 fold higher than baseline. Importantly, this increase was markedly reduced by co-application of either D-APV (1.43±0.07 fold), MK-801 (1.50±0.08 fold), or DXM (1.28±0.10 fold), but little affected by ML204 (2.32±0.29 fold) (Fig. 3.6.E). These data provide strong evidence that leptin triggers Ca^{2+} influx in INS-1 832/13 cells predominantly through NMDARs.

3.3.6. Leptin potentiates NMDAR currents in β-cells

In the hippocampus, leptin has been reported to facilitate long-term potentiation by enhancing NMDAR function(159,160), raising the possibility that leptin may potentiate the function

of NMDARs to trigger the downstream effects in β-cells. To test this possibility we conducted whole-cell voltage-clamp experiments from individual β-cells and induced NMDAR currents by puff application of NMDA before and after the subsequent addition of leptin. We found that NMDAR currents evoked in INS-1 832/13 cells were significantly potentiated by leptin (Fig. 3.7.A, left trace). On average leptin increased NMDAR currents by 164.2±21.7% after 6 min (Fig. 3.7.A,B). The increase could be seen as quickly as 2 min following bath application of leptin and could be sustained for up to 30 min. In 3 out of 8 cells leptin failed to potentiate NMDAR currents indicating that potentiation did not result from repeated NMDA puff applications (see example in Fig. 3.7.A, right trace) and suggested surface leptin receptor heterogeneity among β-cells. Importantly, leptin induced a marked enhancement in NMDA-evoked currents by 187.6±32.7% in human β-cells (Fig. 3.7.C). Taken together, these data reveal a novel link between leptin signaling and the function of NMDARs in β-cells.

3.4. Discussion

Utilizing a combination of biochemical, electrophysiological, and imaging approaches we show that NMDARs play a crucial role in mediating the effect of leptin in β-cells. Together with our previous studies(58,65), we propose a model by which leptin suppresses glucose-stimulated insulin secretion (Fig. 3.8.). At 11 mM glucose under which condition β-cells are depolarized, NMDARs exposed to glutamate and glycine present in the extracellular milieu are able to conduct currents due to Mg^{2+} unblock. Leptin potentiates NMDAR currents, thus increasing Ca^{2+} influx to activate CaMKKβ, which then phosphorylates and activates AMPK to trigger PKA-dependent actin remodeling and trafficking of K_{ATP} and Kv2.1 channels to the cell surface. The increased surface expression of Kv2.1 channels induced by NMDAR activation is expected to shorten action potentials(65) facilitating membrane repolarization while increased K_{ATP} channel abundance would facilitate membrane hyperpolarization to limit voltage-dependent Ca^{2+} influx and inhibit insulin secretion. The expression of functional NMDARs was observed in both rodent and human

β-cells, indicating that this mechanism is highly conserved and likely plays an important role in regulating β-cell function and insulin release.

A recent study by Marquard et al. found that NMDARs were required to limit GSIS and that inhibition of NMDARs could serve as a potential antidiabetic treatment(82). However, how NMDARs regulate insulin secretion remains unknown. Interestingly, these authors showed that inhibition of NMDARs by DXM could enhance GSIS without affecting basal insulin secretion; moreover, the effect of NMDAR inhibition on insulin secretion was absent in Kir6.2 knockout mice, implicating involvement of K_{ATP} channels(82). Our findings provide a molecular mechanism for the observations made by Marquard et al. Specifically, during low glucose, the negative resting β-cell membrane potential prevents NMDARs from opening due to blockade by external Mg^{2+} (143), rendering NMDAR inhibition ineffective. When glucose is high, β-cells depolarize, removing the Mg^{2+} block, allowing Ca^{2+} to enter and trigger channel trafficking, increasing K^+ efflux, and suppressing insulin release. Under this condition, inhibiting NMDARs would enhance insulin release by preventing K^+ channel trafficking.

The co-trafficking of K_{ATP} and Kv2.1 channels by leptin has been shown to require activation of CaMKKβ and its downstream effector AMPK(57,65), which brings into question the potential source of Ca^{2+} influx upstream of CaMKKβ. While it was previously reported that Ca^{2+} influx through TRPC4 channels was the most likely candidate(57), we found that TRPC4 inhibition was unable to prevent recruitment of K_{ATP} and Kv2.1 channels to plasma membrane. Rather, our data show that NMDARs are the primary Ca^{2+} source mediating the effect of leptin, as NMDAR antagonists (competitive and non-competitive) as well as a selective pore blocker inhibited leptin-induced Ca^{2+} influx, activation of AMPK, K_{ATP} and Kv2.1 channel trafficking, and membrane hyperpolarization.

Our finding that NMDAR activation triggers the co-regulation of K_{ATP} and Kv2.1 channels highlights its importance in modulating the excitability of β-cells to control insulin secretion. This

raises questions regarding how Kv2.1 and K_{ATP} channels are sorted within β-cells. For example, are they sorted into specific secretory vesicles from the trans-Golgi network and/or are they endocytosed together for subsequent recycling to the membrane. Knowing how Kv2.1 and K_{ATP} channels are trafficked will undoubtedly provide new avenues for drug development to overcome diseases related to insulin and leptin misregulation.

There is increasing evidence that insulin secretion from β-cells is regulated by glutamate(78). In addition to expressing NMDARs and other glutamate receptors(79–81), pancreatic β-cells express vesicular glutamate transporters VGLUT1 and VGLUT3(161), the excitatory amino acid transporter EAAT2(162), and the glial glutamate transporter 1 (GLT1)(163), suggesting active regulation of intracellular and extracellular glutamate signals. Several possible physiological sources of glutamate for β-cells have been reported, including circulating plasma glutamate in the range of ~20 - 30 μM(164) which is well above the EC_{50} of ~1 μM for NMDARs(143), glutamate released by α-cells(29), glutamate released by β-cells that is not coupled to secretion(165), and finally, glutamate co-released from insulin granules(162). The possibility that β-cells may co-release glutamate during insulin secretion is an intriguing one. Such a mechanism would allow NMDAR activation to be coordinated with periods of insulin release. Thus, NMDAR activation may provide autoinhibitory feedback to prevent the over secretion of insulin perhaps even in the absence of leptin. In this regard, it is interesting to note that glucose stimulation has been reported to promote K_{ATP} channels trafficking to the cell surface(142).

Our results show that leptin potentiates NMDAR currents. Potentiation of NMDAR currents by leptin has been observed in other cells such as hippocampal neurons(77) and cerebellar granule cells(166). How leptin potentiates NMDARs in β-cells is not clear although involvement of Src kinases has been implicated in hippocampal neurons(77). More studies are needed to determine whether a similar mechanism is at play in β-cells and whether these signaling molecules form a complex to confer spatial and temporal specificity.

Analysis of data from immunocytochemistry, electrophysiology and Ca^{2+} imaging experiments revealed non-uniform NMDAR expression and responses to leptin. Studies of dispersed clonal or primary β-cells suggest that ion channel expression and composition in β-cells is heterogeneous(167,168), including a recent report of heterogeneous NMDAR expression in the BRIN-BD11 β-cell line(152). Such cell-to-cell variations may explain controversies regarding β-cell expression of NMDARs(169,170). While heterogeneity amongst β-cells is becoming increasingly evident(171), how these subpopulations contribute to islet function and whether their expression patterns change in response to autocrine or paracrine signals are still open questions. Modeling studies have shown that heterogeneity in individual β-cell electrical properties is largely negated by the electrical coupling of β-cells via gap junctions to give rise to synchronized β-cell activity in islets(172,173). Thus, expression of NMDARs or leptin receptors in every β-cell may not be necessary for glutamate or leptin to exert a significant impact on the overall function of an islet. In this context, NMDAR expressing β-cells may function to trigger waves of hyperpolarization throughout the islet to suppress insulin release. Our immunocytochemistry data on dispersed human islet cells also suggest expression of NMDARs in non-β cells, although the functional significance of this finding awaits further investigation.

In summary, we demonstrate that NMDARs are unequivocally expressed in pancreatic β-cells and contribute to Ca^{2+} and CaMKKβ-dependent trafficking of K_{ATP} and Kv2.1 channels to the plasma membrane. The signaling pathway elucidated here provides a cellular mechanism linking glutamate signaling to NMDAR dependent regulation of insulin secretion to explain the reported antidiabetic effects of NMDAR antagonists, and further reinforces the therapeutic potential of NMDAR in the treatment of diabetes.

3.5. Figures

Table 3. 1. Human islet donor information

Donor (date received)	Age	Gender	BMI	Cause of death	Islet viability	Islet purity
04/10/17[a]	32	M	29.2	Head trauma	97%	80%
04/26/17[a]	26	F	38.9	Stroke	95%	95%
06/30/16[b]	24	M	34.8	Head trauma	97%	95%
07/12/16[b]	58	M	39.3	Anoxia	95%	80%
07/19/16[b]	35	M	24.2	Head trauma	95%	95%
05/29/16[c]	33	F	34.2	Stroke	95%	98%
06/28/16[c]	24	M	34.8	Head trauma	99%	95%
07/10/16[c]	38	F	34.4	Anoxia	95%	95%
07/17/16[c]	35	M	24.2	Head trauma	95%	95%
08/02/16[d]	39	F	24.8	Stroke	90%	85%
08/11/16[d]	63	F	27.4	Stroke	96%	85%
08/24/16[d]	47	M	31.0	Anoxia	96%	85%
09/09/16[d]	56	M	40.1	Stroke	95%	90%

[a]Islets used in Figure 3.1.B.

[b]Islets used in Figure 3.1.F.

[c]Islets used in Figure 3.5.

[d]Islets used in Figure 3.7.C.

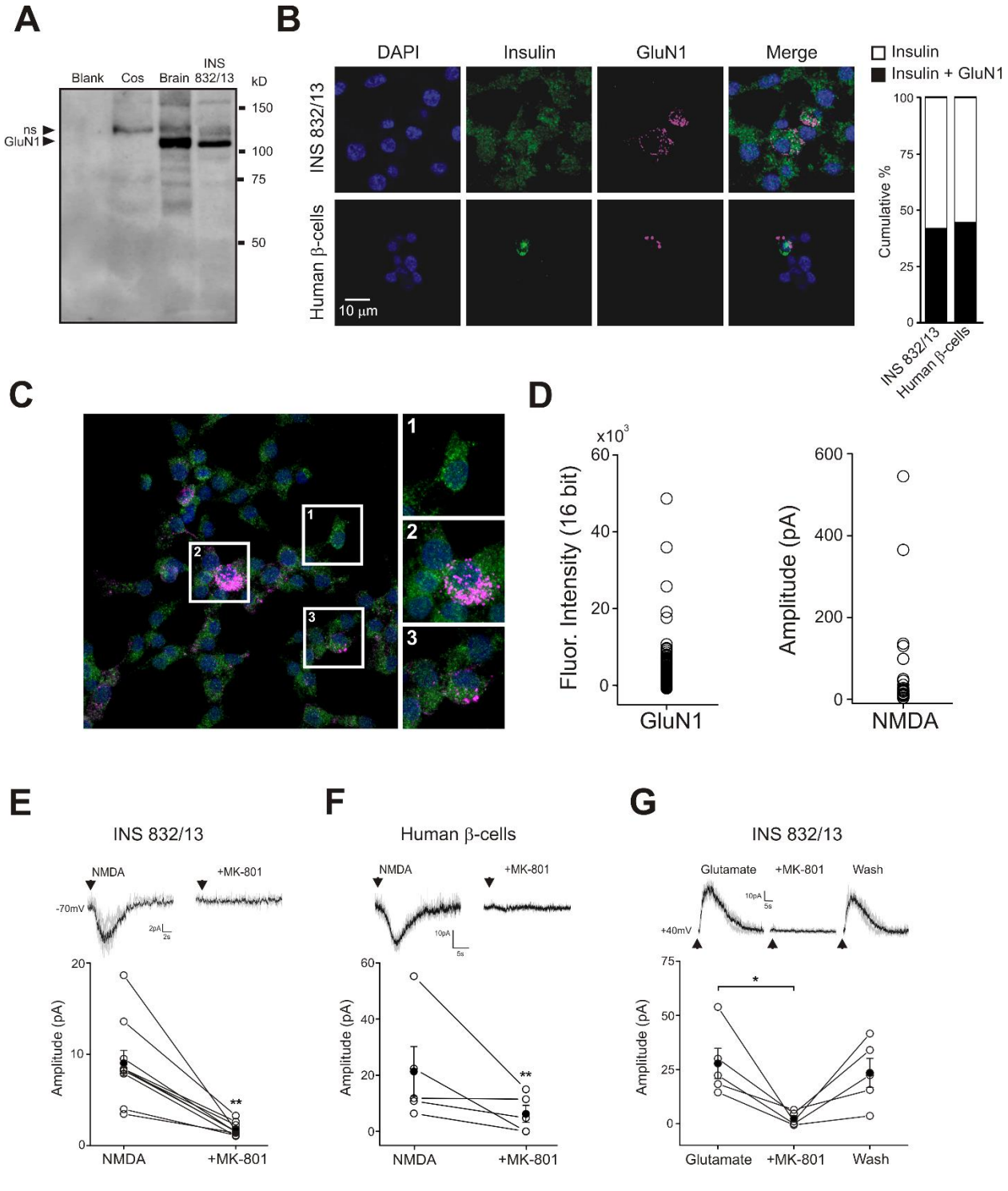
A
Blank
Cos
Brain
INS 832/13
kD
150
100
75
50
ns
GluN1
B
DAPI
Insulin
GluN1
Merge
INS 832/13
Human β-cells
10 μm
Insulin
Insulin + GluN1
Cumulative %
100
75
50
25
0
INS 832/13
Human β-cells
C
1
2
3
D
x10^3
60
40
20
0
Fluor. Intensity (16 bit)
GluN1
600
400
200
0
Amplitude (pA)
NMDA
E
INS 832/13
NMDA
+MK-801
-70mV
2pA
2s
20
10
0
Amplitude (pA)
**
NMDA
+MK-801
F
Human β-cells
NMDA
+MK-801
10pA
5s
60
40
20
0
Amplitude (pA)
**
NMDA
+MK-801
G
INS 832/13
Glutamate
+MK-801
Wash
+40mV
10pA
5s
75
50
25
0
Amplitude (pA)
*
Glutamate
+MK-801
Wash

Figure 3. 1. INS-832/13 and human β-cells express functional NMDARs.

(**A**) Immunoblot showing expression of GluN1 protein (105kD) in whole brain and INS-832/13 cell lysate, but not in lysate prepared from COS cells (ns, non-specific protein band). (**B**) Confocal image of INS-832/13 cells (top panels) and human β-cells (lower panels) immunostained for DNA (DAPI, blue), insulin (green), and GluN1 (magenta). Right, graph showing the percentage of INS-832/13 and human β-cells that expressed GluN1 protein (INS-832/13 = 144 out of 339 cells; human β-cells = 136 out of 296 cells from 2 donors). (**C**) Immunofluorescence image of INS-1 832/13 cells immunostained for insulin (green), GluN1 (magenta), and DNA (DAPI, blue). Zoom-in of numbered boxed regions are shown to the right for cells with no (1), high (2), and low (3) expression of GluN1. (**D**) Distributions of single cell integrated fluorescence intensities of GluN1 (left, n = 282) and single cell NMDA-induced current amplitudes (right, n = 32). (**E** and **F**) Whole-cell voltage clamp traces (holding potential at -70mV) recorded from a single INS-832/13 cell (**E**) or human β-cell (**F**) in response to NMDA (1mM puff) and after the subsequent addition of NMDAR antagonist MK-801 (50μM). (**G**) Whole-cell voltage clamp traces (holding potential at +40mV) recorded from a single INS-1 832/13 cell in response to glutamate (1mM puff), subsequent addition of MK-801, and 10 min after MK-801 washout (wash). For experiments shown in E-G, the external Tyrode's solution was supplemented with 0.1 mM glycine but no Mg^{2+} or glucose. In panels E-G, black traces represent the mean response to 3 consecutive puff evoked currents shown in gray. Arrows denote time of puff. Group data for mean (filled circles ± SEM) and individual (open circles) changes in the amplitude of puff-evoked currents are plotted below. *p < 0.01, **p < 0.001.

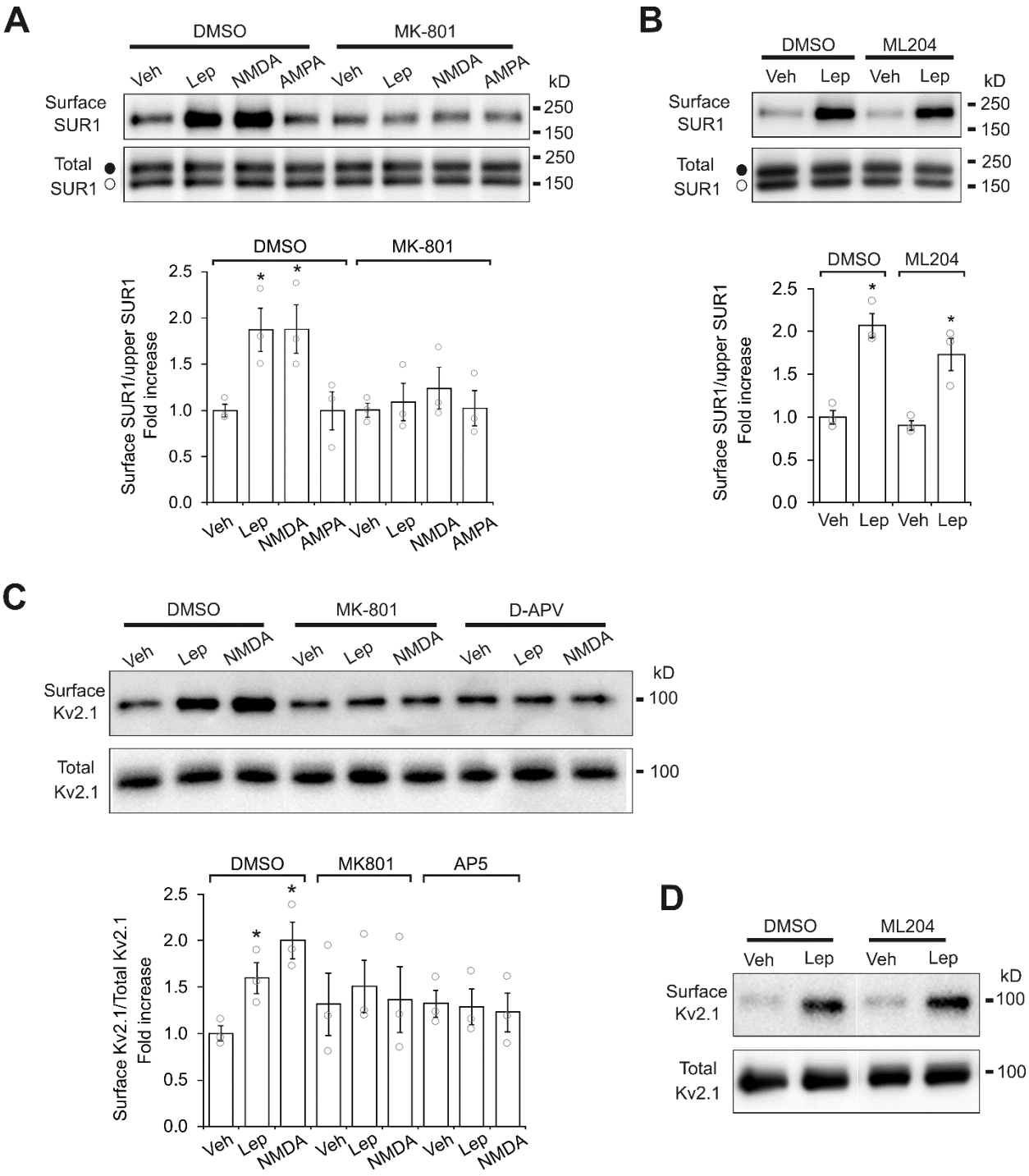
A
DMSO
MK-801
Veh
Lep
NMDA
AMPA
Veh
Lep
NMDA
AMPA
kD
Surface SUR1
250
150
Total SUR1
250
150
DMSO
MK-801
Surface SUR1/upper SUR1 Fold increase
2.5
2.0
1.5
1.0
0.5
0.0
Veh
Lep
NMDA
AMPA
Veh
Lep
NMDA
AMPA
B
DMSO
ML204
Veh
Lep
Veh
Lep
kD
Surface SUR1
250
150
Total SUR1
250
150
DMSO
ML204
Surface SUR1/upper SUR1 Fold increase
2.5
2.0
1.5
1.0
0.5
0.0
Veh
Lep
Veh
Lep
C
DMSO
MK-801
D-APV
Veh
Lep
NMDA
Veh
Lep
NMDA
Veh
Lep
NMDA
kD
Surface Kv2.1
100
Total Kv2.1
100
DMSO
MK801
AP5
Surface Kv2.1/Total Kv2.1 Fold increase
2.5
2.0
1.5
1.0
0.5
0.0
Veh
Lep
NMDA
Veh
Lep
NMDA
Veh
Lep
NMDA
D
DMSO
ML204
Veh
Lep
Veh
Lep
kD
Surface Kv2.1
100
Total Kv2.1
100

Figure 3. 2. Ionotropic function of NMDARs is required for leptin-induced trafficking of SUR1 (K_{ATP} channels) and Kv2.1.

(**A**) Representative immunoblot showing surface biotinylated SUR1 protein (upper blot) and total SUR1 protein (lower blot) from INS-1 832/13 cells pre-treated with DMSO (0.1% DMSO), 10 nM leptin (Lep), 50 µM NMDA, and 50 µM (R,S)-AMPA in the absence or presence of 50 µM MK-801. Total SUR1 antibody recognizes both complex-glycosylated mature (filled circle) and core-glycosylated immature (open circle) SUR1 protein. Group data is shown below from 3 independent experiments. *$p < 0.05$. (**B**) Representative immunoblot showing increase in surface SUR1 protein was not prevented by the TRPC4 inhibitor ML204 (10 µM). Group data is shown below from 3 independent experiments. *$p < 0.05$. (**C**) Representative immunoblot showing surface biotinylated Kv2.1 protein (upper blot) and total Kv2.1 protein (lower blot) from INS-832/13 cells pre-treated with DMSO, leptin, or NMDA in the absence or presence of MK-801 (as in A) or the competitive NMDAR antagonist D-APV (50 µM). Group data from 3 independent experiments is shown below. *$p < 0.05$. (**D**) Example immunoblot showing inhibition of TRPC4 with ML204 did not alter the increase in Kv1.2 surface trafficking by leptin.

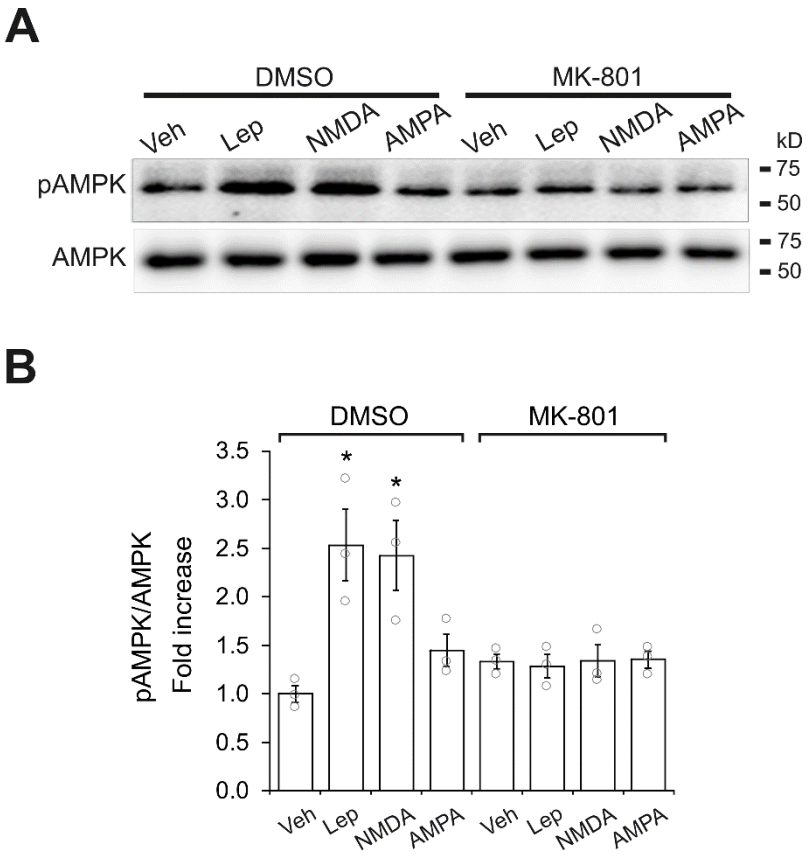

Figure 3. 3. Leptin-induced phosphorylation of AMPK requires NMDARs.

(**A**) Representative immunoblot probed for total and phosphorylated AMPK (pAMPK; phosphorylated at Thr172) protein from INS-1 832/13 cells treated with vehicle, leptin, NMDA, or AMPA in the absence or presence of MK-801 (concentrations as in Fig.2A). (**B**) Fold increase in the mean pAMPK/AMPK ratio for each condition from 3 independent experiments. *$p < 0.05$.

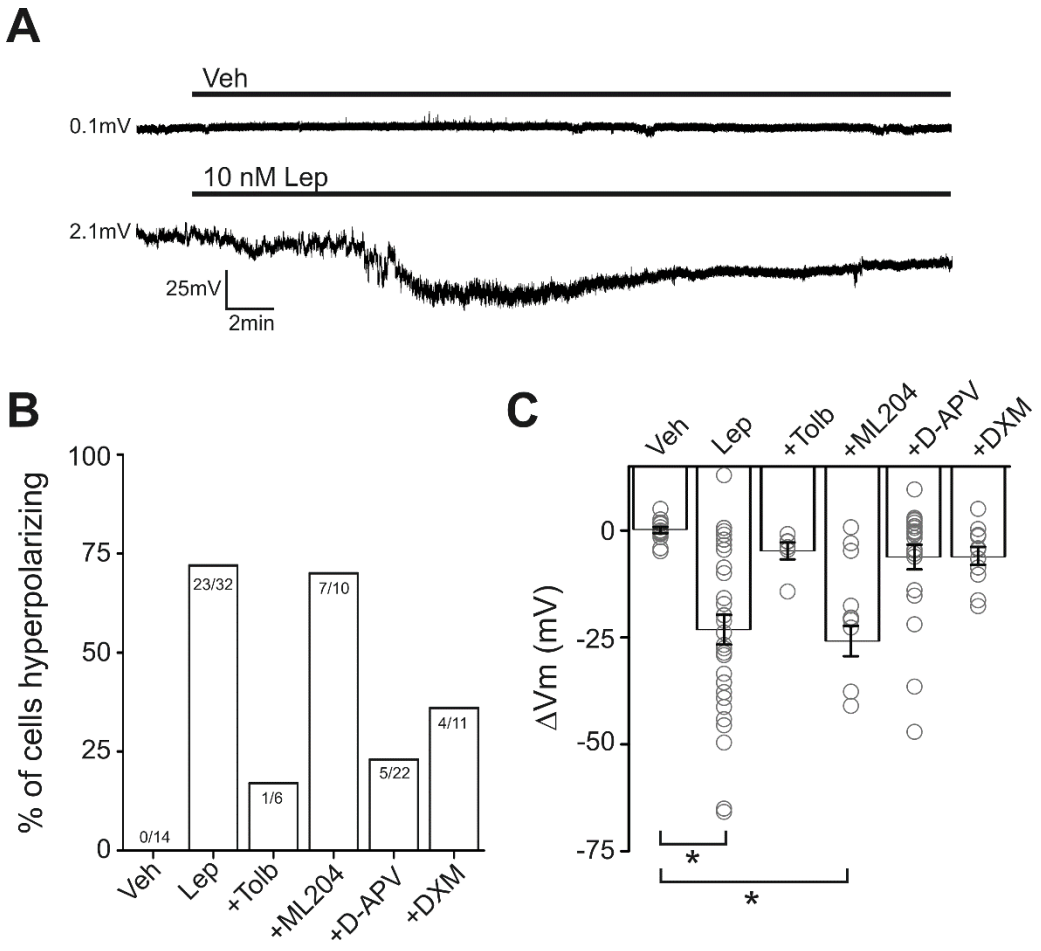

Figure 3. 4. Leptin-induced hyperpolarization of INS-832/13 cells is dependent on K_{ATP} channels and NMDARs but not TRPC4/5 channels.

(**A**) Cell-attached voltage traces recorded from INS-1 832/13 cells incubated in Tyrode's solution supplemented with 0.1 mM glycine and 11 mM glucose before and after perfusion of vehicle (top trace) or 10 nM leptin (bottom trace). The initial membrane potential for each cell, averaged over the first 2 min, is indicated to the left of each trace. (**B**) Bar graph depicting the percentage of cells that hyperpolarized in response to vehicle only or leptin in the absence or presence of the K_{ATP} channel inhibitor, tolbutamide (tolb, 300 µM), ML204 (10 µM), D-APV (50 µM) or dextromethorphan (DXM, 10 µM). The number of cells tested is provided for each condition. The mean baseline potential across conditions was 1.5±9.7 mV (**C**) Group data illustrating the average degree of hyperpolarization for each condition. Data are shown as means ± SEM (bars) along with individual cell responses (open circles). *$p < 0.001$.

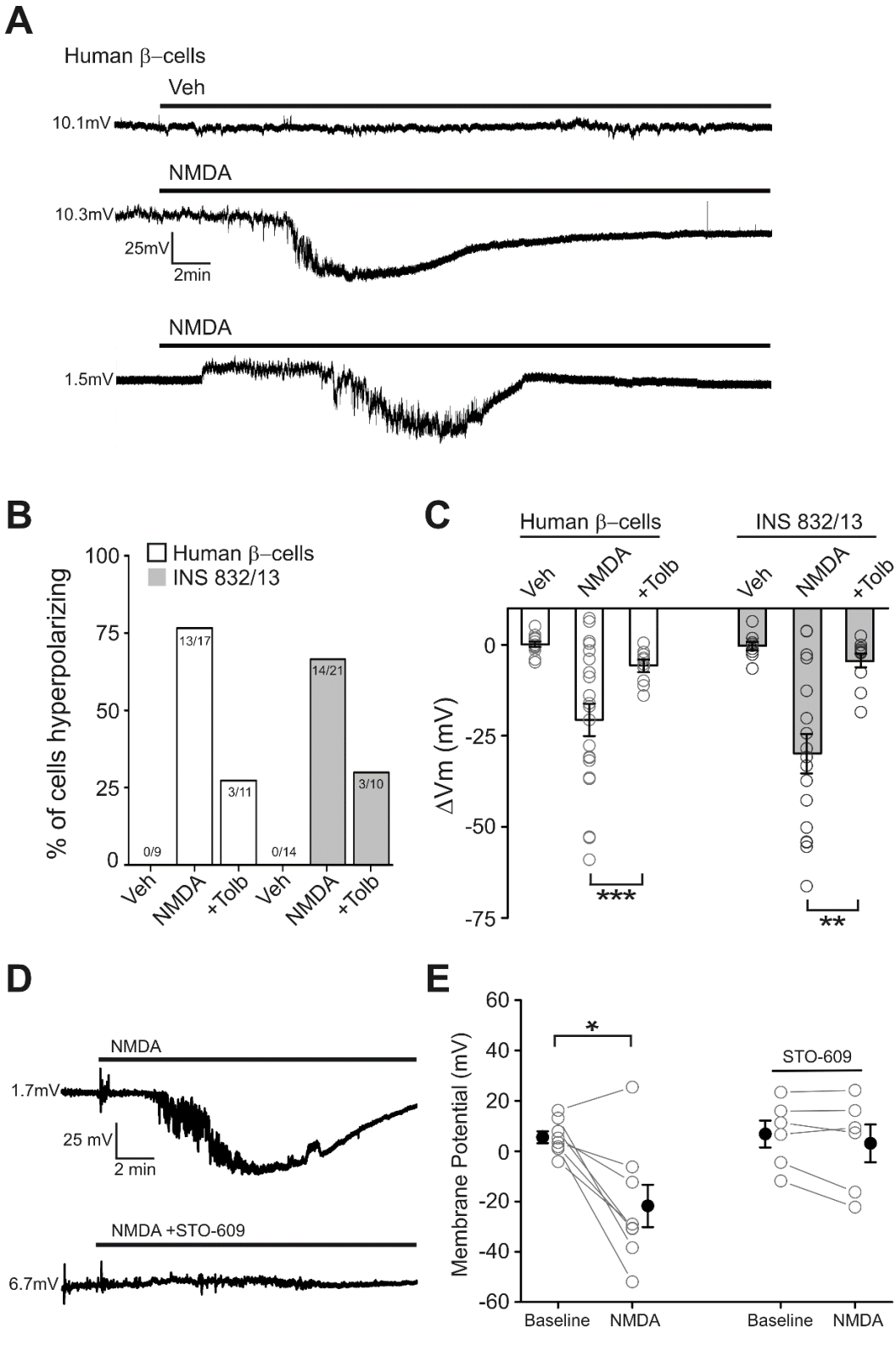
A
Human β–cells
Veh
10.1mV
NMDA
10.3mV
25mV
2min
NMDA
1.5mV
B
Human β–cells
INS 832/13
% of cells hyperpolarizing
100
75
50
25
0
13/17
3/11
14/21
3/10
0/9
0/14
Veh
NMDA
+Tolb
Veh
NMDA
+Tolb
C
Human β–cells
INS 832/13
Veh
NMDA
+Tolb
Veh
NMDA
+Tolb
ΔVm (mV)
0
-25
-50
-75
***
**
D
NMDA
1.7mV
25 mV
2 min
NMDA +STO-609
6.7mV
E
Membrane Potential (mV)
60
40
20
0
-20
-40
-60
*
STO-609
Baseline
NMDA
Baseline
NMDA

Figure 3. 5. Activation of NMDARs is sufficient to induce K_{ATP}-dependent hyperpolarization in INS-832/13 and human β-cells.

(**A**) Representative cell-attached voltage traces recorded from human β-cells incubated in Tyrode's supplemented with 0.1 mM glycine and 11 mM glucose before and after perfusion of vehicle (top trace) or 50 µM NMDA (middle and bottom traces). In a subset of cells tested NMDA also induced a small membrane depolarization prior to the induction of hyperpolarization (bottom trace). The initial membrane potential for each cell, averaged over the first 2 min, is given to the left of each trace. (**B**) Bar graph depicting the percentage of human β-cells (white filled bars) and INS-832/13 cells (grey filled bars) that hyperpolarized in response to vehicle only or NMDA in the absence or presence of tolbutamide. The number of cells tested is provided for each condition. (**C**) Group data illustrating the average degree of hyperpolarization observed in human β-cells and INS-832/13 cells for each condition. Data are shown as means ± SEM (bars) along with individual cell responses (open circles). $^{**}p < 0.01$, $^{***}p < 0.001$. (**D**) Example traces of NMDA induced membrane hyperpolarization in an individual INS-832/13 cell in the absence (top trace) or presence of the CaMKKβ inhibitor STO-609 (10 µM; bottom trace). (**E**) Plot of individual changes (open circles) in membrane potential measured in INS-1 832/13 cells before and after bath application of NMDA in the absence (n=8) or presence of STO-609 (n=6). Means ± SEM are indicated by filled circles. $^{*}p < 0.05$.

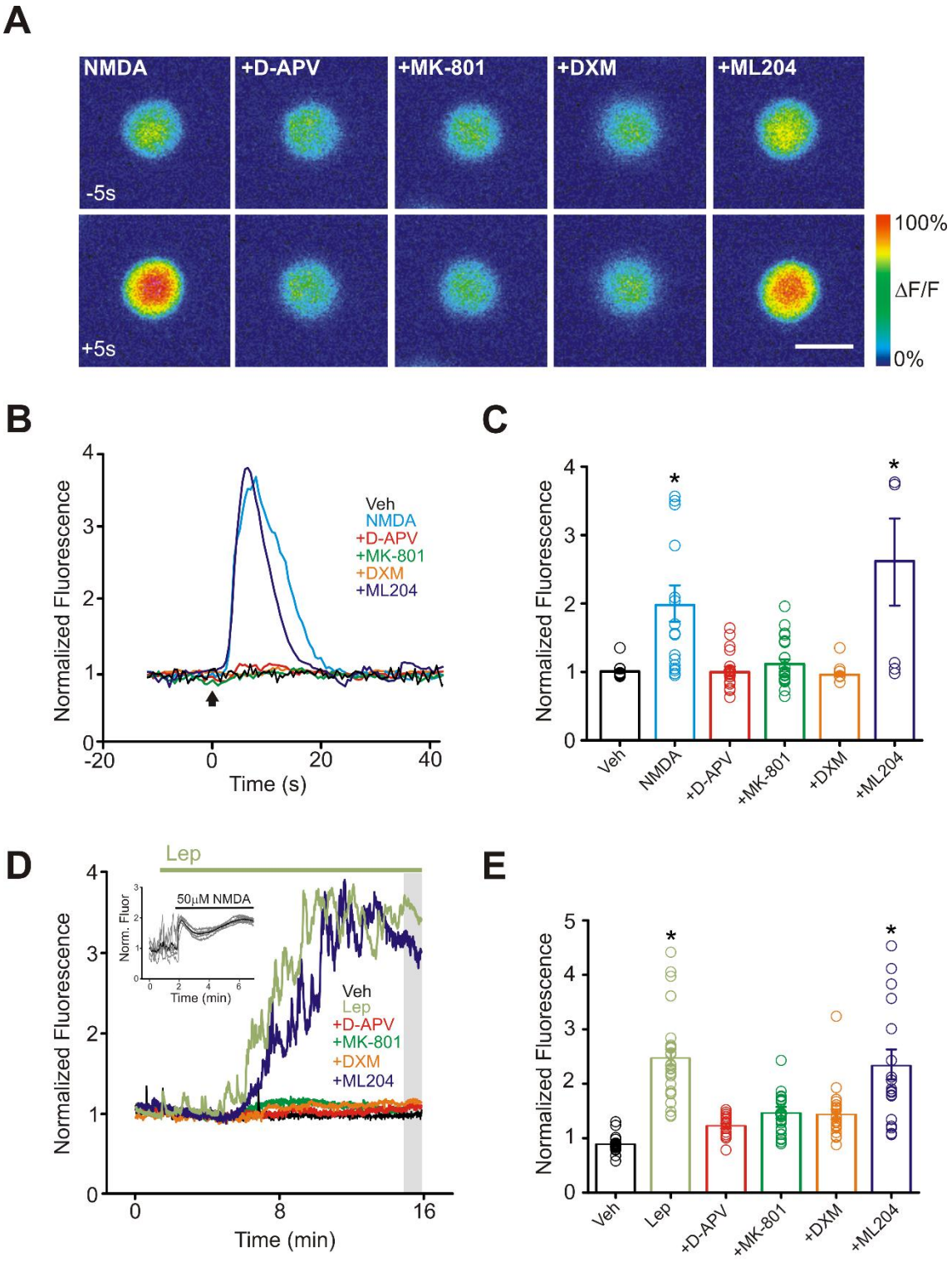
A
NMDA
+D-APV
+MK-801
+DXM
+ML204
-5s
+5s
100%
ΔF/F
0%
B
Normalized Fluorescence
Time (s)
Veh
NMDA
+D-APV
+MK-801
+DXM
+ML204
C
Normalized Fluorescence
Veh
NMDA
+D-APV
+MK-801
+DXM
+ML204
D
Lep
50μM NMDA
Norm. Fluor
Time (min)
Normalized Fluorescence
Time (min)
Veh
Lep
+D-APV
+MK-801
+DXM
+ML204
E
Normalized Fluorescence
Veh
Lep
+D-APV
+MK-801
+DXM
+ML204

Figure 3. 6. Leptin-induced Ca^{2+} increases recorded from INS-832/13 cells require NMDARs.

(**A**) ΔF/F pseudo colored images of individual INS-1 832/13 cells loaded with the Ca^{2+} indicator Fluo-4 AM. Cells were bathed in Tyrode's solution supplemented with 0.1 mM glycine but no Mg^{2+} or glucose during recording (see Experimental Procedures). Images were taken 5s before and 5s after a puff of 100 µM NMDA in the absence or presence of D-APV (50 µM), MK-801 (50 µM), DXM (10 µM), or ML204 (50 µM); scale bar = 10 µm. (**B**) Representative Ca^{2+} transients corresponding to the conditions shown in panel A. Arrow denotes time of the NMDA puff. (**C**) Group data showing the baseline normalized changes in fluorescence for each condition. Color bars correspond to representative Ca^{2+} transients shown in panel B. Data are shown as means ± SEM (bars) along with individual cell responses (open circles). *$p < 0.05$. (**D**) Representative Ca^{2+} transients recorded before and after bath application of 10 nM leptin in the absence or presence of D-APV, MK-801, DXM, or ML204 (10 µM). Gray bar denotes time used to quantify the mean change in fluorescence. Inset shows responses to bath application of 50 µM NMDA. (**E**) Group data for baseline normalized changes in fluorescence for each condition. Color bars correspond to representative Ca^{2+} transients shown in panel D. Data are shown as means ± SEM (bars) along with individual cell responses (open circles). *$p < 0.05$.

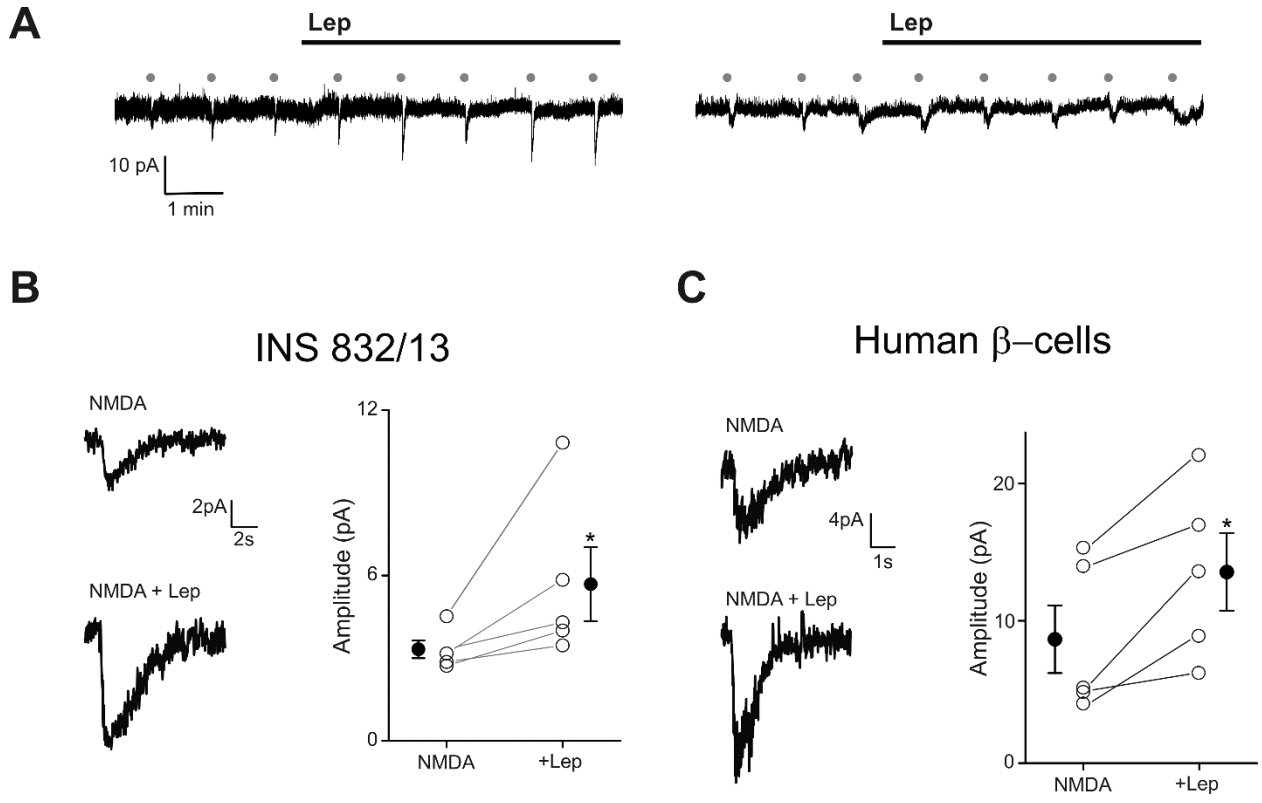

Figure 3. 7. Leptin potentiates NMDAR currents.

(**A**) Whole cell NMDA current responses recorded from an INS-1 832/13 cell bathed in Tyrode's solution supplemented with 0.1 mM glycine but no Mg^{2+} or glucose that potentiated (left) or failed to potentiate (right) in the presence of leptin. Cell were recorded from a holding potential of -70 mV. Small black dots indicate time of NMDA puff. Group data for five INS-1 832/13 cells (**B**) or five human β-cells (**C**) showing the mean (filled circles) and individual (open circles) NMDA current amplitudes before and after leptin. *$p < 0.05$.

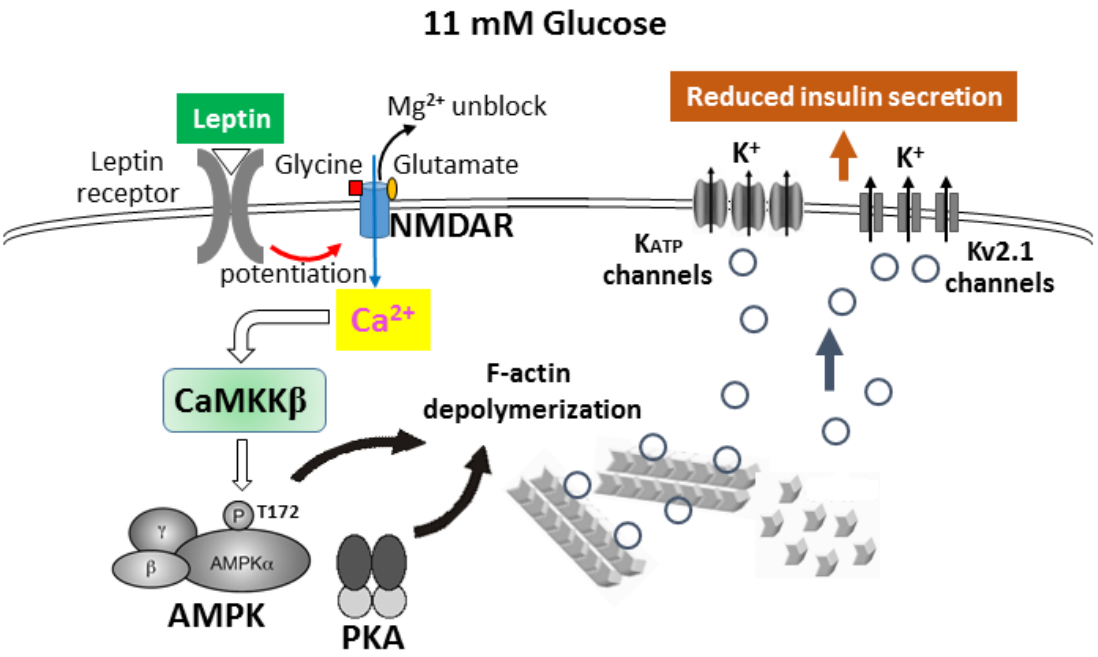

Figure 3. 8. Proposed model depicting leptin signaling through NMDARs to regulate potassium channel trafficking in β-cells.

Under 11 mM glucose, β-cells are depolarized such that NMDARs are not blocked by Mg^{2+} and are activated by glutamate and glycine present in the extracellular milieu. Binding of leptin to its receptor potentiates NMDAR currents, which leads to an increase in Ca^{2+} influx, activation of CaMKKβ and phosphorylation of T172 on AMPKα, which then cause PKA-dependent F-actin depolymerization to promote K_{ATP} and Kv2.1 channel trafficking to the plasma membrane. The increased K^+ efflux through increased surface density of Kv2.1 channels shortens action potentials and facilitates membrane repolarization, while the increased K^+ efflux through increased surface K_{ATP} channels leads to membrane hyperpolarization. Together, they reduce β-cell excitability and suppress insulin secretion.

3.6. Materials and methods

Cell culture. INS-1 832/13 cells were cultured in RPMI 1640 with 11.1 mM D-glucose (Invitrogen) supplemented with 10% fetal bovine serum (FBS), 100 U/ml penicillin, 100 µg/ml streptomycin, 10 mM HEPES, 2 mM glutamine, 1 mM sodium pyruvate, and 50 µM β-mercaptoethanol(64). Human β-cells were dissociated from human islets obtained through the Integrated Islets Distribution Program (IIDP) as described previously(58,65). Briefly, human islets were cultured in RPMI 1640 with 10% FBS and 1% L-Glutamine. For recording, islets were dissociated into single cells by trituration in a solution containing 116 mM NaCl, 5.5 mM D-glucose, 3 mM EGTA, and 0.1% bovine serum albumin (BSA), pH 7.4. Dissociated cells were then plated on gelatin (0.1%)-coated coverslips. For electrophysiological experiments β-cells were identified using 2 separate criteria. The first utilized the high autofluorescence signature of β-cells to 488 nm excitation as these cells have high concentrations of unbound flavin adenine dinucleotide(172) and the second criterion was that cells had an initial depolarizing membrane potential (~0 mV) in response to 11 mM glucose(165). Donor information for specific experiments is provided in Table 4.1.

Drug treatments. Leptin, tolbutamide, glutamate, and dextromethorphan were from Sigma (St. Louis, MO). NMDA, (R,S)-AMPA, MK-801, D-APV, STO-609, and ML204 were from Tocris Bioscience (Bristol, UK). For surface biotinylation experiments, INS-832/13 cells were incubated in regular RPMI 1640 medium without serum for 30 minutes before treatment with leptin or NMDA for 30 minutes. Where stated, pharmacological inhibitors were added 30 minutes before and during the addition of leptin and NMDA.

Immunoblotting. INS-1 832/13 cells were lysed in lysis buffer (50 mM Tris–HCl, 2 mM EDTA, 2 mM EGTA, 100 mM NaCl, 1% Triton-X-100, pH 7.4 with complete protease inhibitor) for 30 min at 4°C and cell lysates cleared by centrifugation at 21,000xg for 10 minutes at 4°C. Proteins were separated by SDS-PAGE (7.5-12.5%) and transferred onto nitrocellulose or PVDF membranes

(Millipore, Bedford, MA). Membranes were incubated overnight at 4°C with a primary antibody diluted in the Tris-buffered saline plus 0.1% Tween-20 (TBST) followed by incubation with horseradish peroxidase-conjugated secondary antibodies in TBST for 1 hour at room temperature. Antibodies against GluN1 and Kv2.1 (clone K89/34) were from NeuroMab (Davis, CA). Antibodies against AMPK and pAMPK were from Cell Signaling (Danvers, MA) and Millipore, respectively. Antibody for SUR1 was generated in rabbit using a C-terminal peptide (KDSVFASFVRADK) of hamster SUR1 as described previously(174). Blots were developed using Super Signal West Femto (Pierce) and imaged with FluorChemE (ProteinSimple, San Jose, CA). Blots were stripped and re-probed with anti-tubulin (Sigma) as a control for loading. The blots were quantified with Image J (NIH) and normalized to the corresponding controls.

Immunocytochemistry. INS-1 832/13 cells were fixed in 2% paraformaldehyde in phosphate-buffered saline (PBS) for 10 min at room temperature, permeabilized with 0.2% Triton X-100, and blocked for 60 min with 1% BSA in PBST (PBS+ 0.1% Tween 20) before being incubated overnight at 4°C with primary antibodies directed against GluN1 (NeuroMab) and insulin (Cell Signaling). Proteins were visualized using Cy3- and Alexa-488-conjugated secondary antibodies. Fluorescent images were acquired using a Zeiss LSM780 confocal microscope equipped with a 63x oil immersion objective. Images were processed and analyzed using NIH Image J software.

Electrophysiology. Electrical recordings were performed using an Axon 200B amplifier (Molecular Devices, Sunnyvale, CA) and were filtered at 2 kHz and digitized and acquired at 20 kHz using pCLAMP software. For whole-cell patch-clamp recordings cells were held at -70 mV or 40 mV using micropipettes pulled from non-heparinized Kimble glass (Thermo Fisher Scientific, Waltham, MA) filled with a solution containing in mM: 140 K-Gluconate, 6 EGTA, 10 HEPES, 5 K_2ATP, 1 $CaCl_2$ (pH 7.2; 3-5 MΩ tip resistance). External Tyrode solution contained in mM: 137 NaCl, 5.4 KCl, 1.8 $CaCl_2$, 0.5 $MgCl_2$, 5 Na-HEPES, 3 $NaHCO_3$, and 0.16 NaH_2PO_4, (pH 7.2). The external solution was supplemented with 0.1 mM glycine or 11 mM glucose, and in some

experiments Mg^{2+} was omitted, as specified in the figure legends. To induce glutamate or NMDA-mediated currents, glutamate (1 mM) or NMDA (1 mM) was puffed (3-5 psi for 0.5 s) with carbogen using 1-0.5 MΩ micropipettes connected to a Multi-function Microforge Controller DMF1000 (World Precision Instruments, Sarasota, FL) equipped with a pressure regulator.

Cell-attached recording electrodes were pulled as described above and filled with 140 mM NaCl, and had tip resistances of 2–6 MΩ. The liquid junction potential was calculated to be 0 mV. Seal resistances ranged from 1-5 GΩ between the recording pipette and the cell membrane. Membrane potentials were recorded in current-clamp mode. Signals were analyzed using Clampfit (pCLAMP).

Surface biotinylation. INS-1 832/13 cells were washed twice with cold PBS and incubated with 1 mg/ml EZ-Link Sulfo-NHS-SS-Biotin (Pierce) in PBS for 30 minutes on ice. The reaction was terminated by incubating cells for 5 minutes with PBS containing 50 mM glycine, followed by three washes with cold PBS. Cells were then lysed in 300 µl of lysis buffer as described above and 500 µg of total lysate was incubated with 100 µL of ~50% slurry of NeutraAvidin Agarose beads (Pierce) overnight at 4°C. Biotinylated proteins were eluted with 2× protein loading buffer for 15 min at room temperature. Both eluent and input samples (50 µg of total cell lysate) were analyzed by immunoblotting using anti-SUR1 or anti-Kv2.1 antibodies described previously(58,65).

Calcium imaging. INS-1 832/13 cells were loaded in the dark with 2 mM Fluo-4 AM (Thermo Fisher Scientific) according the manufacturer's instructions. To prevent indicator extrusion by organic-anion transporters probenecid (2.5 mM) (Thermo Fisher Scientific) was added during loading(175). Cells were then imaged on an upright Leica microscope outfitted with a 40x water immersion objective (0.8 NA) and a Polychrome IV monochromator light source (TILL Photonics, Munich, Germany) and were continuously perfused with Tyrode's solution (with 0.1 mM glycine but no Mg^{2+} or glucose) at room temperature (21–25°C). Note glucose was not included to avoid glucose-induced Ca^{2+} signals, which would make it difficult to discern NMDA or leptin-evoked

Ca^{2+} signals; Mg^{2+} was also not included to avoid blocking of NMDARs under no glucose conditions. Fluo-4 fluorescence was excited at 480 nm, and fluorescence emission was filtered through a 525 (50)-nm single-band bandpass filter (Chroma Technology, Bellows Falls, VT). Images were acquired using a 12 bit ORCA-ER CCD camera (Hamamatsu, Japan) controlled by the Metafluor image acquisition software (Molecular Devices). Images were acquired every 0.5 sec and digitized. Fluorescence intensity was analyzed post hoc in regions of interest (ROIs) manually drawn around individual INS-1 832/13 cells using Metafluor. Changes in intracellular Ca^{2+} concentration were normalized to baseline and expressed as a fold change in $\Delta F/F_0=((F-F_0)/F_0)$, where F_0 is the average, background-subtracted baseline fluorescence and F is the fluorescence intensity immediately following the addition of NMDA or leptin.

Statistical analysis. Results are expressed as mean ± standard error of the mean (SEM). Differences were tested using one-way ANOVA followed by the *post-hoc* Dunnett's test for multiple comparisons. When only two groups were compared, unpaired or paired Student's *t*-tests were used where indicated. The level of statistical significance was set at $p < 0.05$.

Chapter 4: Leptin modulates pancreatic β-cell membrane potential through Src kinase-mediated phosphorylation of NMDA receptors

Veronica A. Cochrane[1], Yi Wu[1], Zhongying Yang[1], Assmaa ElSheikh[1, 2], Jeremy Dunford[3], Paul Kievit[4], Dale A. Fortin[1, 3, †], and Show-Ling Shyng[1,†]

[1]Department of Chemical Physiology and Biochemistry, Oregon Health & Science University, Portland, OR 97239, USA; [2]Department of Medical Biochemistry, Tanta University, Tanta, Egypt; [3]Department of Integrated Physiology and Neuroscience, College of Arts and Sciences, Washington State University, Vancouver, WA 98686; [4]Division of Cardiometabolic Health, Oregon National Primate Research Center, Beaverton, OR 97006.

This work was originally published in

The Journal of Biological Chemistry 2020; 295(50): 17281-17297

DOI: 10.1074/jbc.RA120.015489

[†]To whom correspondence may be addressed: Show-Ling Shyng, Department of Chemical Physiology and Biochemistry, School of Medicine, Oregon Health & Science University, 3181 S.W. Sam Jackson Park Road, Portland, OR 97239, Tel. (503) 494-2694; Fax: (503) 494-3849; Email:shyngs@ohsu.edu; or Dale A. Fortin, Department of Integrated Physiology and Neuroscience, College of Arts and Sciences, Washington State University, 14204 NE Salmon Creek Ave, Vancouver, WA, Tel. (360)456-9720; Email: dale.fortin@wsu.edu.

Author contributions: VC*, YW, and DF designed and performed experiments, analyzed data, and wrote the manuscript; ZY, AE and JD performed experiments; PK provided mouse islets and edited the manuscript; SLS conceived the project, analyzed data and wrote the manuscript. All authors have full access to all the data in the study and take responsibility for the integrity of the data and the accuracy of the data analysis. All authors reviewed the results and approved the final version of the manuscript.
*VC performed experiments in Fig. 1D, Fig. 4A, B, Fig. 5E, F, and Fig. 7.

Acknowledgements: We thank Dr. Christopher Newgard for the rat insulinoma INS-1 clone 832/13 cells. This work was supported by National Institutes of Health grant R01DK057699 and 3R01DK057699-14S1 (to Show-Ling Shyng). Dr. Paul Kievit acknowledges the support of NIH P51 OD011092 for the Oregon National Primate Research Center.

4.1. Abstract

The adipocyte-derived hormone leptin increases trafficking of K_{ATP} and Kv2.1 channels to the pancreatic β-cell surface, resulting in membrane hyperpolarization and suppression of insulin secretion. We have previously shown that this effect of leptin is mediated by the NMDA subtype of glutamate receptors (NMDARs). It does so by potentiating NMDAR activity, thus enhancing Ca^{2+} influx and the ensuing downstream signaling events that drive channel trafficking to the cell surface. However, the molecular mechanism by which leptin potentiates NMDARs in β-cells remains unknown. Here we report that leptin augments NMDAR function via Src kinase-mediated phosphorylation of the GluN2A subunit. Leptin-induced membrane hyperpolarization diminished upon pharmacological inhibition of GluN2A but not GluN2B, indicating involvement of GluN2A-containing NMDARs. GluN2A harbors tyrosine residues which when phosphorylated by Src family kinases potentiate NMDAR activity. We found that leptin increases phosphorylation of Y418 in Src, an indicator of kinase activation. Pharmacological inhibition of Src or overexpression of a kinase-dead Src mutant prevented the effect of leptin, while a Src kinase activator peptide mimicked it. Using mutant GluN2A overexpression, we show that Y1292 and Y1387 but not Y1325 are responsible for the effect of leptin. Importantly, β-cells from *db/db* mice, a type 2 diabetes mouse model lacking functional leptin receptors, or from obese diabetic human donors failed to respond to leptin but hyperpolarized in response to NMDA. Our study reveals a signaling pathway wherein leptin modulates NMDARs via Src to regulate β-cell excitability and suggests NMDARs as a potential target to overcome leptin resistance.

4.2. Introduction

Leptin is an adipocyte-produced hormone, which plays a key role in body weight regulation. The physiological actions and signaling mechanisms of leptin in the central nervous system have been extensively studied. Less well understood is the function and mechanism of leptin signaling in peripheral tissues. In pancreatic islets, leptin has been reported to downregulate glucose-stimulated insulin secretion more than two decades ago(39–42,44,176). Recent studies find that leptin stimulates potassium channel trafficking to the cell surface to reduce β-cell excitability(57,58,65). Specifically, leptin causes a transient increase in the number of ATP-sensitive potassium (K_{ATP}) channels and Kv2.1 channels in the β-cell plasma membrane(65). K_{ATP} channels control β-cell resting membrane potential and couple blood glucose with insulin secretion, while Kv2.1 channels play a prominent role in action potential repolarization to stop insulin secretion(177,178). The increased surface abundance of these channels would reduce β-cell excitability and thus explain how leptin inhibits glucose-stimulated insulin secretion.

Leptin signaling is complex and multiple signal transduction pathways have been described(179,180). The best characterized is JAK2-dependent phosphorylation of STAT3 following activation of the ObRb receptor, but PI3K/Akt, MAPK, AMPK and Src family kinases (SFKs) are also possible downstream effectors(87,180). In addition, transactivation of other cytokine receptors via leptin signaling has also been implicated(180). Studies into the mechanisms by which leptin regulates K_{ATP} and Kv2.1 channel trafficking so far have identified several key molecular players. These include the NMDA subtype glutamate receptors (NMDARs), calcium/calmodulin-dependent protein kinase kinase β (CaMKKβ), AMPK and PKA(181). Evidence that has emerged reveals a novel signaling pathway wherein leptin potentiates NMDAR function to increase Ca^{2+} influx, resulting in activation of CaMKKβ, which phosphorylates and activates AMPK; AMPK in turn causes PKA-dependent actin depolymerization, culminating in increased trafficking of K_{ATP} and Kv2.1 channels to the β-cell surface. A key question of how leptin potentiates NMDAR activity, however, has yet to be addressed.

NMDARs are calcium-permeant ionotropic glutamate receptors that are highly expressed in the brain and are important for learning and memory(145). Although they are extensively studied in the central nervous system, there is growing evidence that they are expressed in pancreatic β-cells and play a role in regulating insulin secretion(78,82,182). Functional NMDARs generally form as heterotetramers of two obligatory glycine-binding GluN1 subunits (also known as NR1) and two glutamate-binding GluN2 (GluN2A-D, or NR2A-D) subunits(183). NMDARs containing GluN2A and 2B subunits are highly sensitive to blockade by extracellular Mg^{2+} under negative membrane potential and require membrane depolarization to remove Mg^{2+} block for activity, while those with GluN2C and 2D subunits are significantly less sensitive to external Mg^{2+} (145,183,184). Additionally, NMDAR activity can be modulated by post-translational modifications. In particular, GluN2A and GluN2B have long cytoplasmic tails which are known to be phosphorylated at serine/threonine and/or tyrosine residues by a variety of kinases including CDK5, PKA, PKC, CaMKII, Casein kinase II, and protein tyrosine kinases(83). In neurons, these phosphorylation modifications have been linked to regulation of NMDAR trafficking, localization and function [reviewed in (185)]. For example, phosphorylation of several tyrosine residues in GluN2A by Src family kinases (SFKs) have been shown to enhance NMDAR activity(84,186). Of note, Src activation is one of the many downstream signaling events that have been reported following stimulation of the ObRb leptin receptor by leptin(77,86,87), raising the possibility that leptin may signal through Src family kinases to modulate NMDAR activity in pancreatic β-cells.

Here, we present evidence that leptin activates Src to phosphorylate GluN2A containing NMDARs in pancreatic β-cells, which results in potentiation of NMDAR currents and increased trafficking of K_{ATP} and Kv2.1 channels to the cell surface to hyperpolarize β-cell membrane potential. Importantly, we show that leptin fails to induce membrane hyperpolarization in β-cells from the leptin-resistant *db/db* mice and obese diabetic human donors. Interestingly, direct activation of NMDARs by NMDA was able to mimic the effect of leptin. As leptin resistance is

frequently associated with obesity-related diabetes, NMDARs may be a potential target to overcome leptin resistance in diabetic β-cells.

4.3. Results

4.3.1. Leptin hyperpolarizes pancreatic β-cells through GluN2A-containing NMDARs

In rodent pancreatic β-cell lines as well as primary human β-cells, leptin induces membrane hyperpolarization at glucose concentrations that depolarize β-cell membrane potential(39,57,58,65,182). Recently, we showed that, both in rat insulinoma INS-1 832/13 cells and human β-cells, this effect is mediated by NMDARs(182). Leptin stimulation increased NMDA currents, leading to increased Ca^{2+} influx and increased surface density of K_{ATP} and Kv2.1 channels(182). To determine the mechanism by which leptin increases NMDA currents, we began by characterizing the NMDARs that are expressed in β-cells. Functional NMDARs that are Ca^{2+} permeant are tetramers of two GluN1 subunits and two of four different GluN2 subunits, GluN2A, 2B, 2C, and 2D(183). The GluN1 subunit is obligatory and is encoded by a single gene *Grin1*. In contrast, GluN2 subunits are encoded by four different genes: *Grin2a*, *Grin2b*, *Grin2c*, and *Grin2d* for GluN2A-D(183). We first examined the expression of these subunits at the mRNA level in INS-1 832/13 cells by RT-PCR. Transcripts for *Grin1*, *Grin2a*, *Grin2b*, and *Grin2d* were clearly detected but not *Grin2c* (Fig. 4.1.A), suggesting that these cells express GluN1, GluN2A, 2B, 2D but not GluN2C.

NMDARs containing GluN2A or 2B are much more sensitive to external Mg^{2+} block than those containing GluN2C or 2D(183,187). We thus tested Mg^{2+} sensitivity of NMDA currents using whole-cell recording as an indicator of the GluN2 subunit composition. Puff application of NMDA (1 mM) at a holding potential of -70mV in Mg^{2+} free external solution elicited NMDA currents that were reduced by >80% upon addition of $MgCl_2$ (100 μM) to the external solution (from 11.3 ± 2.6 pA to 1.3 ± 0.5 pA, n=4; $p<0.05$ by paired t-test) (Fig. 4.1.B, C). The strong Mg^{2+} block observed is characteristic of NMDARs containing GluN2A and/or GluN2B subunits(184,187), suggesting

that NMDARs at the surface of these cells are largely made up of GluN1 and GluN2A and/or GluN2B subunits. Consistently, in western blot experiments, GluN1 and GluN2A were readily detectable in total cell lysate and further enriched in the membrane fraction, whereas GluN2B was barely detectable in total cell lysate but clearly seen in the membrane fraction (Fig. 4.1.D).

Since both GluN2A and 2B could potentially mediate the leptin response, we sought to determine their relative contributions using subunit specific inhibitors: TCN-201 for GluN2A and Ro 25-6981 for GluN2B(183,188,189). Hyperpolarization of membrane potential in Tyrode's solution containing 11mM glucose was used as a readout for leptin response. Because GluN2A inhibition by TCN-201 is dependent on glycine, which at higher concentrations render the drug less effective(189), we reduced the glycine supplement in Tyrode's solution from 100μM to 50μM. These experiments were performed using cell-attached current-clamp recording, which provides a robust assessment of changes in membrane potential while maintaining cell integrity and preventing dialysis of soluble factors that may be important for intracellular signaling(157,190). Bath application of leptin alone (10 nM) induced a mean membrane hyperpolarization of −46.8 ± 8.1 mV, similar to that reported previously(65,182). However, co-application of the GluN2A selective antagonist TCN-201 (50 μM) with leptin only induced a mean hyperpolarization of -14.4 ± 3.9 mV, significantly less than that observed in cells treated with leptin alone (Fig. 4.1.E, F). By contrast, co-application of the GluN2B selective antagonist Ro 25-6981(191) had little effect on the ability of leptin to hyperpolarize INS-1 832/13 cells (Ro 25-6981 at 1μM, ΔV_m= -35.8 ± 3.8 mV; Fig. 4.1.E, F). These results suggest that GluN2A is largely responsible for mediating the effect of leptin. Note, there is evidence that GluN2A can form diheteromeric GluN1/GluN2A or triheteromeric GluN1/GluN2A/GluN2B complexes(183). Since the potency and efficacy of TCN-201 and Ro 25-6981 have been shown to be reduced for triheteromeric GluN1/GluN2A/GluN2B channels especially for Ro25-6981(188,192), the lack of effect by Ro25-6981 in our experiment does not allow us to exclude the involvement of GluN1/GluN2A/GluN2B heteromers, as both

GluN2A and GluN2B (albeit less abundant compared to GluN2A based on western blot of total cell lysate) were detected in membrane fractions prepared from INS-1 832/13 cells by western blot (Fig. 4.1.D).

4.3.2. Leptin regulates NMDAR activity via Src family kinases

In contrast to GluN1 which has a relatively small cytoplasmic domain of ~100 amino acids, GluN2A has a long cytoplasmic tail of ~600 amino acids that contains potential phosphorylation sites for a number of protein kinases, including PKA, PKC, CDK5, and the SFKs(83). Phosphorylation by PKC(193), CDK5(194), and Src(186,195) in particular has been reported to potentiate NMDAR currents. We therefore monitored changes in INS-1 832/13 cell membrane potentials in response to leptin in the absence or presence of inhibitors for the various kinases. Neither roscovitine (Ros; 10 µM), an inhibitor of CDK5 kinase, nor Go 6983 (Go; 10 µM), a broad-spectrum PKC kinase inhibitor had significant effects on leptin-induced hyperpolarization (ΔV_m= -32.4 ± 4.1mV for leptin alone; ΔV_m= -39.3 ± 7.0 mV for roscovitine plus leptin; ΔV_m= -33.7 ± 5.5 mV for Go 6983 plus leptin; Fig. 4.2.A, B). By contrast, AZD0530 (AZD; 10 µM), also known as saracatinib(196), a broad-spectrum inhibitor of Src family kinases, markedly reduced the ability of leptin to induce membrane hyperpolarization (ΔV_m= -4.8 ± 3.1 mV, p<0.0005 compared to leptin alone; Fig.2A, B), but had no effect on membrane hyperpolarization triggered by direct activation of NMDARs via NMDA (NMDA: ΔV_m = -35.3 ± 8.9 mV, n=7; NMDA plus AZD0530: ΔV_m= -30.4 ± 9.9 mV, n=7). Another tyrosine kinase inhibitor, dasatinib (Das; 25 µM)(196) also abrogated the effect of leptin, resulting in only a small hyperpolarization (ΔVm= -7.0 ± 2.4 mV, p<0.0005 compared to leptin alone; Fig. 4.2.B). These results indicate that SFKs but not CDK5 nor PKC are likely involved in the leptin-induced membrane hyperpolarization observed in INS-1 832/13 cells.

Next we determined whether activation of SFKs via an activating phosphopeptide EPQpYEEIPIYL (referred to as YEEI), which binds to SH2 domain to relieve kinase autoinhibition(197,198) could mimic the effects of leptin and induce membrane hyperpolarization.

For these experiments, whole-cell current-clamp recordings of INS-1 832/13 cells were carried out in order to apply YEEI intracellularly through the patch pipet. Under whole-cell conditions with 5mM ATP in the pipet solution (estimated intracellular [ATP] with 11 mM glucose in the bath solution), inclusion of YEEI phosphopeptide induced significant membrane hyperpolarization (ΔV_m = -21.1 ± 4.1 mV from break-in to steady state, n=7) compared to the control without the peptide (ΔV_m = -4.9 ± 4..0 mV from break-in to steady state, n=6) (Fig. 4.2.C,D). The result supports the notion that direct activation of SFKs is sufficient to mimic the effect of leptin and cause β-cell membrane hyperpolarization.

To directly test whether SFKs underlie the potentiation of NMDAR currents by leptin we performed whole-cell recording of NMDAR currents and monitored how current amplitudes were affected by leptin and the SFK inhibitor AZD0530. In the absence of leptin, repeated puff applications of 1mM NMDA at one minute intervals elicited NMDAR currents of similar amplitudes. Bath application of 10nM leptin potentiated NMDA-evoked currents within 5 min of leptin treatment from a baseline of 14.8 ± 8.0 pA to 25.8 ± 13.3 pA (p<0.05 by Friedman's test; Fig. 4.3.), as we reported previously(182). Subsequent co-application of 10 μM AZD0530 with leptin abolished the effect of leptin, with averaged NMDA currents of 15.5 ± 8.7 pA comparable to baseline values (Fig. 4.3.). These results provide direct evidence that leptin-mediated potentiation of NMDAR currents requires SFKs.

4.3.3. Leptin modulation of NMDAR activity requires phosphorylation of GluN2A at Y1292 and Y1387

SFKs have been reported to potentiate NMDAR currents by phosphorylating GluN2(185,199,200). Specifically, three tyrosine residues in GluN2A (Y1292, Y1325 and Y1387) have been identified as targets of SFK-mediated phosphorylation to enhance NMDAR function in different experimental systems(84,186,199,201). To determine whether these sites play a role in leptin-induced membrane hyperpolarization we mutated the three tyrosine residues in GluN2A to

phenylalanines together GluN2A^{Y1292F,Y1325F,Y1387F} as well as individually (GluN2A^{Y1292F}, GluN2A^{Y1325F}, GluN2A^{Y1387F}). To facilitate visualization of expression, a GluN2A construct fused to GFP at its extracellular N-terminus was used(202). INS-1 832/13 cells were then transfected to express WT or phosphomutants. To confirm that exogenously expressed GFP-GluN2A co-assembles with endogenous GluN1, we performed co-immunoprecipitation experiments using an anti-GFP nanobody. Both GluN1 and GFP-GluN2A were present in the immunoprecipitate as detected by anti-GFP, anti-GluN2A, and anti-GluN1 antibodies in western blots (Fig. 4.4.A), indicating association of transfected GluN2A with endogenous GluN1. Surface staining of the GFP tag further demonstrates that transfected WT and mutant GluN2A were expressed in the plasma membrane (Fig. 4.4.B).

Changes in membrane potential following leptin treatment were again monitored using cell-attached current-clamp recording. We first compared cells expressing GFP-GluN2A^{WT} with those expressing the GFP-GluN2A^{Y1292F,Y1325F,Y1387F} triple phenylalanine mutant. GFP-negative cells on the same coverslip were also examined as untransfected controls. Representative membrane potential traces from untransfected and cells expressing GFP-GluN2A^{WT} or triple phosphomutant GFP-GluN2A^{Y1292F,Y1325F,Y1387F} are shown in Fig. 4.4.C. Leptin application to untransfected cells induced a mean hyperpolarization of -51.1 ± 5.6 mV (n=10) that was not statistically different than leptin responses in cells expressing GluN2A^{WT} (-48.0 ± 6.5 mV, n=13). By contrast, leptin had little hyperpolarizing effect in cells expressing the triple phosphomutant (Fig. 4.4.C,D; GluN2A^{Y1292F,Y1325F,Y1387F} ΔV_m = -12.0 ± 1.7 mV; n=18; p<0.0005 by unpaired t-test compared to untransfected cells). The diminished response is not due to disruption of K_{ATP} channel gating or expression as the K_{ATP} activator diazoxide (200 μM) was fully able to hyperpolarize cells expressing GluN2A^{Y1292F,Y1325F,Y1387F} (ΔV_m = -52.7 ± 4.9 mV; n=14) (Fig. 4.4.D). Moreover, we tested the response of cells expressing GluN2A^{Y1292F,Y1325F,Y1387F} to NMDA, which we have shown hyperpolarizes cells in the absence of leptin(182). We found that NMDA hyperpolarized INS-1 832/13 cells by an average of -38.8 ± 7.0 mV (n=11), suggesting that the GluN2A phosphomutant

also did not disrupt NMDAR expression or function (Fig. 4.4.D). To determine the relative contributions of the three tyrosine residues, we next tested the membrane potential response to leptin in cells expressing GluN2A^{Y1292F}, GluN2A^{Y1325F} or GluN2A^{Y1387F}. In this cohort of cells, leptin application caused a mean hyperpolarization of -47 ± 3.8 mV in untransfected (n=26) (Fig. 4.4.E, F). Interestingly, leptin still hyperpolarized cells transfected with GluN2A^{Y1325F} (ΔV_m = -41.7 ± 4.1 mV; n=16), not significantly different from untransfected cells. By contrast, in cells expressing GluN2A^{Y1292F} or GluN2A^{Y1387F} the response to leptin was significantly reduced (Fig. 4.4.E,F; ΔV_m for GluN2A^{Y1292F} = -17.4 ± 4.1 mV, n=19, and ΔV_m for GluN2A^{Y1387F} = -24.3 ± 4.7 mV, n=15; p<0.0005 by unpaired t-test). Taken together, these results identify the tyrosine phosphorylation sites Y1292 and Y1387 in GluN2A as responsible for mediating the leptin effect.

4.3.4. Leptin activates Src kinase in β-cells

The above results suggest that leptin likely activates SFKs to modulate NMDAR currents. Studies of GluN2A phosphorylation using in vitro or the HEK293 cell heterologous expression systems have found that both Src and Fyn can phosphorylate GluN2A(84). Src, when activated, autophosphorylates a highly conserved tyrosine residue Y418 in the catalytic domain of Src kinase, which is required for its full catalytic activity(203,204). Increased phosphorylation of Y418 is therefore indicative of kinase activation. We used an antibody raised against a peptide containing Src-pY418 to monitor Src phosphorylation in order to directly test whether leptin activates Src. Immunocytochemistry experiments were carried out on INS-1 832/13 cells treated with or without leptin (10 nM for 10min) in the presence or absence of the tyrosine kinase inhibitor dasatinib (50 μM). We found that leptin induced a significant increase in Src-pY418 staining as compared to matched controls with prominent staining at the cell periphery (Fig. 4.5.A,B) that was inhibited by co-application of dasatinib (Fig. 4.5.A,B). Further biochemical experiments using similar treatment conditions were carried out. In good agreement with the immunostaining results, leptin increased the ratio of phosphorylated to total Src by 176.0 ± 30.0% as compared to controls

(p<0.05 by unpaired t-test) which was reduced to 102.1 ± 40.4% of controls when co-applied with dasatinib (Fig. 4.5.C,D). Since the Src-pY418 antibody also recognizes conserved corresponding phosphopeptide in other SFKs including Fyn, and since both Src and Fyn are expressed in β-cells(205), we further tested the requirement of Src activity in leptin-induced response by expressing a dominant negative kinase-dead Src mutant(206) (see Materials and methods) in INS-1 832/13 cells. For this, we monitored leptin-induced increase of K_{ATP} channel surface expression by surface biotinylation, as described in our previous studies(58,65). As expected, leptin caused an increase in surface biotinylated SUR1, the regulatory subunit of the β-cell K_{ATP} channel, in control cells. However, in cells transfected with the kinase-dead Src mutant leptin failed to show an increase in surface biotinylated SUR1 (Fig. 4.5.E,F). This result lends further support to the requisite role of Src activity in mediating the effect of leptin on K_{ATP} channel trafficking.

4.3.5. Leptin signaling through Src-mediated phosphorylation of GluN2A is conserved in human β-cells

We have previously shown that leptin induces hyperpolarization that is dependent on NMDARs in human β-cells as in INS-1 832/13 cells(182). Having found that leptin potentiates NMDARs via Src-mediated phosphorylation of GluN2A in INS-1 832/13 cells, we next tested whether the same mechanism applies to human β-cells. Cell-attached current-clamp recordings were made in human β-cells dissociated from islets of three different non-diabetic donors obtained through the Integrated Islets Distribution Program (IIDP). All donor information can be found in Table 4.1. Bath application of leptin alone induced a mean membrane hyperpolarization of −43.7 ± 8.9 mV (n = 9 cells from 3 donors) (Fig. 4.6.A, B). The GluN2A selective inhibitor TCN-201 largely eliminated the leptin response (ΔV_m= -9.1 ± 4.2 mV, n = 12 cells from 3 donors; p<0.05, unpaired t-test) (Fig. 4.6.A, B), suggesting that GluN2A containing NMDARs underlie leptin signaling in human β-cells. We next tested whether leptin modulation of NMDARs and membrane

potential in human β-cells requires Src. As shown in the example traces in Fig.6C, the SFK inhibitor AZD0530 nearly abolished the ability of leptin to hyperpolarize human β-cells (ΔV_m= -0.4 ± 1.2 mV; n = 6 from 2 non-diabetic donors), while another SFK inhibitor dasatinib also diminished leptin-induced hyperpolarization albeit to a lesser extent (ΔV_m= -13.5 ± 2.8 mV, n = 7 cells from 3 donors) compare to human β-cells treated with leptin alone (ΔV_m= -33.5 ± 6.0 mV; n = 17 from 5 non-diabetic donors; p<0.0005 between AZD0530 and control, and p<0.05 between dasatinib and control, Welch's t-test) (Fig. 4.6.D). Taken together, results from both INS-1 832/13 and human β-cells establish a mechanistic link between leptin receptor signaling and modulation of GluN2A containing NMDARs via Src kinase.

4.3.6. Leptin signaling through NMDARs is disrupted in β-cells from *db/db* mice and from human Type 2 diabetic donors.

Leptin resistance is a common pathological feature of type 2 diabetes associated with obesity(207). To test how the leptin signaling pathway pertinent to this study is affected in diabetic β-cells, we examined β-cells from leptin-insensitive *db/db* mice, which harbors a mutation in the leptin receptor gene that renders ObRb signaling defective(208), as well as from human obese type 2 diabetic donors. Cell-attached recordings of membrane potential in β-cells isolated from C57BL/6J (WT) mice showed a clear response to leptin with a ΔV_m of -33.5 ± 5.2 mV (n=8), as expected. By contrast, β-cells isolated from *db/db* mice failed to respond to leptin (10 nM leptin for 15min, ΔV_m = -0.4 ± 0.4 mV, n=6, p<0.0001), although subsequent application of the K_{ATP} channel opener diazoxide (250 μM) evoked large hyperpolarizations (ΔV_m = -44.7 ± 8.0 mV, n=6) (Fig. 4.7.A,B) suggesting that K_{ATP} channels are functionally expressed in these mice. These results also provide clear evidence that leptin-induced hyperpolarization requires functional leptin receptors. Next, we tested whether direct activation of NMDARs using the receptor agonist NMDA can bypass leptin receptor deficiency and cause membrane hyperpolarization in the absence of leptin. Control WT cells hyperpolarized in response to bath application of 50μM NMDA

(ΔV_m = -37.9 ± 5.5 mV, n=9). Strikingly, β-cells from *db/db* mice also showed robust responses to NMDA (ΔV_m = -44.3 ± 6.7 mV, n=9; Fig. 4.7.C,D), indicating that the signaling events downstream of NMDAR activation that lead to increased K_{ATP} and Kv2.1 channel trafficking and membrane hyperpolarization remain intact despite harboring non-functional leptin receptors.

To test whether findings from the monogenic leptin-resistant mouse β-cells are also reproduced in human diabetic β-cells, we examined β-cells from obese (BMI>30) diabetic donors with presumably different genetic background through the IIDP (see Table 4.1. for donor information). We first tested whether these cells were resistant to leptin. Whole-cell recordings were performed to assess K_{ATP} and Kv2.1 current density with or without leptin treatment (10 nM for 30min) as described previously from β-cells taken from normal donors(58,65). In contrast to normal human β-cells(58,65), leptin did not increase the current density of K_{ATP} channels (107.4 ± 23.2 for control versus 75.4 ± 11.7 pA/pF for leptin-treated, n=6), or Kv2.1 channels (683.3 ± 146.3 for control versus 720.3 ± 158.0 pA/pF for leptin-treated, n=10) (Fig. 4.8.A). Moreover, leptin failed to potentiate NMDAR currents in β-cells from diabetic donors (12.4 ± 2.3 pA for control versus 11.3 ± 1.8 pA following leptin treatment, n=5) (Fig. 4.8.B), in contrast to β-cells from normal donors we reported previously(182). Consistent with these results, leptin did not induce membrane hyperpolarization in diabetic human β-cells (ΔV_m=1.3 ± 2.1 mV for leptin, n=8) (Fig. 4.8.C,D). Conversely, application of 50μM NMDA in the bath solution to directly activate NMDARs in β-cells from the same donors used to test leptin response did induce significant hyperpolarization (ΔV_m = -22.0 ± 8.6 mV, n=9) (Fig. 4.8.C,D), indicating that NMDAR function and downstream signaling events were not compromised as was observed in β-cells from *db/db* mice. These results show that β-cells from a sample of obese diabetic donors were leptin resistant but retained the ability to hyperpolarize in response to direct NMDAR activation.

4.4. Discussion

The results presented in this study elucidate the mechanism by which leptin potentiates NMDAR currents to regulate pancreatic β-cell excitability. Multiple lines of evidence support our conclusion that leptin modulation of β-cell membrane potential requires the phosphorylation of GluN2A-containing NMDARs by Src kinase. First, application of TCN-201, a potent and highly selective inhibitor for GluN2A-containing NMDARs, diminished leptin-induced membrane hyperpolarization in both INS-1 832/13 and human β-cells. Second, inhibition of Src-family kinases blocked the ability of leptin to potentiate NMDAR currents and hyperpolarize β-cells. Third, leptin increased phosphorylation of Src at Y418, a site which is required for its catalytic activity(203,204) and dominant-negative suppression of Src activity via a kinase-dead mutant prevented the ability of leptin to increase surface K_{ATP} channels. Finally, mutation of known Src kinase phosphorylation sites, specifically Y1292 and Y1387, located in the C-terminus of GluN2A prevented leptin-induced hyperpolarization. It is worth noting that Src has many downstream targets. For example, Src has been shown to regulate Kv2.1 activity(209) and actin dynamics(210,211). Therefore, results from experiments involving pharmacological or molecular manipulation of Src activity could be due to Src regulation of other targets in addition to phosphorylation of NMDARs and downstream trafficking of K_{ATP} and Kv2.1 channels. Nonetheless, the collective evidence presented in this study together with our previously published studies(58,65,182) points to a signaling pathway in which leptin activates Src kinase to phosphorylate GluN2A of NMDARs, which leads to potentiation of NMDAR currents and increased Ca^{2+} influx. The increased Ca^{2+} influx then activates CaMKKβ and AMPK, resulting in PKA-dependent actin depolymerization and trafficking of K_{ATP} and Kv2.1 channels to the cell surface, which culminates in hyperpolarization of β-cell membrane potential and reduced insulin secretion. Given Ca^{2+} influx is normally associated with β-cell depolarization and insulin secretion, it is likely that the Ca^{2+} influx through NMDARs triggered by leptin is localized and specifically coupled to downstream events that regulate potassium channel trafficking and hyperpolarize the

membrane. Importantly, we demonstrate in β-cells from mice deficient in leptin signaling and obese diabetic human donors that direct activation of NMDARs by NMDA can bypass leptin resistance and induce membrane hyperpolarization, suggesting the signaling pathway downstream of Src kinase modulation of NMDARs remains operational and may be targeted to modulate insulin secretion.

Mechanism of NMDAR potentiation by leptin

NMDARs are allosterically modulated by a variety of endogenous extracellular ions. For example, Mg^{2+} can bind within the pore region of NMDA receptors and cause a voltage-dependent block(183). In addition, Zn^{2+} can promote voltage-dependent and voltage-independent inhibition of NMDAR activity(212–214). Voltage-dependent inhibition, like that observed with Mg^{2+}, occurs at a low-affinity GluN1 Zn^{2+} binding site located within the channel pore(214) while voltage-independent inhibition appears to be mediated by a high-affinity Zn^{2+} binding site located outside the channel pore and is associated with GluN2 subunits(215). Of the GluN2 subunits, GluN2A is 200-fold more sensitive to Zn^{2+} than GluN2B(216,217). The binding of Zn^{2+} to these subunits is thought to trap the receptor in a low open probability state, reducing their activity(212,213). Zn^{2+} has been shown to be co-released with several transmitters including glutamate, and at some glutamatergic synapses within the brain vesicular Zn^{2+} is thought to diminish NMDAR activity(218). Interestingly, β-cells contain and release high levels of Zn^{2+} due to its role in the biosynthesis and packaging of insulin(219). We speculate that NMDARs residing on the β-cell membrane would be subjected to high concentrations of Zn^{2+} inhibition during bouts of insulin secretion. Of note, phosphorylation of GluN2A by Src has been shown to potentiate NMDAR currents by reducing tonic inhibition of the receptor by Zn^{2+} (185,186). A possible scenario is that under high glucose concentrations when β-cells are depolarized to relieve external Mg^{2+} block, NMDAR activity is still limited by Zn^{2+} co-released with insulin. However, inhibition by Zn^{2+}could be reduced by phosphorylating GluN2A via leptin-induced Src activation to regulate K_{ATP} and

Kv2.1 surface expression and tune insulin secretion. In this way, GluN2A phosphorylation affords a mechanism to allow modulation of β-cell response to glucose stimulation by additional inputs such as leptin. Interestingly, in cells overexpressing GluN2A phosphomutants that failed to respond to leptin, bath application of 50μM NMDA still induced membrane hyperpolarization. This suggests NMDAR currents activated by endogenously released ligands and potentiated by leptin represent a fraction of total NMDAR currents that were activated by 50 μM NMDA under our experimental conditions.

Mechanism of Src activation by leptin

Expression of ObRb mRNAs in β-cells has been well documented(38,40,43,48,50,176). It is assumed that leptin binds to ObRb expressed by pancreatic β-cells to suppress glucose-stimulated insulin secretion. However, leptin has also been reported to transactivate other cytokine receptor signaling molecules, including EGFR, IGF-IR, LRP, and VEGFR (180). Our results that *db/db* β-cells lack leptin-induced hyperpolarization lends strong support to the requirement of ObRb for leptin regulation of K^+ channel trafficking. The mechanism by which ObRb activation leads to Src activation in β-cells awaits further investigation. The enzymatic activity of Src is tightly regulated by tyrosine phosphorylation at Y418 in the catalytic domain and Y529 at its C-terminal tail. When Y529 is phosphorylated the C-terminal tail acts as an autoinhibitory peptide to block kinase activity and its dephosphorylation relieves autoinhibition, leading to autophosphorylation of Y418 which further activates the kinase(196). Activation of ObRb is known to activate several tyrosine phosphatases such as Shp2 which could dephosphorylate pY529 to activate the kinase(180,196). Alternatively, direct recruitment of Src via the kinase's SH domains to phosphotyrosine in the activated leptin receptor complex or regulation by other kinases activated by leptin are also possibilities(196).

Tyrosine phosphorylation sites in GluN2A and GluN2B have been extensively investigated in recombinant expression systems and in neurons. The three GluN2A tyrosine residues examined

in our study have all been shown to contribute to NMDAR current modulation(84,186,201). It is interesting that our data suggest phosphorylation of Y1292 and Y1387F but not Y1325 are important for leptin response. This is in contrast to previous findings in the striatum neurons that Y1325 is critical for Src-induced increase of NMDAR activity to regulate depression-related behavior(201). Very recently, Bland et al. showed that leptin controls glutamatergic synaptogenesis and NMDAR trafficking via GluN2B phosphorylation by Fyn(220). Thus, the precise mechanisms and consequences of NMDARs modulation by leptin and SFKs are likely to be cell context dependent.

Implications for leptin resistance and Type 2 diabetes

We find that β-cells from obese type 2 diabetic human donors no longer hyperpolarize in response to leptin as was also seen in β-cells from leptin resistant, obese diabetic *db/db* mice. Examination of K_{ATP} and Kv2.1 currents confirm that the lack of hyperpolarization is due to the lack of increase in trafficking of these channels to the cell surface, indicating leptin signaling was disrupted. Interestingly, we found that NMDAR current density was similar in β-cells from normal and obese diabetic donors with detectable currents [12.26 ± 4.12 pA/pF from normal donors, n=16 [total 35 cells from 5 donors (Table 4.1.), 19 cells had no detectable currents] versus 11.60 ± 2.17 pA/pF from obese diabetic donors, n=20 [total 26 cells from two donors (Table 4.1.), 6 cells had no detectable currents]. Moreover, direct activation of NMDAR by NMDA triggered membrane hyperpolarization in both *db/db* β-cells and β-cells from human diabetic donors. Thus, despite leptin resistance, signaling mechanisms downstream of NMDARs, i.e. activation of CaMKKβ, AMPK, and PKA-dependent actin depolymerization we reported previously(58,65,182), remain functional to promote K_{ATP} and Kv2.1 channel trafficking to modulate β-cell excitability. The ability of leptin to temper glucose-stimulated insulin secretion has been proposed as part of an adipoinsular feedback loop between adipocytes and β-cells to prevent excessive secretion of insulin, an adipogenic hormone, thereby limiting fat mass(1). Disruption of leptin signaling in β-

cells has been shown to disrupt glucose homeostasis in some animal models(48,50), although others argue against a major role of β-cell leptin signaling in glucose homeostasis(51). Whether the controversial findings were due to different mouse strains and genetic models used(221) remains to be resolved. Nonetheless, it is tempting to speculate on the potential of exploiting the leptin signaling pathway we have identified for the prevention and treatment of obesity associated type 2 diabetes. In obese individuals, hyperleptinemia may result in leptin resistance(207,222), which may lead to excessive insulin secretion. Hyperinsulinemia can then cause insulin resistance and hyperglycemia, further fueling obesity, leading to a loss of glucose control and eventually β-cell failure as seen in type 2 diabetes(223). Based on our finding that obese diabetic human β-cells despite not being able to respond to leptin retain response to NMDAR activation, stimulating NMDAR in leptin resistant obese, prediabetic individuals may help to prevent excessive insulin secretion and thereby prevent or slow the development of type 2 diabetes(223). On the other hand, inhibition of NMDARs in individuals who have already developed type 2 diabetes may stimulate insulin secretion and alleviate hyperglycemia, as has been reported by Marquard et al.(82).

In summary, the current study identifies a novel leptin signaling mechanism in β-cells wherein leptin activates Src kinase to phosphorylate GluN2A-containing NMDARs and potentiate NMDAR activity, thereby reducing β-cell excitability and insulin secretion. The findings build on our previously identified signaling pathway and provide a molecular explanation for the action of leptin. Moreover, it raises the therapeutic potential of targeting the pathway for the prevention and treatment of type 2 diabetes.

4.5. Figures

Table 4. 1. Human Islets Donor Information

Donor (date received)	T2D	Age	Gender	BMI	Cause of death	Islet viability(%)	Islet purity(%)
11/21/17[1]	N	62	M	28.9	Stroke	97	80
01/10/18[2]	N	32	M	26.2	Anoxia	98	85
10/09/18[3]	N	47	F	24.1	Stroke	90	90
10/19/18[4]	N	55	F	35.7	Stroke	98	94
04/02/18[5]	N	32	M	32.3	Anoxia	95	85
11/07/18[6]	N	48	M	24.4	Head trauma	90	90
10/27/15[7]	Y	41	F	43.1	Stroke	95	95
08/09/16[8]	Y	52	F	39.9	Anoxia	95	85
08/29/16[9]	Y	57	M	34.6	Head trauma	98	80
11/07/16[10]	Y	55	M	32.5	Anoxia	98	75
04/03/17[11]	Y	65	F	42.6	Anoxia	90	95
06/01/17[12]	Y	42	F	37.0	Head trauma	89	90
12/13/17[13]	Y	37	F	38.1	Stroke	94	85

Fig.6B: donors 4, 5, 6
Fig.6C, D: donors 1, 2, 3, 4, 6
Fig.8A: donor 7, 8, 9
Fig.8B, C, D: donors 10, 11
Total NMDAR currents from normal β-cells: donors 1, 2, 3, 4, 5
Total NMDAR currents from T2D β-cells: donors 12, 13

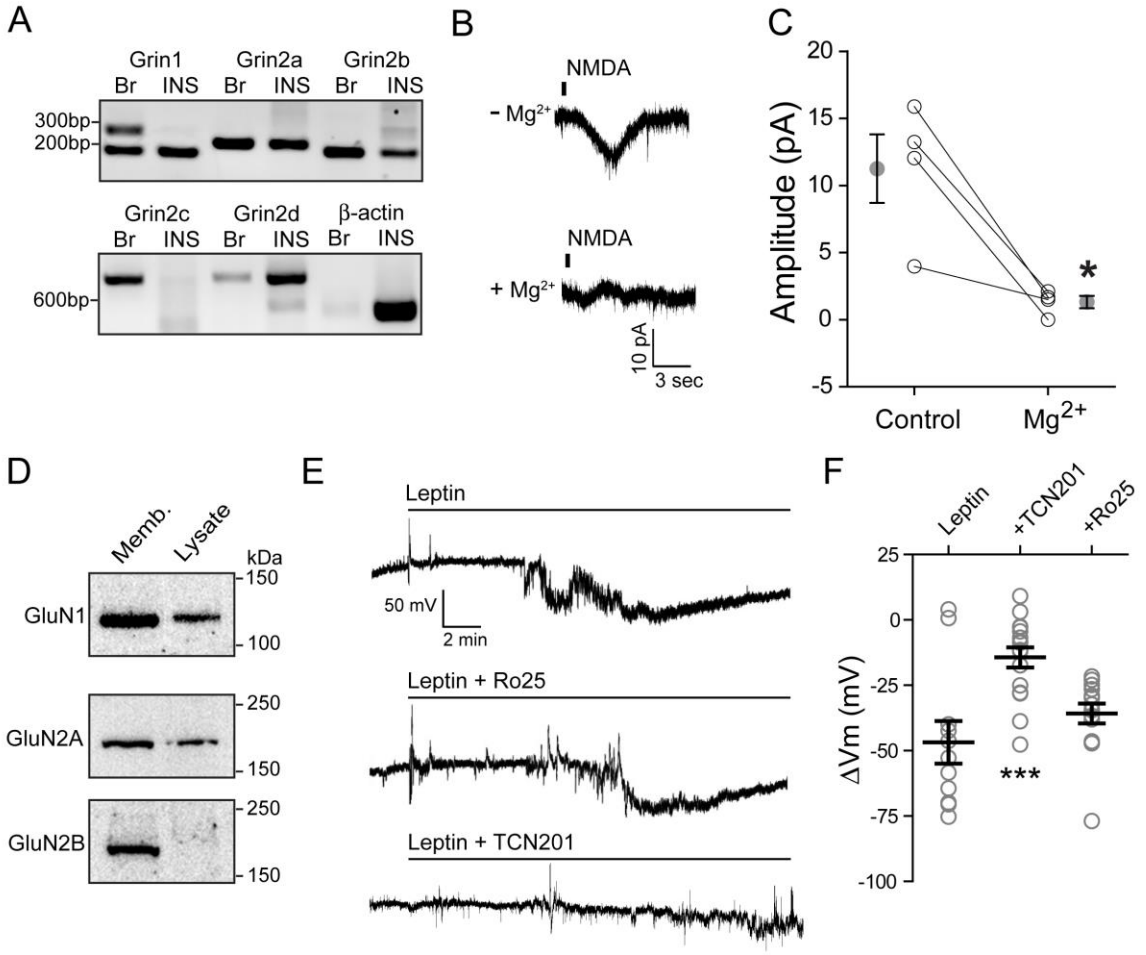

Figure 4. 1. Leptin induces membrane hyperpolarization through GluN2A-containing NMDARs.

(A) Reverse-transcription PCR detection of mRNA for NMDAR subunits, GluN1 (*Grin1*), GluN2A (*Grin2a*), GluN2B (*Grin2b*), GluN2C (*Grin2c*), and GluN2D (*Grin2d*) in rat brain (Br) and INS-1 832/13 cells (INS). β-actin was included as a control. **(B)** Representative traces of NMDAR currents in the absence (top) or presence (bottom) of 100μM Mg^{2+}. **(C)** Sensitivity of NMDA currents (elicited by puff application of 1mM NMDA) to Mg^{2+} block. Averaged current amplitudes before (control) and after 100μM Mg^{2+} for each cell are connected by a straight line. Mean ± SEM values for each group are shown next to individual data points. *p<0.05 by paired t-test. **(D)** Western blots showing protein expression of GluN1, GluN2A, and GluN2B from INS-1 832/13 cell membrane fraction (Memb; 30μg) and total cell lysate (Lysate; 30μg). **(E)** Individual cell attached membrane recordings from INS-1 832/13 cells treated with leptin (10 nM) alone (top), with leptin plus the GluN2B inhibitor Ro 25-6981 (middle; Ro25, 1 μM), or with leptin plus the GluN2A inhibitor TCN201 (bottom, 50μM). **(F)** Group data showing the degree of membrane hyperpolarization in mV for leptin alone (n=11 cells), or leptin co-applied with Ro25 (n=14 cells) or TCN201 (n=16 cells). Here and in subsequent figures, individual cells are represented by symbols and means are indicated by a black line. Error bars represent SEM. *** p<0.0005 by unpaired t-test as compared to leptin.

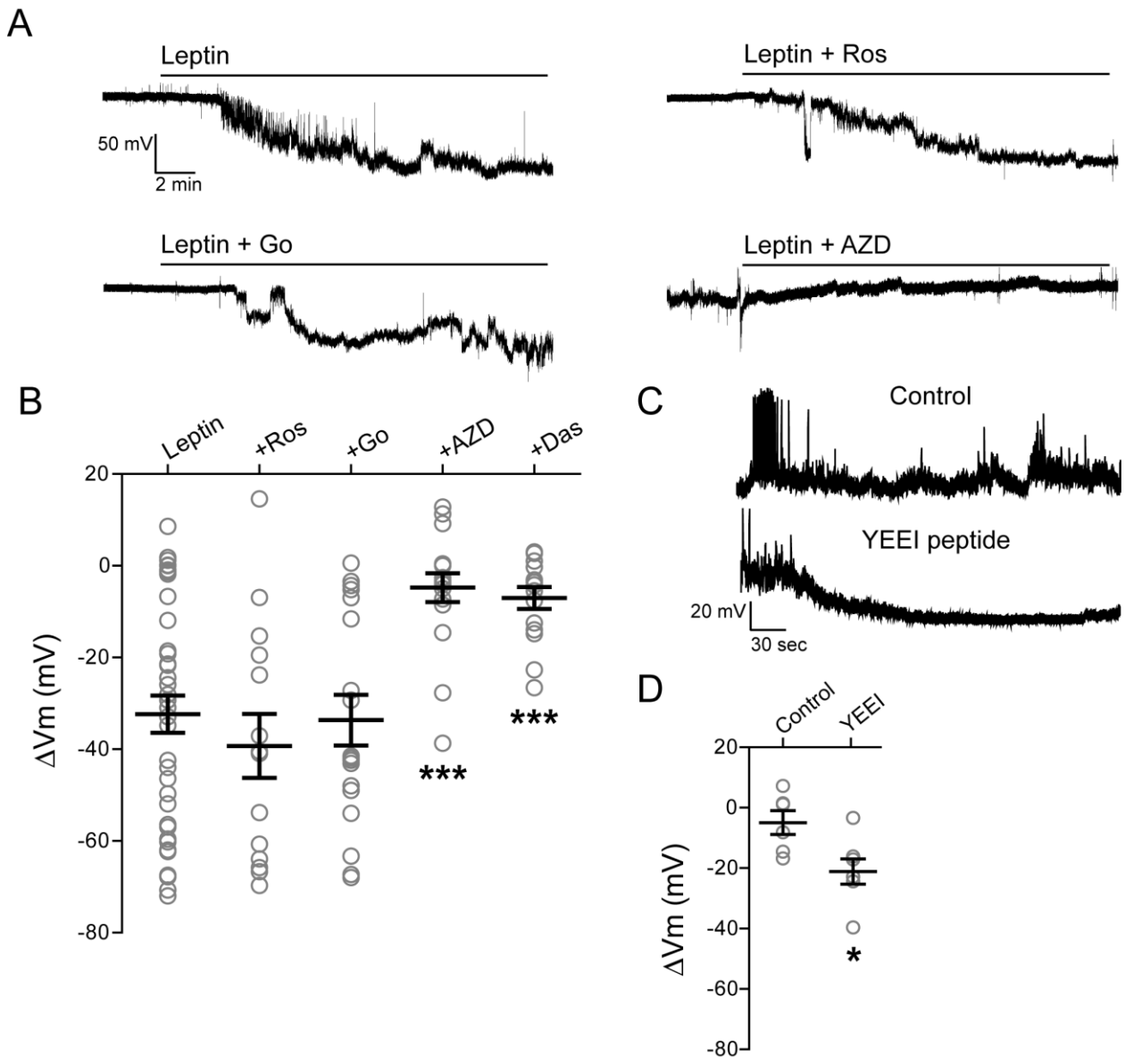

Figure 4. 2. Leptin regulates NMDAR activity via Src family kinases.

(A) Representative cell-attached current-clamp recordings from INS-1 832/13 cells treated with leptin (10 nM) alone (top left), or leptin with the PKC inhibitor Go 6983 (bottom left; Go, 10 µM), the CDK5 inhibitor roscovitine (top right; Ros, 10 µM), or the Src family kinase inhibitor AZD0530 (bottom right; AZD, 10 µM). Inhibitors were applied for 10 min prior to the application of leptin and remained in the solution throughout the recording. **(B)** Group data showing extent of membrane hyperpolarization for leptin alone (n=40 cells), and leptin co-applied with roscovitine (Ros, n=14), Go 6983 (n=18), AZD (n=17), or dasatinib (Das, 25 µM; n=15). ****p*<0.0005 by unpaired t-test as compared to leptin. **(C)** Representative whole-cell current clamp recordings of INS-1 832/13 cells without (top trace) or with (bottom trace) the Src kinase activating peptide YEEI (1 µM) in the pipet solution. **(D)** Group data showing the degree of hyperpolarization for control (n=6) and YEEI peptide (n=7). **p*<0.05, unpaired t-test as compared to control.

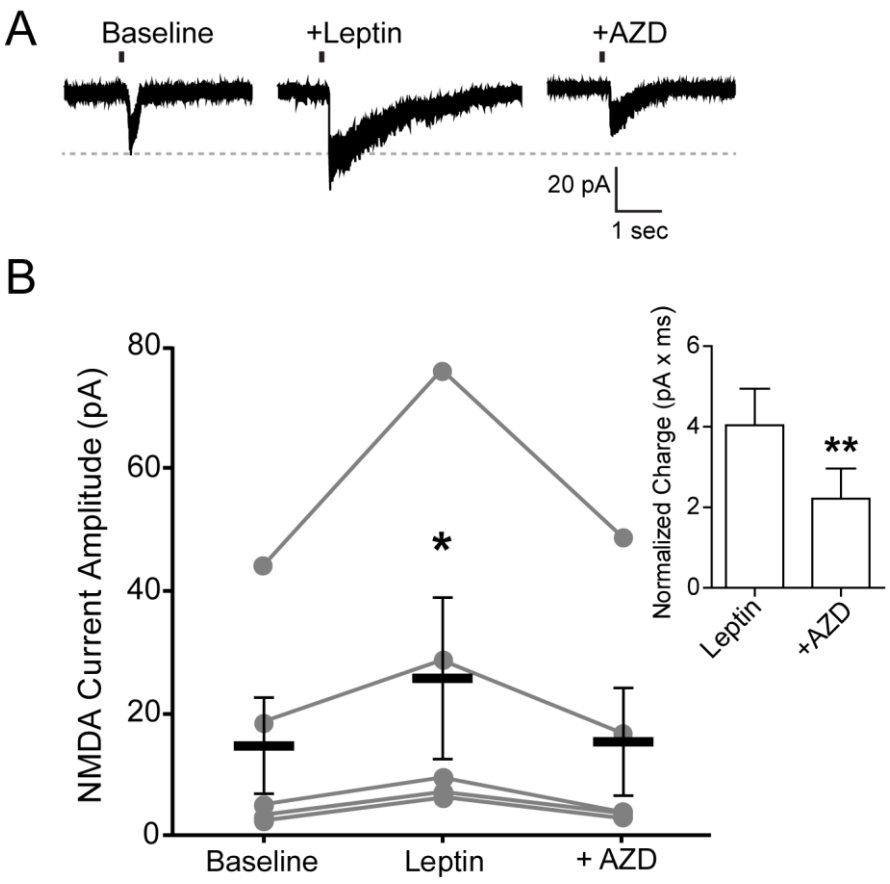

Figure 4. 3. Leptin potentiation of NMDAR currents is prevented by inhibition of Src kinases.

(A) Example of whole-cell currents from a single INS-1 832/13 cell induced by puff application of NMDA (1 mM, vertical line indicates time of puff) during baseline, 5 min after leptin, and following wash-in of AZD (10 µM AZD0350) in the presence of leptin for 5 min. **(B)** Within cell group data showing amplitude of NMDAR currents for each condition (n=5 cells). Means for each condition are depicted as thick black line ± SEM. Statistical analysis was conducted using Friedman's test (p=0.0239) followed by a post hoc Dunn's multiple comparison test with significance set to p<0.05 (*), as compared to baseline. *Inset:* Comparison of total charge (pA x ms) observed for each NMDA puff between leptin and leptin+AZD treatments normalized to baseline. **p<0.005, paired student's t-test as compared to leptin.

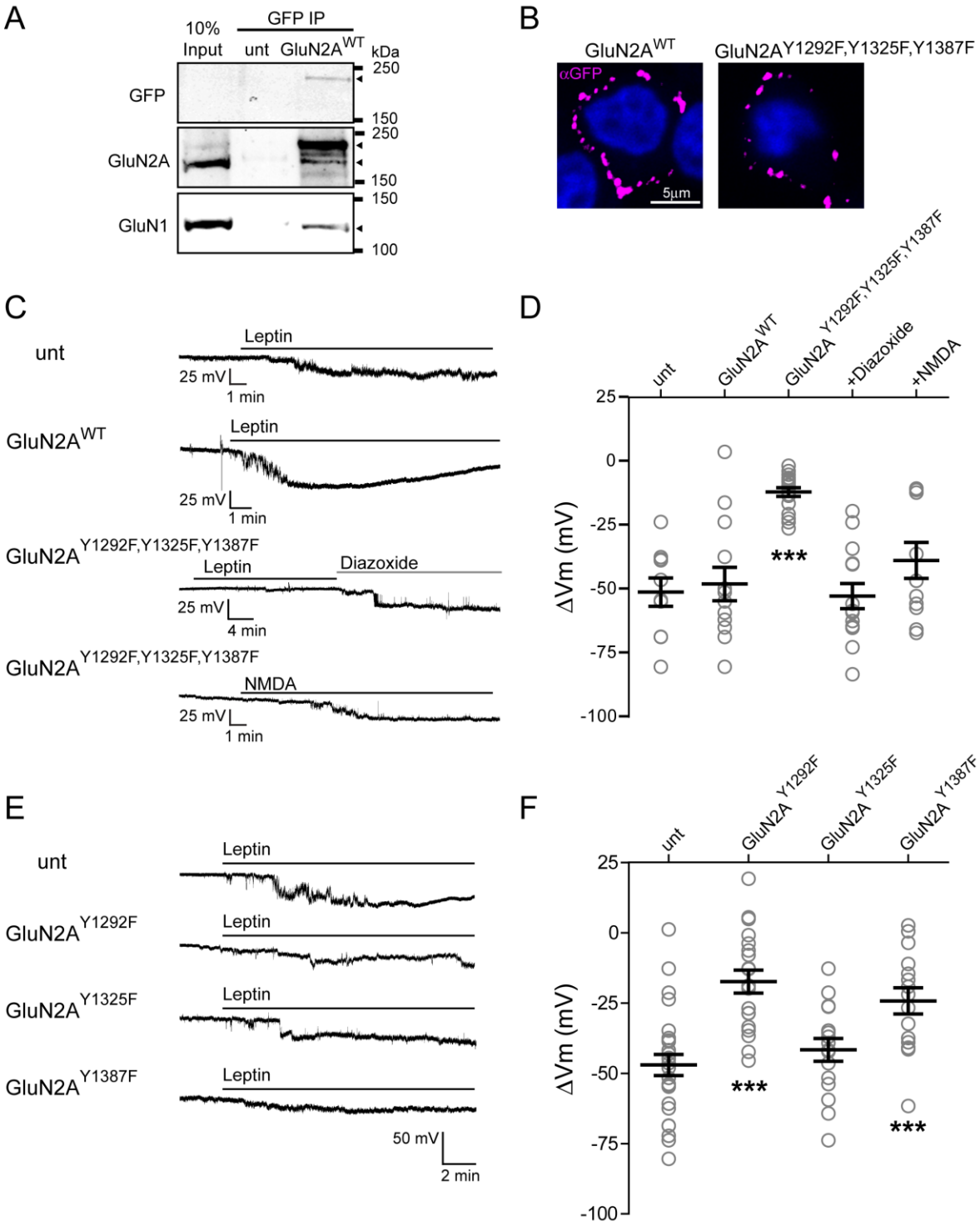
A
10%
Input
GFP IP
unt
GluN2A^WT
kDa
GFP
GluN2A
GluN1
250
150
250
150
150
100
B
GluN2A^WT
GluN2AY1292F,Y1325F,Y1387F
αGFP
5μm
C
unt
Leptin
25 mV
1 min
GluN2A^WT
Leptin
25 mV
1 min
GluN2A^Y1292F,Y1325F,Y1387F
Leptin
Diazoxide
25 mV
4 min
GluN2A^Y1292F,Y1325F,Y1387F
NMDA
25 mV
1 min
D
unt
GluN2A^WT
GluN2A^Y1292F,Y1325F,Y1387F
+Diazoxide
+NMDA
ΔVm (mV)
25
0
-25
-50
-75
-100
***
E
unt
Leptin
GluN2A^Y1292F
Leptin
GluN2A^Y1325F
Leptin
GluN2A^Y1387F
Leptin
50 mV
2 min
F
unt
GluN2A^Y1292F
GluN2A^Y1325F
GluN2A^Y1387F
ΔVm (mV)
25
0
-25
-50
-75
-100
***
***

Figure 4. 4. Leptin-induced membrane hyperpolarization requires phosphorylation of GluN2A Y1292 and Y1387 but not Y1325.

(A) Immunoprecipitation of GFP-GluN2A with anti-GFP followed by immunoblotting using anti-GFP, anti-GluN2A, or anti-GluN1 antibodies showing association of endogenous GluN2A and GluN1 with transfected GFP-GluN2A. Arrowheads next to the blots indicate protein bands corresponding to GFP-GluN2A^{WT} (top blot), GFP-GluN2A^{WT} (upper arrowhead) and endogenous GluN2A (lower arrowhead) (middle blot), and GluN1 (bottom blot). **(B)** Surface staining using anti-GFP antibody showing plasma membrane expression of GFP-GluN2A^{WT} and GFP-GluN2A^{Y1292F,Y1325F,Y1387F}. **(C)** Representative INS-1 832/13 cell-attached current-clamp recordings from an untransfected cell (unt) or a cell transfected with GluN2A^{WT} treated with leptin (10nM), or cells transfected with GluN2A^{Y1292F,Y1325F,Y1387F} and treated with leptin followed by the K_{ATP} channel activator diazoxide (200 µM), or with NMDA (50µM). All GluN2A constructs in this and subsequent panels contain an N-terminal GFP tag. **(D)** Group data showing the degree of hyperpolarization induced by leptin in untransfected cells (n=10), cells transfected with GluN2A^{WT} (n=13), and cells transfected with GluN2A^{Y1292F,Y1325F,Y1387F} (n=18) with subsequent exposure to diazoxide (200 µM; n=14) or treated with NMDA alone (50 µM; n=11). **(E)** Representative cell-attached recordings from unt and three different GluN2A phosphorylation mutants (Y1292F, Y1325F, or Y1387F) treated with 10nM leptin. **(F)** Group data showing the amount of hyperpolarization induced by leptin for unt (n=26) and for single GluN2A phosphorylation mutants (GluN2A^{Y1292F} n=19; GluN2A^{Y1325F} n=16; GluN2A^{Y1387F} n=15). ***p<0.0005 by unpaired t-test as compared to untransfected cells.

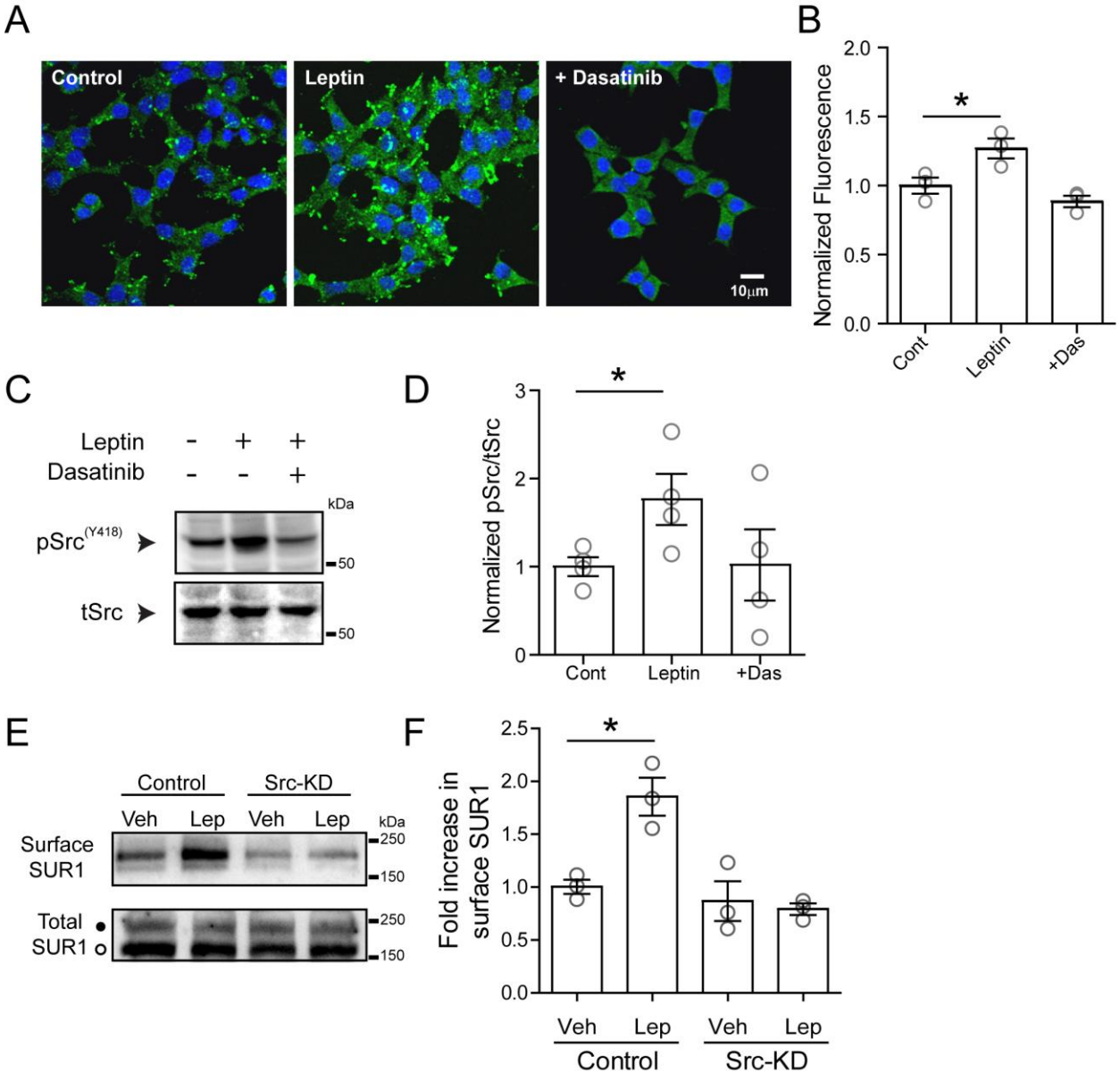
A
Control
Leptin
+ Dasatinib
10μm
B
Normalized Fluorescence
2.0
1.5
1.0
0.5
0.0
*
Cont
Leptin
+Das
C
Leptin - + +
Dasatinib - - +
kDa
pSrc(Y418)
tSrc
50
50
D
Normalized pSrc/tSrc
3
2
1
0
*
Cont
Leptin
+Das
E
Control
Src-KD
Veh
Lep
Veh
Lep
kDa
Surface SUR1
Total SUR1
250
150
250
150
F
Fold increase in surface SUR1
2.5
2.0
1.5
1.0
0.5
0.0
*
Veh
Lep
Veh
Lep
Control
Src-KD

Figure 4. 5. Leptin induces activation of Src kinase.

(A) Immunofluorescence images of cultured INS-1 831/13 cells stained with DAPI (blue) and phosphorylated Src^{Y418} (green) for conditions indicated. Cells were treated with vehicle (control), leptin (10 nM, 10 min), or leptin with dasatinib (25 μM, pretreated for 30 min before leptin was applied). **(B)** Group data for phosphorylated Src^{Y418} fluorescence for each condition normalized to the control (n = 100 cells per condition for each experiment, and the experiment was repeated 3 times). *p<0.05, unpaired student's t-test. **(C)** Representative western blot of phosphorylated Src^{Y418} from cell lysates prepared from INS-1 832/13 cells treated with vehicle, leptin, or leptin co-applied with dasatinib. **(D)** Group data from 4 independent experiments as indicated in panel C. *p<0.05, unpaired student's t-test. **(E)** *Top*: Western blot showing surface SUR1 in response to vehicle or leptin using control cells and cells transfected with a Src kinase-dead mutant (Src-KD). *Bottom*: Total SUR1 showing both the complex glycosylated form (upper band, solid circle) that can traffic to the cell surface and the core-glycosylated form (lower band, open circle) that is in the ER/early Golgi. **(F)** Quantitation of 3 independent surface SUR1 experiments. Data was analyzed by one-way ANOVA (p=0.0019, F=12.95) followed by a post-hoc Dunnett's multiple comparison test with significance set to p<0.05 (*).

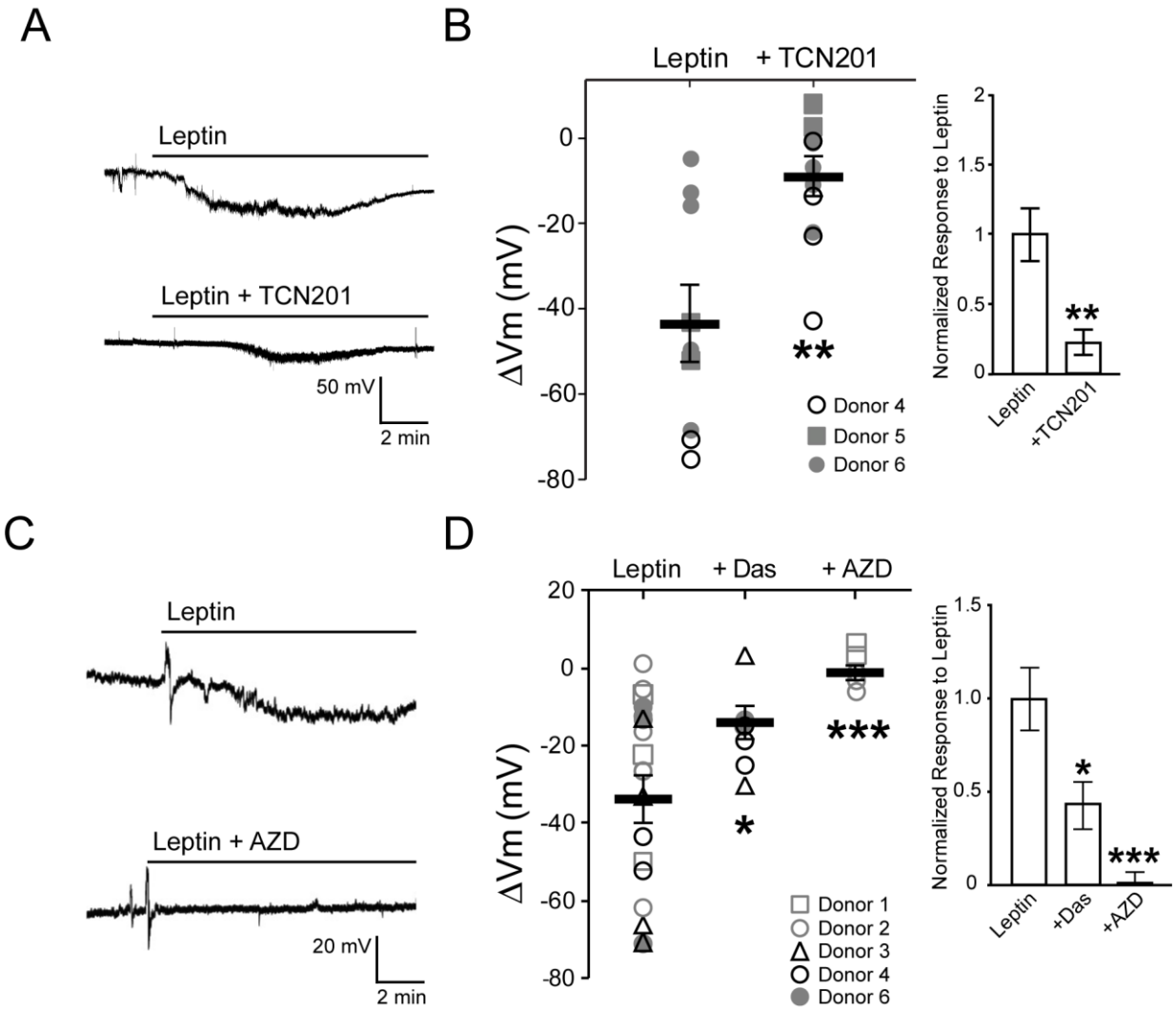

Figure 4. 6. Leptin signaling through GluN2A-containing NMDARs in human β-cells is mediated by Src family kinases.

(A) Individual cell-attached membrane potential recordings from human β-cells isolated from non-diabetic islets treated with leptin (10 nM) alone (top) or leptin together with TCN-201 (bottom, 50 μM). **(B)** Summary data from 3 non-diabetic donors showing the amount of hyperpolarization induced by leptin alone (n=2-5 cells/donor) or when leptin was co-applied with TCN-201 (n=3-4 cells/donor). *Inset*: Normalized responses to leptin across donors in the absence or presence of TCN-201. **(C)** Representative traces of cell-attached current-clamp recordings from human β-cells isolated from non-diabetic islets treated with leptin in the absence or presence of AZD0350 (AZD, 10 μM). **(D)** Summary data from 5 non-diabetic donors showing the extent of membrane hyperpolarization in response to leptin alone (n=19 cells; 3-6 cells/donor) or when leptin was co-applied with dasatinib (Das, 25 μM; n=7 cells; 2-3 cells/donor) or AZD (n=6 cells; 3 cells/donor). *Inset*: Normalized responses to leptin across donors in the absence or presence of Das or AZD. **p*<0.05, ****p*<0.0005, Welch's t-test compared to leptin alone group.

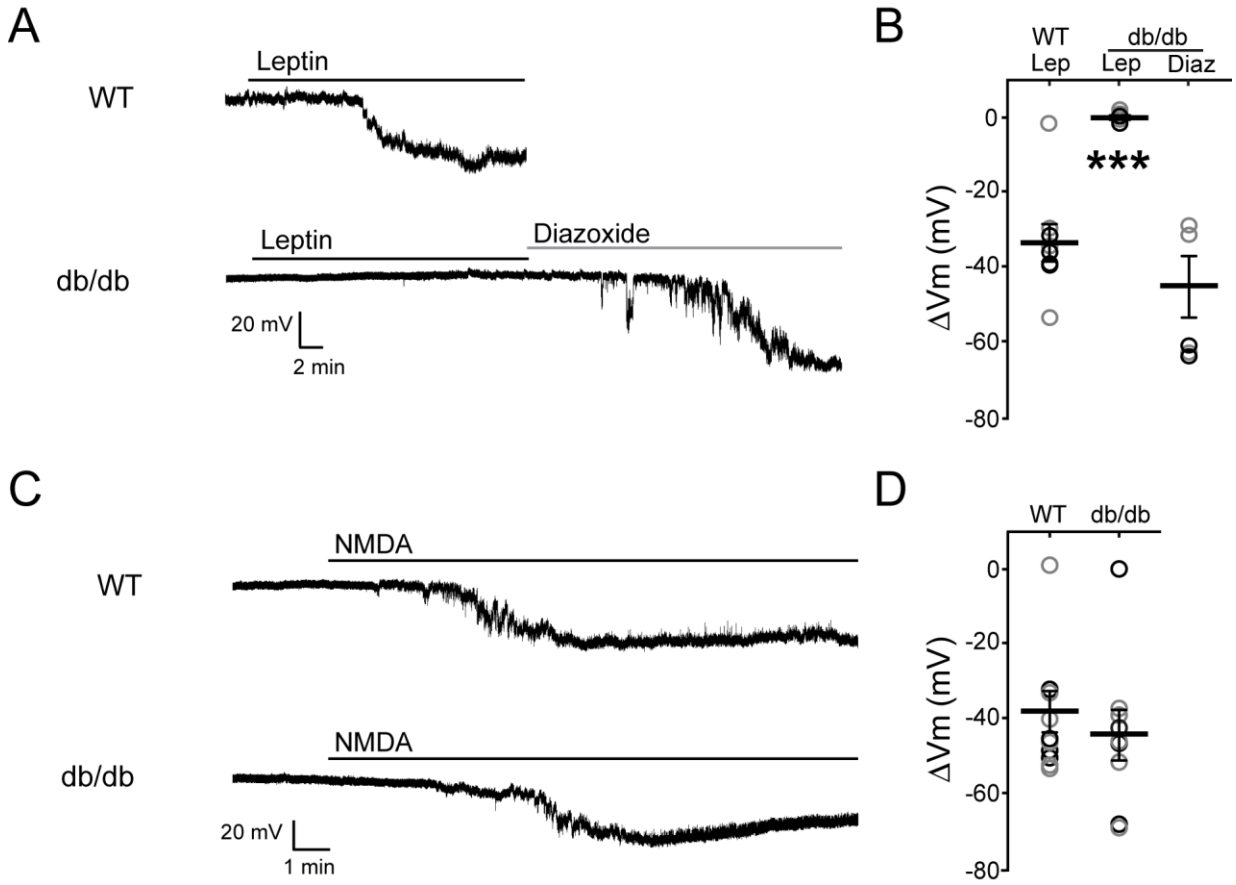

Figure 4. 7. Direct NMDAR activation causes membrane hyperpolarization in mice deficient in leptin receptor signaling.

(A) Representative cell-attached membrane potential recordings from β-cells isolated from C57BL/6J (WT) mice treated with leptin (top trace) or β-cells isolated from db/db mice treated with leptin (10 nM) followed by diazoxide (250 µM; bottom trace). **(B)** Group data showing the degree of membrane hyperpolarization in mV for β-cells isolated from C57BL/6J (WT, n=9) or db/db (n=7) mice for the indicated conditions. Gray and black circles indicate different animals. ****p*<0.0001, unpaired student's t-test compared to WT leptin treated group. **(C)** As described for panel A except β-cells were treated with NMDA (50 µM). **(D)** Group data showing the degree of membrane hyperpolarization in mV for β-cells isolated from C57BL/6J (n=9) or db/db (n=9) mice following NMDA treatment.

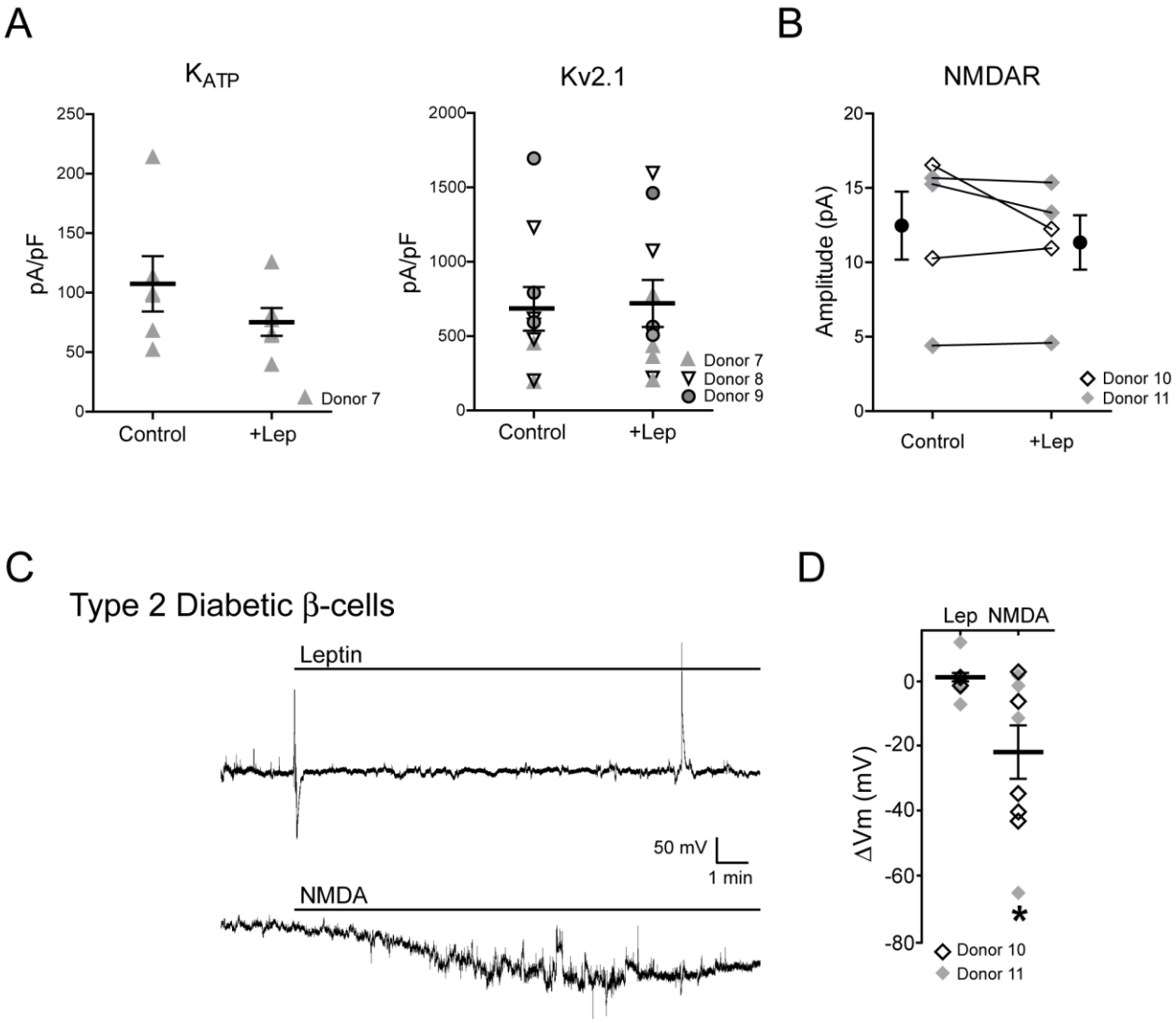

Figure 4. 8. β-cells from obese type 2 diabetic human donors failed to respond to leptin but retained response to NMDA.

(A) Current density of K_{ATP} channels (left) and Kv2.1 channels (right) in β-cells from human diabetic donors treated with vehicle or 10 nM leptin (30 min). Different symbols are used to denote different donors. There is no statistically significant difference between leptin-treated and control groups. **(B)** Whole-cell NMDA currents in β-cells from diabetic donors before leptin application (control) or after 5 min incubation in 10 nM leptin (leptin). The mean (filled circles) and individual cell currents (before and after leptin treatment connected by a solid line) are shown. The open and filled grey diamond represent different donors. **(C)** Representative cell-attached current-clamp recordings from human diabetic β-cells treated with 10 nM leptin (top) or 50 µM NMDA (bottom). Note the spike in the top trace near the end of the recording is a solution suction artifact. **(D)** Group data showing membrane potential response to leptin or NMDA in β-cells isolated from human diabetic donors. *p<0.05, unpaired student's t-test compared to leptin treated group.

4.6. Materials and methods

Chemicals. Leptin was purchased from Sigma (St. Louis, MO). NMDA, Diazoxide, Roscovitine, RO25-6981 and TCN201 were purchased from Tocris Bioscience (Bristol, UK). AZD0530, GO6983 and dasatinib were from Selleckchem (Houston, TX). Src kinase activator peptide (YEEI) was purchased from Santa Cruz (Santa Cruz, CA).

INS-1 832/13 cell culture and transfection. INS-1 832/13 cells were cultured in RPMI 1640 medium (Invitrogen) supplemented with 10% fetal bovine serum (FBS), 100 U/ml penicillin, 100 µg/ml streptomycin, 10 mM HEPES, 2 mM glutamine, 1 mM sodium pyruvate, and 50 µM β-mercaptoethanol. Only cells within passage number of 75 were used for experiments. For experiments involving transfection, cells were prepared as follows. INS-1 832/13 cells were grown on cover slips placed within 35-mm dishes and were transfected with WT (Addgene plasmid # 45445), single GluN2A phosphorylation mutants ($GluN2A^{Y1292F}$, $GluN2A^{Y1325F}$, $GluN2A^{Y1387F}$) or a triple phosphorylation mutant ($GluN2A^{Y1292F,Y1325F,Y1387F}$) using Lipofectamine 2000 (Invitrogen). Plasmids also encoded eGFP at the N-terminus in order to visually discern transfected from non-transfected cells at time of recording 48–72 h after transfection. The kinase-dead Src mutant (pLNCX chick src K295R, a gift from Joan Brugge Addgene plasmid #13659) transfection was carried out in 10-cm plates (cell confluency ~50-60%) using Lipofectamine 2000 (20µg DNA and 40µl lipofectamine 2000) 48 hours prior to experiments.

Dissociation of human pancreatic β-cells. Human β-cells were dissociated from human islets obtained through the Integrated Islets Distribution Program (IIDP) as described previously(58,65,182). Briefly, human islets were cultured in RPMI 1640 medium with 10% FBS and 1% L-glutamine. For recording, islets were dissociated into single cells by trituration in a solution containing 116 mM NaCl, 5.5 mM D-glucose, 3 mM EGTA, and 0.1% bovine serum albumin (BSA), pH 7.4. Dissociated cells were then plated on 0.1% gelatin-coated coverslips placed in 35 mm culture dishes (Falcon 35-3002). For electrophysiological experiments, β-cells

were initially identified using the high autofluorescence signature of β-cells to 488-nm excitation as these cells have high concentrations of unbound flavin adenine dinucleotide(224,225). Dithizone (Sigma-Aldrich) staining was then used to further confirm β-cell identity at the end of each recording(226). Donor information for specific experiments is provided in Table 4.1.

Dissociation of mouse pancreatic β-cells. Mice were purchased from The Jackson Laboratory (Bar Harbor, ME): control (C57BL/6J) and *db/db* [B6.BKS(D)-Lepr^{db}/J]. Pancreatic islets were isolated from the mice as described previously(227) and were performed in compliance with institutional guidelines and approved by the Oregon Health and Science University Animal Care and Use Committee. Following isolation islets were cultured overnight in FBS supplemented RPMI 1640 media at 37ºC and 5% CO_2. Pancreatic β-cells were dissociated from islets using Spinners/EGTA solution. Spinners/EGTA solution in mM: 116 NaCl, 5.37 KCl, 0.8 $MgSO_4$, 26 $NaHCO_3$, 11.67 NaH_2PO_4, 5.5 D-glucose, 3 EGTA, 1% BSA, 1% phenol red (pH 7.4). Islets were incubated twice in Spinners/EGTA for 10 minutes with slight agitation every five minutes. In between incubations with Spinners/EGTA the islets were washed with FBS supplemented RPMI-1640 media. Dissociated cells were plated on glass coverslips coated with 1% gelatin (Sigma-Aldrich) and cultured overnight. The identity of individual β-cells was confirmed by dithizone staining at the end of each experiment(226).

RT-PCR. Total RNA was isolated from mouse brain and INS-1 832/13 cells using RNeasy mini kit (Qiagen, Hilden, Germany) and reverse transcriptase PCR (from 1μg mouse brain RNA and 1.8μg INS-1 832/13 RNA) was performed using the Superscript RT-PCR system (Invitrogen, Carlsbad CA) to examine the mRNA expression of NMDA receptor subunits, Grin1 and Grin2a - 2d. Beta-actin mRNA was used as a standard reference housekeeping gene. The primers used were as follows:

Grin1: (Fwd) 5'-GGTTTGAGATGATGCGAGTCTAC

(Rev) 5'-CAGCAGAGCCGTCACATTCTTGG

Grin2a: (Fwd) 5'-CAATCTGACTGGATCACAGAGC

(Rev) 5'-CTGTCCTTCCCTTGAAAGGATC

Grin2b: (Fwd) 5'-CAATAACCCACCCTGTGAGG

(Rev) 5'-GGTGGGTTGTCACAGTCATAG

Grin2c: (Fwd) 5'-ACATGAAGTATCCAGTATGG

(Rev) 5'-GTTCTGGTTGTAGCTGACAG

Grin2d: (Fwd) 5'-AGGTGTTCTATCAGCGTG

(Rev) 5'-TGTAGCTGTGCATGTCAG

β-actin: (Fwd) 5'- CGTAAAGACCTCTATGCCAA

(Rev) 5'- AGCCATGCCAAATGTGTCAT

Immunoblotting. INS-1 832/13 cells were lysed in lysis buffer (50 mM Tris-HCl, 2 mM EDTA, 2 mM EGTA, 100 mM NaCl, 1% Triton X-100, pH 7.4, with cOmplete EDTA free protease inhibitor cocktail (Roche, Basel, Switzerland) and Halt -phosphatase inhibitor cocktail (Thermo Scientific) for 30 min at 4°C, and cell lysates were cleared by centrifugation (MIKRO 200R, Helmer Scientific, Noblesville, IN) at 14,000 rpm for 10 min at 4°C. In some experiments lysis buffer was replaced with ice cold PBS in order to aid in the isolation of membrane proteins. PBS cell lysates were briefly spun at 3,000 rpm for 5 min at 4°C and the membrane pellet was homogenized in a hypotonic solution containing 15 mM KCl, 10 mM HEPES, 1.5 mM $MgCl_2$ with phosphatase and protease inhibitors by passing 30 times through a 27 ½ gauge needle. Spun at 6,000 rpm at 4°C for 2 min to remove nuclei and cellular debris. Supernatant was collected and transferred to 1.5 ml Beckman Centrifuge tubes and spun at 54,000 rpm at 4°C for 60 min. The resulting membrane pellet was resuspended in solubilization buffer containing 0.2 M NaCl, 0.1 M KCl, 0.05 M HEPES, and proteins were separated by SDS-PAGE (7.5% polyacrylamide gel) and transferred onto PVDF membranes (Millipore, Burlington, MA). Membranes were incubated overnight at 4°C with primary antibody diluted in TBST (Tris-buffered saline plus 0.1% Tween 20) followed by

incubation with horseradish peroxidase-conjugated secondary antibodies in TBST for 1 hr at room temperature. Primary antibodies used were: anti-phosphorylated Src^{Y418} (human Src numbering; rabbit monoclonal; Abcam, ab133460; 1:1000 dilution), anti-c-Src; Abcam, ab16885; 1:100 dilution), anti-GluN1 (NeuroMab, #75-272; 1:1000 dilution), anti-GluN2A (NeuroMab #75-288; 1:1000 dilution), and anti-GluN2B (NeuroMab #75-101; 1:1000 dilution). Blots were developed using Super Signal West Femto (Pierce) and imaged with FluorChemE (ProteinSimple, San Jose, CA), protein bands were quantified using ImageJ (National Institutes of Health) and normalized to the corresponding controls.

Immunocytochemistry. INS-1 832/13 cells were fixed in 2% paraformaldehyde in phosphate-buffered saline (PBS) for 10 min at room temperature, permeabilized with 0.2% Triton X-100 in 1% BSA/PBS, and blocked for 60 min with 1% BSA in PBST (PBS+ 0.1% Tween 20) before being incubated overnight at 4ºC with primary rabbit polyclonal antibodies directed against phospho-Src^{Y418} (Abcam, ab4816). Proteins were visualized using Alexa-488 conjugated secondary antibodies. Fluorescent images were acquired using a Zeiss LSM780 confocal microscope equipped with a 63x oil immersion objective. Images were processed and analyzed using NIH Image J software(228). For surface staining of GFP-$GluN2A^{WT}$ and GFP- $GluN2A^{Y1292F,Y1325F,Y1387F}$, cells were incubated in cold DPBS containing anti-GFP antibody (1:100, ThermoScientific #G10362) at 4ºC for 30 min. Cells were then fixed as described above and surface GFP was visualized using a Cy3 conjugated secondary antibody.

Immunoprecipitation. 48 hours post-transfection of GFP-$GluN2A^{WT}$ cells were collected in DPBS. A membrane pellet was obtained following the protocol described above. The pellet was then solubilized in Co-immunoprecipitation (Co-IP) buffer (0.5mM Tris-HCl, 150mM NaCl, 0.5% Igepal, pH 7.2) and incubated with 25μl of GFP-Trap Dynabeads (Chromotek) overnight at 4ºC. The beads were washed twice with Co-IP buffer. Proteins bound to the beads were then eluted in 2X protein loading buffer for 10 min at 95ºC. Samples were analyzed via immunoblotting for

GFP (1:100, ThermoScientific #G10362), GluN2A (1:1000, NeuroMab #75-288), and GluN1 (1:1000, NeruoMab #75-272) and simultaneously imaged using near infrared secondary antibodies (Licor IRDye).

Surface biotinylation. INS-1 832/13 cells were incubated in RPMI 1640 for 1 hour at 37ºC prior to a 30 min treatment with vehicle or leptin (10nM). Cells were then washed four times with cold DPBS and incubated with 1 mg/ml EZ-Link Sulfo-NHS-SS-Biotin (Pierce) in DPBS with vehicle or leptin for 30 min at 4ºC. The reaction was terminated by incubating cells twice for 5 min with DPBS containing 50 mM glycine followed by two washes with cold DPBS. Cells were then lysed in 300 μl of lysis buffer as described above, and 500 μg of total lysate was incubated with 50 μl of an 50% slurry of NeutraAvidin-agarose beads (Pierce) overnight at 4°C. Biotinylated proteins were eluted with 2X protein loading buffer for 15 min at 37ºC. Both eluent and input samples (50 μg of total cell lysate) were analyzed by immunoblotting using anti-SUR1 antibody (raised against a hamster SUR1 C-terminal peptide KDSVFASFVRADK) as described previously 7.

Electrophysiology. Electrophysiological recordings were conducted using an Axon 200B amplifier (Molecular Devices, Sunnyvale, CA) with Clampex 9.2 (pCLAMP) software. Signals were acquired at 20 kHz and filtered at 2 kHz. Recording electrodes (tip resistances ranged between 3-6 MΩ) were pulled from non-heparinized Kimble glass (Thermo Fisher Scientific, Waltham, MA) using P-97 micropipette puller (Sutter Instruments). For whole-cell recording of NMDA currents, external Tyrode's solution contained in mM: 137 NaCl, 5.4 KCl, 1.8 $CaCl_2$, 0.5 $MgCl_2$, 5 Na-HEPES, 3 $NaHCO_3$, and 0.16 NaH_2PO_4, (pH 7.2). The external solution was supplemented with 0.1 mM glycine and 11 mM glucose, and in some experiments Mg^{2+} was omitted as specified in figure legends. The internal pipette solution contained in mM: 140 K-Gluconate, 6 EGTA, 10 HEPES, 5 K_2ATP, 1 $CaCl_2$ (pH 7.2). To induce NMDA-mediated currents, cells were held at -70mV and NMDA (1 mM) was puffed (3-5 psi for 0.5 sec) with carbogen using 1-0.5 MΩ micropipettes connected to a Multi-function Microforge Controller DMF1000 (World Precision

Instruments, Sarasota, FL) equipped with a pressure regulator. In experiments measuring NMDAR current response to Mg^{2+} block (Fig.1B), leptin (Fig.3, Fig.8B) and leptin plus AZD (Fig.3), 1mM NMDA was puffed repeatedly at 1 min intervals 3-5 times to establish control baseline. Only cells that showed reproducible currents to repeated NMDA puffs during control baseline measurements were subsequently treated with 100μM Mg^{2+}, 10nM leptin or leptin plus AZD for 5min, after which 1mM NMDA was again puffed at 1 min intervals 3-5 times. The currents before and after treatments were then averaged and the averaged values shown as individual data points in figures.

Whole-cell K_{ATP} and Kv2.1 current recordings (Fig.8A) were conducted as described previously(58,65). For K_{ATP} currents, cells were held at −70 mV, and K_{ATP} currents were recorded at two voltage steps (−50 and −90 mV) applied every 2 s. Pipette solution contained (in mM): 140 KCl, 10 K-HEPES, 1 K-EGTA, pH 7.3. The bath solution contained (in mM): 137 NaCl, 5.4 KCl, 1.8 $CaCl_2$, 0.5 $MgCl_2$, 5 Na-HEPES, 3 $NHCO_3$, 0.16 NaH_2PO_4, pH 7.2. Diazoxide (200 μM) was applied to the bath solution immediately after break-in to maximally stimulate K_{ATP} channels. After the current had plateaued, 300 μM tolbutamide (a K_{ATP} channel inhibitor) was applied, and residual currents were subtracted from maximal currents observed in diazoxide and divided by cell capacitance to obtain K_{ATP} current density. For Kv2.1, micropipettes were filled with an internal solution containing (in mM): 140 KCl, 1 $CaCl_2$, 2 $MgCl_2$, 5 EGTA, 5 ATP, 10 glucose and 10 HEPES, pH 7.3. The bath solution contained (in mM) the following: 140 NaCl, 5 KCl, 4 $MgCl_2$, 11 glucose, 10 HEPES, pH 7.3. Ca^{2+} was excluded from the bath solution to eliminate calcium channel currents. A 30-ms prepulse to −10 mV was used to inactivate transient potassium channel currents and voltage-dependent Na^+ currents. The sustained current at +80 mV, after subtracting currents remaining in 10mM of the potassium current blocker tetraethylammonium (TEA), was divided by cell capacitance for Kv2.1 current density calculation.

For cell-attached recording to monitor membrane potentials, micropipettes were filled with 140 mM NaCl. The bath solution contained (in mM): 137 NaCl, 5.4 KCl, 1.8 $CaCl_2$, 0.5 $MgCl_2$, 5 Na-

HEPES, 3 $NHCO_3$, 0.16 NaH_2PO_4, 11 glucose, pH 7.2. The liquid junction potential was measured to be -10 mV and corrected from the recorded V_m. Seal resistances between the recording pipette and the cell membrane ranged between 4-11 GΩ and membrane potentials were monitored in current-clamp mode (I=0). After correction for the liquid junction potential, the average starting V_m was around -4 mV. Note the V_m estimated in this configuration is dependent on the ratio of the seal resistance and the combined patch and cell resistance where the ratio of recorded V_m and true membrane potential = $(R_{seal}/R_{patch}+R_{cell})/[1+(R_{seal}/R_{patch}+R_{cell})(190)$. As such, the recorded V_m is an underestimate of the actual membrane potential (i.e. more depolarized than the actual V_m)(157,190). Since the recorded V_m under this configuration is only a proxy of the true membrane potential we only used it to track changes in membrane potential(157,190). Seal resistance was monitored before and after the recording and only cells which showed stable baseline membrane potential prior to leptin/drug application and which maintained good seal resistance were included for analysis. In addition, the K_{ATP} channel opener diazoxide or inhibitor tolbutamide were used when applicable to ensure cell and patch integrity as we reported previously(182) and in the current study (see Fig. 4.4. and Fig. 4.7.). For whole-cell current-clamp recordings of membrane potential (Fig. 4.2.C, D), pipet solution contained (in mM): 130 K-Gluconate, 10 KCl, 10 HEPES, 6 EGTA, 0.1 $CaCl_2$, 1 $MgCl_2$, and 5 ATP, with or without the SFK activator YEEI phosphopeptide (EPQpYEEIPIYL at 1 µM). All recordings were analyzed using Clampfit 9.2 (pCLAMP).

Statistical analysis. Results are expressed as mean ± standard error of the mean (SEM). One-way ANOVA with a post hoc Dunnett's test (Fig. 4.5.E) or Friedman's test (Fig. 4.3.B) were used for multiple comparisons where different experimental conditions were carried out side-by-side. For most experiments, difference between control and treated groups was tested using paired t-test, or unpaired *t*-tests (for comparable sample sizes) or Welch's t-test (for significantly unequal sample sizes in Fig. 4.6.D) as detailed in figure legends. The level of statistical significance was set at $p<0.05$.

Chapter 5: AKAP79/150 coordinates leptin-induced PKA activation to regulate K_{ATP} channel trafficking in pancreatic β-cells

Veronica A. Cochrane[1, †], Zhongying Yang[1], Mark Dell'Acqua [2], and Show-Ling Shyng[1,†]

[1]Department of Chemical Physiology and Biochemistry, Oregon Health & Science University, Portland, OR 97239, USA; [2]Department of Pharmacology, School of Medicine, University of Colorado Anschutz Medical Campus, Aurora, CO 80045, USA.

Research is In Press at *Journal of Biological Chemistry*.

[†]Correspondence to: Veronica Cochrane (cochranv@ohsu.edu) or Show-Ling Shyng (shyngs@ohsu.edu), Department of Chemical Physiology and Biochemistry, School of Medicine, Oregon Health & Science University, 3181 S.W. Sam Jackson Park Road, Portland, OR 97239.

Author contributions: VC* conceived the project, designed and performed experiments, analyzed data, and wrote the manuscript; ZY performed experiments; MD provided reagents and edited the manuscript; SLS conceived the project, analyzed data and wrote the manuscript. All authors have full access to all the data in the study and take responsibility for the integrity of the data and the accuracy of the data analysis. All authors reviewed the results and approved the final version of the manuscript.
*VC contributed all of the data presented in figures.

Acknowledgements: We thank Dr. Christopher Newgard for the rat insulinoma INS-1 clone 832/13 cells. We also thank Dr. Manuela Zaccolo for the cAMP CUTie sensor plasmids and Dr. John Scott for the AKAP150 shRNAi plasmids. Finally, we thank the Advanced Light Microscopy Core at Jungers (OHSU, Portland, OR) staff for their expertise in image acquisition and analysis. This work was supported by National Institutes of Health grant R01DK057699 and 3R01DK057699-14S1 (to Show-Ling Shyng). Dr. Mark Dell'Acqua acknowledges the support of NIH grant NS040701.

5.1. Abstract

The adipocyte hormone leptin regulates glucose homeostasis both centrally and peripherally. A key peripheral target is the pancreatic β-cell, which secretes insulin upon glucose stimulation. Leptin is known to suppress glucose-stimulated insulin secretion by promoting trafficking of K_{ATP} channels to the β-cell surface, which increases K^+ conductance and causes β-cell hyperpolarization. We have previously shown that leptin-induced K_{ATP} channel trafficking requires protein kinase A (PKA)-dependent actin remodeling. However, whether PKA is a downstream effector of leptin signaling or PKA plays a permissive role is unknown. Using FRET-based reporters of PKA activity, we show that leptin increases PKA activity at the cell membrane and that this effect is dependent on NMDA receptors, CaMKKβ, and AMPK, which are known to be involved in the leptin signaling pathway. Genetic knockdown and rescue experiments reveal that the increased PKA activity upon leptin stimulation requires the membrane-targeted PKA-anchoring protein AKAP79/150, indicating PKA activated by leptin is anchored to AKAP79/150. Interestingly, disrupting protein phosphatase 2B (PP2B) anchoring to AKAP79/150, known to elevate basal PKA signaling, leads to increased surface K_{ATP} channels even in the absence of leptin stimulation. Our findings uncover a novel role of AKAP79/150 in coordinating leptin and PKA signaling to regulate K_{ATP} channel trafficking in β-cells, hence insulin secretion. The study further advances our knowledge of the downstream signaling events that may be targeted to restore insulin secretion regulation in β-cells defective in leptin signaling, such as those from obese individuals with type 2 diabetes.

5.2. Introduction

Pancreatic β-cells produce and secrete insulin making them critical for maintaining glucose homeostasis. In order to secrete insulin in a timely and controlled manner, β-cells must interpret and respond to a myriad of physiological stimuli and hormones. One such hormone is the adipocyte-derived hormone leptin, which regulates serum insulin levels by suppressing glucose-stimulated insulin secretion (GSIS) from β-cells(39,40,42–44). Leptin does so by promoting trafficking of ATP-sensitive potassium (K_{ATP}) channels to the β-cell membrane(57,58,65,182,229). This increased surface expression of K_{ATP} channels increases the total K_{ATP} channel conductance thereby causing membrane hyperpolarization and reducing β-cell electrical activity. Our studies to date have shown that leptin-induced K_{ATP} channel trafficking involves the following series of signaling events(58,65,182,229). Leptin stimulates Src kinase to phosphorylate and potentiate NMDA receptor (NMDAR) activity, resulting in enhanced Ca^{2+} influx that activates calcium/calmodulin-dependent kinase kinase β (CaMKKβ), which then phosphorylates and activates AMP-activated protein kinase (AMPK). Downstream of AMPK actin depolymerization occurs and results in increased trafficking of K_{ATP} channels to the plasma membrane(58,65,182,229). We have shown previously that actin remodeling and subsequent K_{ATP} channel trafficking following AMPK activation requires protein kinase A (PKA). However, it remains elusive whether PKA functions as an active or permissive player in leptin signaling.

PKA is a serine/threonine kinase consisting of two regulatory subunits and two catalytic subunits. Binding of cAMP to the regulatory subunits causes a conformational change that releases the autoinhibition of the catalytic subunits to activate PKA(230,231). Due to the ubiquity of PKA in mammalian cells and the promiscuity of its catalytic subunits, PKA is involved in a multitude of cellular processes. In pancreatic β-cells PKA has been identified by several studies as a positive regulator of insulin granule trafficking and exocytosis(113,114,232–234). However, evidence that PKA promotes K_{ATP} channel trafficking suggests that PKA is also

involved in signaling events that lead to inhibition of insulin secretion(58,142). These findings illuminate the complexity of β-cell signaling and raise the question of how cellular signaling networks are coordinated to fine-tune insulin secretion. It is well established that PKA interacts with a family of scaffolding proteins termed A-kinase anchoring proteins (AKAPs). Different AKAPs direct PKA activity towards specific cell signaling machinery by anchoring PKA and other signaling molecules to distinct subcellular locations(115). Several AKAPs have been identified as having roles in regulating insulin secretion, but the mechanisms by which they do so remain poorly understood(117–120,235,236).

In this study we show that leptin increases PKA signaling at the β-cell membrane, but not in the cytoplasm, through our previously identified pathway involving NMDAR, CaMKKβ, and AMPK. Moreover, we find that anchoring of PKA by AKAP79/150 is necessary for leptin-mediated K_{ATP} channel trafficking and that overexpression of an AKAP79/150 mutant associated with increased basal PKA activity due to a loss of protein phosphatase 2B (PP2B) binding recapitulates the effects of leptin. Additionally, we present evidence that leptin locally increases concentrations of the PKA activator cAMP near AKAP79/150 expressed at the cell membrane. These findings reveal a novel function of the PKA-AKAP79/150 signaling complex for orchestrating leptin signaling to regulate K_{ATP} channel surface expression and thus β-cell excitability.

5.3. Results

5.3.1. Leptin increases PKA activity near the plasma membrane

We have previously shown that leptin promotes trafficking of K_{ATP} channels to the plasma membrane, causing increased K^+ conductance and cell hyperpolarization in rat insulinoma INS-1 832/13 cells as well as primary mouse and human β-cells(58,65,182,229). Our prior work revealed that a critical event for this process is actin remodeling(58), which presumably allows vesicles containing potassium channels to translocate and insert into the β-cell membrane(89–91,237). Furthermore, we found that the ability of leptin to remodel the actin cytoskeleton and increase surface K_{ATP} channel density could be blocked by the protein kinase A (PKA)-specific inhibitor peptide (PKI) suggesting that PKA is essential to this signaling mechanism(58). However, whether leptin stimulation directly enhances PKA signaling remains unknown. To determine whether leptin signaling increases PKA signaling we monitored PKA activity using the FRET-based PKA activity reporter A-kinase activity reporter 4 (AKAR4)(125). AKAR4 contains a PKA substrate motif that is phosphorylated by PKA causing the sensor to undergo a conformational change to increase FRET detected as an increased YFP acceptor/CFP donor emission ratio in response to excitation of the CFP donor. An AKAR4 targeted to the plasma membrane with a farneyslation motif (CAAX; Fig. 1A) as well as an AKAR4 targeted to the cytoplasm by a nuclear export signal (NES; Fig. 1B) were both tested. INS-1 832/13 cells expressing either AKAR4-CAAX or AKAR4-NES were treated with leptin (100 nM) or vehicle. In order to control for the expression level of AKAR4 between cells the potent PKA activator forskolin was administered at the end of each experiment and cells that responded robustly to forskolin with a 10-15% increase in FRET were chosen for analysis. For quantification purposes, FRET traces were normalized to the maximal forskolin response (Fig. 1C,D) and then analyzed for area under the curve (AUC) during the treatment period with vehicle or leptin. In AKAR4-CAAX expressing cells, leptin treatment led to a 6.37-fold increase

in PKA activity ($p<0.0005$, n=24) compared to vehicle treated cells (n=13) (Fig. 1E). In contrast, AKAR4-NES expressing cells showed no change in PKA activity between vehicle (n=9) and leptin (n=10) treatments (Fig. 1F). To confirm that the increase in PKA activity in AKAR4-CAAX expressing cells was due to leptin and not an experimental artifact we tested the effect of various leptin concentrations compared to inactive boiled leptin. While we found that leptin at concentrations of 10 nM and 100 nM increased PKA activity, boiled 100 nM leptin did not (Fig. 1G). This result indicates that leptin does indeed increase PKA activity, as reported by AKAR4-CAAX, and that this increase is spatially restricted to the plasma membrane.

5.3.2. Leptin signals via the NMDAR-CaMKKβ-AMPK axis to activate PKA

Next, we sought to determine the signaling mechanism that underlies an increase in PKA activity. Our previous studies have shown that the leptin signaling pathway leading to increased K_{ATP} channel trafficking involves potentiation of NMDAR activity and Ca^{2+} influx to activate CaMKKβ; this results in phosphorylation and activation of AMPK, which is followed by PKA-dependent actin depolymerization(58,65,182,229). Thus, a logical hypothesis is that leptin upregulates PKA activity via the NMDAR-CaMKKβ-AMPK signaling axis. To test this, we implemented the membrane targeted PKA activity sensor AKAR4-CAAX in conjunction with pharmacological reagents. As shown in Fig.2A, inhibiting the initial potentiation of NMDARs with the competitive NMDAR antagonist D-APV (50 μM) or preventing the ensuing Ca^{2+} influx with the Ca^{2+} chelator BAPTA (10 mM) reduced leptin enhancement of PKA activity by 2.5-fold (n=12) and 5-fold (n=11) respectively, levels that were not significantly different from the vehicle control. Consistent with these findings, inhibiting CaMKKβ with STO-609 (1 μM) also prevented leptin from increasing PKA activity (n=9). Finally, the role of AMPK for leptin activation of PKA was tested using Compound C (CC, also known as Dorsomorphin, 1 μM). Blocking AMPK activity with CC (n=15) greatly diminished the effect of leptin such that PKA activity levels

resembled those of vehicle treated cells. These results support the notion that PKA is activated downstream of AMPK in the leptin signaling cascade.

To further corroborate the above findings, we tested whether pharmacological activation of NMDAR or AMPK could increase PKA activity. Treating AKAR4-CAAX expressing cells with the NMDAR co-agonists NMDA (100 μM) and glycine (100 μM) or the AMPK agonist AICAR (500 μM) significantly increased FRET (Fig. 2B). While direct activation of AMPK caused a 6.25-fold increase ($p<0.001$, $n=20$) over vehicle that was equivalent to leptin treatment, NMDAR co-agonists caused a 10.66-fold increase ($p<0.001$, $n=11$) compared to vehicle, which was 1.67 times ($p<0.01$, $n=11$) greater than that of leptin. This suggests that the direct activation of NMDARs may have caused a greater extent of NMDAR activity and consequently more PKA activity. To confirm that NMDARs signal through the leptin pathway involving AMPK we treated cells with the NMDAR co-agonists NMDA and glycine in the presence of the AMPK inhibitor CC (1 μM) and found that CC significantly reduced the effect of NMDAR on PKA activity ($n=10$, $p<0.001$) (Fig. 2C). On the contrary, the effects of the AMPK agonist AICAR were not blocked by the NMDAR inhibitor D-APV (50 μM) indicating that NMDAR lies upstream of AMPK. Collectively, these findings demonstrate that leptin signaling through the NMDAR-CaMKKβ-AMPK cascade increases PKA activity.

5.3.3. Leptin signaling via PKA requires AKAPs

During the live cell PKA activity imaging experiments it was apparent that leptin increased PKA activity at the cell membrane but not throughout the cytoplasm. This suggests that leptin acts on a subset of cellular PKA that is localized near the plasma membrane. It is widely documented that a high level of regulation and specificity of PKA signaling is maintained by a family of scaffolding proteins known as A-kinase anchoring proteins (AKAPs), which target PKA and its signaling partners to distinct subcellular regions thereby creating PKA signaling microdomains and nanodomains(115,238,239). To test if AKAPs are involved in targeting PKA

to the cell membrane for leptin signaling we used the PKA-AKAP interaction disruptor peptide st-Ht31 (50 μM)(137). This peptide binds the regulatory subunits of PKA and prevents PKA from binding AKAPs. We first introduced st-Ht31 to INS-1 832/13 cells expressing AKAR4-CAAX and monitored PKA activity in response to various stimuli (Fig. 3A). Disrupting the PKA-AKAP interaction with st-Ht31 led to a significant decrease in PKA activity by leptin (3.6-fold decrease, $p<0.01$), NMDAR agonist NMDA (6.4-fold decrease, $p<0.001$, $n=8$), and AMPK activator AICAR (3.4-fold decrease, $p<0.01$, $n=10$). These experiments showed that increased PKA activity at the cell membrane by leptin signaling requires AKAPs.

Having established that PKA-AKAP interactions are necessary for leptin-mediated PKA activity, we wanted to determine if such an interaction is essential for downstream K_{ATP} channel trafficking. To visualize K_{ATP} channels at the plasma membrane, INS-1 832/13 cells were transduced with recombinant adenoviruses containing the K_{ATP} channel subunits Kir6.2 and SUR1 tagged with an N-terminus extracellular bungarotoxin-binding motif (BTX-SUR1)(58); surface K_{ATP} channels were then labeled with Alexa 555-conjugated BTX (BTX) following a 30 min treatment period. Leptin (10 nM) treated cells showed a marked increase in surface BTX staining of BTX-SUR1 compared to vehicle treated cells as expected (Fig. 3B)(58). However, this effect of leptin was greatly attenuated by the presence of st-Ht31 indicating that blocking PKA from binding AKAPs prohibits leptin from increasing K_{ATP} channel surface density. Previously we have shown that the increased abundance of K_{ATP} channels in the membrane enhances total K^+ conductance and causes β-cells to hyperpolarize(58,65,182,229). To further verify the importance of PKA-AKAP interactions for K_{ATP} channel translocation we monitored the effects of st-Ht31 on cell membrane potential following leptin treatment using cell-attached current clamp recording, which is a non-invasive approach for detecting changes in membrane potential without disturbing cellular integrity or compromising intracellular soluble factors important for signaling(157,190). Cell-attached membrane recordings of INS-1 832/13 cells

showed that leptin (10 nM) elicits a mean hyperpolarization extent of -64.76 ± 1.61 mV (n=5) (Fig. 3C, D). However, in the presence of st-Ht31 (50 μM) leptin-induced hyperpolarization was significantly reduced to -14.53 ± 3.96 mV ($p< 0.001$, n=8). This data strongly implicates that an AKAP is required to anchor PKA for leptin-mediated K_{ATP} channel trafficking.

5.3.4. PKA and AKAPs are also required for leptin signaling in human β-cells

Our previous studies have shown that leptin regulation of K_{ATP} channel trafficking is conserved in human β-cells. To test whether PKA and AKAPs are also involved in leptin signaling in human β-cells, we conducted cell-attached current-clamp recording experiments to monitor cell membrane potential response while pharmacologically manipulating PKA activity and the PKA-AKAP interaction as described above for INS-1 832/13 cells. Individual human β-cells dissociated from islets from three different donors (Table 1) were tested and the results were compared to those using INS-1 832/13 cells (Fig. 4). Bath application of 10 nM leptin induced membrane hyperpolarization in human β-cells to a similar extent (-39.40 ± 6.46 mV, n=11) as in INS-1 832/13 cells (-46.49 ± 4.92 mV, n=11) (Fig. 4A, B). Consistent with PKA being required for K_{ATP} channel trafficking, the myristoylated form of the PKA inhibitor PKI (1 μM) significantly reduced leptin-induced hyperpolarization to -5.18 ± 2.65 mV ($p<0.01$, n=6) and -17.82 ± 6.88 mV ($p<0.01$, n=9) in human β-cells and INS-1 832/13 cells, respectively (Fig. 4A, B). Conversely, treatment with the PKA-specific agonist 6-Bnz-cAMP (10 μM) recapitulated the effects of leptin and caused a mean hyperpolarization of -54.84 ± 6.83 mV (n=9) in human β-cells and -56.00 ± 8.15 mV (n=12) in INS-1 832/13 cells. Interestingly, at the concentration used, 6-Bnz-cAMP tended to induce a greater membrane hyperpolarization compared to leptin, which may be due to variation in the degree of PKA activation. The findings in human β-cells agree with those in INS-1 832/13 cells indicating that PKA is both necessary and sufficient to promote K_{ATP} channel trafficking and subsequent membrane hyperpolarization in human β-cells. We then examined whether disrupting the PKA-AKAP interaction would negatively impact leptin-

induced hyperpolarization in human β-cells. Pre-incubating human β-cells with st-Ht31 (50 μM) to disrupt PKA-AKAP interactions occluded the effects of leptin on β-cell membrane potential (-4.81 ± 1.13 mV, $p<0.0001$, n=11). These studies demonstrate the importance of our findings to human biology and support that a PKA-AKAP complex plays an essential role for leptin signaling in human β-cells. In the studies that follow, we will further elucidate the mechanism of PKA-AKAP interaction in leptin signaling using INS-1 832/13 cells as they are more amenable to biochemical and molecular genetic manipulations.

5.3.5. AKAP79/150 coordinates leptin signaling to regulate K_{ATP} channel trafficking

The above results that PKA-AKAP interactions are required for leptin to exert its signaling effect raises the question of which AKAP(s) is involved in localizing PKA. There are more than 50 known AKAPs(115). We chose to focus on AKAPs that have been shown to be expressed in β-cells and localize at the cell membrane based on the observation that increased PKA activity occurs near the plasma membrane upon leptin stimulation (Fig.1). Among the possible candidates, AKAP79/150 (human/murine proteins, *AKAP5* gene) stood out as a most interesting candidate(120,130,240,241), because in neurons AKAP79/150 has been shown to co-immunoprecipitate with NMDARs(242,243), a known player in the leptin signaling pathway being studied here. To test the idea that AKAP79/150 could serve as a scaffold to coordinate a complex of leptin signaling molecules in β-cells and regulate K_{ATP} channel trafficking, we genetically knocked down AKAP150 expression and monitored surface K_{ATP} channels using surface staining, electrophysiology and surface biotinylation experiments.

INS-1 832/13 cells were transiently transfected with AKAP150 shRNAi to knock down AKAP150 (AKAP150 KD) or with the empty pSilencer vector as a control (132,134). AKAP150 KD cells showed a significant decrease in AKAP150 expression compared to control cells regardless of whether they received vehicle or leptin (10 nM) treatment for 30 minutes (Fig. 5A). Surface staining of exogenously expressed BTX-SUR1/Kir6.2 K_{ATP} channels was again used to

visualize K_{ATP} channels in the membrane. Similar to untransfected INS-1 832/13 cells (Fig. 3B), pSilencer transfected control cells also showed increased surface K_{ATP} channel expression when treated with leptin, but this effect appeared to be reduced in AKAP150 KD cells (Fig. 5B). In agreement with this observation, cell-attached current-clamp recordings showed that leptin-induced hyperpolarization was drastically reduced from -60.40 ± 4.60 mV (n=5) in pSilencer control cells to 0.30 ± 0.49 mV ($p<0.0001$, n=6) in AKAP150 KD cells (Fig. 5C). To further substantiate the role of AKAP150 in leptin signaling we carried out surface biotinylation experiments to examine the expression of endogenous K_{ATP} channels at the membrane. Control and AKAP150 KD cells were treated with vehicle or leptin (10 nM) for 30 minutes followed by surface biotinylation and western blot analysis. In pSilencer control cells, leptin caused a significant 2.39-fold increase ($p<0.01$) of surface SUR1 compared to vehicle treatment (Fig. 5D). In contrast, AKAP150 KD cells failed to show an increase of surface K_{ATP} channels upon leptin treatment. Taken together these findings identify a novel relationship between AKAP79/150 and leptin signaling in β-cells.

To determine whether the effect observed with AKAP150 KD is specific, we examined the effect of knockdown of another membrane associated AKAP, AKAP220(244,245). INS-1 832/13 cells were transfected with scramble control siRNA or AKAP220 siRNA (AKAP220 KD) and knockdown of AKAP220 expression was confirmed by western blot analysis (Fig. 5E). Surface biotinylation experiments were then carried out to assess K_{ATP} channel trafficking in response to leptin. As expected, scramble control cells treated with leptin showed a significant 2.30-fold increase ($p<0.01$) in surface SUR1 expression compared to vehicle control (Fig. 5F). AKAP220 KD cells stimulated with leptin also showed a significant 2.19-fold increase ($p<0.01$) in surface SUR1 expression compared to vehicle treated cells. The amount of surface SUR1 in leptin treated AKAP220 KD cells was comparable to scramble control cells treated with leptin

and in stark contrast to AKAP150 KD cells. From these observations we concluded that AKAP220 is not involved and that AKAP79/150 plays a unique role for leptin signaling.

5.3.6. AKAP79/150 mediates leptin signaling via its interaction with PKA

As a PKA anchoring protein, AKAP79/150 presumably participates in leptin signaling by binding to PKA and bringing PKA in proximity to the other signaling molecules. However, in addition to PKA, AKAP79/150 has also been found to anchor protein phosphatase 2B (PP2B; also known as calcineurin; see Fig. 6A)(135,246), which opposes PKA activity by dephosphorylating PKA substrates. This dual specificity of AKAP79/150 coordinates PKA and PP2B signaling and allows anchored-PKA actions on downstream substrates to be tightly regulated. Indeed, AKAP79/150 mutants that lack the PP2B binding PxIxIT-like motif (AKAP79ΔPIX; Fig. 6A)(110,135,246) display increased localized PKA activity(110,134,135,247). To address whether the role of AKAP79/150 in leptin signaling involves AKAP79/150 interaction with PKA, PP2B, or both, we performed AKAP150 KD and rescue experiments using full-length WT AKAP79 (human ortholog of mouse AKAP150), or AKAP79 mutants deficient in PKA or PP2B binding.

First, we performed surface biotinylation experiments in AKAP150 KD cells transfected with WT AKAP79 (AKAP150 KD/AKAP79) to test whether expression of AKAP79 would rescue leptin-induced K_{ATP} channel trafficking in AKAP150 KD cells. In this set of experiments leptin treatment caused a significant 1.47-fold increase ($p<0.001$) of surface SUR1 in pSilencer transfected control cells and a similar 1.42-fold increase ($p<0.01$) was observed in AKAP150 KD/AKAP79 cells demonstrating that AKAP79 successfully rescues a loss of AKAP150 (Fig. 6A, B). This result also confirms that the lack of leptin response in AKAP150 KD cells (Fig. 5D) was not due to off-target effects of the shRNAi. Next, we performed the same experiment using an AKAP79 mutant that lacks the PKA binding motif (AKAP79ΔPKA; Fig. 6A)(110,246) to test the importance of AKAP79/150-anchored PKA for leptin signaling. AKAP150 KD/AKAP79ΔPKA

cells treated with leptin failed to show a significant change in surface K_{ATP} channel expression compared to vehicle treated cells (Fig. 6C) indicating that PKA anchored by AKAP79/150 serves a critical function in the leptin signaling cascade. Lastly, surface biotinylation experiments were performed in AKAP150 KD cells co-transfected with an AKAP79 mutant lacking the PP2B binding motif (AKAP150 KD/AKA79ΔPIX). Interestingly, compared to vehicle pSilencer controls, vehicle treated AKAP150 KD/AKA79ΔPIX cells exhibited a 1.96-fold increase in surface SUR1 expression levels akin to that seen in leptin treated controls (Fig. 6D). Stimulating AKAP150 KD/AKA79ΔPIX cells with leptin led to an even greater 2.87-fold increase in surface K_{ATP} channels, although this increase was not statistically significant when compared to vehicle treated AKAP150 KD/AKA79ΔPIX cells ($p>0.05$). The higher than normal K_{ATP} channel surface expression in unstimulated AKAP150 KD/AKAP79ΔPIX cells implies that PP2B constitutively bound to AKAP79 likely limits anchored-PKA signaling such that disrupting PP2B anchoring mimics the effect of leptin to increase basal PKA signaling and K_{ATP} channel trafficking. The combined results from these experiments provide compelling evidence that leptin increases AKAP79/150-anchored PKA activity and suggest that these actions of PKA are basally opposed by AKAP79/150-anchored PP2B.

5.3.7. Leptin increases cAMP concentrations near AKAP79

The results thus far indicate that leptin increases the activity of AKAP79/150 anchored-PKA to regulate K_{ATP} channel trafficking, but how leptin activates PKA remains to be addressed. PKA is typically activated by cAMP, which binds to PKA regulatory subunits and relieves autoinhibition to unleash the catalytic subunits. Alternatively, inhibiting the opposing activity of PP2B could also enhance net PKA signaling(110,230,238,247,248). Our results above implicating that AKAP150 KD/AKAP79ΔPIX cells have increased basal PKA signaling is consistent with an inhibitory role of PP2B on steady state PKA signaling. However, the observation that AKAP150 KD/AKAP79ΔPIX cells still responded to leptin suggests a PKA

activation mechanism independent of PP2B inhibition. This prompted us to ask whether leptin increases cAMP levels near AKAP79/150. To monitor changes in cAMP near AKAP79/150, we employed the FRET-based cAMP CUTie sensor targeted to AKAP79 (AKAP79-CUTie)(127). AKAP79-CUTie was found to express at the cell membrane where we had also observed increases in PKA activity. Similar to FRET-based PKA activity experiments, we treated the cells with vehicle or leptin (100 nM), normalized the FRET traces to a maximal response, and then analyzed the traces for area under the curve. To generate a maximal response we applied forskolin (20 μM) and IBMX (10 μM), which increases cAMP production by adenylyl cyclases (ACs) and prevents cAMP degradation by phosphodiesterases (PDEs), respectively. During our first set of experiments we did not see a significant difference in cAMP levels between treatments, although there appeared to be a trend toward increased cAMP in leptin treated cells (Fig. 7A). Since AKAPs have also been shown to anchor PDEs to tightly regulate PKA activity via cAMP degradation(115) we repeated the experiments in the presence of IBMX to prevent potential cAMP degradation that could obscure cAMP signals. In the presence of IBMX, leptin treated cells showed a significant 1.53-fold increase ($p<0.0005$, n=16) in AKAP79-CUTie cAMP sensor activity compared to vehicle (n=15) (Fig. 7B). This effect of leptin on cAMP levels appears to be specific to AKAP79 as leptin did not significantly increase cAMP levels monitored by a cytoplasmic AKAP18δ-CUTie sensor (Fig. 7C). Curiously, in the presence of forskolin, leptin accelerated cAMP accumulation as detected by AKAP18δ-CUTie suggesting that leptin may augment cAMP production by forskolin. These results lead us to conclude that leptin signaling activates PKA at least in part by increasing local cAMP levels near AKAP79/150.

5.4. Discussion

The study we present here reveals a novel relationship between leptin and PKA for K_{ATP} channel trafficking in β-cells that is mediated by AKAP79/150. From this work and our previous studies we propose a model in which the PKA-AKAP79/150 complex orchestrates leptin-induced K_{ATP} channel trafficking to suppress GSIS from pancreatic β-cells (Fig. 8). In this model leptin stimulation increases PKA activity anchored by AKAP79/150 through a signaling cascade wherein leptin activates Src kinase which phosphorylates and potentiates NMDARs, resulting in an enhanced Ca^{2+} influx that activates CaMKKβ to phosphorylate and activate AMPK. AMPK then increases PKA activity by elevating cAMP concentrations localized near AKAP79/150, possibly by activating an AC, culminating in actin remodeling and the translocation of K_{ATP} channels. A greater abundance of K_{ATP} channels in the membrane increases the total K^+ conductance causing β-cell membrane hyperpolarization and inhibition of Ca^{2+} influx through voltage-dependent Ca^{2+} channels to prevent insulin exocytosis. Importantly, we found that in human β-cells the ability of leptin to reduce electrical activity was also dependent on PKA-AKAP interactions suggesting that this signaling mechanism serves an important function in the regulation of insulin secretion in humans.

Mechanism of leptin-induced PKA activity

Although our previous studies suggested that PKA-dependent actin remodeling was necessary for leptin to promote K_{ATP} channel trafficking(58), there was very little evidence outside of our own findings for such a signaling relationship between leptin and PKA(249). By implementing FRET-based live cell imaging to monitor PKA activity in combination with pharmacology we demonstrate here that leptin significantly increases PKA activity at the cell membrane via the NMDAR-CaMKKβ-AMPK signaling axis. The finding that AMPK activation can increase PKA activity in β-cells was notable as two prior studies, one in vascular smooth muscle cells and the other in cardiomyocytes, had only tentatively implicated AMPK upstream of

PKA(102,103). One potential mechanism for AMPK to increase PKA signaling is by inhibiting protein phosphatase activity to prevent the dephosphorylation of PKA effectors. While there are some studies to suggest that AMPK may counteract protein phosphatases(250), others show that AMPK is inactivated by protein phosphatases(251,252) or that AMPK increases protein phosphatase activity(253,254). Our experiments using the AKAP79ΔPIX mutant that cannot bind PP2B showed that even vehicle treated cells displayed increased surface K_{ATP} channel expression, which could be the result of a loss of AKAP79-anchored PP2B opposing basal AKAP79-anchored PKA activity. Thus, it is possible that leptin signals via AMPK to inhibit AKAP79-anchored PP2B activity resulting in increased K_{ATP} channel surface density. However, the fact that leptin still increases surface K_{ATP} channels in AKAP150 KD/AKAP79ΔPIX cells, albeit not statistically significant compared to vehicle treated control due to already elevated basal K_{ATP} channel surface expression, suggests leptin increases PKA activity independent of PP2B. In this regard, our finding that leptin stimulation raises cAMP levels near AKAP79-CUTie suggests an alternative mechanism by which AMPK increases PKA activity. It is unlikely that AMPK increases cAMP by inhibiting PDEs as we were only able to detect significantly elevated cAMP levels in the presence of the PDE inhibitor IBMX, and in other contexts AMPK has been shown to increase PDE activity(255). Rather, AMPK may act via ACs either directly or indirectly to cause a rise in cAMP. , Indeed, several ACs have been reported to interact with AKAP79/150(235,256–260). Of note, we observed a small but significant increase in cAMP detected by the cytosolic AKAP18CUTie in response to forskolin stimulation in leptin treated cells compared to vehicle treated cells; this raises the possibility that leptin may also enhance forskolin-induced AC activation in the cytosol, although the significance of this observation awaits further investigation. Other possibilities that AMPK phosphorylates a yet-to-be identified intermediary or directly phosphorylates PKA to induce catalytic activity also need to be

considered(261). It is clear that more work is required to determine the precise mechanism by which AMPK activates PKA.

Spatiotemporal regulation of PKA activity in β-cells

A key observation made during these studies is that leptin causes an increase in PKA activity that is restricted near the cell membrane. While our studies support that leptin signals via PKA to increase K_{ATP} channel surface density, K^+ conductance and subsequent β-cell hyperpolarization known to inhibit GSIS(58,65), others have found that the incretin hormone glucagon-like peptide 1 (GLP-1) signals via PKA to promote insulin granule trafficking(114) and Ca^{2+}-induced exocytosis to augment GSIS(117,232–234). All of these studies have used pharmacological or genetic manipulations of total PKA activity to implicate PKA in either inhibiting or enhancing GSIS. Although some of these discrepancies may be explained in part by differences in experimental design, it is also likely that they are the result of the indiscriminate activation and/or inhibition of total cellular PKA. In contrast, endogenous hormonal and physiological stimuli such as leptin and GLP-1 are likely to act in a more nuanced manner due to high spatial and temporal regulation. This is supported by our data demonstrating that leptin has a much more limited effect on PKA activity compared to the global PKA activator forskolin. Specificity of PKA signaling within cells is attributed primarily to AKAPs, such as AKAP79/150, organizing PKA signaling microdomains. Interestingly, recent work in vascular smooth muscle cells also illustrates how local cAMP-PKA signaling in an AKAP79/150-organized complex can dictate a very different downstream cellular response from that regulated by more global engagement of cAMP and PKA(262). Of note, some AKAPs expressed in β-cells, including AKAP79/150, have already been implicated in either inhibiting or promoting insulin secretion(117–120,235,236). This highlights that a high level of structural cellular organization is essential for β-cells to incorporate multiple complex signaling networks in order to function properly, including the opposing effects of the hormones leptin and GLP-1.

Implications for the role of AKAP79/150 in insulin secretion

Our results that AKAP150 knockdown or expression of AKAP79ΔPKA prevents leptin-induced K_{ATP} channel trafficking indicate that AKAP79/150 coordinates PKA and leptin signaling to impact insulin secretion. Interestingly, neither AKAP150 knockdown nor AKAP79ΔPKA expression affected basal K_{ATP} channel surface expression, suggesting that while AKAP79/150 anchored-PKA is critical for leptin signaling it is unlikely to be involved in constitutive K_{ATP} channel trafficking. On the other hand, our findings that expression of AKAP79ΔPIX, a mutant that cannot bind PP2B, leads to a greater abundance of K_{ATP} channels in the β-cell membrane in the absence of leptin stimulation suggests that increasing AKAP79/150 anchored-PKA activity is sufficient to promote K_{ATP} channel translocation. Note, a previous study has reported that mouse islets lacking AKAP150 exhibit reduced GSIS(120), which was attributed to the effects of AKAP150 on L-type Ca^{2+} channels. Curiously, the same study found that while expressing AKAP150ΔPKA in AKAP150 knockout islets did not affect GSIS, expressing AKAP150ΔPIX significantly reduced GSIS(120). These observations are congruent with our findings in INS-1 832/13 cells that disrupting PKA tethering did not affect basal surface K_{ATP} channel density but disrupting PP2B tethering increases basal surface K_{ATP} channel density. This raises the possibility that the reduced GSIS observed in AKAP150ΔPIX-expressing islets is in part due to increased K_{ATP} channel surface expression. Noteworthy, the activity of PP2B is stimulated by Ca^{2+} raising the question of whether Ca^{2+} influx through NMDARs following leptin stimulation also increase PP2B activity to oppose the effect of leptin on PKA and K_{ATP} channel trafficking. Such a dual mode of Ca^{2+} effect on K_{ATP} channel surface expression may play a role in setting the range of K_{ATP} channel surface density and will be an interesting topic to pursue in the future. It is also worth mentioning that PKA and PP2B have been reported to modulate K_{ATP} channel phosphorylation and subsequently K_{ATP} channel gating in some contexts(263–267). However,

our published(58) data showed that there is little difference in the gating properties of K_{ATP} channels between vehicle treated and leptin treated cells, suggesting the effect of altered PKA and/or PP2B signaling following leptin stimulation affects primarily K_{ATP} channel trafficking rather than gating. Also important, while our current study focuses on the role of AKAP79/150 in mediating PKA signaling by leptin, AKAP79/150 is multifaceted and can coordinate multiple signaling complexes, as has been shown in neurons(133,134,242) and other cell types(262,268). Thus, AKAP79/150 in β-cells may be involved in organizing multiple signaling networks with distinct functions. Finally, increased K_{ATP} channel trafficking has been observed following glucose starvation via activation of AMPK(68), and following high glucose stimulation in a PKA-dependent manner(142). It will be interesting to determine in the future whether these regulations are similarly mediated by AKAP79/150.

In summary, we have identified a novel role of AKAP79/150 in coordinating leptin and PKA signaling to regulate K_{ATP} channel trafficking in β-cells, hence GSIS. Importantly, our recent studies showed that in human β-cells from obese type II diabetic donors and β-cells from obese diabetic *db/db* mice lacking functional leptin receptors leptin fails to promote K_{ATP} channel trafficking and membrane hyperpolarization; however, activation of NMDARs downstream of leptin reenacted the effect of leptin(229). Thus further exploration into the leptin signaling pathway coordinated by AKAP79/150 will likely provide valuable insight into how the β-cell regulates K_{ATP} channel trafficking to tune its function and may even identify potential therapeutic targets to combat type II diabetes.

5.5. Figures

Table 5. 1. Human Islets Donor Information.

Donor (date received)	T2D	Age	Gender	BMI	Cause of death	Islet viability (%)	Islet purity (%)
10/09/18[1]	N	47	F	24.1	Stroke	90	90
10/19/18[2]	N	55	F	35.7	Stroke	98	94
11/07/18[3]	N	48	M	24.4	Head trauma	90	90

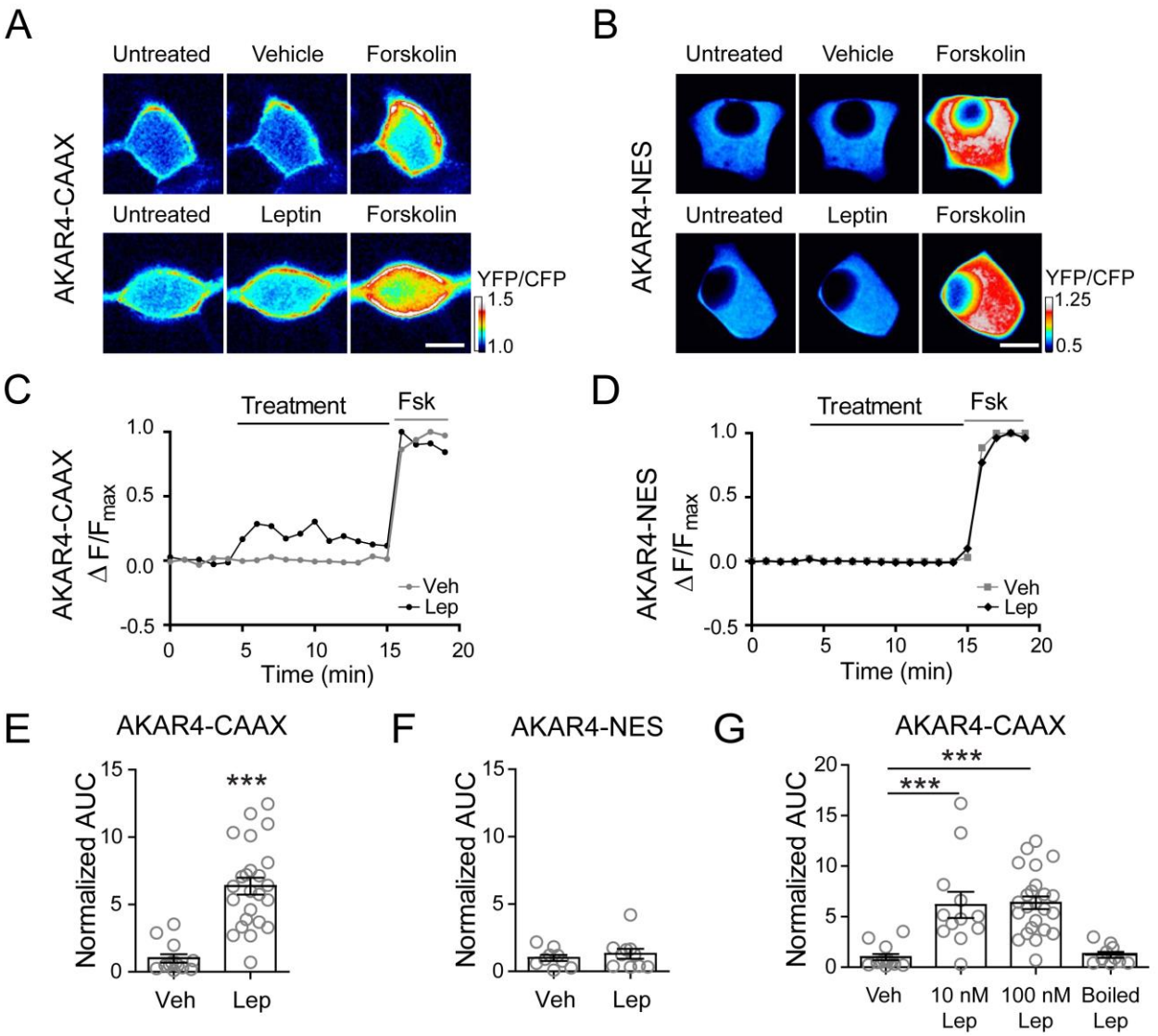

Figure 5. 1. Leptin increases PKA activity.

A, B) Ratiometric images of INS-1 832/13 cells transfected with the FRET-based PKA activity reporter A-kinase activity reporter 4 (AKAR4), which has been targeted to the plasma membrane with a farnesylation motif (AKAR4-CAAX) or to the cytoplasm with a nuclear export signal (AKAR4-NES). Cells were treated with vehicle or leptin (100 nM) followed by the robust PKA activator forskolin (20 μM). *Scale bar, 5 μm*. **C, D)** FRET traces of the cells in **(A, B)** normalized to the maximal forskolin response. **E)** Group analysis of AKAR4-CAAX cell traces. Graph shows the fold-change in area under the curve (AUC) normalized to vehicle treatment (n=13). 100 nM leptin (n=24) was used for these experiments. ***p<0.0001 by unpaired student's t-test. **F)** Group data of AKAR4-NES expressing cells treated with vehicle (n=9) or 100 nM leptin (n=10). **G)** Group analysis for AKAR4-CAAX cells treated with vehicle (n=13), 10 nM leptin (n=12), 100 nM leptin (n=24), or boiled 100 nM leptin (n=10). ***p<0.001 by one-way ANOVA followed by a post-hoc Dunnett's multiple comparison test. In all figures, circles represent individual cells except as otherwise specified.

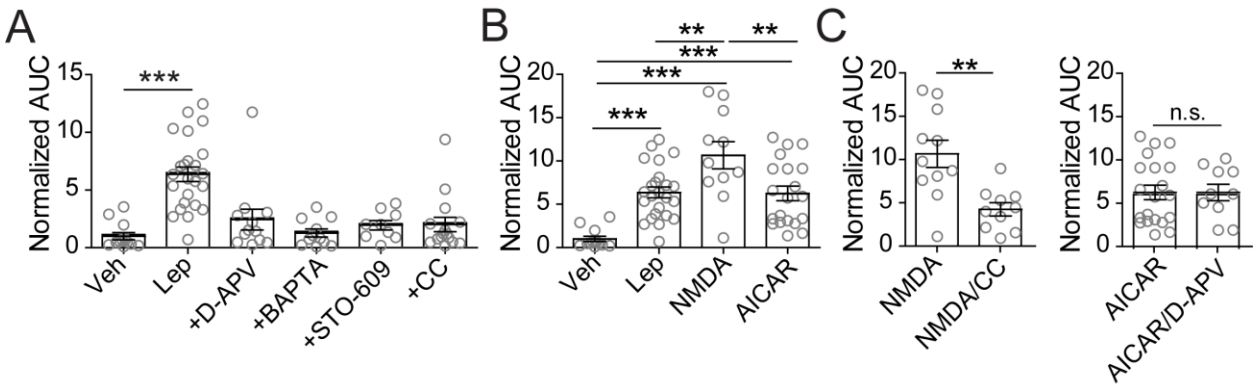

Figure 5. 2. Leptin activates PKA via the NMDAR-CaMKKβ-AMPK signaling cascade.

INS-1 832/13 cells were transfected with AKAR4-CAAX followed by various treatments. **A)** PKA activity in response to 100 nM leptin (n=24) alone or in the presence of the NMDAR inhibitor D-APV (50 μM; n=12), the Ca^{2+} chelator BAPTA (10 mM; n=11), the CaMKKβ inhibitor STO-609 (1 μM; n=9), or the AMPK inhibitor Compound C (CC, 1 μM; n=15). Treatments were compared to vehicle control (n=13). ***p<0.001 as determined by one-way ANOVA ($F_{(4,66)}$ = 12.13, p<0.0001) followed by a post-hoc Dunnett's multiple comparison test. **B)** Effects of NMDAR co-agonists NMDA/glycine (100 μM/100 μM; n=11) and the AMPK activator AICAR (500 μM; n=20) on PKA activity. **p<0.01, ***p<0.001 by one-way ANOVA ($F_{(3,64)}$ = 15.77, p<0.0001) followed by a post-hoc Tukey's multiple comparison test **C)** PKA activity in response to NMDAR activation by NMDA/glycine in the absence or presence of the AMPK inhibitor CC (1 μM; p=0.002, n=10), and to AMPK activation by AICAR in the absence or presence of the NMDAR inhibitor D-APV (50 μM; p=0.99 n=10). Statistical analysis by unpaired student's t-test.

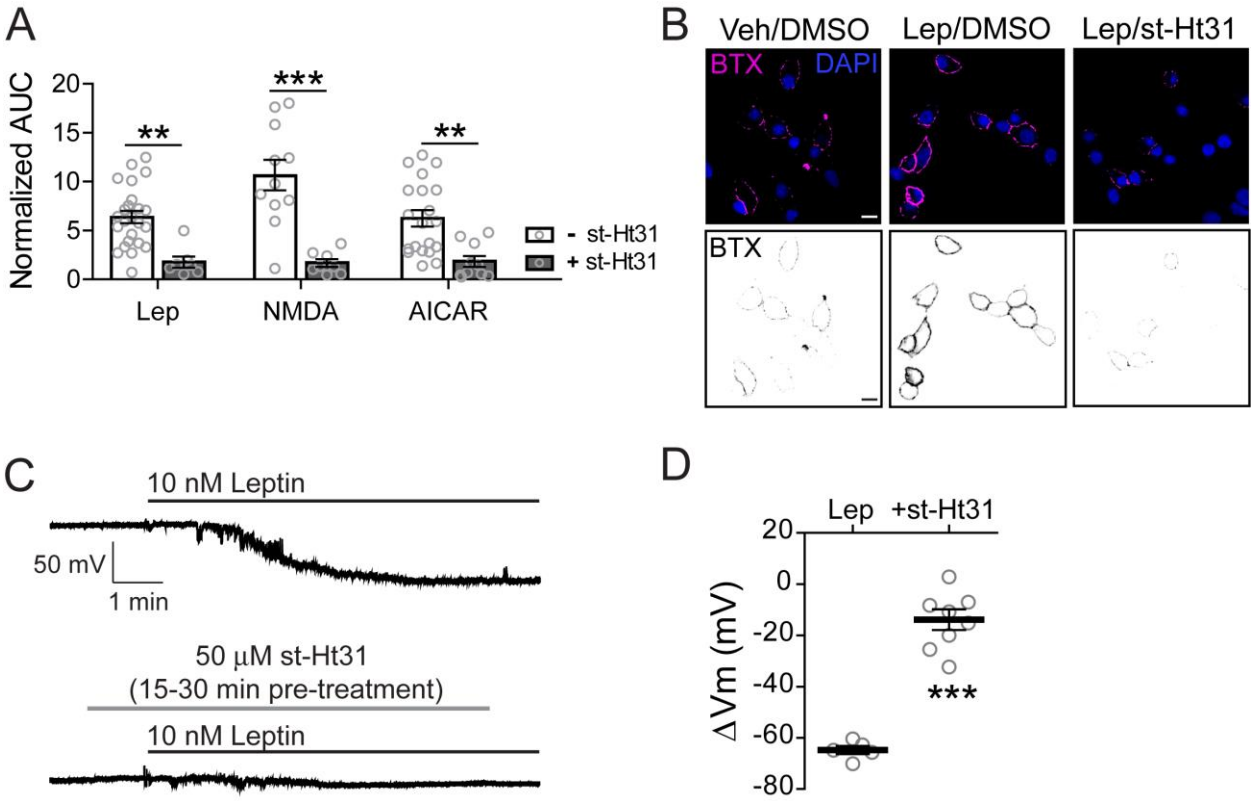

Figure 5. 3. Leptin signaling through PKA requires an A-kinase anchoring protein (AKAP).

A) Effects of the PKA-AKAP interaction disruptor peptide st-Ht31 on PKA activity. Group FRET data of cells expressing AKAR4-CAAX in response to various stimuli: 100 nM leptin (n=7), NMDAR co-agonists NMDA/glycine (100 μM/100 μM) (n=8), and AMPK activator AICAR (500 μM) (n=10) in the presence of st-Ht31 (50 μM). Results are compared to those shown in Fig. 2B of cells treated with leptin (n=24), NMDA/glycine (n=11) and AICAR (n=20) in the absence of st-Ht31**p<0.01, ***p<0.001. Data was analyzed by two-way ANOVA followed by a post hoc Bonferroni's test. Analysis revealed significant main effects of st-Ht31 ($F_{1,74}$ = 54.17, p<0.0001), but no significant main effects of stimuli ($F_{2,74}$ = 2.76, p= 0.07) nor a significant interaction between these variables ($F_{2,74}$ = 3.11, p=0.05). **B)** INS-1 832/13 cells transduced with bungarotoxin binding motif-tagged SUR1 (BTX-SUR1) and Kir6.2 subunits of K_{ATP} channels and treated with leptin (10 nM) for 30 min in the presence of 0.01% DMSO or 50 μM st-Ht31. Surface K_{ATP} channels were then labeled with Alexa 555-conjugated bungarotoxin (BTX) and nuclei were stained with DAPI. Top panels show representative confocal microscopy images. Inverse gray scale representations of BTX-labeled surface K_{ATP} channels are shown in bottom panels. *Scale bar, 10 μm*. **C)** Representative INS-1 832/13 cell-attached membrane recordings in response to leptin (10 nM) in the absence or presence of st-Ht31 (50 μM) pre-incubation (15-30 min). **D)** Group data showing the extent of membrane hyperpolarization in response to leptin without st-Ht31 pre-incubation (-64.76 ± 1.61 mV, n=5) or with st-Ht31 pre-incubation (-14.53 ± 3.96 mV, n=8). ***p<0.001 by unpaired student's t-test. For graph analysis of membrane potential recordings the mean is represented by a thick line with error bars depicting the standard error of the mean.

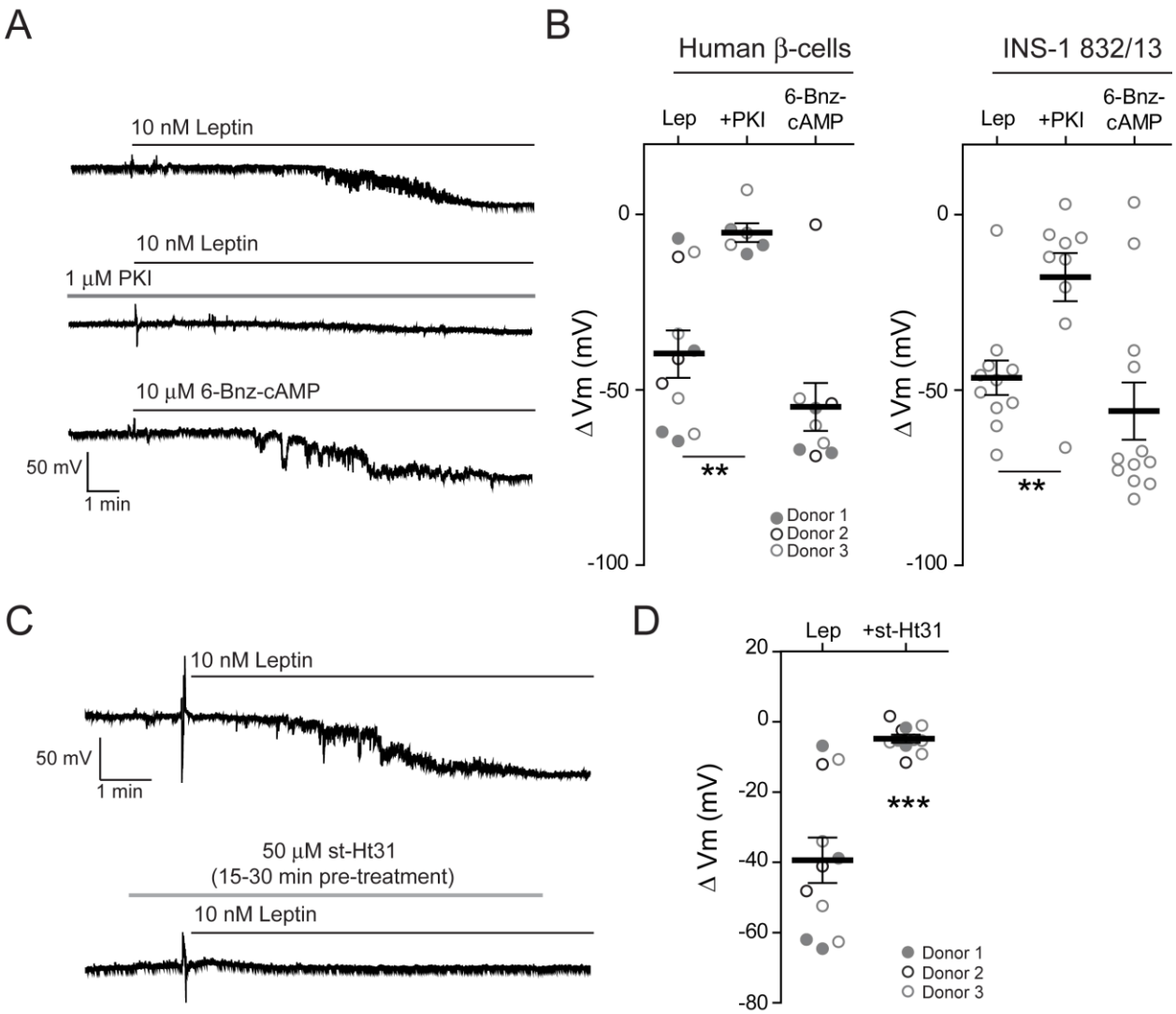

Figure 5. 4. AKAP anchoring of PKA is necessary for leptin-induced hyperpolarization in human β-cells.

A) Representative cell-attached membrane recordings of individual human β-cells treated with 10 nM leptin (top), leptin in the presence of the PKA inhibitor PKI (middle; PKI, 1 μM), or the PKA-specific activator 6-Bnz-cAMP (bottom; 6-Bnz-cAMP, 10 μM). **B)** Group analysis of the extent of membrane hyperpolarization of human β-cells (left) or INS-1 832/13 cells (right) treated with leptin (human β-cells: -39.40 ± 6.46 mV, n=11; INS-1 832/13 cells: -46.49 ± 4.92 mV, n=11), leptin with PKI (human β-cells: -5.18 ± 2.65 mV, n=6; INS-1 832/13 cells: -17.82 ± 6.88 mV, n=9), or 6-Bnz-cAMP (human β-cells: -54.84 ± 6.83 mV, n=9; INS-1 832/13 cells: -56.00 ± 8.15 mV, n=12). **p<0.01 by one-way ANOVA followed by a post-hoc Dunnett's multiple comparison test. **C)** Representative membrane potential recordings of human β-cells in response to leptin (10 nM) following pre-incubation without (top) or with 50 μM st-Ht31 (bottom) for 15-30 min. **D)** Group data of human β-cells showing the degree of membrane hyperpolarization in response to leptin without st-Ht31 pre-incubation (-39.40 ± 6.46 mV, n=11) or with st-Ht31 pre-incubation (-4.81 ± 1.13 mV, n=11). ***p<0.0001 by unpaired student's t-test. Donors are indicated by the circle color and fill.

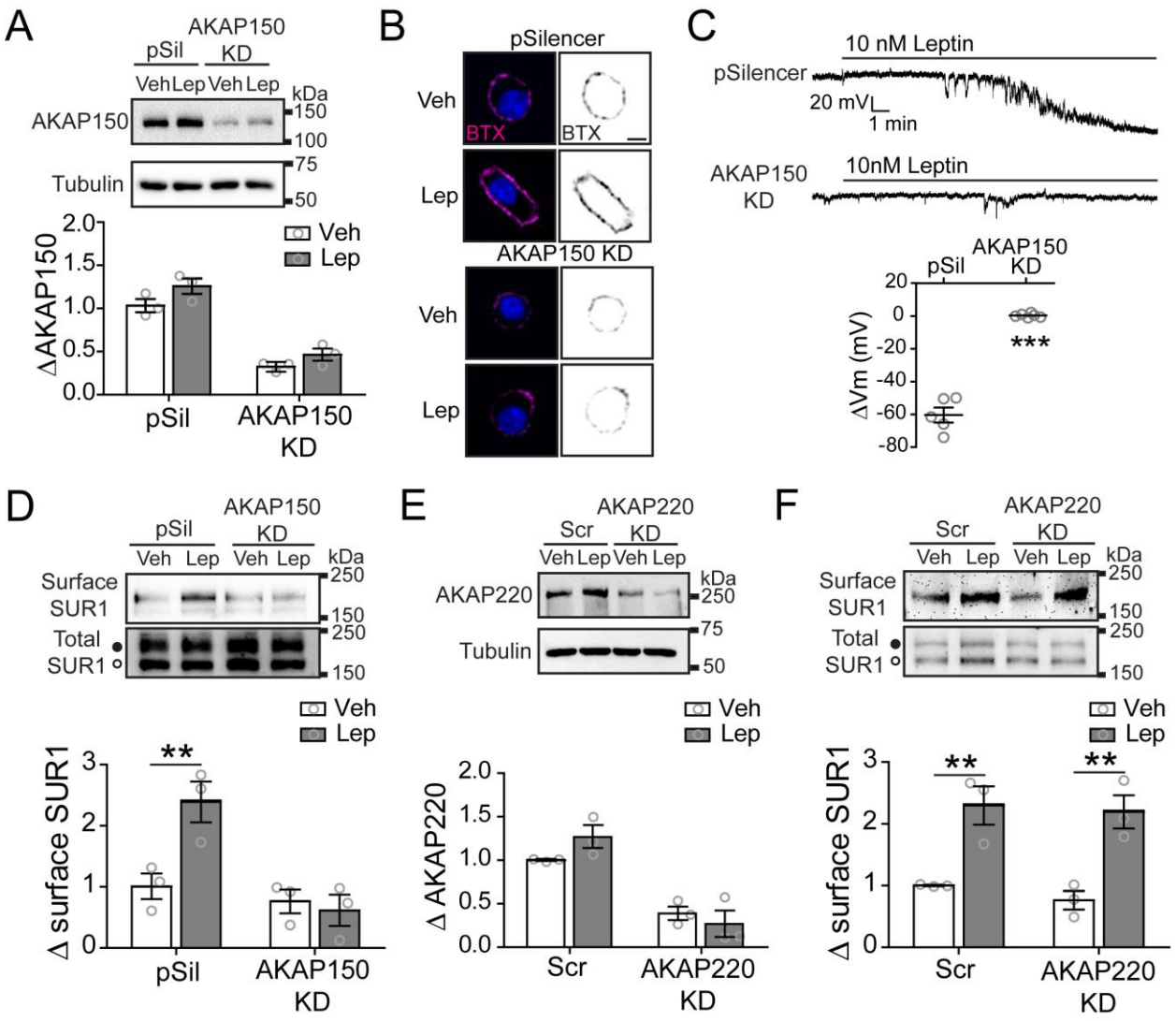

Figure 5. 5. AKAP150 is necessary for leptin-induced K_{ATP} channel trafficking.

A) INS-1 832/13 cells transfected with the control pSilencer vector (pSil) or AKAP150 shRNAi (AKAP150 KD) and analyzed for AKAP150 expression via western blot (top). Graph shows quantification of AKAP150 relative to tubulin (bottom). Analysis determined significant main effects of cells ($F_{(1,8)}$ = 113.37, p<0.0001), treatment ($F_{(1,8)}$ = 6.68, p=0.03), but no significant interaction between these variables ($F_{(1,8)}$ = 0.38, p=0.55). **B)** Confocal images of BTX labeled surface K_{ATP} channels following vehicle or 10 nM leptin treatment in pSil and AKAP150 KD cells (top panels). Bottom panels show inverse gray scale representations. *Scale bar, 5 μm*. **C)** Representative membrane potential recordings from pSil (top; -60.40 ± 4.60 mV, n=5) and AKAP150 KD (bottom; 0.30 ± 0.49 mV, n=6) cells treated with 10 nM leptin. Below the traces is the group analysis of the extent of membrane hyperpolarization. ***p<0.0001 by unpaired student's t-test. **D)** Surface biotinylation experiments. Western blots show surface expression of the K_{ATP} channel subunit SUR1 and total SUR1 in pSil and AKAP150 KD cells treated with vehicle or 10 nM leptin (top). Note, the upper band in the total SUR1 corresponds to the complex-glycosylated SUR1 (filled circles) that traffics to the surface and the lower band corresponds to the ER-core glycosylated SUR1 (open circle). Normalized quantification of

surface SUR1 relative to total upper SUR1 band, which represent mature K_{ATP} channels that may be trafficked to the cell membrane (bottom). Data analysis revealed significant main effects of cells ($F_{(1,8)}$ = 15.79, p=0.004), treatment ($F_{(1,8)}$ = 5.95, p=0.04), and a significant interaction between these variables ($F_{(1,8)}$ = 9.18, p=0.016). **E)** Western blot analysis (top) and quantification (bottom) of AKAP220 expression in control scramble siRNA (Scr) or AKAP220 siRNA (AKAP220 KD) cells. Significant main effects of cells ($F_{(1,8)}$ = 56.41, p<0.0001), no effect of treatment ($F_{(1,8)}$ = 0.43, p=0.53), and no interaction ($F_{(1,8)}$ = 3.16, p=0.11) by two-way ANOVA. **F)** Western blots showing the effects of AKAP220 siRNA on surface SUR1 relative to total SUR1. Analysis determined no effect of cells ($F_{(1,8)}$ = 0.61, p=0.48), a significant effect of treatment ($F_{(1,8)}$ = 38.89, p=0.0002), and no significant interaction between these variables ($F_{(1,8),}$ = 0.10, p=0.76). Biochemical experiments **(A, D, E, F**) were repeated three times (n=3; represented as circles) and normalized to vehicle treated controls. **p<0.01, ***p<0.001 by two-way ANOVA followed by a post-hoc Bonferroni's test unless stated otherwise.

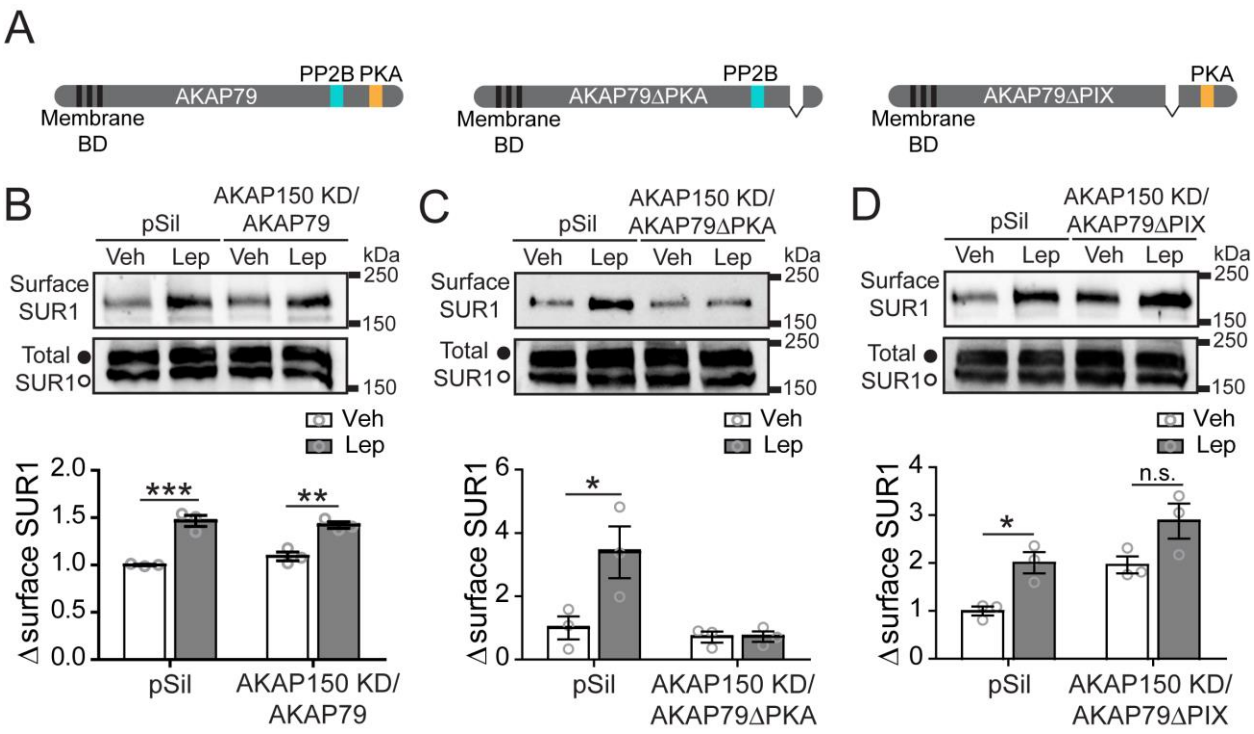

Figure 5. 6. AKAP79 rescues leptin-induced K_{ATP} channel trafficking in AKAP150 KD cells.

A) Schematic of AKAP79 showing key membrane binding domains (BD) as well as PP2B and PKA binding regions. **B)** INS-1 832/13 cells were transfected with control pSilencer vector (pSil) or co-transfected with AKAP150 shRNAi and WT AKAP79 (AKAP150 KD/AKAP79). Transfected cells were treated with vehicle or 10 nM leptin for 30 min followed by surface biotinylation. Western blots show surface SUR1 and total SUR1 (top). Quantification of surface SUR1 relative to total upper SUR1 band (bottom). There was a significant effect of treatment ($F_{(1,8)}$ = 91.33, p<0.0001), no significant effect of cells ($F_{(1,8)}$ = 0.33, p=0.58) and no interaction between these variables ($F_{(1,8)}$ = 2.624, p=0.14). **C)** Same as **(B)** except AKAP150 KD cells were co-transfected with AKAP79 mutants that cannot bind PKA (AKAP150 KD/AKAP79ΔPKA). Both cells ($F_{(1,8)}$ = 10.18, p=0.0128) and treatment ($F_{(1,8)}$ = 6.73, p=0.0319) had significant effects in these experiments, and there was a significant interaction between these variables ($F_{(1,8)}$ = 6.573, p=0.033). **D)** Same as **(B)** except AKAP150 KD cells were co-transfected with AKAP79 mutants that cannot bind PP2B (AKAP150 KD/AKAP79ΔPIX). Analysis of these data revealed that both cells ($F_{(1,8)}$ = 15.08, p=0.0047) and treatment ($F_{(1,8)}$ = 16.61, p=0.0036) had significant effects, but there was no interaction between the two ($F_{(1,8)}$ = 0.039, p=0.8485). Each experiment was performed three independent times (n=3; shown as circles) and results were normalized to vehicle treated control pSil cells. *p<0.05, **p<0.01, ***p<0.001 by two-way ANOVA followed by a post-hoc Bonferroni's test.

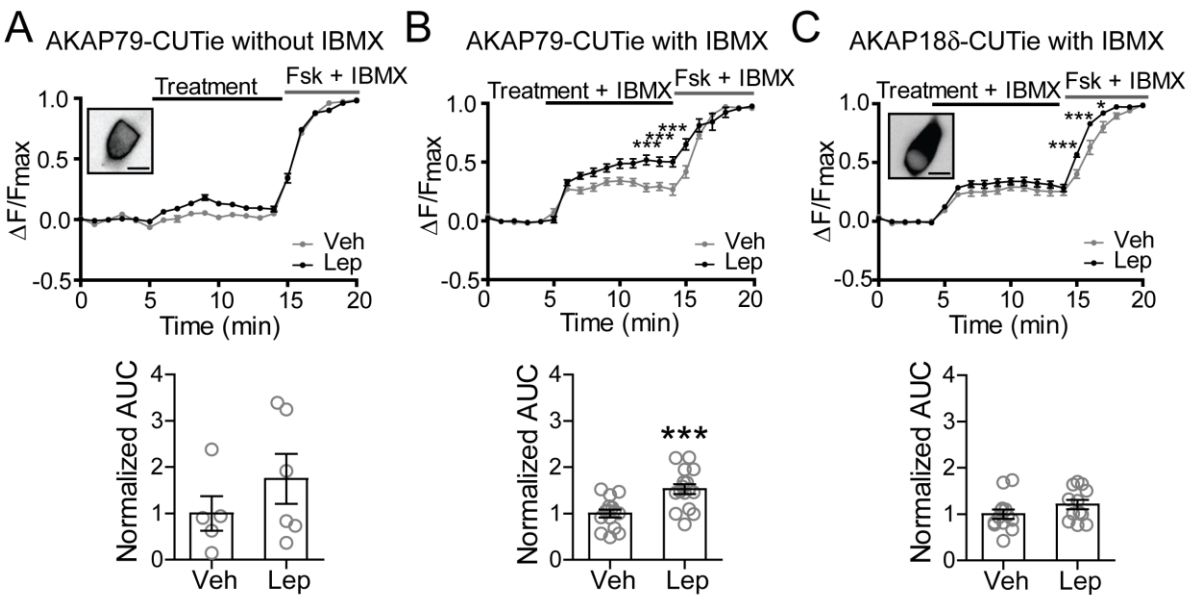

Figure 5. 7. Leptin increases cAMP levels near AKAP79.

A) cAMP CUTie sensor targeted to AKAP79 (human orthologue of AKAP150) was utilized to detect changes in cAMP levels in response to vehicle or 100 nM leptin. The average FRET traces (top) and the group data of FRET traces analyzed for area under the curve (bottom) are shown. *Inset shows INS-1 832/13 cell expressing AKAP79-CUTie sensor. Scale bar, 10 μm*. **B)** Experiments in (A) were repeated in the presence of the phosphodiesterase inhibitor IBMX (50 μM) to prevent rapid degradation of cAMP. Two-way ANOVA analysis of average traces determined a significant effect of treatment ($F_{(1,629)}$ = 40.08, p<0.0001) and time ($F_{(20,629)}$ = 212.5, p<0.0001) and there was a significant interaction between these variables ($F_{(20,629)}$ = 3.96, p<0.0001). This was followed by a post hoc pairwise comparison of time points by Bonferroni's test ***p<0.0001 (top). Below, normalized AUC was analyzed by unpaired student's t-test (***p<0.0005). **C)** Same as **(B)** except cAMP levels were monitored using the AKAP18δ-CUTie sensor, which is largely expressed in the cytosol as shown in the inset. Average traces were analyzed by two-way ANOVA, which revealed a significant effect of treatment ($F_{(1,629)}$ = 46.10, p<0.0001) and time ($F_{(20,629)}$ = 339.8, p<0.0001) and there was a significant interaction between these variables ($F_{(20,629)}$ = 2.27, p=0.0014). *p<0.05, ***p<0.001 by post hoc Bonferroni's test (traces, top). *Scale bar, 10 μm*.

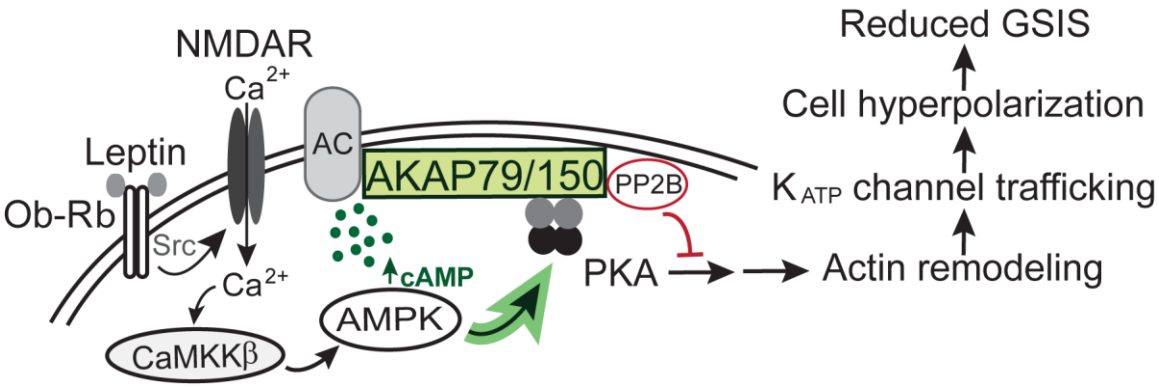

Figure 5. 8. Proposed model depicting AKAP79/150 mediates leptin signaling to regulate K_{ATP} channel trafficking.

AKAP79/150 is a scaffolding protein that creates PKA signaling microdomains localized at cell membranes. AKAP79/150 also anchors PP2B, which opposes PKA activity by dephosphorylating PKA substrates and ACs, which enhance PKA activity by producing the PKA activator cAMP. Signaling complexes coordinated by AKAP79/150 allow for PKA signaling to be tightly regulated. In pancreatic β-cells AKAP79/150 anchoring of PKA renders a localized increase of PKA activity following leptin activation of Src kinase to initiate the NMDAR-CaMKKβ-AMPK signaling cascade. This enhancement of PKA activity may at least in part be due to the leptin signaling axis increasing cAMP levels near AKAP79/150. Actin remodeling downstream of PKA allows for increased K_{ATP} channel trafficking and a subsequent increase in K^+ conductance, which causes cell hyperpolarization and suppresses GSIS.

5.6. Materials and methods

Chemicals. Leptin and glutamate were from Sigma-Aldrich (St. Louis, MO). PKI, 6-Bnz-cAMP, NMDA, Compound C (Dorsomorphin), D-APV, and STO-609 were from Tocris Bioscience (Bristol, UK). AICAR was from Selleck Chemicals (Houston, TX). st-Ht31 inhibitor peptide was from Promega (Madison, WI).

INS-1 832/13 cell culture. INS-1 cells (clone 832/13, referred to herein as INS-1 832/13) were cultured in RPMI 1640 medium with 11.1 mM D-glucose (Invitrogen) supplemented with 10% fetal bovine serum (FBS), 100 units/ml penicillin, 100 µg/ml streptomycin, 10 mM HEPES, 2 mM glutamine, 1 mM sodium pyruvate, and 50 µM β-mercaptoethanol. Only cells within passage numbers 55-75 were used for experiments.

Dissociation of human pancreatic β-cells. Human β-cells were dissociated from human islets obtained through the Integrated Islets Distribution Program (IIDP) as described previously(58,65,182,229). Human islets were cultured in RPMI 1640 medium with 10% FBS and 1% L-glutamine. Islets were dissociated into single cells by trituration in a solution containing 116 mM NaCl, 5.5 mM D-glucose, 3 mM EGTA, and 0.1% bovine serum albumin (BSA), pH 7.4. Dissociated cells were then plated on 0.1% gelatin-coated coverslips and allowed to recover overnight in culture media. For electrophysiological experiments, β-cells were identified by their high level of autofluorescence at 488 nm excitation due to β-cells having high concentrations of unbound flavin adenine dinucleotide(224,225). Dithizone (Sigma-Aldrich) staining confirmed β-cell identity at the end of each experiment(269). Donor information is provided in Table 1.

Plasmids, viruses, and siRNA. pcDNA3-EGFP (Addgene plasmid #13031) was a gift from Doug Golenbock (UMass, MA). pcDNA3-AKAR4-CAAX (Addgene plasmid #61621) and pcDNA3-AKAR4-NES (Addgene plasmid #64727) were gifts from Jin Zhang (UCSD, CA).

AKAP79-CUTie and AKAP18δ-CUTie were gifts from Manuela Zaccolo (Oxford, UK). AKAP150 shRNAi and pSilencer vector were gifts from John Scott (UW, Washington)(132), AKAP79-GFP, AKAP79ΔPIX, and AKAP79ΔPKA were described previously(110,130,134,135). Recombinant rat Kir6.2 and BTX-tag SUR1 adenoviruses were generated in our lab and described previously(58). AKAP220 siRNA (5'-CCAAUGUAAGCA GUAGUCCUCUAA A-3') and scramble siRNA (5'-UUUAGAGGACUACUGCUUACA UUGG-3') were from Millipore (Burlington, MA).

Electrophysiology. Cell-attached recordings were performed using an Axon 200B amplifier (Molecular Devices, Sunnyvale, CA) and pClamp software. Signals were acquired at 20 kHz and filtered at 2 kHz. Micropipettes were pulled from non-heparinized Kimble glass (Thermo Fisher Scientific, Waltham, MA) on a horizontal puller (Sutter Instruments, Novato, CA) and filled with 140 mM NaCl. The bath solution (Tyrode's solution) contained (in mM): 137 NaCl, 5.4 KCl, 1.8 $CaCl_2$, 0.5 $MgCl_2$, 5 Na-HEPES, 3 $NaHCO_3$, and 0.16 NaH_2PO_4, 11 glucose, pH 7.2. Pipette resistance was typically between 2-6 MΩ. The seal resistance between the recording pipette and the cell ranged between 2-8 GΩ. Membrane potentials were recorded in current clamp mode (I=0) and signals were analyzed using Clampfit (pClamp). After correcting for the measured liquid junction potential (-10 mV), the average baseline V_m was around -4 mV. In this configuration the estimated V_m is dependent on the ratio of the seal resistance and the combined patch and cell resistance where the ratio of recorded V_m and true membrane potential = $(R_{seal}/R_{patch}+R_{cell})/[1+(R_{seal}/R_{patch}+R_{cell})]$(190). Note, as the recorded V_m is an underestimate of the actual membrane potential we only used it to track changes in membrane potential(157,190). Seal resistance was monitored before and after the recording. Only cells that showed stable baseline membrane potential prior to leptin/drug application and which maintained good seal resistance were included for analysis.

Live cell FRET imaging. INS-1 832/13 cells were grown in 35-mm dishes and transfected at 50-60% confluency with FRET-based biosensors (2.5 μg plasmid DNA) using Lipofectamine

2000 (6 μl) (Invitrogen). 24 hours post-transfection cells were plated in μ-slide 8 well glass bottom chamber (Ibidi) and allowed to recover overnight. Cells were then imaged at 37°C in Tyrode's solution (described above). Images were acquired every minute using an Olympus IX71 inverted microscope with a 40x, 1.35 NA, oil immersion, UApo objective (Olympus). The microscope was equipped with a Nikon Coolsnap ES2 HQ camera. Image processing was performed using Fiji software (National Institutes of Health)(228). FRET was calculated as the ratio of acceptor fluorophore emission (545 nm) to donor emission (480 nm) in response to donor excitation (435 nm). F/F_{max} was obtained for each time point by subtracting the average baseline FRET ratio and normalizing to the maximal forskolin response. Only cells that showed a 10-15% increase in FRET in response to forskolin were used for analysis. Area under the curve (AUC) was calculated using GraphPad Prism™ for each experimental treatment time course.

Surface staining. INS-1 832/13 cells at ~70% confluency were washed once with phosphate-buffered saline (PBS) and incubated for two hours at 37°C in Opti-MEM (Thermo Fisher Scientific) and a mixture of viruses: tetracycline-inhibited transactivator, tetracycline-inhibited transactivator-regulated construct expressing BTX-SUR1 and Kir6.2(58). The multiplicity of infection for each virus was determined empirically. After two hours the infection mixture was replaced with RPMI 1640 supplemented cell culture media (described above) and were incubated at 37°C. 24 hours post-infection cells were plated on 15-mm, number 1.5 glass coverslips (Thermo Fisher Scientific) and allowed to adhere overnight. In Fig. 3B cells were pre-incubated at 37°C for 30 min in RPMI 1640 without serum and an additional 30 min with 0.01% DMSO or 50 μM st-Ht31 before being treated with 10 nM leptin or vehicle for 30 min. A prior study by our lab determined that leptin stimulation for 30 min is the optimal treatment duration for immunocytochemistry and biochemical experiments(58). Following leptin or vehicle treatment surface BTX-SUR1 was labeled with 1 μg/ml Alexa Fluor® 555 α-bungarotoxin (555-

BTX, Thermo Fisher Scientific) for 1 hour at 4^{o}C. In Fig. 5B cells were co-transfected with AKAP150 shRNAi and EGFP or pSilencer and EGFP at a 5:1 plasmid DNA ratio respectively using Lipofectamine 2000. The next day cells were infected with BTX-SUR1 and Kir6.2. These cells were treated with vehicle or 10 nM leptin for 30 min and surface BTX-SUR1 was labeled as described for Fig. 3B (minus the pre-incubation with DMSO or st-Ht31). All imaging experiments were performed on a Zeiss LSM780 confocal microscope equipped with a 63x, 1.4 NA, oil immersion, PlanApochromat objective (Carl Zeiss). During imaging for Fig. 5B EGFP expression was used to distinguish which cells had been transfected. Images were processed with Fiji (NIH).

Immunoblotting. INS-1 832/13 cells were lysed in triple lysis buffer [50 mM Tris-HCl, 2 mM EDTA, 2 mM EGTA, 100 mM NaCl, 1% Triton X-100, pH 7.4, with cOmplete EDTA free protease inhibitor cocktail (Roche, Basel, Switzerland)] for 30 min at 4°C with rotation, and cell lysates were cleared by centrifugation at 21,000 × *g* for 10 min at 4°C. Proteins were separated by SDS-PAGE (8% acrylamide gel) and transferred to nitrocellulose membranes (Millipore). Membranes were incubated overnight at 4°C with a primary antibody diluted in Tris-buffered saline plus 0.1% Tween 20 (TBST). The antibody for SUR1 (1:500) was generated in rabbit using a C-terminal peptide (KDSVFASFVRADK) of hamster SUR1 as described previously(58). The antibody against AKAP150 (1:1000) was made as described previously(270). The antibody against GFP (1:100) was from Thermo Fisher Scientific. The antibody for tubulin (1:2000) was from Sigma-Aldrich. After three 10 min washes with TBST, blots were incubated for 1 hour at room temperature with horseradish peroxidase-conjugated secondary antibodies in TBST buffer as follows: 1:20,000 donkey anti-rabbit IgG (Jackson ImmunoResearch Laboratories) for SUR1, AKAP150, and GFP; 1:20,000 donkey anti-mouse IgG (Jackson ImmunoResearch Laboratories) for AKAP220 and tubulin. After washing three times for 10 min with TBST, blots were developed using Super Signal West Femto (Pierce) and imaged with FluorChemE

(ProteinSimple, San Jose, CA) or Sapphire Biomolecular Imager (Azure Biosystems). The blots were quantified using Fiji software (NIH) and normalized to corresponding controls.

Surface Biotinylation. INS-1 832/13 cells cultured in 10 cm dishes at 50-60% confluency were transfected with 20 μg of pSilencer or AKAP150 shRNAi plasmid DNA and 40 μl of lipofectamine 2000. 48 hours following transfection the cells were re-plated in new 10 cm dishes. 72 hours post-transfection cells at 70-80% confluency were incubated in RPMI 1640 without serum for 1 hour at 37ºC prior to a 30 min treatment with vehicle or 10 nM leptin. Cells were then washed four times with cold PBS containing 9 mM $CaCl_2$ and 5.9 mM $MgCl_2$ (DPBS) and incubated with 1 mg/ml EZ-Link Sulfo-NHS-SS-Biotin (Pierce) in DPBS for 30 min at 4ºC. The reaction was terminated by incubating cells twice with DPBS containing 50 mM glycine for 5 min at 4ºC, followed by two washes with cold DPBS. Cells were then lysed with 300 μl triple lysis buffer as described above, and 500 μg of total lysate was incubated with 50 μl of 50% slurry Neutravidin-agarose beads (Pierce) overnight at 4ºC. Biotinylated proteins were eluted with 2x protein loading buffer for 10 min at 37ºC. Both eluent and input samples (50 μg total cell lysate) were analyzed by immunoblotting using anti-SUR1. These experiments were repeated with slight variations in the transfection protocol. For AKAP220 KD experiments 30 nM of AKAP220 or scramble siRNA was used for transfection. The transfections for AKAP150 KD rescue experiments with WT AKAP79-GFP, AKAP79ΔPKA, or AKAP79ΔPIX were performed using 20 μg of AKAP150 shRNAi plasmid DNA and 5 μg of WT AKAP79-GFP, AKAP79ΔPKA , or AKAP79ΔPIX plasmid DNA. In addition to immunoblotting for anti-SUR1, input samples were analyzed using anti-AKAP150, anti-AKAP220, and anti-GFP to confirm transfections were successful. Surface SUR1 bands were normalized to the upper band of total SUR1, as the upper band represents the mature population of SUR1 incorporated into K_{ATP} channels that may traffic to the cell membrane. AKAP150 and AKAP220 bands were normalized to the tubulin loading control.

Statistical Analysis. All data were analyzed with the program GraphPad Prism™. Results were expressed as mean ± standard error of the mean (SEM). Two-way analysis of variance (ANOVA) followed by the post hoc Bonferroni's test or one-way analysis of variance (ANOVA) followed by the post hoc Dunnet's test or Tukey's test were used for multiple comparisons as detailed in figure legends. When only two groups were compared, unpaired Student's t-tests was used. The level of statistical significance was set at $p<0.05$.

Chapter 6: Summary, future directions, and concluding remarks

6.1. Summary

The work presented in this thesis focused on leptin-induced K_{ATP} channel trafficking in β-cells as a mechanism to regulate β-cell electrical activity, and hence insulin secretion. Specifically, these studies examined NMDA receptors as a Ca^{2+} source to initiate downstream signaling events and identified a mechanism for leptin activation of PKA to allow for subsequent actin remodeling and K_{ATP} channel translocation. The first portion of this work demonstrates that leptin increases intracellular Ca^{2+} by potentiating NMDAR activity. This was followed by demonstration that NMDAR potentiation occurs as a result of leptin activation of Src kinase, which phosphorylates tyrosine residues on the GluN2A subunit. In the last section of this thesis, it is discovered that leptin signaling via the NMDAR-CaMKKβ-AMPK axis increases PKA activity at the β-cell membrane and that the scaffolding protein AKAP79/150 plays a critical role in anchoring PKA for leptin signaling. Another important aspect of this thesis work is that it demonstrates that human T2D donor β-cells are non-responsive to leptin; however, direct activation of NMDARs can restore the effects of leptin indicating that during the pathology of T2D the connection between leptin and NMDARs may be disrupted. From these findings, a new leptin signaling model is proposed in which leptin activates Src kinase to initiate the NMDAR-CaMKKβ-AMPK signaling axis and increase AKAP79/150-anchored PKA activity resulting in actin remodeling and trafficking of vesicles containing K_{ATP} channels to the β-cell membrane (Fig. 5.8.). Further investigation into the leptin signaling mechanism in β-cells has the potential to advance our understanding of the pathology of T2D and may aid in the development of new therapies for T2D.

6.2. Future directions

6.2.1. Leptin activation of Src kinase

Future studies will aim to decipher how Src kinase is activated to potentiate NMDAR activity. Leptin activation of Src kinase most likely occurs via the long ObRb leptin receptor since leptin had no affect on β-cells from *db/db* mice, which lack the ObRb isoform but retain expression of shorter isoforms, such as ObRa (Chapter 4). Once activated, the ObRb receptor has been reported to activate several tyrosine phosphatases, including SHP-2(271,272). Tyrosine phosphatases may then activate Src by removing the inhibitory phosphorylation mark on Src residue Y527(196). However, in an initial experiment, I found that Src pY527 levels did not change in response to leptin. Following leptin treatment I immunoprecipated Src and analyzed the immunoprecipitate by western blot for pY527 and pY418. While pY418 levels were increased by leptin treatment, indicative of increased Src activity (Fig. 4.5.), pY527 levels were no different between leptin and controls (Appendix i). If this result persists in future experiments, it would suggest that leptin is not activating Src by dephosphorylating Y527. Instead, the activated leptin receptor may recruit and bind the SH2 or SH3 domain of Src, mechanisms that are known to activate Src by relieving intramolecular autoinhibitory interactions(196).

6.2.2. AMPK activation of PKA

The studies in Chapter 5 provide compelling evidence that AMPK increases PKA activity, but the mechanism for AMPK activation of PKA remains elusive. As mentioned in the discussion of Chapter 5 (section: 5.4. Discussion), it is unlikely that AMPK is increasing PKA activity by inhibiting cAMP degradation by PDEs or inhibiting dephosphorylation of PKA effectors by PP2B. However, experiments using a cAMP sensor targeted to AKAP79 (AKAP79-CUTie) did show that leptin increases cAMP levels near AKAP79 suggesting that this may be how leptin signaling activates PKA. I have started to investigate whether leptin signaling via the NMDAR-CaMKKβ-AMPK signaling axis increases cAMP concentrations (Appendix ii. A). At

present, I have determined that NMDAR activation significantly increases cAMP levels. My current data shows that AMPK activation is trending towards increasing cAMP levels, but more data will be required to draw any firm conclusions. If AMPK is found to increase cAMP levels, a plausible target of AMPK would be ACs, which produce cAMP. Interestingly, AKAP79/150 has been shown to localize with several ACs(256–258,260), including AC8 in β-cells(235,259). AC8 is stimulated by Ca^{2+} to produce cAMP(235,273) and has been implicated in Ca^{2+}-induced upregulation of cAMP production and the activation of cAMP effectors, such as PKA, in β-cells(274). Interestingly, the Ca^{2+} chelator BAPTA did not significantly affect basal PKA activity in vehicle treated cells, but BAPTA did significantly reduce AMPK activation of PKA (Appendix ii. B). However, in the presence of BAPTA, AMPK still caused a significant increase of PKA activity compared to vehicle controls (Appendix ii. C). This suggests that AMPK activation of PKA is not necessarily dependent on Ca^{2+}, but that it may be enhanced by a Ca^{2+} influx. Whether AMPK activates PKA by increasing cAMP via potentiation of Ca^{2+}-induced AC8 cAMP production or activation of other ACs is still undetermined, and therefore, other potential mechanisms for AMPK to activate PKA should be considered as well.

Another potential mechanism is that AMPK may directly phosphorylate PKA. The PKA RIIα regulatory subunit contains an AMPK phosphorylation consensus motif [LXRXX(pS/pT)] that may permit AMPK phosphorylation of RIIα residue T314 (Appendix ii. D). Through conversations with Dr. Susan Taylor's lab at UCSD, I was informed that T314 is in a critical region termed the β4-β5 loop that is likely to be important for binding something, although at this time it is not known what the β4-β5 loop is interacting with. One possibility is that, in the cAMP-bound conformation, pT314 may reach over to K386 located in the phosphate binding cassette region and lock the RIIα subunit into the active cAMP-bound conformation (Appendix ii. E, F). This mechanism of AMPK activation of PKA would be dependent on readily available cAMP, which could potentially be enhanced by a Ca^{2+} influx from NMDARs activating AC8. In the event

that AMPK does not increase cAMP levels, direct phosphorylation of PKA by AMPK is an intriguing alternative mechanism that may be explored.

6.2.3. PKA-dependent actin remodeling

Identifying how PKA regulates actin remodeling is a daunting task. This is in part due to PKA having many effectors that are involved in modulating actin dynamics. In an attempt to identify PKA effector proteins, phosphoproteomic analysis is being conducted on INS-1 832/13 cell lysates treated with leptin, the AMPK activator AICAR, or the PKA activator 8-Bromo-cAMP. In addition to this work, studies conducted by a former postdoc in our lab show that leptin signaling via PKA increases phosphorylation of the actin depolymerizing protein cofilin at serine 3 (Appendix iii.). Phosphorylation at serine 3 inhibits cofilin activity and promotes actin polymerization(275), which is opposite of the increased cofilin activity and actin depolymerization typically associated with vesicle exocytosis(276,277). However, cofilin remodeling of the actin cytoskeleton is very complicated and often involves the coordination of localized activation and inactivation of cofilin(278–281). Determining whether cofilin is involved in K_{ATP} channel trafficking will require further investigation. Aside from these efforts, studies performed by another lab have identified Rac as being important for actin remodeling to promote K_{ATP} channel trafficking (see section 1.6.4.1.)(93). Although PKA has been shown to increase Rac activity(282,283), it has yet to be tested if PKA acts via Rac for actin remodeling in the context of K_{ATP} channel translocation. Clearly, much more work is needed to begin unraveling the complex process of PKA-dependent actin remodeling.

6.2.4. Leptin signaling complex

As noted in chapter 5, many of the molecules involved in leptin signaling (Ca^{2+}, cAMP, and PKA) have also been identified as positive regulators of insulin secretion. A primary interest of mine at the start of this thesis was to determine if leptin signaling was spatially localized within β-cells, which could reconcile these paradoxical findings. My observation that leptin

increases PKA activity at the cell membrane but not in the cytoplasm and that the membrane-targeted AKAP79/150 is involved in anchoring PKA for leptin signaling suggest that leptin signaling is indeed localized. Moreover, AKAP79/150 has been reported to co-localize with NMDARs(242,243) and therefore, AKAP79/150 may function as a scaffold to form a complex of leptin signaling molecules. I have attempted to determine if leptin signaling molecules co-localize in INS-1 832/13 cells by using proximity labeling and co-immunoprecipiations techniques. For proximity labeling, the NMDAR GluN2A subunit was tagged at its cytoplasmic C-terminal tail with the TurboID construct(284), which should biotinylate nearby proteins. However, GluN2A-TurboID failed to significantly biotinylate any proteins other than endogenous GluN2A subunits. This is likely due to the location where TurboID was inserted in GluN2A and low expression levels of the GluN2A-TurboID construct. Next, I immunoprecipated out the NMDAR GluN1 subunit and analyzed the eluent for leptin signaling molecules. While the GluN1 immunoprecipitate showed only a faint band for AKAP150, there was an unmistakable band for AMPKα. This suggests that these signaling molecules co-localize in INS-1 832/13 cells. Previous studies have reported that the co-localization of AKAP79/150 with NMDARs is mediated through adaptor proteins such as PSD-95/SAP97(242). An adaptor protein may increase the difficulty of co-immunoprecipitating AKAP150 with GluN1 since AKAP150 would not be directly interacting with GluN1. Modifying the composition of the immunoprecipitation buffer (salts, detergents, etc.) may help to maintain interactions between proteins of interest and improve detection of AKAP150 in the eluent. Ideally, co-localization of leptin signaling molecules would be shown in intact β-cells using imaging techniques such as super resolution microscopy. This will require quality antibodies to detect leptin signaling molecules and a robust staining protocol. Improving these strategies and utilizing additional techniques are predicted to reveal co-localization of leptin signaling molecules. Optimizing the proximity labeling technique is of particular interest as it may also aid in uncovering additional molecules involved in K_{ATP} channel

trafficking. Identifying co-localization of leptin signaling molecules or a leptin signaling complex is expected to provide valuable insight as to how leptin signaling is spatiotemporally regulated within β-cells.

6.2.5. Regulated K_{ATP} channel trafficking

Although glucose metabolism is the primary regulator of β-cell K_{ATP} channel activity and insulin secretion, there is growing evidence that regulated K_{ATP} channel trafficking is an auxiliary mechanism to control β-cell electrical activity. In addition to leptin, glucose has also been implicated in regulating K_{ATP} channel surface density. Briefly, initial exposure to high glucose has been shown to promote K_{ATP} channel endocytosis(285), whereas prolonged exposure has been found to recruit K_{ATP} channels to the β-cell surface(142); also, low glucose concentrations are reported to promote K_{ATP} channel trafficking(57,68). While K_{ATP} channel endocytosis is proposed to enhance β-cell electrical activity and promote insulin secretion, increased K_{ATP} channel surface density reduces β-cell activity to prevent excessive insulin secretion and prime the β-cell for future insulin exocytic events. Thus, regulation of K_{ATP} channel surface expression may complement the effects of glucose metabolism on K_{ATP} channel activity. Interestingly, the leptin signaling molecules PKA and AMPK are also required for high glucose(142) and low glucose-induced(68) K_{ATP} channel trafficking, respectively. These findings were confirmed by a former postdoc in our lab. Furthermore, she found that PKA is required downstream of AMPK at low glucose concentrations, similar to leptin signaling (Appendix v). Collectively, these studies suggest that leptin and glucose may act on a common signaling pathway to promote K_{ATP} channel translocation. I have initiated experiments to determine if, like in leptin signaling, AKAP79/150 plays a role in coordinating glucose-mediated K_{ATP} channel trafficking. So far my findings suggest that at low glucose levels knockdown of AKAP150 blocks K_{ATP} channel trafficking, and that this is not rescued by overexpression of the AKAP79 mutant that cannot bind PKA (AKAP79ΔPKA) indicating that AKAP79/150 also coordinates K_{ATP} channel trafficking

at low glucose levels (Appendix vi). While it is intriguing to consider that a common K_{ATP} channel transport pathway may be influenced by various stimuli, many of the glucose experiments were conducted *in vitro* under non-physiological conditions(68,142) and the physiological relevance of glucose-mediated K_{ATP} channel trafficking remains uncertain.

Sections 6.2.6. – 6.2.8. and 6.3. are adapted and/or modified from a review article originally published by Cochrane V. & Shyng S-L.

International Journal of Molecular Sciences 2019; 20(11): 2660.

DOI: 10.3390/ijms20112660

6.2.6. K_{ATP} channel vesicles

The finding that K_{ATP} channels are rapidly inserted into the plasma membrane in response to leptin without changing the total amount of K_{ATP} channels within cells suggests that K_{ATP} channels exist in a readily available pool of vesicles. However, there is currently no consensus on the intracellular vesicle population in which K_{ATP} channels reside. Insulin granules(286,287), chromogranin positive but insulin negative dense core granules(142), as well as EEA1 positive early endosomes(57) have all been reported to contain K_{ATP} channels. Immunocytochemistry studies by our lab aimed at identifying the vesicles that contain K_{ATP} channels are ongoing. After identifying the vesicles, isolation and analysis of the vesicular contents may reveal other channels or transporters that are regulated by leptin. For example, studies conducted by our lab indicate that leptin signaling also promotes Kv2.1 channel trafficking(65) suggesting that Kv2.1 and K_{ATP} channels may reside in vesicles together. The discovery of additional molecules that are trafficked in response to leptin are expected to provide further insight into β-cell function.

6.2.7. Turning off leptin signaling

As noted earlier, the effect of leptin on K_{ATP} channel surface density is transient. There have been no studies conducted to investigate the transient nature of the leptin response. Although there are several possible steps at which leptin signaling may be shut off, they remain untested. However, in the brain, both suppressor of cytokine signaling 3 (SOCS3)(180) and protein tyrosine phosphatase 1B (PTP1B)(288,289) have been shown to negatively regulate leptin signaling by inhibiting leptin receptor activation and leptin effectors. Moreover, upregulated expression of SOCS3 and PTP1B contribute to the development of leptin resistance in neurons(180). Identifying similar mechanisms in β-cells may explain our finding that T2D donor β-cells are responsive to NMDAR activation but not leptin, and could help us to gain insight into how leptin resistance may occur at the β-cell level in pathological states such as obesity or T2D.

6.2.8. Physiological significance of leptin-mediated K_{ATP} channel trafficking

Despite clear evidence that leptin regulates K_{ATP} channel trafficking to suppress β-cell excitability, a definitive demonstration that leptin's action on β-cells has a role in regulating blood glucose is, surprisingly, still lacking. Most signaling mechanism studies have been conducted using β-cell lines or primary β-cells with biochemical or electrophysiological readouts as endpoints. It would be important to establish that trafficking of K_{ATP} by leptin reduces insulin secretion. Ultimately, it will be critical to define the physiological relevance of this mechanism for regulating serum insulin levels and glucose homeostasis in vivo. The few transgenic mouse studies designed to address this question have so far yielded inconsistent results. While early papers support a role of β-cell leptin signaling in glucose regulation(48–50), this notion was recently challenged(51). The cre line used to knock out leptin receptors in β-cells, the mouse strain used, as well as whether animals were subjected to high fat feeding are all factors that could affect experimental outcomes and data interpretation. Thus, these studies that aimed to

resolve the longstanding question of the physiological importance of leptin signaling in pancreatic β-cells have instead sparked further controversy. It is evident that more work with careful controls is needed to resolve this important question.

6.3. Concluding remarks

In conclusion, the work presented in this thesis significantly advances our understanding of the mechanism underlying leptin-induced K_{ATP} channel trafficking, which has implications for β-cell electrical activity and insulin secretion. Notable findings from this work include: 1) NMDARs are a potential target for overcoming disrupted leptin signaling and 2) leptin signaling is spatially regulated. Moving forward it will be important to translate these findings to *in vivo* models, but it is encouraging that leptin signaling is conserved in isolated human β-cells. Continuing future efforts in delineating downstream leptin signaling mechanisms regulating K_{ATP} channel trafficking in β-cells may offer novel therapeutic targets for improving glycemic control in T2D patients by bypassing leptin-resistance.

Appendices

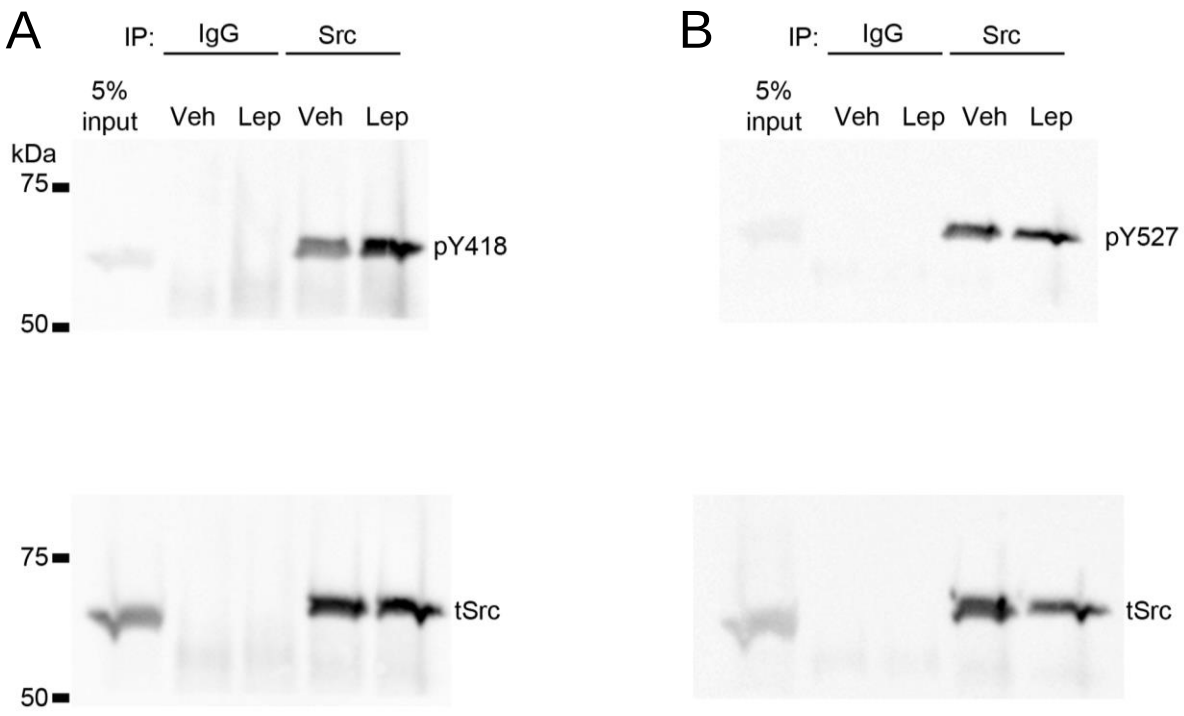

Appendix i. Leptin activation of Src kinase.

Western blot analysis of Src activation following a 15 minute treatment with leptin (10 nM) or vehicle. Following treatments, samples were immunoprecipated with anti-Src or control IgG antibodies. Top blots show immunoblotting for the activating pY418 **(A)** or inhibitory pY527 **(B)** Src residues. The blots were then stripped and re-probed for total Src (bottom).

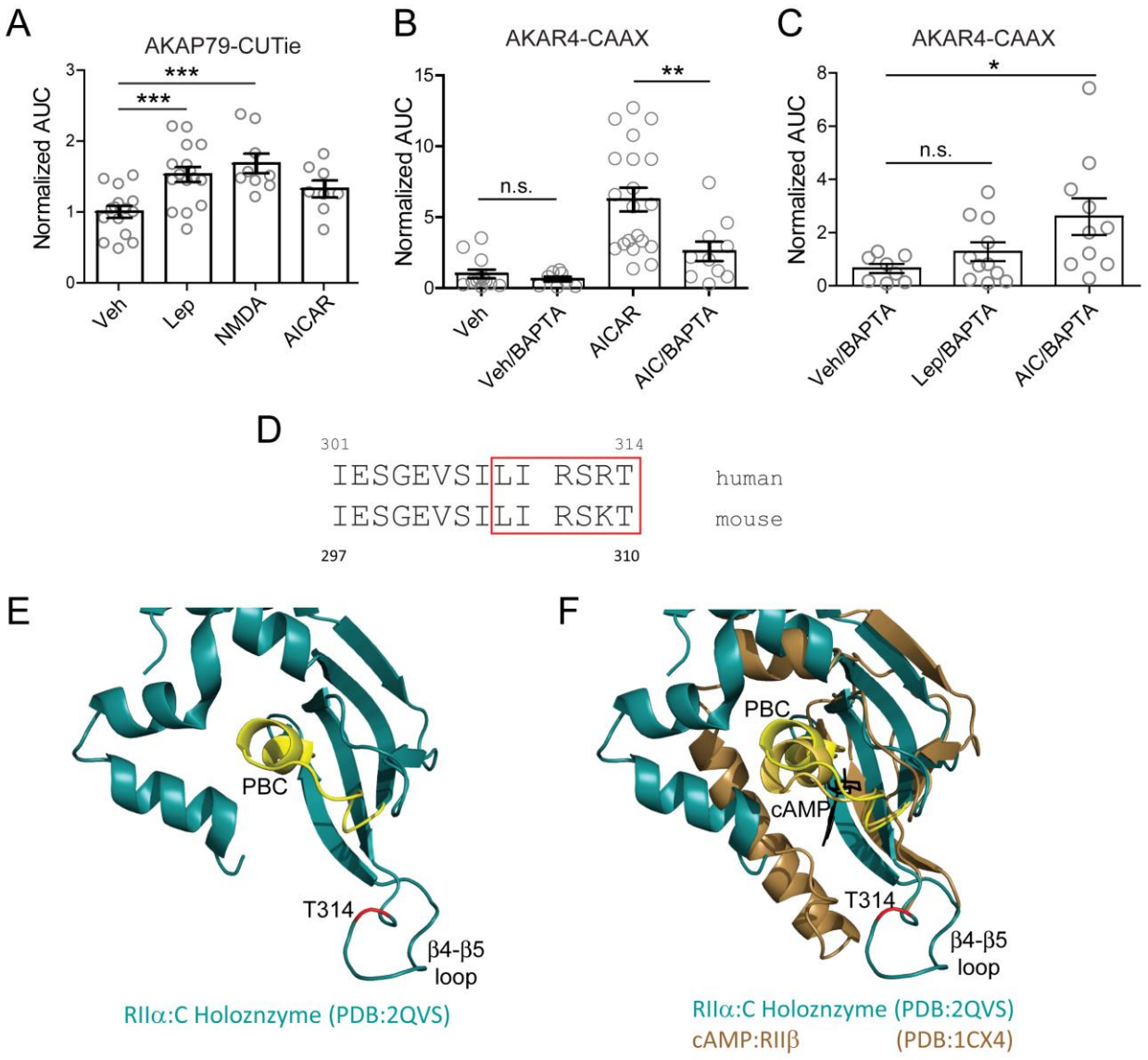

Appendix ii. AMPK activation of PKA.

A) AKAP79-CUTie monitored cAMP levels in response to vehicle, leptin (100nM), NMDA + Glycine (100 μM + 100 μM) and the AMPK activator AICAR (500 μM). ***p<0.001 as determined by one-way ANOVA followed by a post hoc Dunnett's multiple comparison test. **B)** AKAR4-CAAX was utilized to examine the effects of BAPTA on PKA activity levels in vehicle and 500 μM AICAR (p=0.0083) treated cells. Unpaired student's t-test was used to determine statistical significance. **C)** Comparison of vehicle, leptin (100 nM), and AICAR (500 μM) on PKA activity in the presence of BAPTA. *p<0.05 as determined by one-way ANOVA followed by a post hoc Dunnett's multiple comparison test. **D)** AMPK consensus motif [LXRXX(pS/pT)] in the PKA RIIα sequence of both human and mouse. **E)** PKA RIIa structure labeled with the β4-β5 loop, T314, and the phosphate binding cassette (PBC) region where residue K386 is located. **F)** The PKA RIIα structure overlayed with the PKA RIIβ structure bound to cAMP. cAMP is shown in black.

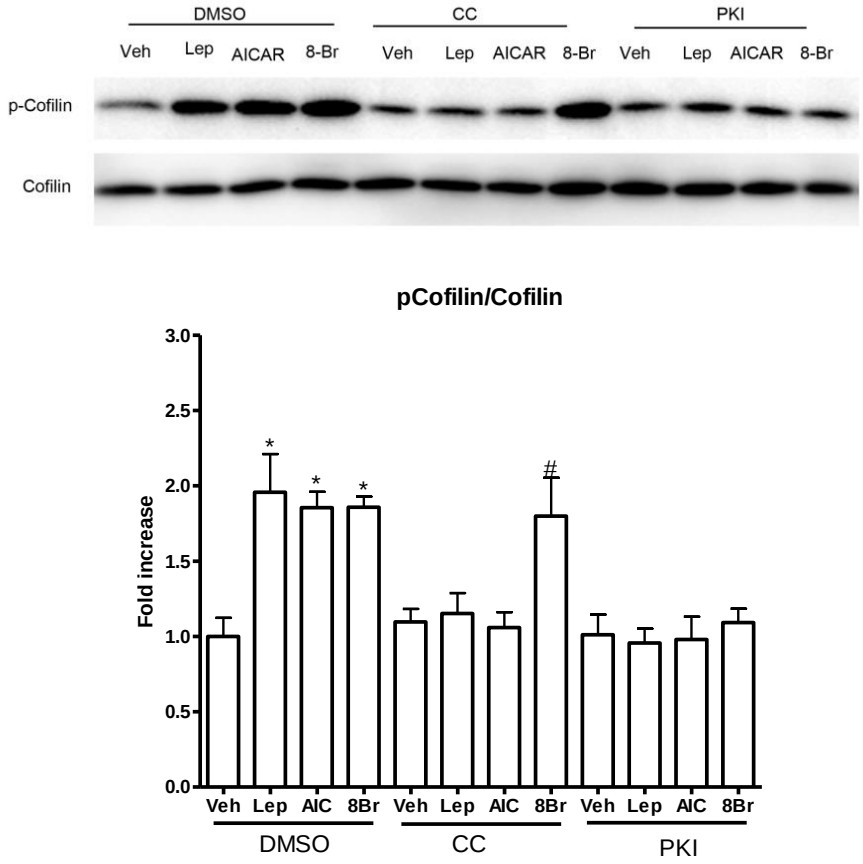

Appendix iii. PKA increases phosphorylation of cofilin.

Western blots of INS-1 832/13 cell lysates probed for phosphorylated cofilin and total cofilin following 30 min treatments with leptin, AICAR (AIC), or 8-Bromo-cAMP (8Br) in the absence or presence of the AMPK inhibitor Compound C (CC) or the PKA inhibitor PKI (top). Bottom graph shows analysis of pcofilin normalized to total cofilin from 4 independent experiments.

Experiments were performed by Pei-Chun Chen.

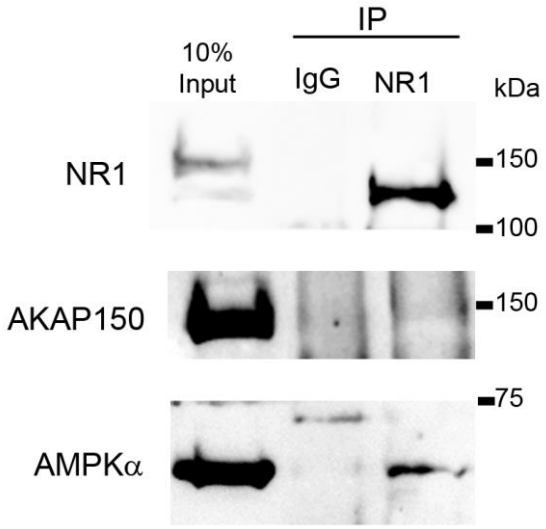

Appendix iv. NR1 co-immunoprecipitates with AKAP150 and AMPKα.

NR1 (GluN1) was immunoprecipitated from INS-1 832/13 cell lysate. Samples were analyzed for AKAP150 and AMPKα by immunoblotting. The AKAP150 blot was then stripped and re-probed for NR1; residual AKAP150 can still be observed in the input lane on the NR1 immunoblot.

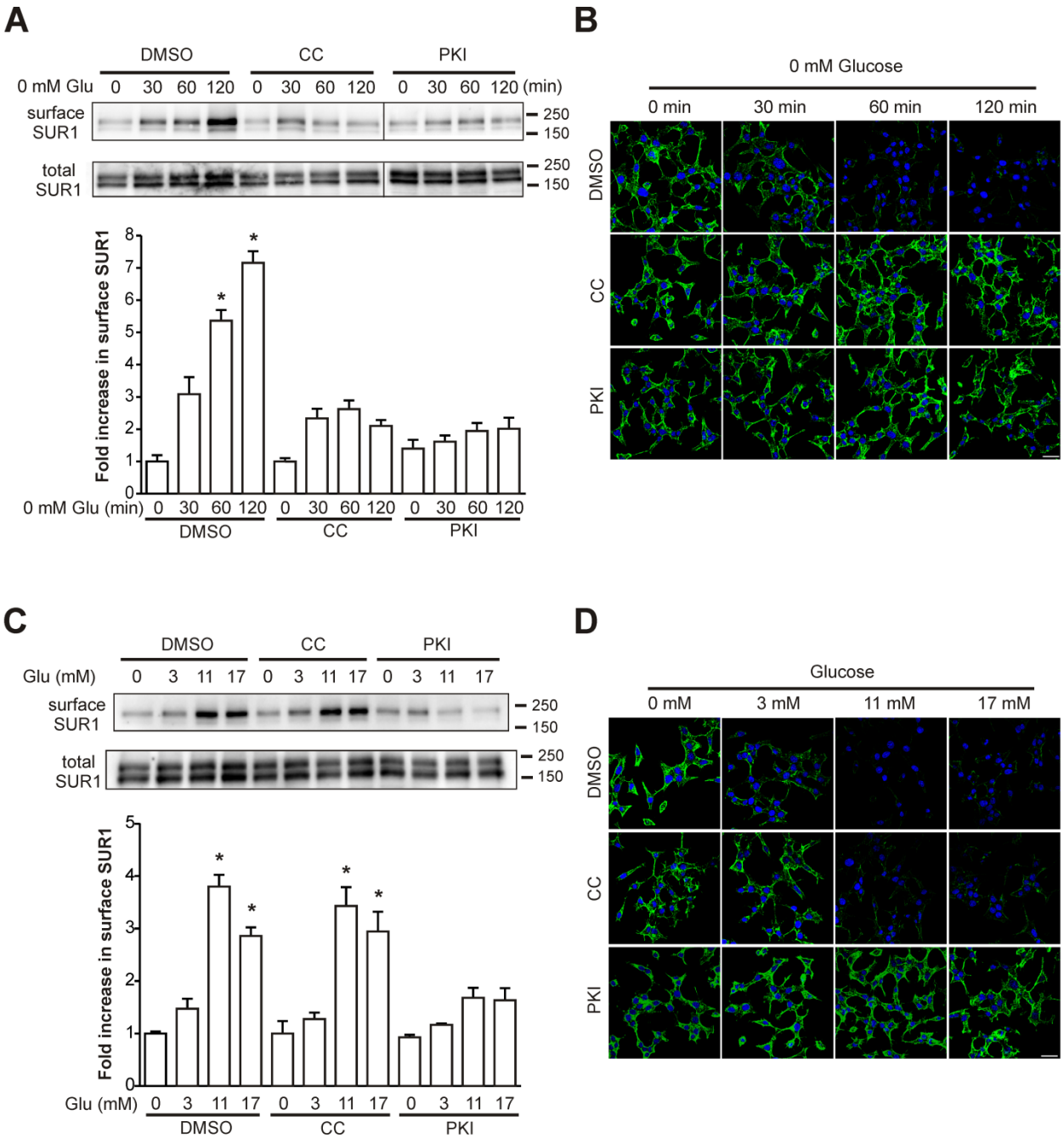

Appendix v. Effects of glucose on K_{ATP} channel surface density.

A) Western blots showing surface SUR1 and total SUR1 in response to a time course of glucose deprivation (0 mM) in the absence or presence of the AMPK inhibitor Compound C (CC) or the PKA inhibitor PKI (top). Graph shows analysis of surface SUR1 normalized to total SUR1. **B)** Fluorescent images of F-actin (green). Nuclei is stained with DAPI (blue). **C, D)** Same as **(A)** and **(B)** but in response to various glucose concentrations for 1 hour.

Experiments were performed by Pei-Chun Chen.

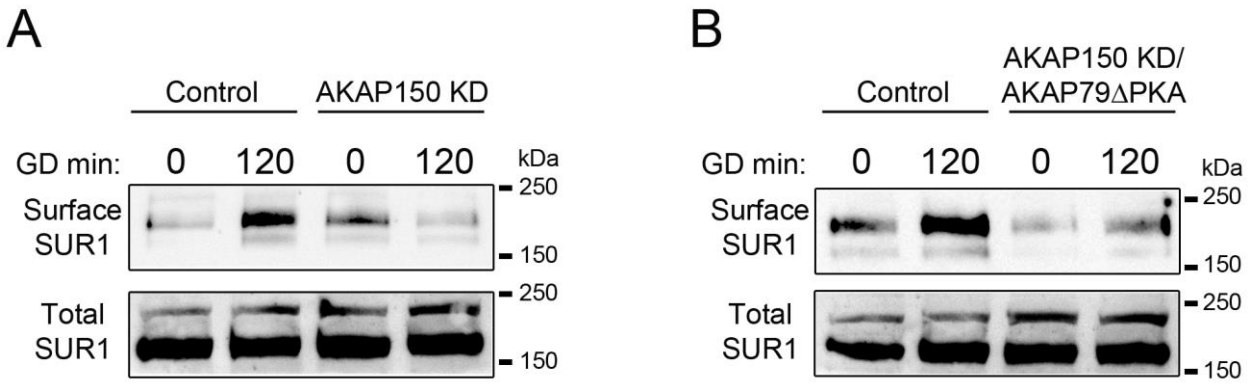

Appendix vi. AKAP79/150 orchestrates glucose deprivation-mediated K_{ATP} channel trafficking.

A) Western blots showing surface SUR1 and total SUR1 in INS-1 832/13 cells transfected with the empty pSilencer vector (control) or AKAP150 shRNAi and exposed to glucose deprivation (GD) for 0 to 120 mins. **B)** Same as **(A)** except cells were co-transfected with AKAP150 shRNAi and the AKAP79ΔPKA mutant construct.

References

1. Kieffer TJ, Habener JF. The adipoinsular axis: effects of leptin on pancreatic beta-cells. Am J Physiol Endocrinol Metab. 2000 Jan;278(1):E1–14.

2. Hummel KP, Dickie MM, Coleman DL. Diabetes, a new mutation in the mouse. Science [Internet]. 1966 Sep 2;153(3740):1127–8. Available from: http://www.ncbi.nlm.nih.gov/pubmed/5918576

3. Coleman DL. Obese and diabetes: two mutant genes causing diabetes-obesity syndromes in mice. Diabetologia [Internet]. 1978 Mar;14(3):141–8. Available from: http://www.ncbi.nlm.nih.gov/pubmed/350680

4. Zhang Y, Proenca R, Maffei M, Barone M, Leopold L, Friedman JM. Positional cloning of the mouse obese gene and its human homologue. Nature [Internet]. 1994 Dec 1;372(6505):425–32. Available from: http://www.ncbi.nlm.nih.gov/pubmed/7984236

5. Moon BC, Friedman JM. The molecular basis of the obese mutation in ob2J mice. Genomics [Internet]. 1997 May 15;42(1):152–6. Available from: http://www.ncbi.nlm.nih.gov/pubmed/9177786

6. Tartaglia LA, Dembski M, Weng X, Deng N, Culpepper J, Devos R, et al. Identification and expression cloning of a leptin receptor, OB-R. Cell [Internet]. 1995 Dec 29;83(7):1263–71. Available from: http://www.ncbi.nlm.nih.gov/pubmed/8548812

7. Lee G-H, Proenca R, Montez JM, Carroll KM, Darvishzadeh JG, Lee JI, et al. Abnormal splicing of the leptin receptor in diabetic mice [Internet]. Vol. 379, Nature. 1996. p. 632–5. Available from: http://www.nature.com/doifinder/10.1038/379632a0

8. Chen H, Charlat O, Tartaglia LA, Woolf EA, Weng X, Ellis SJ, et al. Evidence that the diabetes gene encodes the leptin receptor: identification of a mutation in the leptin receptor gene in db/db mice. Cell [Internet]. 1996 Feb 9;84(3):491–5. Available from: http://www.ncbi.nlm.nih.gov/pubmed/8608603

9. Maffei M, Fei H, Lee GH, Dani C, Leroy P, Zhang Y, et al. Increased expression in adipocytes of ob RNA in mice with lesions of the hypothalamus and with mutations at the db locus. Proc Natl Acad Sci [Internet]. 1995 Jul 18;92(15):6957–60. Available from: http://www.pnas.org/cgi/doi/10.1073/pnas.92.15.6957

10. Chua SC, Chung WK, Wu-Peng XS, Zhang Y, Liu S-M, Tartaglia L, et al. Phenotypes of Mouse diabetes and Rat fatty Due to Mutations in the OB (Leptin) Receptor. Science (80-) [Internet]. 1996 Feb 16;271(5251):994–6. Available from: https://www.sciencemag.org/lookup/doi/10.1126/science.271.5251.994

11. Ghilardi N, Ziegler S, Wiestner A, Stoffel R, Heim MH, Skoda RC. Defective STAT signaling by the leptin receptor in diabetic mice. Proc Natl Acad Sci U S A [Internet]. 1996 Jun 25;93(13):6231–5. Available from: http://www.ncbi.nlm.nih.gov/pubmed/8692797

12. Vaisse C, Halaas JL, Horvath CM, Darnell JE, Stoffel M, Friedman JM. Leptin activation of Stat3 in the hypothalamus of wild-type and ob/ob mice but not db/db mice. Nat Genet [Internet]. 1996 Sep;14(1):95–7. Available from: http://www.ncbi.nlm.nih.gov/pubmed/8782827

13. Bahrenberg G, Behrmann I, Barthel A, Hekerman P, Heinrich PC, Joost H-G, et al. Identification of the critical sequence elements in the cytoplasmic domain of leptin

receptor isoforms required for Janus kinase/signal transducer and activator of transcription activation by receptor heterodimers. Mol Endocrinol [Internet]. 2002 Apr;16(4):859–72. Available from: http://www.ncbi.nlm.nih.gov/pubmed/11923481

14. Bates SH, Stearns WH, Dundon TA, Schubert M, Tso AWK, Wang Y, et al. STAT3 signalling is required for leptin regulation of energy balance but not reproduction. Nature [Internet]. 2003 Feb 20;421(6925):856–9. Available from: http://www.ncbi.nlm.nih.gov/pubmed/12594516

15. Pelleymounter M, Cullen M, Baker M, Hecht R, Winters D, Boone T, et al. Effects of the obese gene product on body weight regulation in ob/ob mice. Science (80-) [Internet]. 1995 Jul 28;269(5223):540–3. Available from: http://www.sciencemag.org/cgi/doi/10.1126/science.7624776

16. Halaas J, Gajiwala K, Maffei M, Cohen S, Chait B, Rabinowitz D, et al. Weight-reducing effects of the plasma protein encoded by the obese gene. Science (80-) [Internet]. 1995 Jul 28;269(5223):543–6. Available from: https://www.sciencemag.org/lookup/doi/10.1126/science.7624777

17. Coleman DL, Hummel KP. Hyperinsulinemia in pre-weaning diabetes (db) mice. Diabetologia [Internet]. 1974 Nov;10(S1):607–10. Available from: http://link.springer.com/10.1007/BF01221993

18. Dubuc PU. The development of obesity, hyperinsulinemia, and hyperglycemia in ob/ob mice. Metabolism [Internet]. 1976 Dec;25(12):1567–74. Available from: http://www.ncbi.nlm.nih.gov/pubmed/994838

19. Dubuc PU, Willis PL. Postweaning development of diabetes in obob mice. Metabolism [Internet]. 1979;28(6):633–40. Available from: http://www.sciencedirect.com/science/article/pii/0026049579900167

20. Genuth SM. Hyperinsulinism in mice with genetically determined obesity. Endocrinology [Internet]. 1969 Feb;84(2):386–91. Available from: http://www.ncbi.nlm.nih.gov/pubmed/4884801

21. Levi J, Gray SL, Speck M, Huynh FK, Babich SL, Gibson WT, et al. Acute disruption of leptin signaling in vivo leads to increased insulin levels and insulin resistance. Endocrinology. 2011;152(9):3385–95.

22. Schwartz MW, Baskin DG, Bukowski TR, Kuijper JL, Foster D, Lasser G, et al. Specificity of leptin action on elevated blood glucose levels and hypothalamic neuropeptide Y gene expression in ob/ob mice. Diabetes. 1996;45(4):531–5.

23. Rahier J, Wallon J, Henquin JC. Cell populations in the endocrine pancreas of human neonates and infants. Diabetologia [Internet]. 1981 May;20(5):540–6. Available from: http://www.ncbi.nlm.nih.gov/pubmed/6116638

24. Saito K, Iwama N, Takahashi T. Morphometrical analysis on topographical difference in size distribution, number and volume of islets in the human pancreas. Tohoku J Exp Med [Internet]. 1978 Feb;124(2):177–86. Available from: http://www.ncbi.nlm.nih.gov/pubmed/347635

25. Dolenšek J, Rupnik MS, Stožer A. Structural similarities and differences between the human and the mouse pancreas. Islets [Internet]. 2015 Jan 2;7(1):e1024405. Available from: http://www.tandfonline.com/doi/full/10.1080/19382014.2015.1024405

26. In't Veld P, Marichal M. Microscopic anatomy of the human islet of Langerhans. Adv Exp Med Biol [Internet]. 2010;654:1–19. Available from: http://www.ncbi.nlm.nih.gov/pubmed/20217491

27. Langerhans P, Morrison H. CONTRIBUTIONS TO THE MICROSCOPIC ANATOMY OF THE PANCREAS. Bull Inst Hist Med [Internet]. 1937 Dec 3;5(3):259–97. Available from: http://www.jstor.org/stable/44438182

28. Zhou Q, Melton DA. Pancreas regeneration. Nature [Internet]. 2018 May 16;557(7705):351–8. Available from: http://www.nature.com/articles/s41586-018-0088-0

29. Cabrera O, Jacques-Silva MC, Speier S, Yang S-N, Köhler M, Fachado A, et al. Glutamate is a positive autocrine signal for glucagon release. Cell Metab [Internet]. 2008 Jun;7(6):545–54. Available from: http://www.ncbi.nlm.nih.gov/pubmed/18522835

30. Brissova M, Fowler MJ, Nicholson WE, Chu A, Hirshberg B, Harlan DM, et al. Assessment of human pancreatic islet architecture and composition by laser scanning confocal microscopy. J Histochem Cytochem [Internet]. 2005 Sep;53(9):1087–97. Available from: http://www.ncbi.nlm.nih.gov/pubmed/15923354

31. Bosco D, Armanet M, Morel P, Niclauss N, Sgroi A, Muller YD, et al. Unique Arrangement of - and -Cells in Human Islets of Langerhans. Diabetes [Internet]. 2010 May 1;59(5):1202–10. Available from: http://diabetes.diabetesjournals.org/cgi/doi/10.2337/db09-1177

32. Roscioni SS, Migliorini A, Gegg M, Lickert H. Impact of islet architecture on β-cell heterogeneity, plasticity and function. Nat Rev Endocrinol [Internet]. 2016 Dec 2;12(12):695–709. Available from: http://www.nature.com/articles/nrendo.2016.147

33. Kim A, Miller K, Jo J, Kilimnik G, Wojcik P, Hara M. Islet architecture: A comparative study. Islets [Internet]. 2009 Sep 27;1(2):129–36. Available from: http://www.tandfonline.com/doi/abs/10.4161/isl.1.2.9480

34. Kharouta M, Miller K, Kim A, Wojcik P, Kilimnik G, Dey A, et al. No mantle formation in rodent islets—The prototype of islet revisited. Diabetes Res Clin Pract [Internet]. 2009 Sep;85(3):252–7. Available from: https://linkinghub.elsevier.com/retrieve/pii/S0168822709002708

35. Nichols CG. KATP channels as molecular sensors of cellular metabolism. Nature [Internet]. 2006 Mar 22;440(7083):470–6. Available from: http://www.nature.com/articles/nature04711

36. Ashcroft FM, Rorsman P. KATP channels and islet hormone secretion: new insights and controversies. Nat Rev Endocrinol [Internet]. 2013 Nov 17;9(11):660–9. Available from: http://www.nature.com/articles/nrendo.2013.166

37. Martin GM, Chen P-CC, Devaraneni P, Shyng S-LL. Pharmacological rescue of trafficking-impaired ATP-sensitive potassium channels. Front Physiol [Internet]. 2013 Dec 24;4 DEC(December):1–16. Available from: http://www.ncbi.nlm.nih.gov/pubmed/24399968

38. Kieffer TJ, Heller RS, Habener JF. Leptin Receptors Expressed on Pancreatic β-Cells. Biochem Biophys Res Commun [Internet]. 1996 Jul;224(2):522–7. Available from: http://linkinghub.elsevier.com/retrieve/pii/S0006291X96910591

39. Kieffer TJ, Heller RS, Leech CA, Holz GG, Habener JF. Leptin Suppression of Insulin

Secretion by the Activation of ATP-Sensitive K + Channels in Pancreatic p-Cells. Diabetes. 1997;46:1087–93.

40. Emilsson V, Liu YL, Cawthorne M a, Morton NM, Davenport M. Expression of the functional leptin receptor mRNA in pancreatic islets and direct inhibitory action of leptin on insulin secretion. Diabetes [Internet]. 1997;46(November 1996):313–6. Available from: http://diabetes.diabetesjournals.org/content/46/2/313.long

41. Fehmann HC, Peiser C, Bode HP, Stamm M, Staats P, Hedetoft C, et al. Leptin: A potent inhibitor of insulin secretion. Peptides. 1997;18(8):1267–73.

42. Kulkarni RN, Wang ZL, Wang RM, Hurley JD, Smith DM, Ghatei MA, et al. Leptin rapidly suppresses insulin release from insulinoma cells, rat and human islets and, in vivo, in mice. J Clin Invest. 1997;100(11):2729–36.

43. Seufert J, Kieffer TJ, Leech CA, Holz GG, Moritz W, Ricordi C, et al. Leptin Suppression of Insulin Secretion and Gene Expression in Human Pancreatic Islets: Implications for the Development of Adipogenic Diabetes Mellitus [1]. J Clin Endocrinol Metab [Internet]. 1999;84(2):670–6. Available from: https://academic.oup.com/jcem/article-lookup/doi/10.1210/jcem.84.2.5460

44. Ookuma K, Ookuma M, York DA. Effects of Leptin on Insulin Secretion From Isolated Rat Pancreatic Islets. Diabetes. 1998;47(2):219–23.

45. Tanizawa Y, Okuya S, Ishihara H, Asano T, Yada T, Oka Y. Direct Stimulation of Basal Insulin Secretion by Physiological Concentrations of Leptin in Pancreatic β Cells. Endocrinology [Internet]. 1997 Oct;138(10):4513–6. Available from: https://academic.oup.com/endo/article-lookup/doi/10.1210/endo.138.10.5576

46. Leclercq-Meyer V, Malaisse W. Failure of human and mouse leptin to affect insulin, glucagon and somatostatin secretion by the perfused rat pancreas at physiological glucose concentration. Mol Cell Endocrinol [Internet]. 1998 Jun;141(1–2):111–8. Available from: https://linkinghub.elsevier.com/retrieve/pii/S0303720798000872

47. Ahrén B, Havel PJ. Leptin inhibits insulin secretion induced by cellular cAMP in a pancreatic B cell line (INS-1 cells). Am J Physiol Integr Comp Physiol [Internet]. 1999 Oct 1;277(4):R959–66. Available from: https://www.physiology.org/doi/10.1152/ajpregu.1999.277.4.R959

48. Covey SD, Wideman RD, McDonald C, Unniappan S, Huynh F, Asadi A, et al. The pancreatic beta cell is a key site for mediating the effects of leptin on glucose homeostasis. Cell Metab [Internet]. 2006 Oct;4(4):291–302. Available from: http://www.ncbi.nlm.nih.gov/pubmed/17011502

49. Gray SL, Donald C, Jetha A, Covey SD, Kieffer TJ. Hyperinsulinemia precedes insulin resistance in mice lacking pancreatic beta-cell leptin signaling. Endocrinology. 2010;151(9):4178–86.

50. Morioka T, Asilmaz E, Hu J, Dishinger JF, Kurpad AJ, Elias CF, et al. Disruption of leptin receptor expression in the pancreas directly affects β cell growth and function in mice. J Clin Invest [Internet]. 2007 Oct 1;117(10):2860–8. Available from: http://www.jci.org/cgi/doi/10.1172/JCI30910

51. Soedling H, Hodson DJ, Adrianssens AE, Gribble FM, Reimann F, Trapp S, et al. Limited impact on glucose homeostasis of leptin receptor deletion from insulin- or proglucagon-

expressing cells. Mol Metab [Internet]. 2015;4(9):619–30. Available from: http://dx.doi.org/10.1016/j.molmet.2015.06.007

52. Harvey J, McKenna F, Herson PS, Spanswick D, Ashford MLJ. Leptin activates ATP-sensitive potassium channels in the rat insulin-secreting cell line, CRI-G1. J Physiol [Internet]. 1997 Nov 1;504(3):527–35. Available from: http://www.ncbi.nlm.nih.gov/pubmed/9401961

53. Harvey J, Ashford MLJ. Insulin occludes leptin activation of ATP-sensitive K+ channels in rat CRI-G1 insulin secreting cells. J Physiol. 1998;511(3):695–706.

54. Ning K, Miller LC, Laidlaw HA, Burgess LA, Perera NM, Downes CP, et al. A novel leptin signalling pathway via PTEN inhibition in hypothalamic cell lines and pancreatic beta-cells. EMBO J [Internet]. 2006;25(11):2377–87. Available from: http://www.pubmedcentral.nih.gov/articlerender.fcgi?artid=1478173&tool=pmcentrez&rendertype=abstract

55. Harvey J, McKay NG, Walker KS, Van der Kaay J, Downes CP, Ashford ML. Essential role of phosphoinositide 3-kinase in leptin-induced K(ATP) channel activation in the rat CRI-G1 insulinoma cell line. J Biol Chem [Internet]. 2000 Feb 18;275(7):4660–9. Available from: http://www.ncbi.nlm.nih.gov/pubmed/10671495

56. Harvey J, Hardy SC, Irving AJ, Ashford ML. Leptin activation of ATP-sensitive K+ (KATP) channels in rat CRI-G1 insulinoma cells involves disruption of the actin cytoskeleton. J Physiol [Internet]. 2000 Aug 15;527 Pt 1:95–107. Available from: http://www.pubmedcentral.nih.gov/articlerender.fcgi?artid=2270061&tool=pmcentrez&rendertype=abstract

57. Park S-H, Ryu S-Y, Yu W-J, Han YE, Ji Y-S, Oh K, et al. Leptin promotes KATP channel trafficking by AMPK signaling in pancreatic -cells. Proc Natl Acad Sci [Internet]. 2013 Jul 30;110(31):12673–8. Available from: http://www.pnas.org/cgi/doi/10.1073/pnas.1216351110

58. Chen P-C, Kryukova YN, Shyng S-L. Leptin Regulates K ATP Channel Trafficking in Pancreatic β-Cells by a Signaling Mechanism Involving AMP-activated Protein Kinase (AMPK) and cAMP-dependent Protein Kinase (PKA). J Biol Chem [Internet]. 2013 Nov 22;288(47):34098–109. Available from: http://www.jbc.org/lookup/doi/10.1074/jbc.M113.516880

59. Ning K, Miller LC, Laidlaw HA, Watterson KR, Gallagher J, Sutherland C, et al. Leptin-dependent phosphorylation of PTEN mediates actin restructuring and activation of ATP-sensitive K+ channels. J Biol Chem. 2009;284(14):9331–40.

60. Ashcroft FM, Rorsman P. Electrophysiology of the pancreatic β-cell. Prog Biophys Mol Biol [Internet]. 1989 Jan;54(2):87–143. Available from: https://linkinghub.elsevier.com/retrieve/pii/0079610789900138

61. Shyng, S. NCG. Membrane Phospholipid Control of Nucleotide Sensitivity of KATP Channels. Science (80-) [Internet]. 1998 Nov 6;282(5391):1138–41. Available from: https://www.sciencemag.org/lookup/doi/10.1126/science.282.5391.1138

62. Lee Y-R, Chen M, Pandolfi PP. The functions and regulation of the PTEN tumour suppressor: new modes and prospects. Nat Rev Mol Cell Biol [Internet]. 2018 Sep 1;19(9):547–62. Available from: http://www.nature.com/articles/s41580-018-0015-0

63. Terzic A, Kurachi Y. Actin microfilament disrupters enhance K(ATP) channel opening in patches from guinea-pig cardiomyocytes. J Physiol [Internet]. 1996 Apr 15;492 (Pt 2:395–404. Available from: http://www.ncbi.nlm.nih.gov/pubmed/9019537

64. Hohmeier HE, Mulder H, Chen GX, Henkel-Rieger R, Prentki M, Newgard CB. Isolation of INS-1-derived cell lines with robust ATP- sensitive K+ channel-dependent and -independent glucose- stimulated insulin secretion. Diabetes [Internet]. 2000;49(3):424–30. Available from: http://fox.novo.dk/netacgi/getref.pl?ref=C-85654800015

65. Wu Y, Shyng SL, Chen PC. Concerted trafficking regulation of Kv2.1 and KATP channels by leptin in pancreatic beta-cells. J Biol Chem. 2015;290(50):29676–90.

66. Rorsman P, Braun M. Regulation of Insulin Secretion in Human Pancreatic Islets. Annu Rev Physiol [Internet]. 2013;75(1):155–79. Available from: http://www.annualreviews.org/doi/10.1146/annurev-physiol-030212-183754

67. Garcia D, Shaw RJ. AMPK: Mechanisms of Cellular Energy Sensing and Restoration of Metabolic Balance. Mol Cell [Internet]. 2017 Jun;66(6):789–800. Available from: https://linkinghub.elsevier.com/retrieve/pii/S1097276517303969

68. Lim A, Park S-H, Sohn J, Jeon J, Park J, Song D, et al. Glucose Deprivation Regulates K ATP Channel Trafficking via AMP-Activated Protein Kinase in Pancreatic β-Cells. Diabetes [Internet]. 2009 Dec;58(12):2813–9. Available from: http://diabetes.diabetesjournals.org/lookup/doi/10.2337/db09-0600

69. Beall C, Piipari K, Al-Qassab H, Smith MA, Parker N, Carling D, et al. Loss of AMP-activated protein kinase α2 subunit in mouse β-cells impairs glucose-stimulated insulin secretion and inhibits their sensitivity to hypoglycaemia. Biochem J [Internet]. 2010;429(2):323–33. Available from: http://biochemj.org/lookup/doi/10.1042/BJ20100231

70. Minokoshi Y, Kim Y-B, Peroni OD, Fryer LGD, Müller C, Carling D, et al. Leptin stimulates fatty-acid oxidation by activating AMP-activated protein kinase. Nature [Internet]. 2002 Jan;415(6869):339–43. Available from: http://www.nature.com/articles/415339a

71. Minokoshi Y, Alquier T, Furukawa N, Kim Y-B, Lee A, Xue B, et al. AMP-kinase regulates food intake by responding to hormonal and nutrient signals in the hypothalamus. Nature [Internet]. 2004 Apr 17;428(6982):569–74. Available from: http://www.nature.com/articles/nature02440

72. Marcelo KL, Ribar T, Means CR, Tsimelzon A, Stevens RD, Ilkayeva O, et al. Research Resource: Roles for Calcium/Calmodulin-Dependent Protein Kinase Kinase 2 (CaMKK2) in Systems Metabolism. Mol Endocrinol [Internet]. 2016 May 1;30(5):557–72. Available from: https://academic.oup.com/mend/article/30/5/557/2556685

73. Bootman MD, Collins TJ, Mackenzie L, Roderick HL, Berridge MJ, Peppiatt CM. 2-Aminoethoxydiphenyl borate (2-APB) is a reliable blocker of store-operated Ca 2+ entry but an inconsistent inhibitor of InsP 3 -induced Ca 2+ release. FASEB J [Internet]. 2002 Aug;16(10):1145–50. Available from: https://onlinelibrary.wiley.com/doi/abs/10.1096/fj.02-0037rev

74. Peppiatt CM, Collins TJ, Mackenzie L, Conway SJ, Holmes AB, Bootman MD, et al. 2-Aminoethoxydiphenyl borate (2-APB) antagonises inositol 1,4,5-trisphosphate-induced calcium release, inhibits calcium pumps and has a use-dependent and slowly reversible action on store-operated calcium entry channels. Cell Calcium [Internet]. 2003 Jul;34(1):97–108. Available from:

https://linkinghub.elsevier.com/retrieve/pii/S0143416003000265

75. Hong DH, Choi I-W, Son YK, Kim D-J, Na SH, Jung W-K, et al. The effect of PI3 kinase inhibitor LY294002 on voltage-dependent K+ channels in rabbit coronary arterial smooth muscle cells. Life Sci [Internet]. 2013 May;92(17–19):916–22. Available from: https://linkinghub.elsevier.com/retrieve/pii/S0024320513001744

76. Iacobucci GJ, Popescu GK. NMDA receptors: linking physiological output to biophysical operation. Nat Rev Neurosci [Internet]. 2017 Apr 1;18(4):236–49. Available from: http://www.nature.com/articles/nrn.2017.24

77. Shanley LJ, Irving AJ, Harvey J. Leptin enhances NMDA receptor function and modulates hippocampal synaptic plasticity. J Neurosci [Internet]. 2001 [cited 2017 Mar 31];21(24):RC186. Available from: http://www.jneurosci.org/content/jneuro/21/24/RC186.full.pdf

78. Otter S, Lammert E. Exciting Times for Pancreatic Islets: Glutamate Signaling in Endocrine Cells. Trends Endocrinol Metab [Internet]. 2016 Mar;27(3):177–88. Available from: https://linkinghub.elsevier.com/retrieve/pii/S1043276015002489

79. Molnár E, Váradi A, McIlhinney RAA, Ashcroft SJH. Identification of functional ionotropic glutamate receptor proteins in pancreatic beta-cells and in islets of Langerhans. FEBS Lett [Internet]. 1995;371(3):253–7. Available from: http://www.ncbi.nlm.nih.gov/pubmed/7556603

80. Inagaki N, Kuromi H, Gonoi T. Expression and role of ionotropic glutamate receptors in pancreatic islet cells. Faseb J. 1995;9(8):686–91.

81. Gonoi T, Mizuno N, Inagaki N, Kuromi H, Seino Y, Miyazaki J, et al. Functional neuronal ionotropic glutamate receptors are expressed in the non-neuronal cell line MIN6. J Biol Chem [Internet]. 1994 Jun 24;269(25):16989–92. Available from: http://www.ncbi.nlm.nih.gov/pubmed/8006003

82. Marquard J, Otter S, Welters A, Stirban A, Fischer A, Eglinger J, et al. Characterization of pancreatic NMDA receptors as possible drug targets for diabetes treatment. Nat Med [Internet]. 2015 Mar 16;21(4):363–72. Available from: http://www.nature.com/doifinder/10.1038/nm.3822

83. Chen B-S, Roche KW. Regulation of NMDA receptors by phosphorylation. Neuropharmacology [Internet]. 2007 Sep;53(3):362–8. Available from: https://linkinghub.elsevier.com/retrieve/pii/S0028390807001542

84. Yang M, Leonard JP. Identification of mouse NMDA receptor subunit NR2A C-terminal tyrosine sites phosphorylated by coexpression with v-Src. J Neurochem [Internet]. 2001 Dec 20;77(2):580–8. Available from: http://doi.wiley.com/10.1046/j.1471-4159.2001.00255.x

85. Nakazawa T, Komai S, Tezuka T, Hisatsune C, Umemori H, Semba K, et al. Characterization of Fyn-mediated Tyrosine Phosphorylation Sites on GluRε2 (NR2B) Subunit of the N -Methyl-d-aspartate Receptor. J Biol Chem [Internet]. 2001 Jan 5;276(1):693–9. Available from: http://www.jbc.org/lookup/doi/10.1074/jbc.M008085200

86. Heida N-M, Leifheit-Nestler M, Schroeter MR, Müller J-P, Cheng I-F, Henkel S, et al. Leptin Enhances the Potency of Circulating Angiogenic Cells Via Src Kinase and Integrin αvβ5. Arterioscler Thromb Vasc Biol [Internet]. 2010 Feb;30(2):200–6. Available from:

https://www.ahajournals.org/doi/10.1161/ATVBAHA.109.192807

87. Jiang L, Li Z, Rui L. Leptin Stimulates Both JAK2-dependent and JAK2-independent Signaling Pathways. J Biol Chem [Internet]. 2008 Oct 17;283(42):28066–73. Available from: http://www.jbc.org/lookup/doi/10.1074/jbc.M805545200

88. Meunier FA, Gutiérrez LM. Captivating New Roles of F-Actin Cortex in Exocytosis and Bulk Endocytosis in Neurosecretory Cells. Trends Neurosci [Internet]. 2016 Sep;39(9):605–13. Available from: https://linkinghub.elsevier.com/retrieve/pii/S016622361630073X

89. Aunis D, Bader MF. The cytoskeleton as a barrier to exocytosis in secretory cells. J Exp Biol [Internet]. 1988 Sep;139:253–66. Available from: http://www.ncbi.nlm.nih.gov/pubmed/3062121

90. Tomas A, Yermen B, Min L, Pessin JE, Halban PA. Regulation of pancreatic beta-cell insulin secretion by actin cytoskeleton remodelling: role of gelsolin and cooperation with the MAPK signalling pathway. J Cell Sci [Internet]. 2006 May 15;119(Pt 10):2156–67. Available from: http://jcs.biologists.org/cgi/doi/10.1242/jcs.02942

91. Johnson JL, Monfregola J, Napolitano G, Kiosses WB, Catz SD. Vesicular trafficking through cortical actin during exocytosis is regulated by the Rab27a effector JFC1/Slp1 and the RhoA-GTPase–activating protein Gem-interacting protein. Brill J, editor. Mol Biol Cell [Internet]. 2012 May 15;23(10):1902–16. Available from: https://www.molbiolcell.org/doi/10.1091/mbc.e11-12-1001

92. Park SH, Ho WK, Jeon JH. AMPK regulates KATP channel trafficking via PTEN inhibition in leptin-treated pancreatic β-cells. Biochem Biophys Res Commun [Internet]. 2013;440(4):539–44. Available from: http://dx.doi.org/10.1016/j.bbrc.2013.09.099

93. Han Y-E, Lim A, Park S-H, Chang S, Lee S-H, Ho W-K. Rac-mediated actin remodeling and myosin II are involved in KATP channel trafficking in pancreatic β-cells. Exp Mol Med [Internet]. 2015 Oct 16;47(10):e190. Available from: http://www.nature.com/doifinder/10.1038/emm.2015.72

94. Chi X, Wang S, Huang Y, Stamnes M, Chen J-L. Roles of rho GTPases in intracellular transport and cellular transformation. Int J Mol Sci [Internet]. 2013 Mar 28;14(4):7089–108. Available from: http://www.ncbi.nlm.nih.gov/pubmed/23538840

95. Han J, Luby-Phelps K, Das B, Shu X, Xia Y, Mosteller RD, et al. Role of substrates and products of PI 3-kinase in regulating activation of Rac-related guanosine triphosphatases by Vav. Science [Internet]. 1998 Jan 23;279(5350):558–60. Available from: http://www.sciencemag.org/cgi/doi/10.1126/science.279.5350.558

96. Fleming IN, Gray A, Downes CP. Regulation of the Rac1-specific exchange factor Tiam1 involves both phosphoinositide 3-kinase-dependent and -independent components. Biochem J [Internet]. 2000 Oct 1;351(Pt 1):173–82. Available from: http://www.ncbi.nlm.nih.gov/pubmed/10998360

97. Shinohara M, Terada Y, Iwamatsu A, Shinohara A, Mochizuki N, Higuchi M, et al. SWAP-70 is a guanine-nucleotide-exchange factor that mediates signalling of membrane ruffling. Nature [Internet]. 2002 Apr;416(6882):759–63. Available from: http://www.nature.com/articles/416759a

98. Papadopulos A, Tomatis VM, Kasula R, Meunier FA. The Cortical Acto-Myosin Network:

From Diffusion Barrier to Functional Gateway in the Transport of Neurosecretory Vesicles to the Plasma Membrane. Front Endocrinol (Lausanne) [Internet]. 2013;4. Available from: http://journal.frontiersin.org/article/10.3389/fendo.2013.00153/abstract

99. Klussmann E, Maric K, Wiesner B, Beyermann M, Rosenthal W. Protein kinase A anchoring proteins are required for vasopressin-mediated translocation of aquaporin-2 into cell membranes of renal principal cells. J Biol Chem [Internet]. 1999 Feb 19;274(8):4934–8. Available from: http://www.ncbi.nlm.nih.gov/pubmed/9988736

100. Nedvetsky PI, Tamma G, Beulshausen S, Valenti G, Rosenthal W, Klussmann E. Regulation of aquaporin-2 trafficking. Handb Exp Pharmacol [Internet]. 2009;(190):133–57. Available from: http://www.ncbi.nlm.nih.gov/pubmed/19096775

101. Butterworth MB, Frizzell RA, Johnson JP, Peters KW, Edinger RS. PKA-dependent ENaC trafficking requires the SNARE-binding protein complexin. Am J Physiol Renal Physiol [Internet]. 2005 Nov;289(5):F969-77. Available from: http://www.ncbi.nlm.nih.gov/pubmed/15972388

102. Stone JD, Narine A, Tulis DA. Inhibition of vascular smooth muscle growth via signaling crosstalk between AMP-activated protein kinase and cAMP-dependent protein kinase. Front Physiol [Internet]. 2012;3. Available from: http://journal.frontiersin.org/article/10.3389/fphys.2012.00409/abstract

103. Kobashigawa LC, Xu YC, Padbury JF, Tseng Y-T, Yano N. Metformin Protects Cardiomyocyte from Doxorubicin Induced Cytotoxicity through an AMP-Activated Protein Kinase Dependent Signaling Pathway: An In Vitro Study. López M, editor. PLoS One [Internet]. 2014 Aug 15;9(8):e104888. Available from: http://dx.plos.org/10.1371/journal.pone.0104888

104. Geron E, Boura-Halfon S, Schejter ED, Shilo B-Z. The Edges of Pancreatic Islet β Cells Constitute Adhesive and Signaling Microdomains. Cell Rep [Internet]. 2015 Jan;10(3):317–25. Available from: https://linkinghub.elsevier.com/retrieve/pii/S2211124714010602

105. Idevall-Hagren O, Tengholm A. Metabolic regulation of calcium signaling in beta cells. Semin Cell Dev Biol [Internet]. 2020 Jul;103:20–30. Available from: https://linkinghub.elsevier.com/retrieve/pii/S1084952118303100

106. Rizzuto R. Close Contacts with the Endoplasmic Reticulum as Determinants of Mitochondrial Ca2+ Responses. Science (80-) [Internet]. 1998 Jun 12;280(5370):1763–6. Available from: https://www.sciencemag.org/lookup/doi/10.1126/science.280.5370.1763

107. Cárdenas C, Miller RA, Smith I, Bui T, Molgó J, Müller M, et al. Essential Regulation of Cell Bioenergetics by Constitutive InsP3 Receptor Ca2+ Transfer to Mitochondria. Cell [Internet]. 2010 Jul;142(2):270–83. Available from: https://linkinghub.elsevier.com/retrieve/pii/S009286741000629X

108. Dingreville F, Panthu B, Thivolet C, Ducreux S, Gouriou Y, Pesenti S, et al. Differential Effect of Glucose on ER-Mitochondria Ca 2+ Exchange Participates in Insulin Secretion and Glucotoxicity-Mediated Dysfunction of β-Cells. Diabetes [Internet]. 2019 Sep;68(9):1778–94. Available from: http://diabetes.diabetesjournals.org/lookup/doi/10.2337/db18-1112

109. Tengholm A, Gylfe E. cAMP signalling in insulin and glucagon secretion. Diabetes, Obes

Metab. 2017;19(March):42–53.

110. Murphy JG, Sanderson JL, Gorski JA, Scott JD, Catterall WA, Sather WA, et al. AKAP-anchored PKA maintains neuronal L-type calcium channel activity and NFAT transcriptional signaling. Cell Rep [Internet]. 2014 Jun 12;7(5):1577–88. Available from: http://www.ncbi.nlm.nih.gov/pubmed/24835999

111. Dyachok O, Gylfe E. Ca 2 +-induced Ca 2 + Release via Inositol 1,4,5-trisphosphate Receptors Is Amplified by Protein Kinase A and Triggers Exocytosis in Pancreatic β-Cells. J Biol Chem [Internet]. 2004 Oct 29;279(44):45455–61. Available from: http://www.jbc.org/lookup/doi/10.1074/jbc.M407673200

112. Kawasaki H, Springett GM, Mochizuki N, Toki S, Nakaya M, Matsuda M, et al. A Family of cAMP-Binding Proteins That Directly Activate Rap1. Science (80-) [Internet]. 1998 Dec 18;282(5397):2275–9. Available from: https://www.sciencemag.org/lookup/doi/10.1126/science.282.5397.2275

113. Seino S, Shibasaki T. PKA-dependent and PKA-independent pathways for cAMP-regulated exocytosis. Physiol Rev [Internet]. 2005 Oct;85(4):1303–42. Available from: http://www.ncbi.nlm.nih.gov/pubmed/16183914

114. Renström E, Eliasson L, Rorsman P. Protein kinase A-dependent and -independent stimulation of exocytosis by cAMP in mouse pancreatic B-cells. J Physiol [Internet]. 1997 Jul 1;502(1):105–18. Available from: http://www.ncbi.nlm.nih.gov/pubmed/9234200

115. Wong W, Scott JD. AKAP signalling complexes: focal points in space and time. Nat Rev Mol Cell Biol. 2004;5(December):959–70.

116. Faruque OM, Le-Nguyen D, Lajoix A-D, Vives E, Petit P, Bataille D, et al. Cell-permeable peptide-based disruption of endogenous PKA-AKAP complexes: a tool for studying the molecular roles of AKAP-mediated PKA subcellular anchoring. Am J Physiol Physiol [Internet]. 2009 Feb;296(2):C306–16. Available from: https://www.physiology.org/doi/10.1152/ajpcell.00216.2008

117. Lester LB, Langeberg LK, Scott JD. Anchoring of protein kinase A facilitates hormone-mediated insulin secretion. Proc Natl Acad Sci U S A [Internet]. 1997 Dec 23;94(26):14942–7. Available from: http://www.ncbi.nlm.nih.gov/pubmed/9405718

118. Fraser IDC. A novel lipid-anchored A-kinase Anchoring Protein facilitates cAMP-responsive membrane events. EMBO J [Internet]. 1998 Apr 15;17(8):2261–72. Available from: http://emboj.embopress.org/cgi/doi/10.1093/emboj/17.8.2261

119. Josefsen K, Lee YC, Thams P, Efendic S, Nielsen JH. AKAP 18 alpha and gamma have opposing effects on insulin release in INS-1E cells. FEBS Lett [Internet]. 2010;584(1):81–5. Available from: http://www.ncbi.nlm.nih.gov/entrez/query.fcgi?cmd=Retrieve&db=PubMed&dopt=Citation&list_uids=19896945%5Cnhttp://www.sciencedirect.com/science?_ob=MImg&_imagekey=B6T36-4XMKBBY-2-G&_cdi=4938&_user=4853037&_pii=S0014579309008886&_origin=gateway&_coverDate=01

120. Hinke SA, Navedo MF, Ulman A, Whiting JL, Nygren PJ, Tian G, et al. Anchored phosphatases modulate glucose homeostasis. EMBO J [Internet]. 2012;31(20):3991–4004. Available from: http://emboj.embopress.org/cgi/doi/10.1038/emboj.2012.244

121. Asfari M, Janjic D, Meda P, Li G, Halban PA, Wollheim CB. Establishment of 2-mercaptoethanol-dependent differentiated insulin-secreting cell lines. Endocrinology [Internet]. 1992 Jan;130(1):167–78. Available from: https://academic.oup.com/endo/article-lookup/doi/10.1210/endo.130.1.1370150

122. Schwiening CJ. A brief historical perspective: Hodgkin and Huxley. J Physiol [Internet]. 2012 Jun 1;590(11):2571–5. Available from: http://doi.wiley.com/10.1113/jphysiol.2012.230458

123. Hamill OP, Marty A, Neher E, Sakmann B, Sigworth FJ. Improved patch-clamp techniques for high-resolution current recording from cells and cell-free membrane patches. Pflügers Arch - Eur J Physiol [Internet]. 1981 Aug;391(2):85–100. Available from: http://link.springer.com/10.1007/BF00656997

124. Gee KR, Brown KA, Chen W-NU, Bishop-Stewart J, Gray D, Johnson I. Chemical and physiological characterization of fluo-4 Ca2+-indicator dyes. Cell Calcium [Internet]. 2000 Feb;27(2):97–106. Available from: https://linkinghub.elsevier.com/retrieve/pii/S0143416099900957

125. Depry C, Allen MD, Zhang J. Visualization of PKA activity in plasma membrane microdomains. Mol Biosyst [Internet]. 2011;7(1):52–8. Available from: http://www.ncbi.nlm.nih.gov/pubmed/20838685

126. Herbst KJ, Allen MD, Zhang J. Spatiotemporally Regulated Protein Kinase A Activity Is a Critical Regulator of Growth Factor-Stimulated Extracellular Signal-Regulated Kinase Signaling in PC12 Cells. Mol Cell Biol [Internet]. 2011 Oct 1;31(19):4063–75. Available from: http://mcb.asm.org/cgi/doi/10.1128/MCB.05459-11

127. Surdo NC, Berrera M, Koschinski A, Brescia M, MacHado MR, Carr C, et al. FRET biosensor uncovers cAMP nano-domains at b-adrenergic targets that dictate precise tuning of cardiac contractility. Nat Commun [Internet]. 2017;8:1–14. Available from: http://dx.doi.org/10.1038/ncomms15031

128. Carr DW, Stofko-Hahn RE, Fraser ID, Cone RD SJ. Localization of the cAMP-dependent protein kinase to the postsynaptic densities by A-kinase anchoring proteins. Characterization of AKAP 79. J Biol Chem. 1992;25(267(24)):16816–23.

129. Bregman DB, Bhattacharyya N RC. High affinity binding protein for the regulatory subunit of cAMP-dependent protein kinase II-B. Cloning, characterization, and expression of cDNAs for rat brain P150. J Biol Chem. 1989;15(264(8)):4648–56.

130. Dell'Acqua ML, Faux MC, Thorburn J, Thorburn A, Scott JD. Membrane-targeting sequences on AKAP79 bind phosphatidylinositol-4, 5-bisphosphate. EMBO J [Internet]. 1998 Apr 15;17(8):2246–60. Available from: http://www.ncbi.nlm.nih.gov/pubmed/9545238

131. Klauck TM, Faux MC, Labudda K, Langeberg LK, Jaken S, Scott JD. Coordination of Three Signaling Enzymes by AKAP79, a Mammalian Scaffold Protein. Science (80-) [Internet]. 1996 Mar 15;271(5255):1589–92. Available from: https://www.sciencemag.org/lookup/doi/10.1126/science.271.5255.1589

132. Hoshi N, Langeberg LK, Scott JD. Distinct enzyme combinations in AKAP signalling complexes permit functional diversity. Nat Cell Biol [Internet]. 2005 Nov 16;7(11):1066–73. Available from: http://www.nature.com/articles/ncb1315

133. Zhang J, Bal M, Bierbower S, Zaika O, Shapiro MS. AKAP79/150 Signal Complexes in G-Protein Modulation of Neuronal Ion Channels. J Neurosci [Internet]. 2011 May 11;31(19):7199–211. Available from: http://www.jneurosci.org/cgi/doi/10.1523/JNEUROSCI.4446-10.2011

134. Oliveria SF, Dell'Acqua ML, Sather WA. AKAP79/150 Anchoring of Calcineurin Controls Neuronal L-Type Ca2+ Channel Activity and Nuclear Signaling. Neuron [Internet]. 2007 Jul;55(2):261–75. Available from: https://linkinghub.elsevier.com/retrieve/pii/S0896627307004898

135. Dell'Acqua ML, Dodge KL, Tavalin SJ, Scott JD. Mapping the protein phosphatase-2B anchoring site on AKAP79. Binding and inhibition of phosphatase activity are mediated by residues 315-360. J Biol Chem [Internet]. 2002 Dec 13;277(50):48796–802. Available from: http://www.ncbi.nlm.nih.gov/pubmed/12354762

136. Carr DW, Stofko-Hahn RE, Fraser ID, Bishop SM, Acott TS, Brennan RG SJ. Interaction of the regulatory subunit (RII) of cAMP-dependent protein kinase with RII-anchoring proteins occurs through an amphipathic helix binding motif. J Biol Chem. 1991;266(22):14188–92.

137. Carr DW, Hausken ZE, Fraser ID, Stofko-Hahn RE, Scott JD. Association of the type II cAMP-dependent protein kinase with a human thyroid RII-anchoring protein. Cloning and characterization of the RII-binding domain. J Biol Chem [Internet]. 1992 Jul 5;267(19):13376–82. Available from: http://www.ncbi.nlm.nih.gov/pubmed/1618839

138. Aguilar-Bryan L, Bryan J. Molecular Biology of Adenosine Triphosphate-Sensitive Potassium Channels*. Endocr Rev [Internet]. 1999 Apr 1;20(2):101–35. Available from: https://academic.oup.com/edrv/article/20/2/101/2530810

139. Ashcroft FM, Proks P, Smith PA, Ämmälä C, Bokvist K, Rorsman P. Stimulus-secretion coupling in pancreatic β cells. J Cell Biochem [Internet]. 1994;55(S1994A):54–65. Available from: http://doi.wiley.com/10.1002/jcb.240550007

140. Jacobson DA, Kuznetsov A, Lopez JP, Kash S, Ämmälä CE, Philipson LH. Kv2.1 Ablation Alters Glucose-Induced Islet Electrical Activity, Enhancing Insulin Secretion. Cell Metab [Internet]. 2007 Sep;6(3):229–35. Available from: https://linkinghub.elsevier.com/retrieve/pii/S1550413107002227

141. MacDonald PE, Sewing S, Wang J, Joseph JW, Smukler SR, Sakellaropoulos G, et al. Inhibition of Kv2.1 Voltage-dependent K + Channels in Pancreatic β-Cells Enhances Glucose-dependent Insulin Secretion. J Biol Chem [Internet]. 2002 Nov 22;277(47):44938–45. Available from: http://www.jbc.org/lookup/doi/10.1074/jbc.M205532200

142. Yang SN, Wenna ND, Yu J, Yang G, Qiu H, Yu L, et al. Glucose Recruits KATP Channels via Non-Insulin-Containing Dense-Core Granules. Cell Metab. 2007;6(3):217–28.

143. Traynelis SF, Wollmuth LP, McBain CJ, Menniti FS, Vance KM, Ogden KK, et al. Glutamate Receptor Ion Channels: Structure, Regulation, and Function. Pharmacol Rev [Internet]. 2010 Sep 1;62(3):405–96. Available from: http://pharmrev.aspetjournals.org/cgi/doi/10.1124/pr.109.002451

144. Saneyoshi T, Wayman G, Fortin D, Davare M, Hoshi N, Nozaki N, et al. Activity-Dependent Synaptogenesis: Regulation by a CaM-Kinase Kinase/CaM-Kinase I/βPIX

Signaling Complex. Neuron [Internet]. 2008 Jan;57(1):94–107. Available from: https://linkinghub.elsevier.com/retrieve/pii/S0896627307009749

145. Paoletti P, Bellone C, Zhou Q. NMDA receptor subunit diversity: impact on receptor properties, synaptic plasticity and disease. Nat Rev Neurosci [Internet]. 2013;14(6):383–400. Available from: http://www.ncbi.nlm.nih.gov/pubmed/23686171

146. Mairet-Coello G, Courchet J, Pieraut S, Courchet V, Maximov A, Polleux F. The CAMKK2-AMPK Kinase Pathway Mediates the Synaptotoxic Effects of Aβ Oligomers through Tau Phosphorylation. Neuron [Internet]. 2013 Apr;78(1):94–108. Available from: https://linkinghub.elsevier.com/retrieve/pii/S0896627313001335

147. Thornton C, Bright NJ, Sastre M, Muckett PJ, Carling D. AMP-activated protein kinase (AMPK) is a tau kinase, activated in response to amyloid β-peptide exposure. Biochem J [Internet]. 2011 Mar 15;434(3):503–12. Available from: https://portlandpress.com/biochemj/article/434/3/503/80037/AMPactivated-protein-kinase-AMPK-is-a-tau-kinase

148. Shen K-Z, Johnson SW. Ca2+ Influx through NMDA-Gated Channels Activates ATP-Sensitive K+ Currents through a Nitric Oxide-cGMP Pathway in Subthalamic Neurons. J Neurosci. 2010 Feb;30(5):1882–93.

149. Shen K-Z, Yakhnitsa V, Munhall AC, Johnson SW. AMP kinase regulates K-ATP currents evoked by NMDA receptor stimulation in rat subthalamic nucleus neurons. Neuroscience [Internet]. 2014 Aug;274:138–52. Available from: https://linkinghub.elsevier.com/retrieve/pii/S0306452214004230

150. Corless M, Kiely A, McClenaghan NH, Flatt PR, Newsholme P. Glutamine regulates expression of key transcription factor, signal transduction, metabolic gene, and protein expression in a clonal pancreatic β-cell line. J Endocrinol [Internet]. 2006 Sep;190(3):719–27. Available from: https://joe.bioscientifica.com/view/journals/joe/190/3/1900719.xml

151. Atouf F, Czernichow P, Scharfmann R. Expression of Neuronal Traits in Pancreatic Beta Cells. J Biol Chem [Internet]. 1997 Jan 17;272(3):1929–34. Available from: http://www.jbc.org/lookup/doi/10.1074/jbc.272.3.1929

152. Patterson S, Irwin N, Guo-Parke H, Moffett RC, Scullion SM, Flatt PR, et al. Evaluation of the role of N-methyl-D-aspartate (NMDA) receptors in insulin secreting beta-cells. Eur J Pharmacol [Internet]. 2016;771:107–13. Available from: http://dx.doi.org/10.1016/j.ejphar.2015.12.015

153. Nakanishi S. Molecular diversity of glutamate receptors and implications for brain function. Science (80-) [Internet]. 1992 Oct 23;258(5082):597–603. Available from: https://www.sciencemag.org/lookup/doi/10.1126/science.1329206

154. Wu Z-Y, Zhu L-J, Zou N, Bombek LK, Shao C-Y, Wang N, et al. AMPA Receptors Regulate Exocytosis and Insulin Release in Pancreatic β Cells. Traffic [Internet]. 2012 Aug;13(8):1124–39. Available from: http://doi.wiley.com/10.1111/j.1600-0854.2012.01373.x

155. Weaver CD, Yao TL, Powers AC, Verdoorn TA. Differential Expression of Glutamate Receptor Subtypes in Rat Pancreatic Islets. J Biol Chem [Internet]. 1996 May 31;271(22):12977–84. Available from: http://www.jbc.org/lookup/doi/10.1074/jbc.271.22.12977

156. Miller M, Shi J, Zhu Y, Kustov M, Tian J, Stevens A, et al. Identification of ML204, a Novel Potent Antagonist That Selectively Modulates Native TRPC4/C5 Ion Channels. J Biol Chem [Internet]. 2011 Sep 23;286(38):33436–46. Available from: http://www.jbc.org/lookup/doi/10.1074/jbc.M111.274167

157. Mason MJ, Simpson AK, Mahaut-Smith MP, Robinson HPC. The interpretation of current-clamp recordings in the cell-attached patch-clamp configuration. Biophys J [Internet]. 2005 Jan;88(1):739–50. Available from: http://www.ncbi.nlm.nih.gov/pubmed/15516522

158. Gribble FM, Reimann F. Sulphonylurea action revisited: the post-cloning era. Diabetologia [Internet]. 2003 Jul 1;46(7):875–91. Available from: http://link.springer.com/10.1007/s00125-003-1143-3

159. Luo X, McGregor G, Irving AJ, Harvey J. Leptin Induces a Novel Form of NMDA Receptor-Dependent LTP at Hippocampal Temporoammonic-CA1 Synapses. eneuro [Internet]. 2015 May;2(3):ENEURO.0007-15.2015. Available from: http://eneuro.org/lookup/doi/10.1523/ENEURO.0007-15.2015

160. Shanley LJ, O'Malley D, Irving AJ, Ashford ML, Harvey J. Leptin inhibits epileptiform-like activity in rat hippocampal neurones via PI 3-kinase-driven activation of BK channels. J Physiol [Internet]. 2002 Dec;545(3):933–44. Available from: https://onlinelibrary.wiley.com/doi/10.1113/jphysiol.2002.029488

161. Bai L, Zhang X, Ghishan FK. Characterization of vesicular glutamate transporter in pancreatic α- and β-cells and its regulation by glucose. Am J Physiol Liver Physiol [Internet]. 2003 May 1;284(5):G808–14. Available from: https://www.physiology.org/doi/10.1152/ajpgi.00333.2002

162. Gammelsaeter R, Coppola T, Marcaggi P, Storm-Mathisen J, Chaudhry FA, Attwell D, et al. A Role for Glutamate Transporters in the Regulation of Insulin Secretion. Maedler K, editor. PLoS One [Internet]. 2011 Aug 11;6(8):e22960. Available from: https://dx.plos.org/10.1371/journal.pone.0022960

163. Di Cairano ES, Davalli AM, Perego L, Sala S, Sacchi VF, La Rosa S, et al. The glial glutamate transporter 1 (GLT1) is expressed by pancreatic ??-cells and prevents glutamate-induced ??-cell death. J Biol Chem. 2011;286(16):14007–18.

164. Aliprandi A, Longoni M, Stanzani L, Tremolizzo L, Vaccaro M, Begni B, et al. Increased Plasma Glutamate in Stroke Patients Might Be Linked to Altered Platelet Release and Uptake. J Cereb Blood Flow Metab [Internet]. 2005 Apr 19;25(4):513–9. Available from: http://journals.sagepub.com/doi/10.1038/sj.jcbfm.9600039

165. Feldmann N, del Rio RM, Gjinovci A, Tamarit-rodriguez J, Wollheim CB, Wiederkehr A, et al. Reduction of plasma membrane glutamate transport potentiates insulin but not glucagon secretion in pancreatic islet cells. Mol Cell Endocrinol [Internet]. 2011 May;338(1–2):46–57. Available from: http://dx.doi.org/10.1016/j.mce.2011.02.019

166. Irving AJ, Wallace L, Durakoglugil D, Harvey J. Leptin enhances NR2B-mediated N-methyl-d-aspartate responses via a mitogen-activated protein kinase-dependent process in cerebellar granule cells. Neuroscience [Internet]. 2006 Jan;138(4):1137–48. Available from: https://linkinghub.elsevier.com/retrieve/pii/S0306452205013357

167. Braun M, Ramracheya R, Bengtsson M, Zhang Q, Karanauskaite J, Partridge C, et al. Voltage-Gated Ion Channels in Human Pancreatic -Cells: Electrophysiological Characterization and Role in Insulin Secretion. Diabetes [Internet]. 2008 Jun

1;57(6):1618–28. Available from: http://diabetes.diabetesjournals.org/cgi/doi/10.2337/db07-0991

168. Smolen P, Rinzel J, Sherman A. Why pancreatic islets burst but single beta cells do not. The heterogeneity hypothesis. Biophys J [Internet]. 1993 Jun;64(6):1668–80. Available from: https://linkinghub.elsevier.com/retrieve/pii/S000634959381539X

169. Marroquí L, Gonzalez A, Ñeco P, Caballero-Garrido E, Vieira E, Ripoll C, et al. Role of leptin in the pancreatic β-cell: effects and signaling pathways. J Mol Endocrinol [Internet]. 2012 Aug;49(1):R9-17. Available from: http://www.ncbi.nlm.nih.gov/pubmed/22448029

170. Allison MB, Myers MG. 20 YEARS OF LEPTIN: Connecting leptin signaling to biological function. J Endocrinol [Internet]. 2014 Oct;223(1):T25–35. Available from: https://joe.bioscientifica.com/view/journals/joe/223/1/T25.xml

171. Liu JSE, Hebrok M. All mixed up: defining roles for β-cell subtypes in mature islets. Genes Dev [Internet]. 2017 Feb 1;31(3):228–40. Available from: http://genesdev.cshlp.org/lookup/doi/10.1101/gad.294389.116

172. Benninger RKP, Zhang M, Head WS, Satin LS, Piston DW. Gap Junction Coupling and Calcium Waves in the Pancreatic Islet. Biophys J [Internet]. 2008 Dec;95(11):5048–61. Available from: https://linkinghub.elsevier.com/retrieve/pii/S000634950878932X

173. Silva JR, Cooper P, Nichols CG. Modeling K,ATP-Dependent Excitability in Pancreatic Islets. Biophys J [Internet]. 2014 Nov;107(9):2016–26. Available from: https://linkinghub.elsevier.com/retrieve/pii/S000634951401011X

174. Bruederle CE, Gay J, Shyng S-L. A Role of the Sulfonylurea Receptor 1 in Endocytic Trafficking of ATP-Sensitive Potassium Channels. Traffic [Internet]. 2011 Sep;12(9):1242–56. Available from: http://doi.wiley.com/10.1111/j.1600-0854.2011.01227.x

175. Di Virgilio F, Fasolato C, Steinberg TH. Inhibitors of membrane transport system for organic anions block fura-2 excretion from PC12 and N2A cells. Biochem J [Internet]. 1988 Dec 15;256(3):959–63. Available from: https://portlandpress.com/biochemj/article/256/3/959/25346/Inhibitors-of-membrane-transport-system-for

176. Poitout V, Rouault C, Guerre-Millo M, Briaud I, Reach G. Inhibition of Insulin Secretion by Leptin in Normal Rodent Islets of Langerhans. Endocrinology [Internet]. 1998 Mar;139(3):822–6. Available from: https://academic.oup.com/endo/article-lookup/doi/10.1210/endo.139.3.5812

177. Jacobson DA, Shyng S-L. Ion Channels of the Islets in Type 2 Diabetes. J Mol Biol [Internet]. 2020 Mar;432(5):1326–46. Available from: https://linkinghub.elsevier.com/retrieve/pii/S0022283619305236

178. Rorsman P, Ashcroft FM. Pancreatic β-Cell Electrical Activity and Insulin Secretion: Of Mice and Men. Physiol Rev [Internet]. 2018;98(1):117–214. Available from: http://www.ncbi.nlm.nih.gov/pubmed/29212789

179. Friedman J. The long road to leptin. J Clin Invest [Internet]. 2016;126(12):4727–34. Available from: http://www.ncbi.nlm.nih.gov/pubmed/27906690

180. Wauman J, Zabeau L, Tavernier J. The Leptin Receptor Complex: Heavier Than Expected? Front Endocrinol (Lausanne) [Internet]. 2017 Feb 21;8. Available from:

http://journal.frontiersin.org/article/10.3389/fendo.2017.00030/full

181. Cochrane V, Shyng S-L. Leptin-induced trafficking of K<inf>ATP</inf> channels: A mechanism to regulate pancreatic β-cell excitability and insulin secretion. Int J Mol Sci. 2019;20(11).

182. Wu Y, Fortin DA, Cochrane VA, Chen P-C, Shyng S-L. NMDA receptors mediate leptin signaling and regulate potassium channel trafficking in pancreatic β-cells. J Biol Chem [Internet]. 2017 Sep 15;292(37):15512–24. Available from: http://www.jbc.org/lookup/doi/10.1074/jbc.M117.802249

183. Hansen KB, Yi F, Perszyk RE, Furukawa H, Wollmuth LP, Gibb AJ, et al. Structure, function, and allosteric modulation of NMDA receptors. J Gen Physiol [Internet]. 2018 Aug 6;150(8):1081–105. Available from: https://rupress.org/jgp/article/150/8/1081/43759/Structure-function-and-allosteric-modulation-of

184. Wrighton DC, Baker EJ, Chen PE, Wyllie DJA. Mg 2+ and memantine block of rat recombinant NMDA receptors containing chimeric NR2A/2D subunits expressed in Xenopus laevis oocytes. J Physiol [Internet]. 2008 Jan 1;586(1):211–25. Available from: http://doi.wiley.com/10.1113/jphysiol.2007.143164

185. Salter MW, Kalia L V. Src kinases: a hub for NMDA receptor regulation. Nat Rev Neurosci [Internet]. 2004 Apr;5(4):317–28. Available from: http://www.nature.com/articles/nrn1368

186. Zheng F, Gingrich MB, Traynelis SF, Conn PJ. Tyrosine kinase potentiates NMDA receptor currents by reducing tonic zinc inhibition. Nat Neurosci [Internet]. 1998;1(3):185–91. Available from: http://www.nature.com/doifinder/10.1038/634

187. Kuner T, Schoepfer R. Multiple Structural Elements Determine Subunit Specificity of Mg 2+ Block in NMDA Receptor Channels. J Neurosci [Internet]. 1996 Jun 1;16(11):3549–58. Available from: http://www.jneurosci.org/lookup/doi/10.1523/JNEUROSCI.16-11-03549.1996

188. Stroebel D, Casado M, Paoletti P. Triheteromeric NMDA receptors: from structure to synaptic physiology. Curr Opin Physiol [Internet]. 2018 Apr;2:1–12. Available from: https://linkinghub.elsevier.com/retrieve/pii/S2468867317300275

189. Edman S, McKay S, MacDonald LJ, Samadi M, Livesey MR, Hardingham GE, et al. TCN 201 selectively blocks GluN2A-containing NMDARs in a GluN1 co-agonist dependent but non-competitive manner. Neuropharmacology [Internet]. 2012 Sep;63(3):441–9. Available from: https://linkinghub.elsevier.com/retrieve/pii/S0028390812001633

190. Perkins KL. Cell-attached voltage-clamp and current-clamp recording and stimulation techniques in brain slices. J Neurosci Methods [Internet]. 2006 Jun 30;154(1–2):1–18. Available from: http://www.ncbi.nlm.nih.gov/pubmed/16554092

191. Fischer G, Mutel V, Trube G, Malherbe P, Kew JN, Mohacsi E, Heitz MP KJ. Fischer G, Mutel V, Trube G, Malherbe P, Kew JN, Mohacsi E, Heitz MP, Kemp JA. J Pharmacol Exp Ther. 1997;283(3):1285.

192. Yi F, Mou T-C, Dorsett KN, Volkmann RA, Menniti FS, Sprang SR, et al. Structural Basis for Negative Allosteric Modulation of GluN2A-Containing NMDA Receptors. Neuron [Internet]. 2016 Sep;91(6):1316–29. Available from:

https://linkinghub.elsevier.com/retrieve/pii/S0896627316305062

193. Grant ER, Guttmann RP, Seifert KM, Lynch DR. A region of the rat N-methyl-D-aspartate receptor 2A subunit that is sufficient for potentiation by phorbol esters. Neurosci Lett [Internet]. 2001 Sep;310(1):9–12. Available from: https://linkinghub.elsevier.com/retrieve/pii/S0304394001020857

194. Li B-S, Sun M-K, Zhang L, Takahashi S, Ma W, Vinade L, et al. Regulation of NMDA receptors by cyclin-dependent kinase-5. Proc Natl Acad Sci [Internet]. 2001 Oct 23;98(22):12742–7. Available from: http://www.pnas.org/cgi/doi/10.1073/pnas.211428098

195. Yang K, Trepanier C, Sidhu B, Xie Y-F, Li H, Lei G, et al. Metaplasticity gated through differential regulation of GluN2A versus GluN2B receptors by Src family kinases. EMBO J [Internet]. 2012 Feb 15;31(4):805–16. Available from: http://emboj.embopress.org/cgi/doi/10.1038/emboj.2011.453

196. Roskoski R. Src protein-tyrosine kinase structure, mechanism, and small molecule inhibitors. Pharmacol Res [Internet]. 2015 Apr;94:9–25. Available from: https://linkinghub.elsevier.com/retrieve/pii/S1043661815000055

197. Boggon TJ, Eck MJ. Structure and regulation of Src family kinases. Oncogene [Internet]. 2004 Oct 18;23(48):7918–27. Available from: http://www.nature.com/articles/1208081

198. Liu X, Brodeur SR, Gish G, Songyang Z, Cantley LC, Laudano AP PT. Regulation of c-Src tyrosine kinase activity by the Src SH2 domain. Oncogene. 1993;8(5):1119–26.

199. Köhr G, Seeburg PH. Subtype-specific regulation of recombinant NMDA receptor-channels by protein tyrosine kinases of the src family. J Physiol [Internet]. 1996 Apr 15;492(2):445–52. Available from: http://doi.wiley.com/10.1113/jphysiol.1996.sp021320

200. Wang W-S, Chen Z-G, Liu W-T, Chi Z-Q, He L, Liu J-G. Dorsal hippocampal NMDA receptor blockade impairs extinction of naloxone-precipitated conditioned place aversion in acute morphine-treated rats by suppressing ERK and CREB phosphorylation in the basolateral amygdala. Br J Pharmacol [Internet]. 2015 Jan;172(2):482–91. Available from: http://doi.wiley.com/10.1111/bph.12671

201. Taniguchi S, Nakazawa T, Tanimura A, Kiyama Y, Tezuka T, Watabe AM, et al. Involvement of NMDAR2A tyrosine phosphorylation in depression-related behaviour. EMBO J [Internet]. 2009 Dec 2;28(23):3717–29. Available from: http://emboj.embopress.org/cgi/doi/10.1038/emboj.2009.300

202. Barria A, Malinow R. Subunit-Specific NMDA Receptor Trafficking to Synapses. Neuron [Internet]. 2002 Jul;35(2):345–53. Available from: https://linkinghub.elsevier.com/retrieve/pii/S0896627302007766

203. Roskoski R. Src kinase regulation by phosphorylation and dephosphorylation. Biochem Biophys Res Commun [Internet]. 2005 May;331(1):1–14. Available from: https://linkinghub.elsevier.com/retrieve/pii/S0006291X05004857

204. Pucheta-Martínez E, Saladino G, Morando MA, Martinez-Torrecuadrada J, Lelli M, Sutto L, et al. An Allosteric Cross-Talk Between the Activation Loop and the ATP Binding Site Regulates the Activation of Src Kinase. Sci Rep [Internet]. 2016 Jul 11;6(1):24235. Available from: http://www.nature.com/articles/srep24235

205. Yoder SM, Dineen SL, Wang Z, Thurmond DC. YES, a Src Family Kinase, Is a Proximal Glucose-specific Activator of Cell Division Cycle Control Protein 42 (Cdc42) in Pancreatic

Islet β Cells. J Biol Chem [Internet]. 2014 Apr 18;289(16):11476–87. Available from: http://www.jbc.org/lookup/doi/10.1074/jbc.M114.559328

206. Socodato R, Santiago FN, Portugal CC, Domith I, Encarnação TG, Loiola EC, et al. Dopamine promotes NMDA receptor hypofunction in the retina through D1 receptor-mediated Csk activation, Src inhibition and decrease of GluN2B phosphorylation. Sci Rep [Internet]. 2017 Mar 18;7(1):40912. Available from: http://www.nature.com/articles/srep40912

207. Könner AC, Brüning JC. Selective Insulin and Leptin Resistance in Metabolic Disorders. Cell Metab [Internet]. 2012 Aug;16(2):144–52. Available from: https://linkinghub.elsevier.com/retrieve/pii/S1550413112002811

208. Chen H, Charlat O, Tartaglia LA, Woolf EA, Weng X, Ellis SJ, et al. Evidence That the Diabetes Gene Encodes the Leptin Receptor: Identification of a Mutation in the Leptin Receptor Gene in db/db Mice. Cell [Internet]. 1996 Feb;84(3):491–5. Available from: https://linkinghub.elsevier.com/retrieve/pii/S0092867400812945

209. Song M-Y, Hong C, Bae SH, So I, Park K-S. Dynamic Modulation of the Kv2.1 Channel by Src-Dependent Tyrosine Phosphorylation. J Proteome Res [Internet]. 2012 Feb 3;11(2):1018–26. Available from: https://pubs.acs.org/doi/10.1021/pr200770v

210. Destaing O, Sanjay A, Itzstein C, Horne WC, Toomre D, De Camilli P, et al. The Tyrosine Kinase Activity of c-Src Regulates Actin Dynamics and Organization of Podosomes in Osteoclasts. Brugge J, editor. Mol Biol Cell [Internet]. 2008 Jan;19(1):394–404. Available from: https://www.molbiolcell.org/doi/10.1091/mbc.e07-03-0227

211. Olivares MJ, González-Jamett AM, Guerra MJ, Baez-Matus X, Haro-Acuña V, Martínez-Quiles N, et al. Src Kinases Regulate De Novo Actin Polymerization during Exocytosis in Neuroendocrine Chromaffin Cells. Buday L, editor. PLoS One [Internet]. 2014 Jun 5;9(6):e99001. Available from: https://dx.plos.org/10.1371/journal.pone.0099001

212. Amico-Ruvio SA, Murthy SE, Smith TP, Popescu GK. Zinc Effects on NMDA Receptor Gating Kinetics. Biophys J [Internet]. 2011 Apr;100(8):1910–8. Available from: https://linkinghub.elsevier.com/retrieve/pii/S0006349511002621

213. Dolino DM, Chatterjee S, MacLean DM, Flatebo C, Bishop LDC, Shaikh SA, et al. The structure–energy landscape of NMDA receptor gating. Nat Chem Biol [Internet]. 2017 Dec 9;13(12):1232–8. Available from: http://www.nature.com/articles/nchembio.2487

214. Jalali-Yazdi F, Chowdhury S, Yoshioka C, Gouaux E. Mechanisms for Zinc and Proton Inhibition of the GluN1/GluN2A NMDA Receptor. Cell [Internet]. 2018 Nov;175(6):1520-1532.e15. Available from: https://linkinghub.elsevier.com/retrieve/pii/S0092867418313990

215. Fayyazuddin A, Villarroel A, Le Goff A, Lerma J, Neyton J. Four Residues of the Extracellular N-Terminal Domain of the NR2A Subunit Control High-Affinity Zn2+ Binding to NMDA Receptors. Neuron [Internet]. 2000 Mar;25(3):683–94. Available from: https://linkinghub.elsevier.com/retrieve/pii/S0896627300810703

216. Paoletti P, Ascher P, Neyton J. High-Affinity Zinc Inhibition of NMDA NR1–NR2A Receptors. J Neurosci [Internet]. 1997 Aug 1;17(15):5711–25. Available from: http://www.jneurosci.org/lookup/doi/10.1523/JNEUROSCI.17-15-05711.1997

217. Traynelis SF, Burgess MF, Zheng F, Lyuboslavsky P, Powers JL. Control of Voltage-

Independent Zinc Inhibition of NMDA Receptors by the NR1 Subunit. J Neurosci [Internet]. 1998 Aug 15;18(16):6163–75. Available from: http://www.jneurosci.org/lookup/doi/10.1523/JNEUROSCI.18-16-06163.1998

218. Vogt K, Mellor J, Tong G, Nicoll R. The Actions of Synaptically Released Zinc at Hippocampal Mossy Fiber Synapses. Neuron [Internet]. 2000 Apr;26(1):187–96. Available from: https://linkinghub.elsevier.com/retrieve/pii/S0896627300811496

219. Dodson G, Steiner D. The role of assembly in insulin's biosynthesis. Curr Opin Struct Biol [Internet]. 1998 Apr;8(2):189–94. Available from: https://linkinghub.elsevier.com/retrieve/pii/S0959440X98800377

220. Bland T, Zhu M, Dillon C, Sahin GS, Rodriguez-Llamas JL, Appleyard SM, et al. Leptin Controls Glutamatergic Synaptogenesis and NMDA-Receptor Trafficking via Fyn Kinase Regulation of NR2B. Endocrinology [Internet]. 2020 Feb 1;161(2). Available from: https://academic.oup.com/endo/article/doi/10.1210/endocr/bqz030/5678106

221. Fontaine DA, Davis DB. Attention to Background Strain Is Essential for Metabolic Research: C57BL/6 and the International Knockout Mouse Consortium. Diabetes [Internet]. 2016 Jan 22;65(1):25–33. Available from: http://diabetes.diabetesjournals.org/lookup/doi/10.2337/db15-0982

222. Zhao S, Kusminski CM, Elmquist JK, Scherer PE. Leptin: Less Is More. Diabetes [Internet]. 2020 May;69(5):823–9. Available from: http://diabetes.diabetesjournals.org/lookup/doi/10.2337/dbi19-0018

223. Erion K, Corkey BE. β-Cell Failure or β-Cell Abuse? Front Endocrinol (Lausanne) [Internet]. 2018 Sep 13;9. Available from: https://www.frontiersin.org/article/10.3389/fendo.2018.00532/full

224. Smelt MJ, Faas MM, de Haan BJ, de Vos P. Pancreatic beta-cell purification by altering FAD and NAD(P)H metabolism. Exp Diabetes Res [Internet]. 2008;2008:165360. Available from: http://www.ncbi.nlm.nih.gov/pubmed/18670618

225. Van De Winkel M, Pipeleers D. Autofluorescence-activated cell sorting of pancreatic islet cells: purification of insulin-containing B-cells according to glucose-induced changes in cellular redox state. Biochem Biophys Res Commun [Internet]. 1983 Jul 29;114(2):835–42. Available from: http://www.ncbi.nlm.nih.gov/pubmed/6349638

226. Redick SD, Leehy L, Rittenhouse AR, Blodgett DM, Derr AG, Kucukural A, et al. Recovery of viable endocrine-specific cells and transcriptomes from human pancreatic islet-engrafted mice. FASEB J [Internet]. 2020 Jan 10;34(1):1901–11. Available from: https://onlinelibrary.wiley.com/doi/abs/10.1096/fj.201901022RR

227. Tennant KG, Lindsley SR, Kirigiti MA, True C, Kievit P. Central and Peripheral Administration of Fibroblast Growth Factor 1 Improves Pancreatic Islet Insulin Secretion in Diabetic Mouse Models. Diabetes [Internet]. 2019 Jul;68(7):1462–72. Available from: http://diabetes.diabetesjournals.org/lookup/doi/10.2337/db18-1175

228. Schindelin J, Arganda-Carreras I, Frise E, Kaynig V, Longair M, Pietzsch T, et al. Fiji: an open-source platform for biological-image analysis. Nat Methods [Internet]. 2012 Jul 28;9(7):676–82. Available from: http://www.nature.com/articles/nmeth.2019

229. Cochrane VA, Wu Y, Yang Z, ElSheikh A, Dunford J, Kievit P, et al. Leptin modulates pancreatic β-cell membrane potential through Src kinase-mediated phosphorylation of

NMDA receptors. J Biol Chem [Internet]. 2020 Oct 9; Available from: http://www.ncbi.nlm.nih.gov/pubmed/33037073

230. Taylor SS, Zhang P, Steichen JM, Keshwani MM, Kornev AP. PKA: Lessons learned after twenty years. Biochim Biophys Acta - Proteins Proteomics [Internet]. 2013 Jul;1834(7):1271–8. Available from: http://www.ncbi.nlm.nih.gov/pubmed/19772347

231. Kim C, Cheng CY, Saldanha SA, Taylor SS. PKA-I Holoenzyme Structure Reveals a Mechanism for cAMP-Dependent Activation. Cell [Internet]. 2007 Sep;130(6):1032–43. Available from: https://linkinghub.elsevier.com/retrieve/pii/S0092867407009555

232. Gromada J, Bokvist K, Ding WG, Holst JJ, Nielsen JH, Rorsman P. Glucagon-like peptide 1 (7-36) amide stimulates exocytosis in human pancreatic beta-cells by both proximal and distal regulatory steps in stimulus-secretion coupling. Diabetes [Internet]. 1998 Jan 1;47(1):57–65. Available from: http://diabetes.diabetesjournals.org/cgi/doi/10.2337/diab.47.1.57

233. Suga S, Kanno T, Nakano K, Takeo T, Dobashi Y, Wakui M. GLP-I(7-36) amide augments Ba2+ current through L-type Ca2+ channel of rat pancreatic beta-cell in a cAMP-dependent manner. Diabetes [Internet]. 1997 Nov;46(11):1755–60. Available from: http://www.ncbi.nlm.nih.gov/pubmed/9356022

234. Kaihara KA, Dickson LM, Jacobson DA, Tamarina N, Roe MW, Philipson LH, et al. β-Cell-specific protein kinase A activation enhances the efficiency of glucose control by increasing acute-phase insulin secretion. Diabetes [Internet]. 2013 May;62(5):1527–36. Available from: http://www.ncbi.nlm.nih.gov/pubmed/23349500

235. Willoughby D, Masada N, Wachten S, Pagano M, Halls ML, Everett KL, et al. AKAP79/150 Interacts with AC8 and Regulates Ca 2+ -dependent cAMP Synthesis in Pancreatic and Neuronal Systems. J Biol Chem [Internet]. 2010 Jun 25;285(26):20328–42. Available from: http://www.jbc.org/lookup/doi/10.1074/jbc.M110.120725

236. Lester LB, Faux MC, Nauert JB, Scott JD. Targeted protein kinase A and PP-2B regulate insulin secretion through reversible phosphorylation. Endocrinology. 2001;142(3):1218–27.

237. Muallem S, Kwiatkowska K, Xu X, Yin HL. Actin filament disassembly is a sufficient final trigger for exocytosis in nonexcitable cells. J Cell Biol [Internet]. 1995 Feb 15;128(4):589–98. Available from: https://rupress.org/jcb/article/128/4/589/29147/Actin-filament-disassembly-is-a-sufficient-final

238. Pawson T, Scott JD. Signaling through scaffold, anchoring, and adaptor proteins. Science [Internet]. 1997 Dec 19;278(5346):2075–80. Available from: https://www.sciencemag.org/lookup/doi/10.1126/science.278.5346.2075

239. Smith FD, Langeberg LK, Scott JD. The where's and when's of kinase anchoring. Trends Biochem Sci [Internet]. 2006 Jun;31(6):316–23. Available from: http://www.ncbi.nlm.nih.gov/pubmed/16690317

240. Nauert JB, Rigas JD, Lester LB. Identification of an IQGAP1/AKAP79 complex in beta-cells. J Cell Biochem [Internet]. 2003 Sep 1;90(1):97–108. Available from: http://www.ncbi.nlm.nih.gov/pubmed/12938160

241. Purkey AM, Woolfrey KM, Crosby KC, Stich DG, Chick WS, Aoto J, et al. AKAP150 Palmitoylation Regulates Synaptic Incorporation of Ca2+-Permeable AMPA Receptors to

Control LTP. Cell Rep [Internet]. 2018 Oct;25(4):974-987.e4. Available from: https://linkinghub.elsevier.com/retrieve/pii/S2211124718315456

242. Colledge M, Dean RA, Scott GK, Langeberg LK, Huganir RL, Scott JD. Targeting of PKA to glutamate receptors through a MAGUK-AKAP complex. Neuron [Internet]. 2000 Jul;27(1):107–19. Available from: http://www.ncbi.nlm.nih.gov/pubmed/10939335

243. Lee J, Chung M-K, Ro JY. Activation of NMDA receptors leads to phosphorylation of TRPV1 S800 by protein kinase C and A-Kinase anchoring protein 150 in rat trigeminal ganglia. Biochem Biophys Res Commun [Internet]. 2012 Jul 27;424(2):358–63. Available from: http://www.ncbi.nlm.nih.gov/pubmed/22789851

244. Logue JS, Whiting JL, Tunquist B, Sacks DB, Langeberg LK, Wordeman L, et al. AKAP220 protein organizes signaling elements that impact cell migration. J Biol Chem [Internet]. 2011 Nov 11;286(45):39269–81. Available from: http://www.ncbi.nlm.nih.gov/pubmed/21890631

245. Radeva MY, Kugelmann D, Spindler V, Waschke J. PKA compartmentalization via AKAP220 and AKAP12 contributes to endothelial barrier regulation. PLoS One [Internet]. 2014;9(9):e106733. Available from: http://www.ncbi.nlm.nih.gov/pubmed/25188285

246. Oliveria SF, Gomez LL, Dell'Acqua ML. Imaging kinase--AKAP79--phosphatase scaffold complexes at the plasma membrane in living cells using FRET microscopy. J Cell Biol [Internet]. 2003 Jan 6;160(1):101–12. Available from: http://www.ncbi.nlm.nih.gov/pubmed/12507994

247. Dittmer PJ, Dell'Acqua ML, Sather WA. Ca2+/calcineurin-dependent inactivation of neuronal L-type Ca2+ channels requires priming by AKAP-anchored protein kinase A. Cell Rep [Internet]. 2014 Jun 12;7(5):1410–6. Available from: http://www.ncbi.nlm.nih.gov/pubmed/24835998

248. Taylor SS, Buechler JA, Yonemoto W. cAMP-dependent protein kinase: framework for a diverse family of regulatory enzymes. Annu Rev Biochem [Internet]. 1990;59:971–1005. Available from: http://www.ncbi.nlm.nih.gov/pubmed/2165385

249. Mehebik N, Jaubert A-M, Sabourault D, Giudicelli Y, Ribière C. Leptin-induced nitric oxide production in white adipocytes is mediated through PKA and MAP kinase activation. Am J Physiol Physiol [Internet]. 2005;289(2):C379–87. Available from: http://www.physiology.org/doi/10.1152/ajpcell.00320.2004

250. Zheng S, Qu Z, Zanetti M, Lam B, Chin-Sang I. C. elegans PTEN and AMPK block neuroblast divisions by inhibiting a BMP-insulin-PP2A-MAPK pathway. Development [Internet]. 2018 Dec 1;145(23):dev166876. Available from: http://dev.biologists.org/lookup/doi/10.1242/dev.166876

251. Kudo N, Gillespie JG, Kung L, Witters LA, Schulz R, Clanachan AS, et al. Characterization of 5'AMP-activated protein kinase activity in the heart and its role in inhibiting acetyl-CoA carboxylase during reperfusion following ischemia. Biochim Biophys Acta [Internet]. 1996 May 31;1301(1–2):67–75. Available from: http://www.ncbi.nlm.nih.gov/pubmed/8652652

252. Davies SP, Helps NR, Cohen PT, Hardie DG. 5'-AMP inhibits dephosphorylation, as well as promoting phosphorylation, of the AMP-activated protein kinase. Studies using bacterially expressed human protein phosphatase-2C alpha and native bovine protein phosphatase-2AC. FEBS Lett [Internet]. 1995 Dec 27;377(3):421–5. Available from:

http://www.ncbi.nlm.nih.gov/pubmed/8549768

253. Kim K, Baek A, Hwang J-E, Choi YA, Jeong J, Lee M-S, et al. Adiponectin-Activated AMPK Stimulates Dephosphorylation of AKT through Protein Phosphatase 2A Activation. Cancer Res [Internet]. 2009 May 1;69(9):4018–26. Available from: http://www.ncbi.nlm.nih.gov/pubmed/19366811

254. Yuan D, Zhou S, Liu S, Li K, Zhao H, Long S, et al. The AMPK-PP2A axis in insect fat body is activated by 20-hydroxyecdysone to antagonize insulin/IGF signaling and restrict growth rate. Proc Natl Acad Sci [Internet]. 2020 Apr 28;117(17):9292–301. Available from: http://www.pnas.org/lookup/doi/10.1073/pnas.2000963117

255. Johanns M, Lai Y-C, Hsu M-F, Jacobs R, Vertommen D, Van Sande J, et al. AMPK antagonizes hepatic glucagon-stimulated cyclic AMP signalling via phosphorylation-induced activation of cyclic nucleotide phosphodiesterase 4B. Nat Commun [Internet]. 2016;7(101):10856. Available from: http://www.nature.com/doifinder/10.1038/ncomms10856

256. Johnstone TB, Agarwal SR, Harvey RD, Ostrom RS. cAMP Signaling Compartmentation: Adenylyl Cyclases as Anchors of Dynamic Signaling Complexes. Mol Pharmacol [Internet]. 2018;93(4):270–6. Available from: http://www.ncbi.nlm.nih.gov/pubmed/29217670

257. Efendiev R, Samelson BK, Nguyen BT, Phatarpekar P V., Baameur F, Scott JD, et al. AKAP79 Interacts with Multiple Adenylyl Cyclase (AC) Isoforms and Scaffolds AC5 and -6 to α-Amino-3-hydroxyl-5-methyl-4-isoxazole-propionate (AMPA) Receptors. J Biol Chem [Internet]. 2010 May 7;285(19):14450–8. Available from: http://www.jbc.org/lookup/doi/10.1074/jbc.M110.109769

258. Bauman AL, Soughayer J, Nguyen BT, Willoughby D, Carnegie GK, Wong W, et al. Dynamic Regulation of cAMP Synthesis through Anchored PKA-Adenylyl Cyclase V/VI Complexes. Mol Cell [Internet]. 2006 Sep;23(6):925–31. Available from: https://linkinghub.elsevier.com/retrieve/pii/S1097276506005260

259. Tenner B, Getz M, Ross B, Ohadi D, Bohrer CH, Greenwald E, et al. Spatially compartmentalized phase regulation of a Ca2+-cAMP-PKA oscillatory circuit. Elife [Internet]. 2020 Nov 17;9. Available from: https://elifesciences.org/articles/55013

260. Zhang M, Patriarchi T, Stein IS, Qian H, Matt L, Nguyen M, et al. Adenylyl Cyclase Anchoring by a Kinase Anchor Protein AKAP5 (AKAP79/150) Is Important for Postsynaptic β-Adrenergic Signaling. J Biol Chem [Internet]. 2013 Jun 14;288(24):17918–31. Available from: http://www.jbc.org/lookup/doi/10.1074/jbc.M112.449462

261. Haushalter KJ, Casteel DE, Raffeiner A, Stefan E, Patel HH, Taylor SS. Phosphorylation of protein kinase A (PKA) regulatory subunit RIα by protein kinase G (PKG) primes PKA for catalytic activity in cells. J Biol Chem [Internet]. 2018;293(12):4411–21. Available from: http://www.jbc.org/lookup/doi/10.1074/jbc.M117.809988

262. Prada MP, Syed AU, Reddy GR, Martín-Aragón Baudel M, Flores-Tamez VA, Sasse KC, et al. AKAP5 complex facilitates purinergic modulation of vascular L-type Ca2+ channel CaV1.2. Nat Commun [Internet]. 2020;11(1):5303. Available from: http://www.ncbi.nlm.nih.gov/pubmed/33082339

263. Wilson AJ, Jabr RI, Clapp LH. Calcium modulation of vascular smooth muscle ATP-

sensitive K(+) channels: role of protein phosphatase-2B. Circ Res [Internet]. 2000 Nov 24;87(11):1019–25. Available from: http://www.ncbi.nlm.nih.gov/pubmed/11090547

264. Orie NN, Thomas AM, Perrino BA, Tinker A, Clapp LH. Ca2+/calcineurin regulation of cloned vascular K ATP channels: crosstalk with the protein kinase A pathway. Br J Pharmacol [Internet]. 2009 Jun;157(4):554–64. Available from: http://www.ncbi.nlm.nih.gov/pubmed/19422382

265. Beguin P. PKA-mediated phosphorylation of the human KATP channel: separate roles of Kir6.2 and SUR1 subunit phosphorylation. EMBO J [Internet]. 1999 Sep 1;18(17):4722–32. Available from: http://emboj.embopress.org/cgi/doi/10.1093/emboj/18.17.4722

266. Lin Y-F, Jan YN, Jan LY. Regulation of ATP-sensitive potassium channel function by protein kinase A-mediated phosphorylation in transfected HEK293 cells. EMBO J [Internet]. 2000 Mar 1;19(5):942–55. Available from: http://emboj.embopress.org/cgi/doi/10.1093/emboj/19.5.942

267. Light PE, Manning Fox JE, Riedel MJ, Wheeler MB. Glucagon-Like Peptide-1 Inhibits Pancreatic ATP-Sensitive Potassium Channels via a Protein Kinase A- and ADP-Dependent Mechanism. Mol Endocrinol [Internet]. 2002 Sep;16(9):2135–44. Available from: https://academic.oup.com/mend/article-lookup/doi/10.1210/me.2002-0084

268. Nystoriak MA, Nieves-Cintrón M, Nygren PJ, Hinke SA, Nichols CB, Chen C-Y, et al. AKAP150 Contributes to Enhanced Vascular Tone by Facilitating Large-Conductance Ca 2+ -Activated K + Channel Remodeling in Hyperglycemia and Diabetes Mellitus. Circ Res [Internet]. 2014 Feb 14;114(4):607–15. Available from: https://www.ahajournals.org/doi/10.1161/CIRCRESAHA.114.302168

269. Hansen WA, Christie MR, Kahn R, Norgaard A, Abel I, Petersen AM, et al. Supravital dithizone staining in the isolation of human and rat pancreatic islets. Diabetes Res [Internet]. 1989 Feb;10(2):53–7. Available from: http://www.ncbi.nlm.nih.gov/pubmed/2545405

270. Brandao KE, Dell'Acqua ML, Levinson SR. A-kinase anchoring protein 150 expression in a specific subset of TRPV1- and CaV 1.2-positive nociceptive rat dorsal root ganglion neurons. J Comp Neurol [Internet]. 2012 Jan 1;520(1):81–99. Available from: http://www.ncbi.nlm.nih.gov/pubmed/21674494

271. Bjørbæk C, Buchholz RM, Davis SM, Bates SH, Pierroz DD, Gu H, et al. Divergent Roles of SHP-2 in ERK Activation by Leptin Receptors. J Biol Chem [Internet]. 2001 Feb 16;276(7):4747–55. Available from: http://www.jbc.org/lookup/doi/10.1074/jbc.M007439200

272. Banks AS, Davis SM, Bates SH, Myers MG. Activation of Downstream Signals by the Long Form of the Leptin Receptor. J Biol Chem [Internet]. 2000 May 12;275(19):14563–72. Available from: http://www.jbc.org/lookup/doi/10.1074/jbc.275.19.14563

273. Willoughby D. Ca2+ stimulation of adenylyl cyclase generates dynamic oscillations in cyclic AMP. J Cell Sci [Internet]. 2006 Mar 1;119(5):828–36. Available from: http://jcs.biologists.org/cgi/doi/10.1242/jcs.02812

274. Lønsmann I, Bak LK. Potential role of adenylyl cyclase 8 signaling complexes in regulating insulin secretion from pancreatic beta cells. Cell Signal [Internet]. 2020 Aug;72:109635. Available from: https://linkinghub.elsevier.com/retrieve/pii/S0898656820301121

275. Ridley AJ. Rho GTPases and actin dynamics in membrane protrusions and vesicle trafficking. Trends Cell Biol [Internet]. 2006 Oct;16(10):522–9. Available from: https://linkinghub.elsevier.com/retrieve/pii/S0962892406002236

276. Lee CW, Han J, Bamburg JR, Han L, Lynn R, Zheng JQ. Regulation of acetylcholine receptor clustering by ADF/cofilin-directed vesicular trafficking. Nat Neurosci [Internet]. 2009 Jul 31;12(7):848–56. Available from: http://www.nature.com/articles/nn.2322

277. Hanley JG. Actin-dependent mechanisms in AMPA receptor trafficking. Front Cell Neurosci [Internet]. 2014 Nov 12;8. Available from: http://journal.frontiersin.org/article/10.3389/fncel.2014.00381/abstract

278. Miklavc P, Ehinger K, Sultan A, Felder T, Paul P, Gottschalk K-E, et al. Actin depolymerisation and crosslinking join forces with myosin II to contract actin coats on fused secretory vesicles. J Cell Sci [Internet]. 2015 Mar 15;128(6):1193–203. Available from: http://jcs.biologists.org/cgi/doi/10.1242/jcs.165571

279. Bamburg JR, Bernstein BW. Actin dynamics and cofilin-actin rods in alzheimer disease. Cytoskeleton [Internet]. 2016 Sep;73(9):477–97. Available from: http://doi.wiley.com/10.1002/cm.21282

280. Bravo-Cordero JJ, Sharma VP, Roh-Johnson M, Chen X, Eddy R, Condeelis J, et al. Spatial regulation of RhoC activity defines protrusion formation in migrating cells. J Cell Sci [Internet]. 2013 Aug 1;126(15):3356–69. Available from: http://jcs.biologists.org/cgi/doi/10.1242/jcs.123547

281. Bravo-Cordero JJ, Oser M, Chen X, Eddy R, Hodgson L, Condeelis J. A Novel Spatiotemporal RhoC Activation Pathway Locally Regulates Cofilin Activity at Invadopodia. Curr Biol [Internet]. 2011 Apr;21(8):635–44. Available from: https://linkinghub.elsevier.com/retrieve/pii/S0960982211003113

282. Dormond O, Rüegg C. Regulation of endothelial cell integrin function and angiogenesis by COX-2, cAMP and Protein Kinase A. Thromb Haemost [Internet]. 2003 Dec 5;90(10):577–85. Available from: http://www.thieme-connect.de/DOI/DOI?10.1160/TH03-03-0196

283. O'Connor KL, Mercurio AM. Protein Kinase A Regulates Rac and Is Required for the Growth Factor-stimulated Migration of Carcinoma Cells. J Biol Chem [Internet]. 2001 Dec 21;276(51):47895–900. Available from: http://www.jbc.org/lookup/doi/10.1074/jbc.M107235200

284. Branon TC, Bosch JA, Sanchez AD, Udeshi ND, Svinkina T, Carr SA, et al. Efficient proximity labeling in living cells and organisms with TurboID. Nat Biotechnol [Internet]. 2018 Oct 23;36(9):880–7. Available from: http://www.nature.com/articles/nbt.4201

285. Han Y-E, Chun JN, Kwon MJ, Ji Y-S, Jeong M-H, Kim H-H, et al. Endocytosis of K ATP Channels Drives Glucose-Stimulated Excitation of Pancreatic β Cells. Cell Rep [Internet]. 2018 Jan;22(2):471–81. Available from: https://linkinghub.elsevier.com/retrieve/pii/S2211124717318739

286. Geng X, Li L, Watkins S, Robbins PD, Drain P. The insulin secretory granule is the major site of K(ATP) channels of the endocrine pancreas. Diabetes [Internet]. 2003 Mar;52(3):767–76. Available from: http://www.ncbi.nlm.nih.gov/pubmed/12606519

287. Varadi A, Grant A, McCormack M, Nicolson T, Magistri M, Mitchell KJ, et al. Intracellular

ATP-sensitive K+ channels in mouse pancreatic beta cells: against a role in organelle cation homeostasis. Diabetologia [Internet]. 2006 Jul;49(7):1567–77. Available from: http://www.ncbi.nlm.nih.gov/pubmed/16752175

288. Zabolotny JM, Bence-Hanulec KK, Stricker-Krongrad A, Haj F, Wang Y, Minokoshi Y, et al. PTP1B Regulates Leptin Signal Transduction In Vivo. Dev Cell [Internet]. 2002 Apr;2(4):489–95. Available from: https://linkinghub.elsevier.com/retrieve/pii/S153458070200148X

289. Lund IK, Hansen JA, Andersen HS, Møller NPH, Billestrup N. Mechanism of protein tyrosine phosphatase 1B-mediated inhibition of leptin signalling. J Mol Endocrinol [Internet]. 2005 Apr;34(2):339–51. Available from: https://jme.bioscientifica.com/view/journals/jme/34/2/0340339.xml